Working fluid and system optimisation of organic Rankine cycles via computer-aided molecular design

A review

Markides, Christos N.; Bardow, André; De Paepe, Michel; De Servi, Carlo; Groß, Joachim; Haslam, Andrew J.; Lecompte, Steven; Papadopoulos, Athanasios I.; Oyewunmi, Oyeniyi A.; More Authors

Citation (APA)
Markides, C. N., Bardow, A., De Paepe, M., De Servi, C., Groß, J., Haslam, A. J., Lecompte, S., Papadopoulos, A. I., Oyewunmi, O. A., & More Authors (2025). Working fluid and system optimisation of organic Rankine cycles via computer-aided molecular design: A review. *Progress in Energy and Combustion Science*, *107*, Article 101201. https://doi.org/10.1016/j.pecs.2024.101201
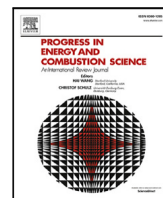
Important note
To cite this publication, please use the final published version (if applicable).
Please check the document version above.

Review article

Working fluid and system optimisation of organic Rankine cycles via computer-aided molecular design: A review

Christos N. Markides [a],[*], André Bardow [b], Michel De Paepe [c], Carlo De Servi [d], Joachim Groß [e], Andrew J. Haslam [a], Steven Lecompte [c], Athanasios I. Papadopoulos [f], Oyeniyi A. Oyewunmi [a], Panos Seferlis [f],[g], Johannes Schilling [b], Patrick Linke [h], Hua Tian [i], Gequn Shu [i],[j]

[a] *Clean Energy Processes (CEP) Laboratory and The Sargent Centre for Process Systems Engineering, Department of Chemical Engineering, Imperial College London, London SW7 2AZ, UK*
[b] *Energy & Process Systems Engineering, ETH Zürich, 8092 Zürich, Switzerland*
[c] *Ghent University, Faculty of Engineering and Architecture, Department of Electrical Energy, Metals, Mechanical Constructions & Systems, Ghent 9000, Belgium*
[d] *Propulsion & Power, Faculty of Aerospace Engineering, Delft University of Technology, Delft, Netherlands*
[e] *Institute of Thermodynamics and Thermal Process Engineering, University of Stuttgart, Stuttgart 70569, Germany*
[f] *Chemical Process and Energy Resources Institute, Centre for Research and Technology Hellas, 57001, Thessaloniki, Greece*
[g] *Department of Mechanical Engineering, Aristotle University of Thessaloniki, Thessaloniki, 54124, Greece*
[h] *Department of Chemical Engineering, Texas A&M University at Qatar, PO Box 23874, Education City, Doha, Qatar*
[i] *State Key Laboratory of Engines, Tianjin University, Tianjin 300072, China*
[j] *University of Science and Technology of China, Hefei, China*

ARTICLE INFO

ABSTRACT

Organic Rankine cycle (ORC) systems are a class of distributed power-generation systems that are suitable for the efficient conversion of low-to-medium temperature thermal energy to useful power. These versatile systems have significant potential to contribute in diverse ways to future clean and sustainable energy systems through, *e.g.*, deployment for waste-heat recovery in industrial facilities, but also the utilisation of renewable-heat sources, thereby improving energy access and living standards, while reducing primary energy consumption and the associated emissions. The energetic and economic performance, but also environmental sustainability of ORC systems, all depend strongly on the working fluid employed, and therefore a significant effort has been made in recent years to select, but also to design novel working fluids for ORC systems. In this context, computer-aided molecular design (CAMD) techniques have emerged as highly promising approaches with which to explore the key role of working fluids, and present an opportunity, by focusing on the design of new eco-friendly fluids with low environmental footprints, to identify alternatives to traditional refrigerants with improved characteristics. In this review article, an overview of working-fluid and system optimisation methodologies that can be used for the design and operation of next-generation ORC systems is provided. With reference to wide-ranging applications from waste-heat recovery in industrial and automotive applications, to biomass, geothermal and solar-energy conversion and/or storage, this review represents a comprehensive, forward-looking exposition of the application of CAMD to the design of ORC technology.

Contents

---

* Corresponding author.
  E-mail addresses: c.markides@imperial.ac.uk (C.N. Markides), o.oyewunmi@imperial.ac.uk (O.A. Oyewunmi).

1. Introduction

Despite recent progress in the development of renewable energy technologies and their increased deployment, global energy consumption is still dominated by non-renewable sources such as coal, oil, and natural gas [1]. Given this persisting reliance on fossil fuels and the significant amount of heat that is inherently wasted from a diverse range of processes, important opportunities exist for the recovery, integration, use and/or conversion of this waste heat into electricity or useful work [2,3], thus enabling energy efficiency improvements, primary fuel consumption minimisation and, consequently, associated emissions abatement [4,5]. The recovery and utilisation of industrial waste-heat streams has the potential to provide an additional 8 EJ of energy towards the annual energy consumption in Europe, thereby reducing annual primary-energy use by over 15% [6]. The significant opportunities that exist for technologies suitable for heat recovery and energy integration are then apparent.

A wide variety of thermal power cycles have been studied for the purpose of industrial energy integration and power generation from lower-temperature thermal sources, including the Kalina cycle [7–10], the Goswami cycle [11,12], carbon dioxide cycles [13,14], trilateral cycles [15–17] and organic Rankine cycles [18–24], along with various combined cycles [25,26]. Beyond these cycles, more novel and niche alternative cycles have also been proposed for waste-heat recovery and conversion applications, including various thermoacoustic and thermofluidic heat engines [27–30], as well as phase-change unsteady heat engines such as the non-inertive-feedback thermofluidic engine (NIFTE) [31–37] and the Up-THERM engine [6,38–42].

Nomenclature

Abbreviations / acronyms

μCHP	Micro combined heat and power
A	Primary characteristic point on saturated liquid curve
ANN	Artificial neural network
ASOG	Analytical solution of groups (activity-coefficient model)
B&B	Branch-and-bound
B&C	Branch-and-cut
BARON	Branch-and-reduce optimisation navigator
C	Critical point
CAM^{2}PD	Computer-aided molecular and multi-operating process design
CAM^{b}D	Computer-aided mixture and blend design
CAMD	Computer-aided molecular design
CAMPCD	Computer-aided molecular process and control design
CAMPD	Computer-aided molecular and process design
CE	Chapman–Enskog
CFC	Chlorofluorocarbon
CFD	Computational fluid dynamics
CHP	Combined heat and power
CMR	Continuous-molecular representation
CoMT	Continuous-molecular targeting
COSMO	Conductor-like screening model
COSMO-RS	COSMO for realistic solvents
COSMO-SAC	COSMO segment activity-coefficient model
DRORC	Dual-stage regenerative ORC
EI99	Eco-indicator 99
EoS	Equation of state
FVM	Finite-volume model
GA	Genetic algorithm
GC	Group-contribution
GT	Gas turbine
GWP	Global-warming potential
HCFC	Hydrochlorofluorocarbon
HCFO	Hydrochlorofluoroolefin
HELD	Helmholtz free energy Lagrangian dual
HEX	Heat exchanger
HFC	Hydrofluorocarbon
HFO	Hydrofluoroolefin
HHS	Hammersley-sequence sampling
HT	High-temperature
HTS	High-throughput screening
ICE-CHP	Internal-combustion engine with combined heat and power
KCORC	Knowledge center on ORC technology
L	Liquid phase
LatHS	Latin-hypercube sampling
lb	Lower bound
LCA	Life Cycle Assessment
LHC	Long haul cycle
LHS	Left-hand side

LINMAP	Linear-programming technique for multi-dimensional analysis of preference
LMTD	Logarithmic-mean temperature difference
LNG	Liquified natural gas
LT	Low-temperature
M	Secondary characteristic point on saturated vapour curve (higher temperature)
MAiNGO	McCormick-based algorithm for mixed-integer nonlinear global optimisation
MBM	Moving-boundary model
MDM	Octamethyltrisiloxane
MILP	Mixed-integer linear programming
MINLP	Mixed-integer nonlinear programming
MIOCP	Mixed-integer optimal control problem
MIQP	Mixed-integer quadratic problem
ML	Machine-learning
MM	Hexamethyldisiloxane
MOO	Multi-objective optimisation
MPC	Model predictive control
MUSCOD	MUltiple Shooting CODe for Optimal Control
N	Secondary characteristic point on saturated vapour curve (lower temperature)
NIFTE	Non-inertive-feedback thermofluidic engine
NLP	Non-linear programming
NPV	Net present value
NRTL	Non-random two-liquid (activity-coefficient model)
NSGA	Non-dominated sorting genetic algorithm
NTU	Number of transfer units
OA	Outer-approximation
OCP	Optimal control problem
ODP	Ozone depletion potential
ODS	Ozone-depleting substances
OFC	Organic flash cycle
ORC	Organic Rankine cycle
ORCLFE	ORC with liquid-flooded expansion
ORCSC	ORC with solution circuit
PC-SAFT	Perturbed-chain SAFT
PEM	Proton-exchange membrane
PEORC	Partially evaporating organic Rankine cycle
PFA	Poly-fluoroalkyl substances
PGS-COM	Particle generating set-complex algorithm
PI	Proportional-integral
PSO	Particle-swarm optimisation
PSRK	Predictive-SRK (EoS)
PTES	Pumped-thermal electricity storage
PTORC	Parallel two-stage ORC
QSAR	Quantitative structure–activity relationship
QSPR	Quantitative structure–property relationship
RHS	Right-hand side
RO	Robust optimisation
SA	Simulated annealing
SAFT	Statistical associating fluid theory
SAFT-VR	SAFT for chain molecules with attractive potentials of variable range
SIC	Specific investment cost
SMILES	Simplified molecular-input line-entry system

SOFC	Solid-oxide fuel cell
SOO	Single-objective optimisation
SPT	SMILES-to-property transformer
SQP	Sequentially quadratic programming
SRK	Soave–Redlich–Kwong (EoS)
SRORC	Single-stage regenerative ORC
SS	Sobol sampling
STORC	Series two-stage ORC
TCI	Total capital investment
TIC	Total investment costs
TLC	Trilateral cycle
TOPSIS	Technique for order preference by similarity to ideal situation
UA	Global conductance
ub	Upper bound
UNIFAC	UNIQUAC functional-group activity coefficients
UNIQUAC	Universal quasichemical activity coefficients
V	Vapour phase
VCC	Vapour-compression cycle
VECTO	Vehicle energy-consumption tool
VTPR	Volume-Translated Peng–Robinson
WF	Working fluid
WHR	Waste-heat recovery
Z	Primary characteristic point on saturated vapour curve

Constants

R	Universal gas constant

Variables (Greek symbols)

α	Ansatz in cubic equations of state
ΔT_{SH}	Degree of superheating (K)
η	Viscosity (Pa s)
η^*	Dimensionless viscosity
η_{carnot}	Carnot efficiency
η_{ex}	Exergetic efficiency
η_{th}	Thermal efficiency
ω	Acentric factor, defined as $-\log_{10}(p_{sat}/p_c) - 1$ at $T_r = 0.7$
ρ	Molar density
ξ	Variable indicating if a fluid is dry, isentropic or wet

Variables

$\dot{m}$	Mass flow rate ($kg\,s^{-1}$)
$\dot{Q}$	Heat flow rate, or thermal power (W)
$\dot{W}_n$	Net power output (kW)
A^{IDEAL}	Ideal free energy
c_p	Isobaric specific heat capacity ($J\,K^{-1}\,kg^{-1}$, or $J\,K^{-1}\,mol^{-1}$)
c_p^0	Ideal-gas (isobaric) specific heat capacity ($J\,K^{-1}\,kg^{-1}$, or $J\,K^{-1}\,mol^{-1}$)
f	Objective function
g	Inequality constraints of the process and molecular properties
G^E	Excess Gibbs energy

h	Equality constraints of the process and molecular properties
k	Inequality constraints of the CAMD formulation
k_{ij}	Binary interaction parameter
p	Pressure (Pa, or bar)
p_c	Critical pressure (Pa, or bar)
P_{net}	Net power output (W)
p_{sat}	Saturation (or vapour) pressure (Pa, or bar)
Q	Heat (J)
s	Specific (or molar) entropy ($J\,kg^{-1}\,K^{-1}$, or $J\,mol^{-1}\,K^{-1}$)
s^{ig}	Ideal-gas specific entropy ($J\,kg^{-1}\,K^{-1}$, or $J\,mol^{-1}\,K^{-1}$)
s^{res}	Residual specific entropy ($J\,kg^{-1}\,K^{-1}$, or $J\,mol^{-1}\,K^{-1}$)
T	Temperature (K, or °C)
T_c	Critical temperature (K, or °C)
T_H	Temperature of the high-temperature thermal reservoir (heat source) of a power cycle (K, or °C)
T_L	Temperature of the low-temperature thermal reservoir (heat sink) of a power cycle (K, or °C)
T_r	Reduced (dimensionless) temperature, defined as T/T_c (with T and T_c in absolute units)
V_c	Critical specific volume ($m^3\,kg^{-1}$ or $m^3\,mol^{-1}$)
x	Process degrees of freedom
x	Vapour quality
y	Molecular structure of the working fluid
k	Number of objective functions in an MOO problem

Amongst all of these options, particular interest has been observed in organic Rankine cycle (ORC) systems due to their applicability to the efficient conversion of lower grade heat to useful power [2,4]. ORC technology has been experiencing increasingly wider adoption in comparison to competing solutions due to continued performance improvements and cost reductions, as well as its versatility in being suited to a wide-ranging mix of heat sources and applications. However, it remains beset by a number of technical challenges; in particular, working-fluid design and selection are key areas of ongoing attention and research focus [18,21,43–45]. The working fluid is an important and integral element of ORC systems as it has a direct bearing on the design and specifications of key components and overall system size and also affects important operational procedures. Therefore it has a controlling role in determining not only the technical and thermodynamic performance but also the capital/investment and operational costs of these systems and, thus, ultimately, their financial viability and potential deployment in real applications.

Traditionally, working-fluid selection for ORC systems has been performed via *ad hoc* selection rules and predefined screening lists and criteria [46–52]. Following this conventional practice is inevitably time-consuming and sub-optimal. Typically, multiple system-level optimisation studies are undertaken, drawing from a database of known, pre-existing fluids of known chemical families, of which the thermophysical properties are readily available [53,54]. The process is complicated by the numerous chemical families and working-fluid options available, with a risk of missing suitable fluids if these are not included *a priori* in the search database. Such approaches can also lead to sub-optimal system designs and limit the flexibility in the design of working fluids for ORCs, especially when one considers the possible use of fluid mixtures [4]. A further complication is that differing ORC applications generally have different requirements, whereby this approach can neither be used to identify new and potentially novel

working fluids nor be used to inform on the prospective manufacturing processes required.

Computer-aided molecular design (CAMD) offers a more holistic approach to the design of working fluids for ORC power systems across a wide range of applications, wherein the molecular structure of prospective working fluids is optimised simultaneously alongside the ORC system design and operation in a single optimisation problem. This has been facilitated by the development of advanced fluid theories rooted in interactions on the molecular scale, providing an opportunity for the intelligent design of working fluids for any ORC system configuration [4,55], and bypassing the pre-emptive screening criteria of traditional methods. When applying CAMD to ORC systems, potential working fluids are described by functional groups; these groups can be combined in different ways to form novel molecules such that a handful of groups can be used to describe a large number of potential working fluids across multiple chemical families. This presents a powerful tool for understanding the impact of the working fluid on the design, performance, sizing, environmental impact, and operation of ORC power systems.

With CAMD, several molecular groups with free bonding sites are defined; these could be individual single/double/triple bonds or multiple combinations of these, (*e.g.*, $-CH_3$, $=CH_2$, $>CH_2$, $>CH-$, $>C<$, $=CH-$). These molecular groups can then be combined accordingly to form a large number of different hydrocarbon molecules. Theoretically, a collection of such molecular groups (including those with halogenated groups to form refrigerants) can be used to describe any arbitrary molecule, so long as all relevant groups present in the molecule are incorporated in the decision space. While CAMD was initially applied to solvent-design problems considering molecular target functions [56], it has been further developed to integrate the design of process models to consider a process-based target function (thus, the development of computer-aided molecular and process design, CAMPD), to advance the integrated design and optimisation of solvent and separation processes [57–60].

Aside from the required process models and constraints, such CAMPD problems require molecular feasibility constraints to ensure that the solutions generated from the combination of the molecular groups represent genuine molecules [61–63]. A group-contribution equation of state (EoS) is also typically required to provide accurate estimates of the fluid properties of a molecule based on the constituent molecular groups. Group-contribution models like those of Joback and Reid [64] can provide pure-component property values as inputs to cubic EoS, whereas group-contribution activity coefficient models such as UNI-FAC [65] can be combined with such EoS to account for both the vapour and liquid phase behaviour of working fluids. While those are empirical in nature, an alternative would be to deploy molecular EoS such as those based on the statistical associating fluid theory (SAFT) [66,67]; group-contribution versions of these EoS are also readily available [68–79] (see Section 4 for a discussion). By means of such group-contribution EoS one can predict the properties of a working fluid based on its constituent molecular groups, and the molecular structure of the fluid can be optimised simultaneously alongside the system, potentially identifying novel working fluids which may otherwise be overlooked [4]. Finally, an optimisation algorithm is required to provide a solution to the problem formulation; such algorithms are usually of the mixed-integer nonlinear programming (MINLP) type due to the integer nature of the molecular groups (and possibly other process variables) involved in the problem.

In this paper, a comprehensive review of CAMD techniques as applied to ORC systems design is presented in the context of the efficient and economically feasible conversion of heat to power. The discussed design techniques are relevant to a diverse range of energy applications featuring a variety of heat sources, from geothermal and biomass to solar and waste heat. The details involved in formulating and solving the optimisation problems describing the ORC system and working-fluid design simultaneously are examined, while the important role of
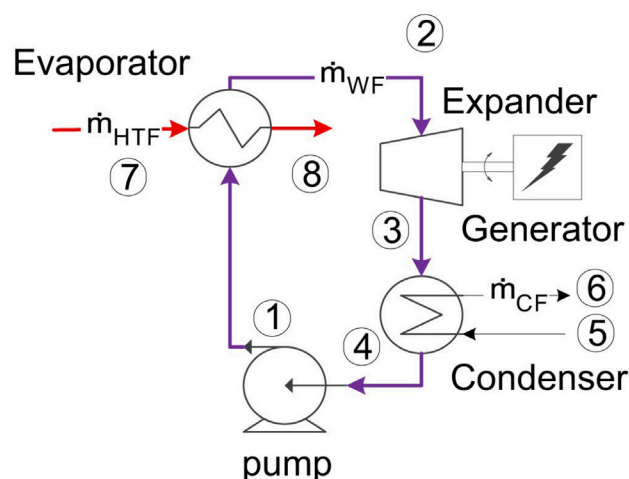
Fig. 1. A simple Rankine-cycle system configuration with key components and flows.
Source: Reprinted with permission from Lecompte et al. [80].
© 2015 Elsevier.

working-fluid property prediction *via* various equation-of-state models is also explored. Finally, the review is concluded with a discussion of the outlook of working-fluid design for ORC power systems, their impact on technology development in important energy applications, and current challenges and opportunities, along with promising future research directions.

2. Overview of organic Rankine cycle power systems

2.1. State-of-the-art

Rankine cycles are a well-known principle in power production today. In a Rankine cycle, water (*i.e.*, the working fluid) is evaporated in the evaporator. This evaporated working fluid then flows through an expander, effectively transforming heat into work. Subsequently, the working fluid condenses by rejecting thermal energy to a heat sink. Finally, a pump pressurises the working fluid, closing the loop. This cycle is often used with water in large-capacity thermal plants where the heat source comes either from combustion, nuclear fission, or other relatively high-temperature heat (> 300 °C) from, for example, solar sources. In Fig. 1, we show the main components, overall configuration and flows in a simple Rankine cycle system.

This cycle can also use other working fluids instead of water. Usually these are organic in nature, and the cycle is then referred to as an organic Rankine cycle (ORC), with the working fluid being typically a compound that exhibits its boiling point at lower temperatures than water. Throughout the article, when using the terms "ORC" (without any qualifier), or "simple ORC", we are referring to the cycle as illustrated in Fig. 1, either with or without superheating. We note that some authors use the term "basic ORC" equivalently, although to avoid confusion we avoid this terminology since it is sometimes used to indicate exclusively the cycle without superheat.

ORCs are hereby applicable as power-production cycles on lower-temperature ranges where the traditional vapour Rankine cycle is too inefficient or costly to operate. In Fig. 2, we show the operation range for typical ORCs based on the temperature of the heat source and the electrical power of the installation. The figure is divided into different regions: ocean thermal energy conversion (OTEC), micro combined heat and power (μCHP) systems, steam Rankine cycles and mainstream ORC systems. Mainstream ORC systems typically use waste heat, geothermal energy or heat from biomass combustion as the heat source. However, the applicability of ORC applications keeps extending. This is partly due to new cycle topologies but also due to the introduction of

Fig. 2. Heat-source temperature and power-rating application range for ORC structures [81].
Source: Reprinted with permission from Colonna et al. [82].
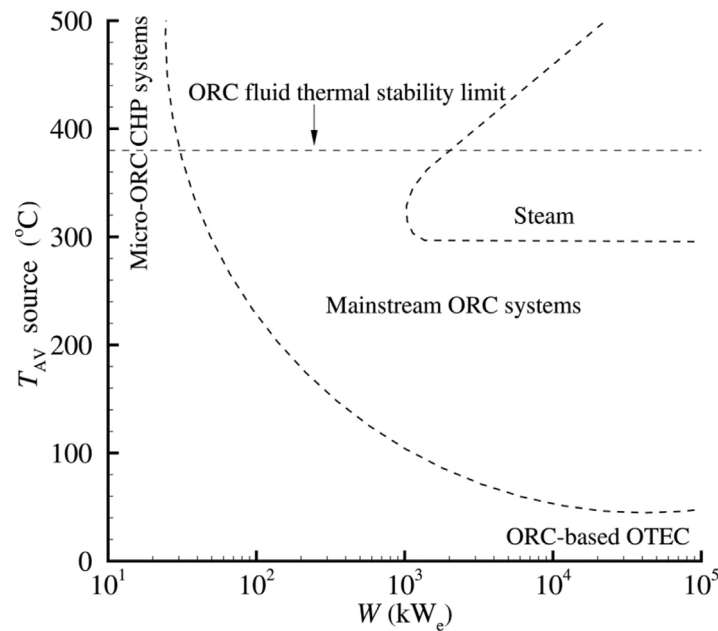© 2015 ASME.

new working fluids that, for example, extend the ORC fluid thermal stability limit to higher temperatures. It is important to note that ORC efficiency is significantly impacted when the power rating and/or heat source temperature decrease. The temperature impact follows from thermodynamic (Carnot efficiency) limitations, while size has an impact on the relative losses and investment potential for increased optimisation. Fig. 2 suggests that larger ORC systems with a higher power-rating can offset the detrimental effect of attempting to operate with reduced heat-source temperatures, and can remain cost-effective when used in lower temperature applications.

2.2. ORC market and potential

The ORC is a key technology in increasing the effective use of medium and low-temperature heat sources. The ORC can be applied to convert a wide variety of heat sources [83], but currently, it is primarily used in geothermal, waste-heat recovery (WHR), and biomass applications [84]. These three together form 99% of the installed ORC power. Other smaller utilised sources are waste-to-energy, solar, and ocean thermal energy. The Knowledge Center on Organic Rankine Cycle technology (KCORC) [85] performed market reports in 2016 and 2020, which showed that the installed power at the end of 2020 was 4.1 GW, of which 29% was installed in the last 4 years. Another 430 MW has been installed or is planned to be installed since December 2020 [84]. This indicates the clear growth of this technology, in particular for manufacturers of large (1 MW) ORC installations (ORMAT, Turboden, and EXERGY), which have all increased their installed capacity by around 40%–50% in the past four years [84]. Yet, also manufacturers of small ORC units have substantially increased their installed capacity.

In assessing the potential of this technology, we can consider the available global waste-heat resource that can be technically recovered. Waste heat has been found to account for over half of the global primary energy [86]. As such, waste heat alone was in 2012 globally estimated [87] to be around 68 PWh with a Carnot potential of 13 PWh. In particular, significant unutilised low-grade waste heat is rejected from industrial facilities to the environment [88,89]. This untapped resource has been found to amount to 15%–20% of the total industrial energy consumption in the EU, UK and USA [90–92].

Looking at the KCORC [85] reports, only a very small fraction of that potential is exploited. Economic considerations could affect the exploitation potential. When comparing the specific investment cost of ORC systems relative to other installations (*e.g.*, internal combustion engines, gas turbines, hydro, wind, or solar), the specific cost of an ORC should be around 2500–3500 Euro/kW to be economically viable [93] (2017). This only takes into account the revenue of the power output and no indirect costs are considered such as related to environmental impact and reliability. The investment cost for an ORC unit can be estimated around 2000–4000 Euro/kW [94] (2016), where the higher values are typically for smaller installations. Efforts should be taken to reduce the specific cost, especially for small-scale installations, and that research should include thermodynamic, economic, and technical aspects to be optimised [93]. Also the importance of the electricity cost from the grid should not be neglected, as was also found in case studies [95].

2.3. Selection of optimal working fluids

Working-fluid selection is an important and intrinsic part of ORC design. There are no *a priori* "best" working fluids for ORC applications because the choice of the optimal fluid depends on several design aspects which are application-dependent and do not concern only the plant energy performance. For instance, working-fluid characteristics also influence the safety and cost of the installation [96–99]. These are:

- Specific cost; this has a rather direct impact on the ORC unit cost, especially for large power capacity.
- Flammability; flammable fluids, such as hydrocarbons, are in use in ORC plants, but they induce additional safety complications and consequently increase the cost.
- Toxicity; toxic fluids can be used, but they bring with them extra safety measurements and costs.
- Material compatibility; the working fluid has to be compatible with all materials within the installation. This includes the metals and elastomer seals of the machines but also lubricating oil(s).
- Environmental impact; while there are many indexes that would need to be considered to enable a comprehensive environmental impact assessment [100], two indexes have been mainly used in

the published literature: the Ozone Depletion Potential (ODP) and the Global Warming Potential (GWP). The ODP is the amount of degradation a fluid causes to the ozone layer compared to CFC-11, which has a fixed ODP of 1. Similarly, the GWP gives a measure of the effect as a greenhouse gas relative to CO_2 over a time frame of 100 years.

- Thermal stability; the risk that working fluids will decompose to other chemical constituents. While this will have a direct effect on the original fluid thermodynamic and thermophysical properties, it can also degrade heat transfer, introduce non-condensable gasses, or lead to corrosion problems.

Working-fluid thermodynamic characteristics that are important for the cycle performance [96–99] are:

- Critical point; the critical point is important for multiple reasons. Firstly, it determines the type of cycle. If the critical pressure is above the maximum operating pressure, the cycle is subcritical, as shown in Fig. 1. When the critical pressure is above the maximum operating pressure, the cycle is transcritical, as explained later. The optimal critical temperature range is typically closely related to the temperature of the thermal source. In practice [99], the chosen critical temperature is often slightly larger than the targeted evaporation temperature in subcritical ORCs. As such, a better match with the heat transfer-fluid is achieved, resulting in a higher average temperature during heat addition and, therefore, higher thermal efficiency. Note that close to the critical point, the specific heat of vaporisation is small, leading to higher pump work [101].
- Dew-curve slope; a working fluid can be either defined as dry, isentropic, or wet depending on the slope of the saturation vapour-pressure curve on the $T–s$ diagram, i.e., $\xi = (\mathrm{d}s/\mathrm{d}T)_{x=1}$, where s is the specific entropy, T the temperature and x the vapour quality. A fluid is defined as 'dry' when $\xi > 0$, 'isentropic' when $\xi = 0$, and 'wet' when $\xi < 0$. A dry fluid is considered beneficial because droplets, which may impinge on turbine blades, cannot be formed along the expansion process as the fluid expands through a superheated-vapour region. However, for very dry fluids, the condenser load can become significantly high due to the high degree of superheating reached by the vapour at the end of the expansion process. It is noted, with respect to the above, that the fluid classification based on the dew-curve slope has been the traditional classification approach of pure working fluids, introduced by Tabor and Bronicki [102], and later Badr et al. [103]. In a more recent approach, Györke et al. [104] identifies limitations with this classification, and introduces a new categorisation approach comprising eight distinct fluid classes: ACZ, ACZM, AZCM, ANZCM, ANCZM, ANCMZ, ACNZM, ACNMZ. This new approach is useful as it further facilitates the identification of working fluids for ORCs.
- Density; a low density leads to high volume flow rates. This leads to higher pressure drops in the heat exchangers and a larger size of the expander, thus increasing the cost of the plant. At the same time, a low fluid density facilitates the realisation of turbomachines also in small power-capacity applications.
- Enthalpy of vaporisation; a high enthalpy of vaporisation is preferred as it increases the thermal efficiency due to 'carnotisation of the cycle' as more heat is added during evaporation [105,106]. However, other authors [107,108] say that low enthalpy of vaporisation is better. In this way the temperature profile of the working fluid matches better with the heat transfer-fluid and this effectively increases the second-law efficiency.
- Viscosity; a low viscosity is beneficial in achieving low frictional losses and promotes better heat transfer rates.
- Thermal conductivity; this must be high to achieve high heat-transfer rates per surface area.

- Melting temperature; the working fluid should never solidify within the ORC circuits. The melting temperature should thus be below the lowest possible ambient temperature.
- Condensing pressure; a condensing pressure above atmospheric is advisable to reduce the risk of infiltration of non-condensable gasses, which would lead to degradation of the system performance [109]. Another benefit is the reduction in expander price due to the smaller volumetric ratio.
- Evaporating pressure; a higher evaporating pressure results in higher component cost and more-stringent safety considerations.
- Boiling point; a lower boiling point allows the working fluid to evaporate from low-temperature heat sources.

The design of a cycle and choice of working fluid, which should be performed simultaneously, can be based on various figures of merit, depending on the application:

- Thermal efficiency [110,111]; the thermal efficiency is defined as the net output work divided by the input thermal energy [110]. The maximum thermal efficiency of any power cycle between two infinite thermal reservoirs at temperatures T_L (low) and T_H (high) is the Carnot efficiency, defined as $\eta_{carnot} = 1 - T_L/T_H$. For non-infinite reservoirs a logarithmic mean temperature can be used. The thermal efficiency is a common figure of merit for cycle design.
- Exergy efficiency [112] (also known as the second-law efficiency); This is defined as the net output power divided by the incoming exergy flow of the heat transfer-fluid. This efficiency is often used for low-grade heat-recovery applications because the thermal efficiency does not take into account the finite thermal capacity of the heat source.
- Cost-effectiveness; not only the thermodynamic efficiencies are important but the cost of the installation can influence the decision as well. It is possible to optimise the design based on a thermo-economic objective function, as in [45]. As an alternative, the ratio of the total heat-exchanger surface area to the net produced power is a good measurement for the cost per unit of power of the ORC unit [113]. This is not to been further substantiated against actual ORC prices.

A working fluid should be chosen considering the above figures of merit, given the chosen cycle configuration. There is a wide variety of possible working-fluid choices: chlorofluorocarbons (CFCs); hydrochlorofluorocarbons (HCFCs); hydrochlorofluoroolefin (HCFOs); hydrofluorocarbons (HFCs); hydrofluoroolefin (HFOs); siloxanes; and many others [114]. Some of these may no longer be used due to legislation. For example, due to the Montreal Protocol, 98% of ozone-depleting substances (ODS) have been phased out globally compared to 1990 levels. These regulations primarily imposed restrictions on the utilisations of CFCs and HCFCs. Nowadays, refrigerants with high GWP are in the process of being phased out. Depending on the country, there are different regulations, but the trend is to ban the use of fluids with GWP to 150 by 2030. Current GWP values are set at IPCC 4, but all refrigerants have been reassessed during IPCC 6 [114]. Refrigerants are also classified according to whether they can be found in nature or not. The natural refrigerants include ammonia, water, carbon dioxide, and hydrocarbons. They exhibit zero ODP and low GWP values and, in general, are compatible with elastomers of common use in industry. Another important benefit is that they do not contain chlorine or fluorine. Thus, they do not form aggressive acids when coming into contact with water, a common cause of system failure in plants operating with synthetic refrigerants [115].

Some refrigerants are actually mixtures of various refrigerants. For example, R410a is a specific mixture of R32 and R125. These mixtures can be azeotropic, showing no temperature glide during phase change, or zeotropic. In this case, a temperature glide is observed during phase change. This can be beneficial for a better temperature profile matching
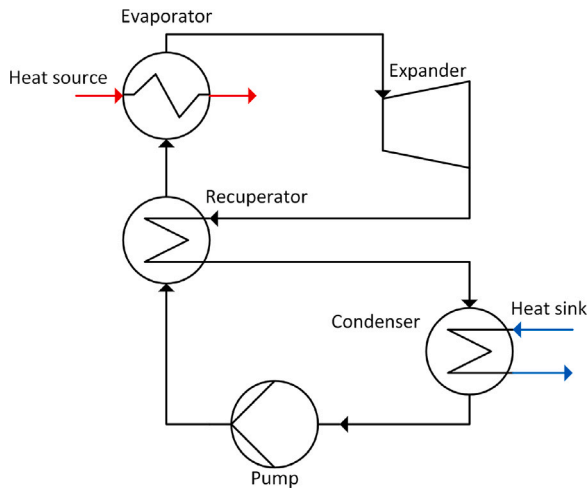
Fig. 3. Configuration of a recuperated ORC system.

with the heat source or sink. Changing the mixture percentage has an influence on the amount of temperature glide [116]. The mixture composition gives immense flexibility in the optimal selection of working fluids, therefore CAMD can be an important asset [117–119].

2.4. ORC architectures and operating conditions

In this section, different cycle configurations will be discussed and described. The simple ORC system, as shown in Fig. 1, is the first possible architecture, as also introduced in Section 2.1.

A first possible adaption is the addition of a recuperator (Fig. 3), whose purpose is to recover part of the thermal energy of the vapour after expansion to preheat the working fluid pumped to the evaporator. With respect to the simple ORC system, this results in a higher power output per unit of heat input, or a higher thermal efficiency [110]. The use of a recuperator does require that the vapour exhibit some degree of superheating at the expander outlet, meaning that dry fluids are necessary. It is important to note that the additional heat exchanger also increases the installation cost and the overall pressure drop in the working-fluid loop.

Another possibility is to cascade ORC systems, as shown in Fig. 4, where a two-stage ORC system is presented. The heat exchanger that works as an evaporator for the bottom cycle functions also as a condenser for the topping cycle. The expander design can be further optimised for each working-fluid loop according to the selected temperature and pressure ranges. Selection of the optimal combination of working fluids could be achieved with CAMD. It is also important to note that the thermal input is fully determined by the topping unit, while the thermal input in the cascaded cycles depends on the thermal energy rejected during condensation in the working-fluid loops above [120,121].

The addition of turbine bleeding and direct-contact heat exchangers (Fig. 5) leads to so-called regenerative ORC system configurations. Turbine bleeding refers to the process of extracting a portion of the steam or gas from a turbine during operation. The preheating effect achieved is similar to that in recuperator cycles. The difference, however, lies in the type of heat exchanger used to preheat the liquid leaving the condenser and the source of thermal energy used for this purpose. It has been shown that regenerative cycles have higher thermal efficiencies than the simple ORC system, and that the irreversibilities are smaller, resulting in higher second-law efficiencies [122]. However, the authors also note that this improvement heavily depends on the used working fluid; the improvements in efficiency were negligible for some working fluids, which would not justify the additional component
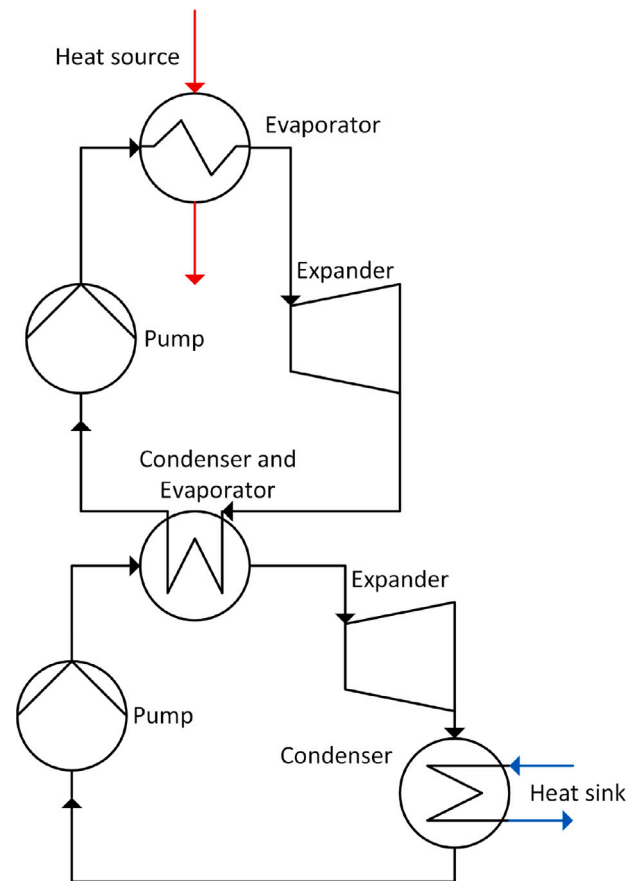
Fig. 4. Configuration of a cascade ORC system.

cost in practice. Furthermore, any performance improvements must more than compensate for the added capital investment and operating/maintenance costs. Therefore, these substantial modifications are typically reserved for larger-scale systems, for which the implementation cost is lower relative to the performance benefits. In addition, in many low-temperature applications, such as geothermal, waste or other renewable heat sources, it will not result in a higher output power or fuel reduction.

Another possibility is to combine different cycle adaptations. The regenerative cycle with a recuperator is a common example of such a combination.

Another way to reduce the irreversibilities associated with heat transfer is to realise a cycle with multiple pressure levels, as shown in Fig. 6. Here, the thermal energy is added to the cycle through two evaporators operating at two different pressure levels.

In Fig. 7 we illustrate an additional configuration known as the organic flash cycle (OFC). With respect to the simple ORC system configuration, a flash tank is installed downstream of the heat exchanger, where the working fluid is heated up. The reason is that no working-fluid evaporation occurs during the heat-transfer process. The dry vapour needed to power the turbine is then generated in the flash tank, which introduces a pressure drop causing a fraction of the working fluid to evaporate. The same tank performs the function of separating the resulting two-phase flow. The saturated vapour is routed to the expander, while the saturated liquid is immediately routed to the condenser over a throttling valve. The advantage of this cycle configuration is the good temperature profile match with the heat source if the working fluid is well chosen. A drawback, instead, is that saturated vapour is fed into the turbine. This means that for wet working fluids, the vapour quality diminishes along the expansion process. This has to be accounted for
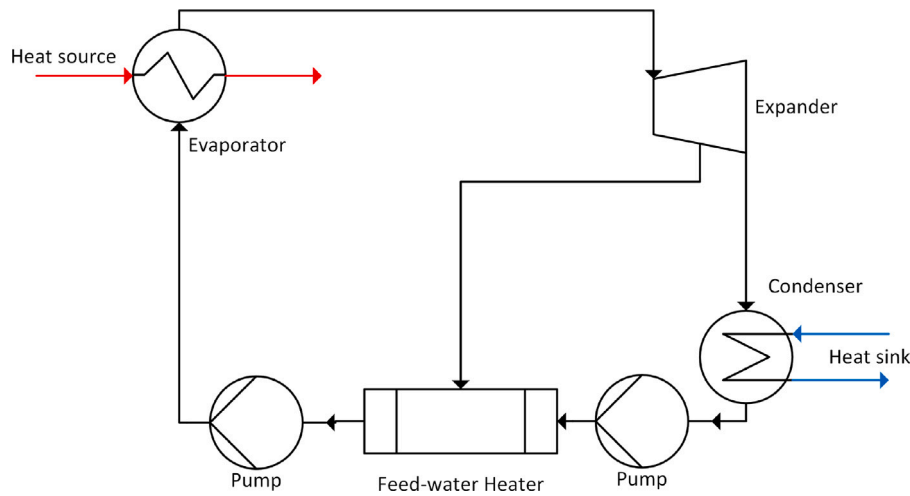
Fig. 5. Configuration of a regenerative ORC system.
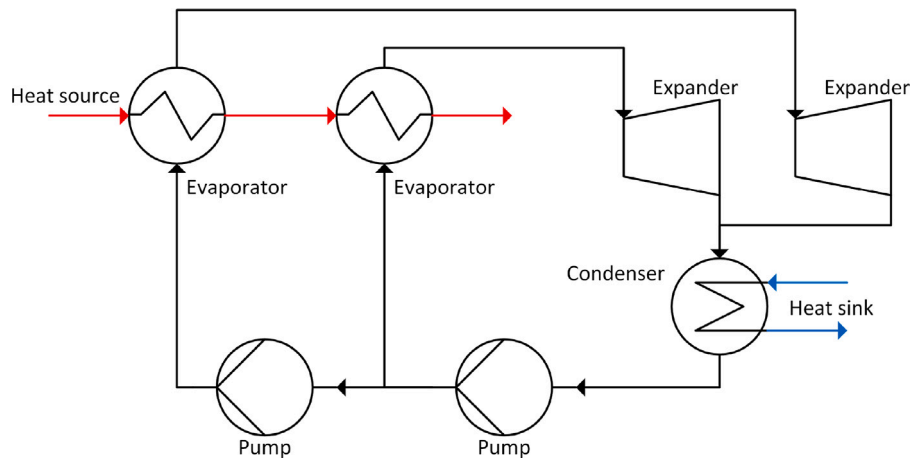
Fig. 6. Configuration of an ORC system with two distinct pressure levels.

in the expander design, which increases the production cost. Another important drawback are the associated throttling irreversibilities over the expansion valves. In Fig. 7, we show only the most simple OFC system configuration. Different variations are possible, for instance, by including in the system multiple flash tanks, phase separators, and expanders to split the corresponding thermodynamic transformations over different pressure levels.

There are also other ways to reduce the irreversibilities associated with heat transfer. The cycle configurations discussed in the following share the same configuration as the simple ORC (Fig. 1), but they differ in their operating principles. Firstly, in the trilateral cycle (TLC), the working fluid is heated up only to saturated-liquid conditions before it is fed to the expander. The TLC operating principle is thus similar to that of the OFC presented earlier. The difference lies in the fact that no flash tank is adopted: the fluid directly expands from a liquid state in the expander. The temperature-profile matching in the heat exchanger interconnected with the thermal source, also called the primary heat exchanger, results in higher second-law efficiencies of the TLC compared to the simple ORC [17]. Nevertheless, the overall thermal efficiency of the TLC tends to be lower due to the relatively low critical temperature of organic fluids [123]. This makes the TLC more applicable as a bottoming cycle. A bottoming cycle utilises waste heat from a primary cycle, leading to increased power output. The bottoming cycle therefore operates at lower temperatures then the top cycle in the cascade. Another drawback of this solution is that the fluid volume flow rate drastically increases compared to the simple
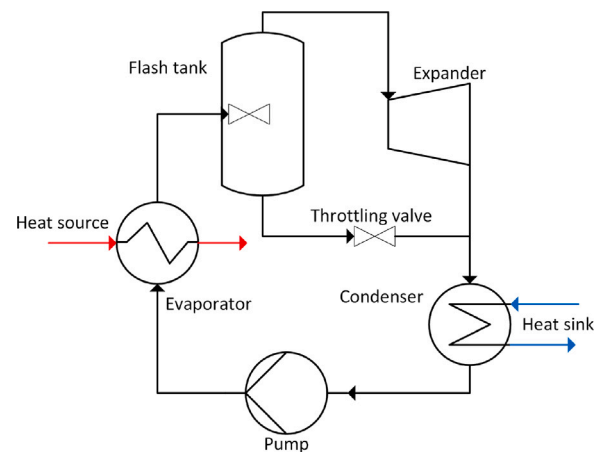
Fig. 7. Configuration of an organic flash cycle system.

ORC. A second option is to partially evaporate the working fluid in the primary heat exchanger, realising a cycle known as the partially evaporating ORC (PEORC). The achievable second-law efficiency and specific volume flow rate are somewhere between those of a simple ORC and a TLC. It has been shown [124] that the PEORC can increase

the net power output of the system compared to the TLC. However, both the TLC and PEORC do require an expander capable of handling two-phase flows, and this technology is not readily available.

Lastly, it is possible to increase the maximum pressure of the cycle above the fluid critical pressure. This results in a transcritical cycle. Because the working-fluid heating happens in supercritical conditions, the temperature profile can be matched to the heat source, depending on the working fluid. Similarly to the TLC, the transcritical cycle could show lower thermal efficiencies (due to high pumping power) in favour of increased heat addition to the cycle and reduced irreversibilities (neglecting possible increased pressure drop) in the vapour generator [125]. An interesting working fluid for transcritical cycles is carbon dioxide [126]. Due to the low critical temperature (31 ° C), the supercritical state can already be achieved for low temperature heat sources. Because it is a natural refrigerant, it also has a small environmental impact as mentioned before.

A final adaptation is to use zeotropic mixtures, resulting in non-isothermal phase changes depending on the mixture composition. These fluids can be used in all topologies and configurations mentioned earlier. Their benefit is that their temperature profiles during phase change can be matched to the heat transfer-fluid or heat sink, reducing the irreversibilities and thus increasing the plant efficiency. It was shown [19] that the best second-law efficiencies for zeotropic simple ORC cycles are obtained by matching the temperature profiles of the working fluid and the heat sink. Literature about zeotropic refrigerants combined with various cycle architectures is scarce. In some studies [19,127] it has been shown that zeotropic mixtures do improve the exergy efficiency of supercritical cycles and cycles with a recuperator.

As can be seen from the above brief review, many cycle configurations and operating principles exist. The system performance does not depend on only the cycle configuration and heat-source characteristics, but also the chosen working medium and its composition in the case of a zeotropic mixture [128]. This means that choosing an optimal design is no simple feat, and the assistance of CAMD for working-fluid design and selection is a much-welcome tool.

2.5. Off-design operation

Cycles are typically designed around their nominal working conditions. However, they should still operate in off-design conditions as the heat source or the heat sink are frequently transient in nature. Furthermore, due to component selection based on availability and cost, the actual operation can deviate from the original design conditions. Part-load operation, meaning that the work output is modulated according to a set-point, is less common. ORCs typically operate at full power, extracting the maximum work out of a heat transfer-fluid. The temperature and mass flow rates of these flows have a significant influence on the system performance [129]. The mass flow rate of the heat transfer-fluid is a key variable in net power generation. However, contrary to expectation, the plant efficiency could decrease due to the faster increase of condensing pressure resulting from increasing heat-source flow rate and temperature [130]. A key component in off-design cycle performance is the expander, as its isentropic efficiency and filling factor vary with suction pressure and temperature and with discharge pressure, influencing the system thermal efficiency [131]. The filling factor is defined as the ratio of the actual volume flow rate of gas drawn into expander to the theoretical volume flow rate based on its working chamber geometry and the expander speed. A low filling factor is detrimental as the expander is not utilised effectively. However, a high filling factor does not necessarily mean that a higher power output is achieved. It is possible that due to leakage paths the flow bypasses much of the expansion process.

In literature, three methods are applied for simulating off-design conditions [132]: a constant-efficiency method, a polynomial regression method, and a semi-empirical method. The constant-efficiency method, as its name suggests, is based on an assumption of constant component efficiencies and filling factors independent of the operational design conditions. In the polynomial regression method, one adapts the component efficiencies and filling factors to the operating conditions by means of a polynomial function. A second-order multivariate polynomial [132] is frequently used. Lastly, in the semi-empirical method, one models the components by means of physically-based equations. On a component level, the discrepancies with experimental data of a polynomial regression method and a semi-empirical method can give comparable results. The coupling of polynomial regression methods could show unreliability on the system level, while this is not the case for a semi-empirical method [132]. Zeotropic mixtures are also interesting for off-design conditions, even though not a lot of literature covers this topic. However, it was shown that a zeotropic ORC outperforms a simple ORC in off-design conditions [133]. The authors investigated a composition-adjustable ORC, where the zeotropic mixture can be altered by adding or removing one of the two components online. They concluded that there is an increase in performance, but that it is not worth the extra investment cost and cycle complexity.

3. Computer-aided design of ORC power systems

3.1. Overview of fluid and ORC design problem challenges

By definition, the goal of CAMD is to determine the chemical structures of molecules that optimise a set of properties that represent desired performance targets [56]. Both parts of this definition, i.e., the "chemical structures" and the "properties", have very significant effects on the working-fluid and ORC design procedures and their performance [134].

In conventional approaches, the working fluid in an ORC system is selected from a set of pre-determined molecular structures that usually results from prior know-how about the suitability of some fluids for the given process [135,136]. Such fluids are hereafter described as conventional working fluids. This is very limiting in view of the vast number of molecular structures (billions) [137] that could be considered as ORC working-fluid options. Such an approach prohibits the discovery of novel molecular structures that may be worth synthesising, or of molecular structures that exist and are commercially available but have never before been used in ORCs and may therefore be considered novel ORC working fluid options [98]. In CAMD, the molecular structures result from the combination of molecular fragments that could be functional groups, atoms, or bonds [138]. This is because the properties of a molecule can be estimated through contributions from its fragments [139]. Systematic approaches are often used that facilitate the evaluation of combinations of these molecular fragments until a chemical composition is identified that exhibits the highest performance according to the selected figures of merit. The advantage of this approach is that vast numbers of molecular structures may be attained by forming combinations from a finite set of less than 200 molecular fragments [140]. This enables the discovery of novel molecular structures. Furthermore, there is no need to derive a database of pre-existing molecules, hence avoiding the arbitrary exclusion of molecular structures that could exhibit high performance when used in an ORC. The immense number of combinations makes the fluid-design problem computationally challenging, even for pure working fluids.

These computational requirements have not prevented researchers from targeting the design of fluid mixtures, which enable higher exergetic performance than pure fluids for certain ORC applications [21]. In the context of CAMD, the identification of the desired ORC mixture requires the simultaneous determination of (i) the number of pure components that will comprise the mixture, (ii) the chemical composition of each pure component, and (iii) the concentration of each component in the mixture [141]. It is clear that this induces additional combinatorial complexity, which has been addressed through various approaches over the years for the design of both pure and mixed working fluids [134]. Optimisation algorithms appear to be the most efficient among the

existing approaches, as the synthesis of the chemical structure(s) is systematically guided by the algorithmic operations in order to avoid the exhaustive enumeration of all options [142].

The above are major requirements that pertain to the identification of appropriate ORC working fluids with respect to their chemical structure. The determination and calculation of the "desired properties" that may lead to the appropriate working fluids raise additional, significant challenges. The development of CAMD has been based on the advent of group contribution (GC) methods [65]. These provide quantitative structure–activity relationships (QSPRs) that enable the prediction of the working-fluid properties based on their molecular-fragment constituents. The original CAMD implementation in ORCs [98] was based on GC QSPRs [143] for the prediction of pure-component properties at standard conditions [139]. Such QSPRs can be used as input to cubic EoS to predict the vapour–liquid behaviour of mixtures as well as enthalpies and other important properties. In recent years, advanced EoS have also been developed that introduce physical molecular characteristics in the prediction of mixture properties, hence avoiding the use of QSPRs; these include SAFT [66,67] and its many variants, including PC-SAFT [144], SAFT-VR Mie [145] and SAFT-γ Mie [79]. In the case of PC-SAFT, the CAMD problem formulation was further changed into one where discrete molecular structure decisions were replaced by continuous targeting of molecules [57]. All these developments are important and have been used in ORC molecular or molecular-and-process design applications [51,134,146]. Depending on the performance metric against which the ORC system is optimised, different "desired properties" are of interest. To determine the relevant properties as well as their search directions, the relationships between economic and thermodynamic performance criteria commonly employed in ORC design and working-fluid properties have been developed [147]. In addition to core criteria related to thermodynamic efficiency and economics, additional criteria related to safety and environmental impacts of working fluids, such as toxicity or GWP, have been considered [98].

The advantage of using molecular or mixture properties as targets in CAMD is that the need to develop and incorporate an ORC model is avoided, with beneficial effects on the ease of implementation and computational complexity. Such approaches have succeeded in identifying efficient working fluids [98,137], as shown in subsequent studies that performed an exhaustive evaluation of millions of working-fluid structures using ORC model simulations [148] or thermodynamic analysis of the atomic chemistries of the derived fluids [149]. However, as the working fluids are inherent components of the ORC system, their design or selection procedure should account for the prevailing ORC operating conditions and equipment characteristics in order to evaluate the economic and environmental behaviour of the system in which they will be used. Depending on the level of detail of the employed ORC model, it is possible to capture the equipment interactions at the ORC system level, the dynamics of the processes in view of disturbances, the changes in the temperature of the thermal energy sources and sinks, or even local heat and mass transfer phenomena. All these characteristics may affect the selection of the working fluid, putting emphasis on the specific application needs and eventually expediting the development and delivery of such systems. Clearly, the simultaneous evaluation of the widest possible set of fluid and ORC system options with models of high resolution, both in space and time, would be highly desirable in order to attain designs that are both optimum and realistic prior to their practical implementation. However, such a formulation would result in an intractable computational problem. The need to address these challenges has fostered the development of various methods that:

(a) Consider the design or selection of single fluids or mixtures[1];

(b) Implement exhaustive enumeration of all design options or employ optimisation algorithms, considering single or multiple criteria;

(c) Integrate ORC models either as part or after the design or selection of fluids;

(d) Consider ORC equipment models of varying resolutions or ORC and heat source/sink configurations of varying structures;

(e) Account for the uncertainties in the property prediction or in the ORC equipment models;

(f) Propose designs considering steady-state or off-design operation.

To this end, important approaches have been developed that implement CAMD (*i.e.*, the determination of molecular structures of ORC working fluids) considering some of the above features. These approaches will be discussed in Section 5. In the current section, we will address how the above considerations have been accounted for as part of fluid-selection approaches. The latter is not without significant challenges. For example, the simultaneous mixture-selection and process-design problem requires the use of efficient optimisation formulations and algorithms to attain high-quality designs, whereas the consideration of high-resolution models in fluid selection requires very intense computations. In all the above areas, there are important fluid-selection and ORC-design contributions that need to be discussed in order to highlight the following:

- Opportunities and challenges in future research efforts, as existing CAMD approaches will move to integrate additional features;
- The features of the different methods and models, as prerequisites for the understanding of the CAMD methods in Section 5;
- The benefits of CAMD over fluid selection approaches.

With respect to points (a), (b), (c), in this section, we review works that include mixture-selection problems, using either single- or multi-objective optimisation algorithms. The focus is on the most-advanced approaches that exhibit interesting methodological insights. The results of straightforward implementations of such approaches, or of approaches that employ either single or mixed fluids in an exhaustive enumeration of options and eventually present mainly technological insights with respect to ORC operation, are not within the scope of this section. The selection of mixtures is more challenging than that of pure fluids because of the higher combinatorial complexity (mixture concentration or composition are additional design variables) but also because the non-ideal phase-change behaviour of mixtures introduces numerical challenges. These features often result in different, non-trivial optimisation approaches in order to address the increased computational effort. In points (d), (e), and (f), we are covering contributions with either pure or mixed fluids, exhaustive enumeration, or optimisation approaches. These points include considerably fewer works and represent directions for future developments.

3.2. Mixture selection using optimisation algorithms

In this section, we present approaches where the concentration of mixtures comprising fluids of pre-specified structures, or the mixture composition itself (*i.e.*, the type and combination of pre-specified fluid structures that comprise the mixture), are optimisation variables, together with the ORC design parameters. The considered ORC configurations are mainly of the simple or of the recuperated type, whereas in a few cases, the ORC extracts heat or provides power to more-extensive process systems. The reviewed studies include single-objective (SOO) and muti-objective optimisation (MOO) formulations, which integrate not only models for thermodynamic-cycle calculations but also models for preliminary sizing of the ORC components, such as heat exchangers and expanders. Within this review we aim to highlight key features of the presented algorithms or design approaches in a sequence of increasing complexity in terms of the employed models or optimisation formulations. Key features of the reviewed works are summarised in Table 1

---

[1] The mixture-selection problem refers to the determination of the optimum number of components and/or concentration of a mixed fluid, using an initial set of pure components with pre-specified chemical structures. The mixture-design problem includes the determination of the chemical structure of at least one of the components.

Table 1

Overview of key features presented in Section 3.2 (details available in Table A.1, in the Appendix).

Work context	Categories	Reference (s)
Mixture formulation approach	Pre-specified mixture compositions	[19,150–165]
	Mixtures resulting from combinations of pure components	[166–171]
Optimisation problem formulation	Single objective optimisation (SOO)	[19,150–157,166–170]
	Multi-objective optimisation (MOO)	[158–165,171]
Optimisation algorithm	Meta-heuristic (PSO, GA, SA, other evolutionary approach)	[152–154,156–162,164–167]
	Deterministic	[19,151,163,168,169,171]
	Both	[170]
	Other software specific routine	[150,155]

and presented in more detail in Table A.1, in Appendix. Table A.1 contains information about the number and type of the considered working fluids, the optimisation problem formulation (*i.e.*, MOO or SOO and objective functions used), the employed optimisation algorithm, and the specifics of the design variables used during optimisation.

3.2.1. Pre-specified mixture compositions

Angelino and Colonna [150] investigated a ternary mixture with pre-specified concentration, but it is worth mentioning because it was one of the first studies incorporating an optimisation approach for the ORC conceptual design. The optimisation enabled the identification of important trade-offs between plant cooling power consumption and the air-cooled condenser surface area.

Chys et al. [151] investigated the use of 13 mixtures in a recuperated ORC system for low-to-medium thermal-source temperatures. They considered both binary and ternary mixtures, and they performed the optimisation of the cycle parameters for every mixture. They used a deterministic, non-linear programming algorithm (NLP). The cycle was optimised for each binary mixture separately, and a third component was added afterwards in the tertiary mixtures. In addition to the optimisation, they performed a parametric evaluation of the thermal efficiency and the net generated electricity of the optimum solutions. The authors noted that the use of mixtures may lead to fractionation (a large amount of one component in the liquid phase and a large amount of the other in the vapour phase); mixtures that may exhibit fractionation in the heat exchangers should be avoided. This is because in a case of leakage the mixture concentration would change very fast, with detrimental effects on system performance. This constraint is commonly overlooked in current studies dealing with the assessment of fluid mixtures for ORC applications. It is also recommended to avoid linear interpolation of pure-fluid heat-transfer coefficients as a method for mixture heat-transfer coefficient prediction, as the latter is often smaller than what is predicted from linear interpolation.

Victor et al. [152] proposed the optimisation of the concentration of pre-specified working fluids for a simple ORC system, using simulated annealing (SA) as the optimisation algorithm. The concentration of the pre-specified mixture compositions was the optimisation parameter.

Lecompte et al. [19] optimised the ORC operating conditions and mixture concentration for a set of binary fluids with pre-specified fluid structures. After attaining the optimum results for given design conditions, a parametric sensitivity analysis was performed where the design variables were re-optimised for variable operating conditions and design assumptions. These included varying the heat-source temperature, the pinch-point temperature difference, and the glide slope of the cooling fluid. Based on the definition provided by the authors, the term pinch-point temperature difference refers to the temperature of the heat carrier at the point of minimum temperature difference between working fluid and heat carrier.

Garg and Orosz [153] used particle swarm optimisation (PSO) to optimise the concentration of 10 binary mixtures of pre-specified components, together with several ORC operating parameters and the condenser area. The binary mixtures resulted from shortlisting and combining five pure components that exhibited optimum performance

when adopted as working fluids of the ORC system. The optimisation was performed for all the binary mixtures considering a fixed power capacity of the plant of 5 kW and a wide heat-source temperature range.

Kolahi et al. [154] investigated six binary mixtures of pre-specified compositions for the optimisation of an ORC in a geothermal binary flash cycle. Each mixture was evaluated, optimising the highest and lowest ORC temperatures in their entire concentration range with a coarse step change of 10 %. At the optimum ORC design solution, the authors selected the concentration range where the mixtures exhibited their highest performance in terms of power output, thermal efficiency, exergy destruction, and exergy efficiency. In a subsequent optimisation step, the concentration was treated as a continuous parameter, together with the operating ORC parameters, to find the overall optimum design of the ORC unit.

The above studies included thermodynamic models of the ORC, which mainly consist of mass and energy balances. The calculation of heat-transfer areas requires models for heat-exchanger (HEX) sizing. A few such studies that are based on SOO formulations are reported below. MOO fluid-mixture selection and ORC design approaches without or with HEX sizing models are reported subsequently. This classification is performed here to highlight that some works include more challenging optimisation problems due to the need for HEX sizing. Details regarding the modelling and the types of HEX are reported in Section 3.4.2.

Heberle and Brüggemann [155] evaluated several mixtures and fluids in an ORC system at various temperatures within the range 80–180 °C. The authors first identified the optimum operating conditions and fluid concentrations of the cycle using the second-law efficiency as an indicator. For a few selected highly performing mixtures, the authors performed cycle simulations using a model for the heat exchangers that included correlations for heat transfer.

Wang et al. [156] determined the concentration of several binary mixtures of pre-specified concentrations through optimisation of a simple ORC. The goal was to evaluate the ORC performance of each mixture considering different criteria, including the cycle network output with or without leakage and the carbon footprint of the cycle. The ORC model included the calculation of the evaporator area. A carbon-footprint model was employed to calculate the emissions during cycle construction, operation, and decommissioning (including disposal and recycling of materials and working fluids). A leakage model was used to account for the leak rate of the fluid and the operation of the cycle with different amounts of the working fluid at different time instants. Equilibrium models and correlations were used for the leakage and carbon-footprint calculations, respectively. The PSO algorithm was used for optimisation, implemented for all fluids considering one of the three different criteria in each case. In this study the authors introduced unconventional criteria related to the environmental performance of the cycle, which should be accounted for during mixture selection or design.

Han et al. [157] investigated the performance of binary mixtures of pre-specified compositions in an ORC system that was part of a geothermal flash cycle and a proton-exchange membrane (PEM) electrolyser that used the ORC power output for the production of hydrogen. In the

optimisation, the authors aimed to maximise the ORC power output using the high and low cycle temperatures and binary-mixture concentration (mass fraction of one component) as optimisation variables. The PSO algorithm was implemented for each binary mixture. Through this study the authors showed that working-fluid selection impacts the design of the entire system where an ORC is used.

MOO formulations include the work of Feng et al. [158], who investigated the performance of a binary mixture in a simple ORC system, considering simultaneously the optimisation of the mixture concentration and the ORC operating conditions. A MOO genetic algorithm (GA) was used to derive Pareto-optimum solutions that simultaneously maximised the exergetic efficiency and minimised the levelised energy cost of the cycle. The authors initially implemented the optimisation considering four different cases of evaporating and condensing temperature values. Alternatives that had the shortest distance from the ideal solution were selected using the technique for order preference by similarity to ideal situation (TOPSIS) [172]. For the optimum mixture concentration and the two pure components of the mixture, the authors fitted polynomials of the levelised energy costs as a function of exergetic efficiency for each model. They then compared the performance of pure and mixed fluids and found that the performance of the mixture is overcome by the pure fluids in some of the evaporating and condensing temperatures explored.

In a follow-up study, Feng et al. [159] used the same optimisation approach to evaluate the performance of a pentane-R245fa mixture. In addition to the TOPSIS technique to select the most favourable options from the generated Pareto front, they used the Shannon entropy technique [173] and the linear programming technique for multi-dimensional analysis of preference (LINMAP) [174]. The authors found that TOPSIS was the most efficient of the three. Finally, Tiwari et al. [160] investigated four mixtures using GA in a straightforward MOO formulation, deriving useful technical insights from the Pareto fronts.

In the case of MOO formulations, studies that address the sizing of heat exchangers also exist. Andreasen et al. [161] used an ORC model considering heat-transfer features in the heat exchangers to assess the performance of three fluids, including one mixture of pre-specified composition and concentration, separately. Although in this work the mixture concentration and composition are pre-specified, it has some interesting features. MOO was used to consider 11 cycle parameters as design variables, including parameters pertaining to the internals of the boiler and of the condenser (*i.e.*, number of tubes, inner tube diameter, and baffle spacing). The optimisation procedure was also interesting, as the authors performed the calculations following a sequence that included simulation without considering pressure losses, design of the heat exchangers, and simulation with pressure losses considered to facilitate the computational effort in view of the rigorous heat-exchange models. The sequence was repeated in every iteration of the GA. An unusually large population number of 30000 individuals was used, possibly to address the multiple design parameters, several of which are continuous.

Oyewunmi and Markides [162] optimised a simple ORC system configuration for two mixtures of pre-specified composition, where predictions were performed using SAFT-VR. This is an important EoS, as discussed in subsequent sections. An NLP algorithm was used for optimisation. The cycle was optimised for all mixture concentrations, including the pure-component cases, in 10% intervals. The authors initially used a single objective (net power output), whereas an MOO implementation was further used (equipment cost), and the Pareto fronts were presented.

Noriega Sanchez et al. [163] considered 28 mixtures of pre-defined composition that were evaluated through an ORC system. The sizing of the heat exchangers was performed using the logarithmic-mean temperature-difference method (LMTD). Further discretisation was performed of the pressure difference across the turbine in order to evaluate the vapour quality and to ensure that no liquid will be formed, which

usually results in corrosion. The mixture concentration was one of the optimisation variables, along with the evaporation pressure, the condensation temperature, and the minimum temperature difference approach in the evaporator. The net power output, the second-law efficiency, and the size of the heat exchangers (represented as global conductance-UA values) were the objective functions. The NSGA-II algorithm was implemented using a large population and executed several times. The repeated executions revealed that for the selected algorithmic parameters, the Pareto front changed insignificantly.

Nasir et al. [164] investigated a case of an ORC system that was combined with a vapour-compression cycle (VCC), either using separate condensers or using a shared condenser. The authors investigated single working fluids for both the ORC and the VCC, but they tested 12 different combinations, together with the optimisation of both cycles. The latter were optimised in terms of 11 operating parameters, so the problem was challenging due to the increased model size (ORC and VCC) and the number of design variables.

Rodriguez-Sotomonte et al. [165] investigated the performance of an ORC in power and cooling cogeneration plant, considering a few different fluids. An interesting feature of this work was that the authors determined the number of individuals used in the GA through a 3k factorial design of the design variables. The LINMAP approach was used to select designs from the Pareto fronts.

The models used to size the heat exchangers during optimisation have significant differences in the employed heat transfer correlations. In most of them correlations are used that include the Nusselt number but use different overall forms of the correlations (e.g., with different coefficients). Furthermore, some works model only few of the heat transfer phenomena, whereas other works provide more comprehensive models. For example, Wang et al. [156] use a formula only for the single- phase heat transfer in the shell side, whereas Heberle and Bruggemann [155] additionally provide correlations for the evaporation of pure working fluids on a plain tube considering pool boiling and for the condensation of a pure working fluid in plain tubes. In addition to using different models, the optimisation studies also often use different objective functions (see Table A.1 in Appendix). Therefore, the results are only valid for the specific heat exchangers under investigation in each case and the specific assumptions made. The effects of different heat transfer correlations in heat exchanger model predictions and ORC performance are further discussed in Section 3.4.3.

3.2.2. Derivation of mixtures from pure components

In this section, we discuss studies in which the mixture composition (number and type of fluids in the mixture) and concentration (amount of components in the mixture) are design variables. In all cases, the mixture compositions are derived from a list of pre-specified pure components.

Micheli et al. [166] investigated various siloxane mixtures in a regenerative ORC system, aiming to identify the optimum mixture composition and concentration. An initial set of 11 pure components was searched freely by an evolutionary algorithm. As the optimisation search proceeded, components that exhibited zero concentration were gradually excluded until, eventually, 11 binary and five ternary mixtures were shortlisted as promising options. The off-design assessment was also performed for a randomly selected pure component. In this case, the turbine was modelled using the Stodola ellipse method [175], allowing both the efficiency and expansion ratio to vary with the load. The evaporator and condenser pressures were the design variables.

Andreasen et al. [167] identified the optimum mixture composition, concentration, and ORC operating conditions, in a work where pre-specified pure components were combined into binary mixtures by the optimisation algorithm. Mixtures of up to five components of pre-specified compositions and concentrations were also included in the database and compared with the designed binary mixtures. Optimisation results for the ORC were reported for each mixture (for either the designed binary options or the pre-specified options). When the binary

mixture composition and concentration were optimisation variables, the mixture composition identified in up to 500 generations of the GA was kept fixed for another 200 generations, where the concentration, the turbine inlet state, and the hot-fluid outlet temperature were optimised. This approach was followed because, as noted, the optimum results varied at different executions of the GA. To facilitate the search, when a mixture exhibited lower performance than that of its pure-fluid constituents, it was removed from the list. The ORC model accounted for both subcritical and supercritical conditions. The discretisation of the boiler (pre-heater, evaporator, and superheater) was coarse for subcritical pressures, as the pinch point could be easily located at the saturated-liquid point. When the pressure of the resulting design solution was close to or higher than supercritical, the optimisation of the cycle and the mixture concentration was performed again using a higher number of segments in the boiler to improve the accuracy of the pinch point prediction.

Molina-Thierry and Flores-Tlacuahuac [168] proposed the simultaneous blend (*i.e.*, mixture) selection and ORC system design in an NLP formulation, testing several different objective functions in independent SOO problems. The number of working fluids participating in the mixture, the type of working fluids that formed the mixture, and the mixture concentration were optimised together with the ORC operating conditions. The working fluids that were used to attain mixture combinations were selected from a pre-specified set of 3, 11 or 6 pure fluids in the performed case studies. The results in the different objective functions indicated mainly binary or ternary mixtures as optimum solutions.

Satanphol et al. [169] developed a mixture-selection and ORC-design approach, where the mixtures were generated and selected from a pool of 24 pure components. A maximum of six components were allowed in the mixture, and the optimisation algorithm freely varied the mass flow rate of each component, together with the ORC design variables. Each time that the mass flow rate of one component was reduced to zero, that component was replaced with another one from the pool. Two quaternary mixtures were shortlisted as optimum, and their pure constituents were used to generate binary and ternary mixtures. Indeed, it was observed that at least one ternary mixture could outperform the quaternary mixture from which it was generated. The ORC model was not based on the simultaneous solution of all the equations, as in Molina-Thierry and Flores-Tlacuahuac [168], but in a tear-stream approach. Internally to the sequentially quadratic programming (SQP) optimisation algorithm used here, two loops were used to ensure the ORC model convergence. These included a procedure for the determination of the upper bound on the evaporator pressure to avoid the assumption of setting it to the critical temperature of the pure constituent with the highest value. The procedure further included a gradual increase of the evaporation temperature until convergence could not be achieved in the corresponding flash.

Lee and Mitsos [170] developed a mixture selection and ORC optimisation approach in order to recover the maximum exergy from an LNG stream. A total of 1771 mixtures of up to three components were derived from a pool of 23 pure components. The presence or not of a pure component in the mixture was represented through binary variables, whereas three continuous variables represented the component concentrations in the mixture and the condensation pressure. The condenser was discretised in 100 segments. The area minimisation between the hot- and cold-temperature curves was used as the objective function instead of minimising the exergy loss because the entropy calculations were avoided, and the problem could be solved faster. A hybrid algorithm (Fig. 8) was used comprising a GA to initially handle the MINLP problem formulation. The mixture composition attained from the GA was then used in a subsequent NLP formulation which included the two mixture concentrations and the condenser pressure as design variables. This was done in order to improve the solution attained from the GA with respect to the continuous variables. It was noted that multiple executions of the GA resulted in the same solution

with respect to the integer variables (*i.e.*, the mixture composition). The NLP was decomposed into several subproblems where constraints were added gradually to provide good starting points for the subsequent subproblem, until the entire problem was solved. Specific focus was placed on avoiding trivial solutions of the cubic EoS. BARON [176] was used in the NLP stage. The authors noted that although the NLP methodology solved the problem globally, the decomposition approach did not provide global optimality.

Whereas in all the above works SOO formulations were used, Bernal-Lara and Flores-Tlacuahuac [171] extended the previous work of Molina-Thierry and Flores-Tlacuahuac [168] towards incorporating rigorous heat-exchanger models in a MOO formulation. The authors considered 10 pure working fluids, which were used freely by the algorithm to generate multi-component mixtures and any concentration. The goal was to optimise the cycle thermal efficiency and total annualised costs simultaneously.

3.2.3. Key observations

Tables 1 and A.1 (in the Appendix) indicate that mixture-selection approaches where the components of the mixture are pre-specified, considered very few options. On several occasions, the authors pre-selected the mixtures from literature sources, mainly using criteria pertaining to their GWP and ODP *etc*. In the case where the mixtures were derived from pure components, Lee and Mitsos [170] indicated that a much larger number of 1771 mixtures can be generated, hence significantly increasing the possibilities of identifying a suitable fluid for the requirements of a particular application. CAMD approaches can be much more efficient as they may generate and assess billions of molecular structures.

Among the employed optimisation algorithms, it appears that SA, GA, and PSO have been used more frequently because they are easy to attain (*e.g.*, through commercial software such as MATLAB) or to implement. These metaheuristic algorithms can avoid local minima, enable derivative-free optimisation, and are suitable for problems where the lack of information, noise, non-smoothness, and discontinuities prohibit the use of deterministic methods, as noted in Boukouvala et al. [177]. The same authors note that metaheuristic algorithms can be used with black- or grey-box models and in cases where large systems of partial differential equations are coupled with nonlinear correlations to represent systems including design aspects, heat transfer, fluid dynamics, *etc*. These are useful features for ORC systems design, and in the future, such algorithms could be used to introduce models of high resolution in the simulations (*e.g.*, turbine CFD). The downside of such algorithms is that repeated executions result in a distribution of locally optimum solutions. They could, therefore, be used to shortlist a few promising solutions out of millions of options, which can then be explored more rigorously. Apparently, they are not appropriate if the optimum solution is desired with first- or second-derivative guarantees, although they can be combined with deterministic algorithms to attain guarantees for the NLP part of the problem, as in Lee and Mitsos [170]. Another downside is that metaheuristic algorithms often include multiple control parameters and require large populations in order to attain convergence [161]. The determination of the algorithmic parameters should also follow a certain, rigorous procedure in order to be able to statistically assess the quality of the optimum solution [178]. Such issues are important, but they were not addressed in most reviewed implementations, where the control parameters were defined arbitrarily. The factorial design of Rodriguez Sotomonte et al. [165] was an interesting exception. The time-consuming performance of such algorithms is largely due to the lack of mechanisms to avoid revisiting the same design points. More-advanced implementations exploit records of past solutions to skip the re-evaluation of the expensive model when a design point was simulated at a previous instant [179].

Deterministic algorithms provide mathematical guarantees about local or global optimality within finite runtime. Relaxations of the
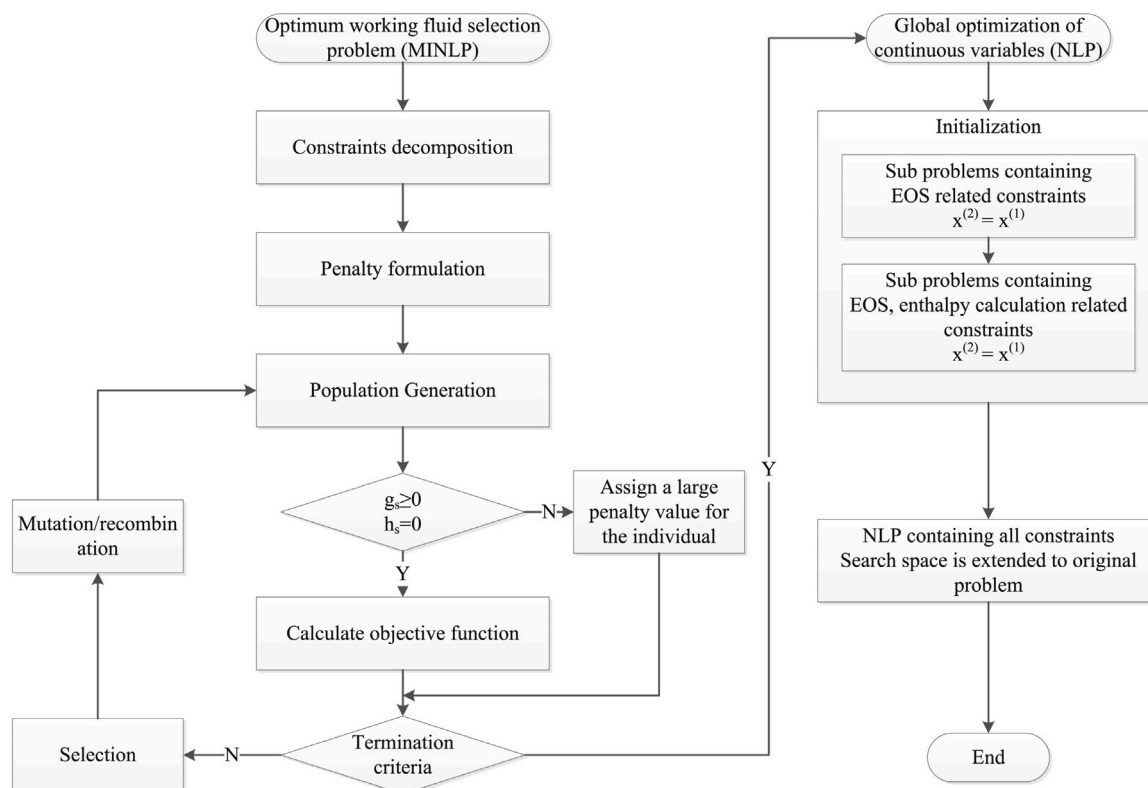
Fig. 8. Hybrid algorithm of Lee and Mitsos [170].
Source: Reprinted with permission from Lee and Mitsos [170].
© 2017 Elsevier.

constraints are used in global algorithms (*e.g.*, branch-and-bound approaches) until a desired tolerance is reached [180]. Their execution is faster than metaheuristics because they exploit gradient information, as opposed to a random search. Lee and Mitsos [170] provided very useful insights regarding optimisation strategies that can be used with such algorithms in ORCs. They proposed the gradual addition of constraints in the calculations in order to generate starting points for the solution of the subsequent problem with more constraints until the full problem is solved. They noted that such strategies facilitate algorithmic execution, but global optimality cannot be guaranteed when they are used. These algorithms are not without challenges either, as they require the identification of a feasible starting point, which is usually done through multi-start strategies. Different starting points often result in a distribution of different locally optimum solutions when non-convex, MINLP formulations are used [60]. The phase-equilibrium calculations may also introduce discontinuities in the constraints of the phase-behaviour and other numerical issues that also affect the non-linear solvers, irrespective of the type of optimisation algorithm (metaheuristic or deterministic). An excellent discussion is presented in Gopinath et al. [60], along with strategies to address such challenges. In this study the authors address multiphase separation processes, but the discussed approaches are very relevant to ORCs. In Satanphol et al. [169], the numerical solution of ORC models has been facilitated through the use of tear-stream approaches in order to avoid the need for simultaneous solution of large equation systems. In such approaches, recycle streams are broken into an input and output stream, where an iterative procedure allows the continuation of the calculations around the units in the recycle loop until these streams match [181]. Although these are easy to implement in simple ORC structures, their use in more-advanced structures and in superstructure approaches is difficult. The need to identify and use the non-trivial roots of the EoS is also very important and should be considered in the area of ORCs [170].

In recent years, the incorporation of approximation algorithms in deterministic approaches is becoming increasingly relevant [182]. Such approaches are likely to enable the use of surrogates of high-resolution models with deterministic algorithms. Huster et al. [180] presented an algorithm where artificial neural network (ANN) models were fitted for 20 different cases of pure-working-fluid–ORC model combinations to perform thermo-economic optimisation. The global deterministic algorithm MAiNGO [183] was used in both MOO and SOO formulations. Approximations are also very relevant for metaheuristic algorithms, where integrated material selection, process and controllability assessment problems can be addressed efficiently [184].

Another important feature of the above studies is the use of MOO. There is a large volume of publications on MOO for the design of ORCs or the selection of pure fluids [185]. The evaluation of different mixtures based on thermodynamic calculations includes indicators that exhibit conflicting behaviour. For example, as the pure components of binary mixtures move towards equal concentrations, the ORC exergy efficiency increases, whereas the thermal efficiency decreases [141]. MOO can help select mixtures that exhibit optimum trade-offs. Insights on the influence of mixture concentration may be unveiled, as a mixture with the same composition may participate in a Pareto front at different concentrations. Opposing trends may also be observed in economic and thermal indicators or in economic and environmental, health, or safety indicators. Several of the previously reviewed studies proposed methods for the selection of Pareto solutions that exhibit the shortest distance from an ideal point. An important feature of MOO approaches that has been overlooked is how to generate Pareto points that are distributed evenly, and that approximate the Pareto front as efficiently as possible. This is very challenging because the search space may be nonconvex due to the underlying ORC models and integer variables. The Pareto front itself may be discontinuous and non-convex. Important algorithms that address such issues, such as the sandwich algorithm

Table 2

Overview of key features presented in Section 3.3 (details available in Table A.2, in the Appendix).

Work context	Categories	Reference (s)
Component selection scope	Pure fluids	[189–208]
	Mixtures	[209–212]
	Both	[190,213]
Design scope	Pre-specified ORC configuration	[189–193,209,213]
	Advanced ORC configuration (superstructure or other generic, evolvable structure)	[194,196–202,210,214]
	Integration with heat source	[195,203,204,206–208,211,212,215]
Optimisation problem formulation	Single objective optimisation — SOO	[189–192,194–197,200,202–204,206–208,210–212,214,215]
	Multi-objective optimisation — MOO	[193,213]
	Both	[198,199,201,209]
Optimisation algorithm	Meta-heuristic (PSO, GA, SA, other evolutionary approach	[189,193,202,209–213]
	Deterministic	[192,194,195,200,203,204,207,208,215]
	Both	[196–199,201,214]
	Other software-specific routine	[190,191]

with multi-level single linkage, have been developed and applied in CAMD problems recently [186].

A cradle-to-grave analysis of ORC equipment and fluids was performed by Wang et al. [156] to calculate the equivalent greenhouse-gas emissions, also accounting for working-fluid leakage scenarios. Clearly, issues of environmental, health, and safety impacts are very important and should be accounted for during mixture selection or design. The evaluation of such mixture properties is much more challenging than for pure fluids because the former often exhibit non-ideal behaviour. For example, mixtures exhibit minimum or maximum flash points, *i.e.*, flash points that are not between the flash points of the pure components [187]. Flash points are indicators of safety, and vapour–liquid equilibrium calculations are needed for their prediction in the case of mixtures. Liquid–liquid equilibrium calculations are also needed to determine the solubility of mixtures in water in cases of leakage into the environment. Frameworks for the incorporation of holistic sustainability calculations in CAMD [100] and CAMPD [188] of solvents have been developed that could also be used for ORC working-fluid selection and system design.

Finally, it is worth discussing the work of Schwöbel et al. [148] and the follow-up work of Preißinger et al. [216]. Although the authors did not use optimisation algorithms or mixtures in these studies, the key feature was the assessment of a database comprising 72 million molecular structures. The authors applied thermodynamic filtering criteria and initially reduced the candidates to approximately two million options. After applying quantum-chemical calculations on those options, they shortlisted 3174 fluids which were evaluated using ORC simulations. While Schwöbel et al. [148]s used the cycle thermal efficiency as a criterion, Preißinger et al. [216] employed a multi-criteria approach where other aspects such as environmental impacts, toxicity, and flammability were also considered. These studies are noteworthy due to the sheer number of evaluated molecules as well as due to the use of advanced thermodynamic and quantum-chemical models. The investigated molecules were part of the PubChem database, which is available publicly. It is worth noting that the attainable structural space that is generated through CAMD is much wider, as it may comprise up to billions of options [137]. With the use of optimisation algorithms, it is not necessary to evaluate all options exhaustively. It is sufficient to evaluate up to a few hundred thousand options [217] in order to identify the molecular structure that optimally matches the desired criteria.

### 3.3. Fluid selection and optimum design of advanced ORC systems

In this section, we discuss different structural ORC and heat-recovery options that go beyond conventional layouts and the systematic representation approaches that are often used to derive and evaluate them. Key features of the studies reviewed are summarised in Table 2 and presented in more detail in Table A.2, in Appendix. Table A.2 contains similar sections as those of Table A.1 in addition to details on the type of ORC configuration (*e.g.*, single, dual-loop, regenerative, *etc.*).

3.3.1. Pre-specified ORC structures

In this section, we review studies that include pre-selected ORC structures with different pressurisation levels or separation of working-fluid streams, to name but a few options. In all of these, multiple different fluids are considered but their selection is not part of the optimisation problem formulation. The operating conditions of the ORC structure are optimised for each one of the considered fluids.

Xi et al. [189] optimised a simple ORC and two regenerative ORC configurations considering few pure fluids. The first configuration included the single-stage regenerative ORC (SRORC), where part of the vapour at the turbine outlet circumvents the condenser and is used in a feed-water heater to preheat the remaining part of the working fluid that has been condensed, before entering the evaporator. In this configuration one pump was used after the condenser to pump the liquid to the feed-water heater, where the liquid came into contact with the vapour from the turbine. Another pump followed to drive the overall liquid to the evaporator. In the dual-stage regenerative ORC (DRORC), one stream was directed to the condenser after the turbine, whereas two other vapour streams (instead of one in the SRORC) were directed to two feed-water heaters, hence the system has three pumps. The GA used for optimisation included deterministic selection, simple arithmetic crossover and mutation, and an elite preservation strategy as operators. Each ORC structure was optimised separately for each working fluid.

Woodland et al. [190] performed operating optimisation of advanced ORC system configurations (Fig. 9), even at transcritical conditions, considering up to two unconventional mixtures. The ORC with liquid-flooded expansion (ORCLFE) is a cycle where the expander is flooded with a subcooled liquid in equilibrium with the working fluid when the latter is expanded. The flooding liquid operates as a heat source, helping to maintain a constantly high temperature during the expansion, bringing it closer to the ideal isothermal expansion. The ORC with solution circuit (ORCSC) uses a mixture of the primary

(a) ORCLFE structure
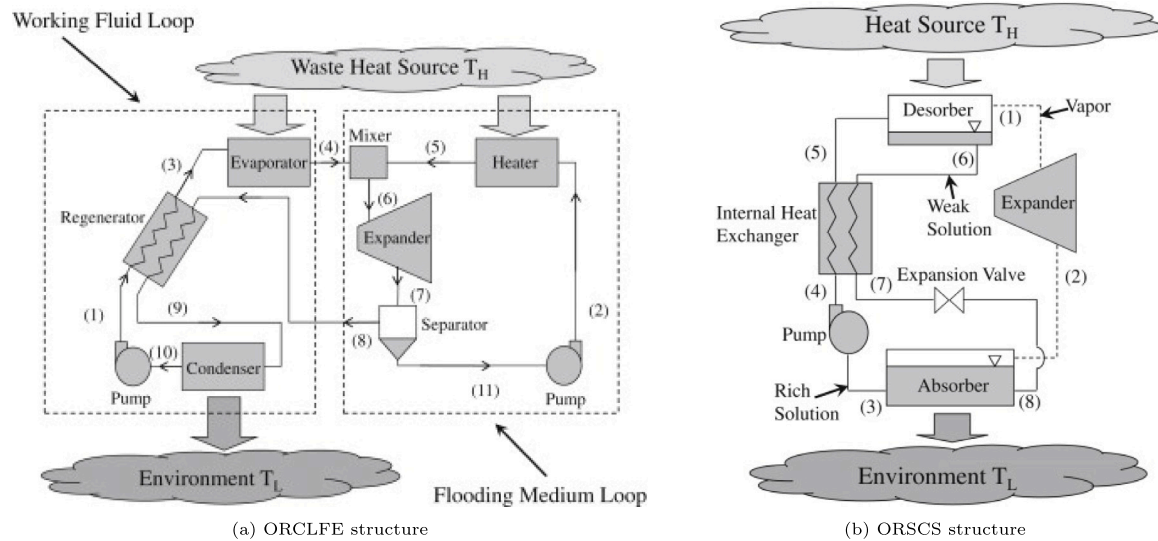
(b) ORSCS structure

Fig. 9. The ORCLFE structure and ORSCS structure.
Source: Reprinted with permission from Woodland et al. [190].
© 2013 Elsevier.

working fluid and an absorbent with a high boiling-point difference. The cycle exploits the temperature glide in the evaporator/ desorber due to the use of the mixture to enable increased exergetic efficiency. The absorbent is desorbed during the heat addition, hence enabling an almost pure working fluid to be expanded in the turbine. The ORCLFE enables higher efficiency than the simple ORC, but a positive displacement expander is needed. The ORCSC facilitates better capacity control and can have lower working pressures than the typical ORC, but its efficiency is lower. In terms of working fluids, investigations should be performed to find more efficient options, as the cycles have received little attention. The ORCSC cycle shares common features with the operation of absorption refrigeration cycles (ammonia–water is a typical fluid for such a cycle) hence similar fluid options may be considered [218,219]. Despite the interesting features of these cycles, additional capital expenditures are introduced due to the additional equipment, whereas the separation and absorption processes in these cycles need to be very efficient.

Walraven et al. [191] investigated different working fluids in a single-pressure recuperative and a double-pressure ORC configuration. In the latter, part of the working fluid in the intermediate pressure level goes through the boiler and into the turbine, whereas the other part is pre-heated at the intermediate pressure level and is then driven to the higher pressure level before it is expanded in the turbine. The operating conditions of the ORC (*e.g.*, temperatures, pressures, *etc.*) were optimised simultaneously with the HEX geometrical characteristics (*e.g.*, tube lengths, *etc.*). An NLP solver was used [220] with automatic gradient differentiation [221]. The authors [222] mention that the gradient-based algorithm using finite-differencing results in slow calculation and low accuracy. These issues were avoided by calculating the gradients with automatic differentiation in reverse/adjoint mode. Multi-pressure configurations enable higher work extraction than single-pressure ones. The number of pressure levels, the type of turbine used (*e.g.*, expansion, induction), and their placement in the multi-pressure cascade should be accounted for during optimisation as they greatly affect the minimisation of exergy losses [194].

Sadeghi et al. [209] investigated several mixtures of up to five components of pre-specified composition and concentration in a simple, a parallel two-stage (PTORC) and a series two-stage ORC (STORC). The PTORC includes separation and pressurisation of the saturated liquid from the condenser into two pressure levels, using two pumps, prior to absorbing heat from two evaporators placed in series. The high-pressure fluid absorbs heat from the hot fluid that enters the first

evaporator, whereas the low-pressure fluid absorbs heat in the second evaporator from the heat source fluid that exits the first evaporator. The two streams then enter the turbine where power is generated, and one outlet stream is led to the condenser. In the STORC, the working fluid after the condenser is pressurised to the low-pressure level. It is then separated into two streams; one stream is led directly to the turbine, whereas the other is pressurised to the high-pressure level and then led to the turbine. The selection was performed in three stages. In the first stage, a parametric analysis was performed with all fluids and configurations, and the authors found that the STORC configuration is the most efficient based on first- and second-law efficiency criteria. In the second stage, specific STORC cycle parameters for all fluids were varied, using the net power output and the turbine-sizing parameter as cycle-performance criteria. The third stage included multi-objective optimisation, using specific STORC cycle parameters as design variables for mixture R32/R125/R134a, and the two criteria of the second stage as objective functions. It was observed that the STORC configuration with the selected fluid enables the highest power output with the second-lowest turbine size.

Theamtat and Koonsrisuk [192] investigated different working fluids in subcritical, supercritical, and trilateral cycles. The latter is an advanced layout where the working fluid enters the expander in a saturated-liquid instead of a saturated-vapour state. A two-phase expansion occurs, reducing the heat-rejection requirements at the condenser. In all cases, the golden-section search algorithm was used to identify a locally optimum solution for the working fluid flow rate that maximised the work output.

Wang et al. [213] investigated a dual-loop ORC considering different working-fluid mixtures for the low-temperature (LT) and the high-temperature (HT) loops. In the dual cycles, heat is extracted firstly in the HT loop and then in the LT loop. An internal heat exchanger acts as the condenser of the HT loop, where the fluid of the LT loop is pre-heated after the pump. An MOO approach was used with the NSGA-II algorithm, using the TOPSIS technique to identify the optimum solution. Thermal, economic, and environmental criteria (emissions) were used in the optimisation. Gray relational analysis was further used to identify the optimum pair of fluid mixtures for the two cycles.

Emadi et al. [193] investigated a dual ORC configuration to exploit the heat from a solid-oxide fuel cell (SOFC) with a gas turbine (GT) (Fig. 10). In this cycle, all the heat is extracted from the HT evaporator (ORC1), whereas its condenser acts as the LT evaporator (ORC2
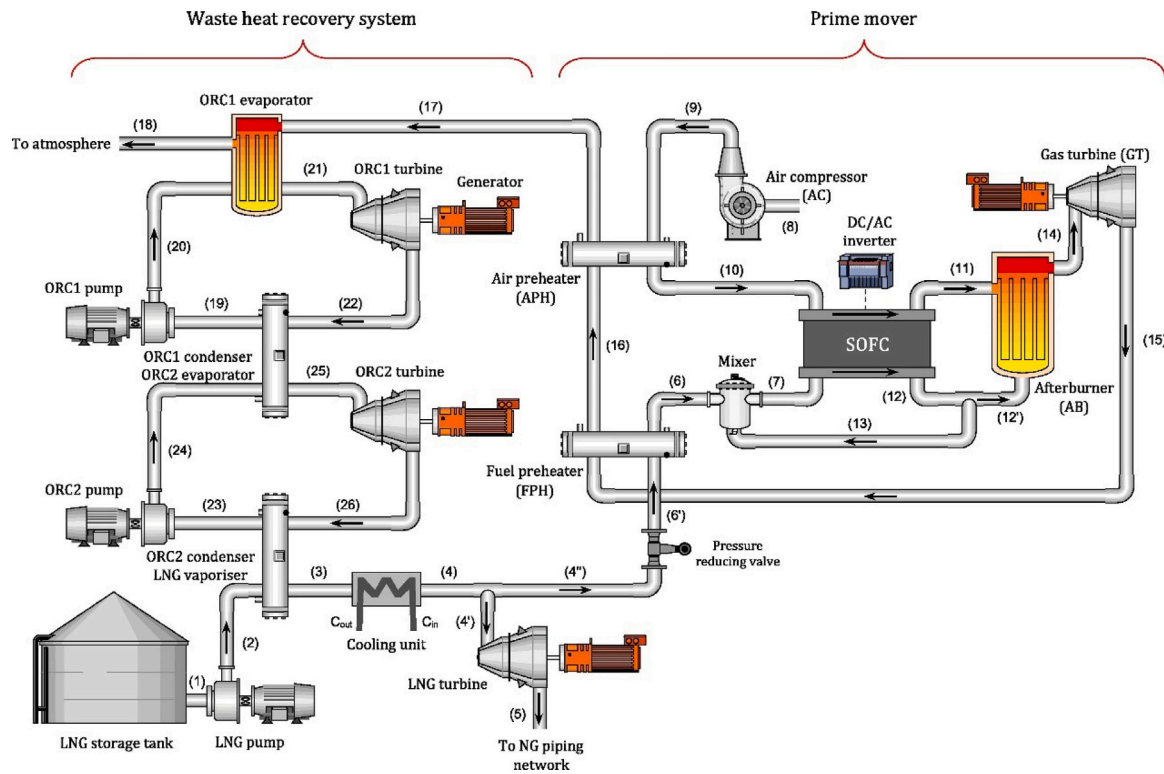
Fig. 10. Layout of dual-loop cycle in Emadi et al. [193].
Source: Reprinted with permission from Emadi et al. [193].
© 2020 Elsevier.

evaporator). An MOO approach was used with GA as the optimisation approach. ANNs were used to generate a model of the SOFC–GT–ORC that facilitated the implementation of the GA. The time-consuming simulations of the rigorous SOFC–GT–ORC model where thus avoided. The LINMAP technique was used to select the optimum solution from the generated Pareto front. The combination of two different fluids for the top (R601) and bottom (ethane) cycle resulted in the optimum trade-off between efficiency and cost.

3.3.2. Design of ORC structures

The previous section included studies where the ORC configuration was pre-determined, and an optimisation algorithm was used to further determine the optimum operating conditions. In this section we consider studies in which the ORC configuration itself is a design variable, and the optimisation algorithm is used to guide the search towards structural features that optimise a performance indicator. In these cases, superstructure-based approaches (*e.g.*, [210]) may include pre-determined structural options which are activated or deactivated during the search. There are also superstructure-free approaches (*e.g.*, [196] or [198]), where the optimisation algorithm adds or removes options, and the ORC structure evolves and results from the optimisation search. There are a few such works, and hence the superstructure-free approaches are discussed here even if there is no selection of working fluids.

Stijepovic et al. [194] proposed a generic approach for the design of multi-pressure ORC networks, built on a mathematical representation of the exergy composite curves approach [223]. This approach is an extension of the original Pinch analysis method [224] where temperature-enthalpy diagrams of the heat source fluid and the working fluid represent the composite curves and determine the amount of heat that is available for recovery from the heat source. In the exergy composite curves, the temperature is replaced by the Carnot factor $(1 - T_0/T)$. The area between the heat source fluid curve and

the enthalpy axis in the Carnot factor-enthalpy diagram represents the maximum work that can be generated, whereas the area between the heat source fluid and working fluid composite curves corresponds to the exergy loss or the ideal work equivalent lost in heat transfer. With the proposed representation (Fig. 11) the authors could determine the optimum configuration of the heat-exchange operations between the external pressure loop and the heat source and between the internal heat-exchange processes within the different pressure loops. Expansion and induction turbines were design options, with the latter enabling different pressure loops to be contacted. The number of pressure levels could be increased if the addition of a new level improved the performance of the previous one. An induction turbine is essentially a layout that may be represented as single stage turbine units connected in series. The working fluid vapour from the high-pressure evaporator first flows into the high-pressure turbine and the pressure decreases to the low-stage evaporation pressure. The exhaust from the high-pressure turbine and the vapour from the low-pressure evaporator flow into the low-pressure turbine together, and the vapour pressure decreases to the condensation pressure [225].

Toffolo [196] presented an approach for the synthesis of ORC systems, where the ORC is represented through two basic components, an expander, and a compressor, allowing for interruptions (thermal cuts) between them in the cycle path. The thermal cuts represent the heat-transfer processes within the cycle components or between the cycle components and the environment. The optimisation algorithm may freely select the optimum number of thermal cuts and basic components, allowing for stream splitting and mixing, different temperature and pressure levels, and numbers of basic cycles. This was called the HEATSEP method (Fig. 12) and was based on the original work of Lazzaretto and Toffolo [226] for the synthesis of thermal processes. Toffolo further proposed a two-level formulation of the optimisation problem. Externally, he showed how to model the structural design options within the operations of an MOO evolutionary algorithm such
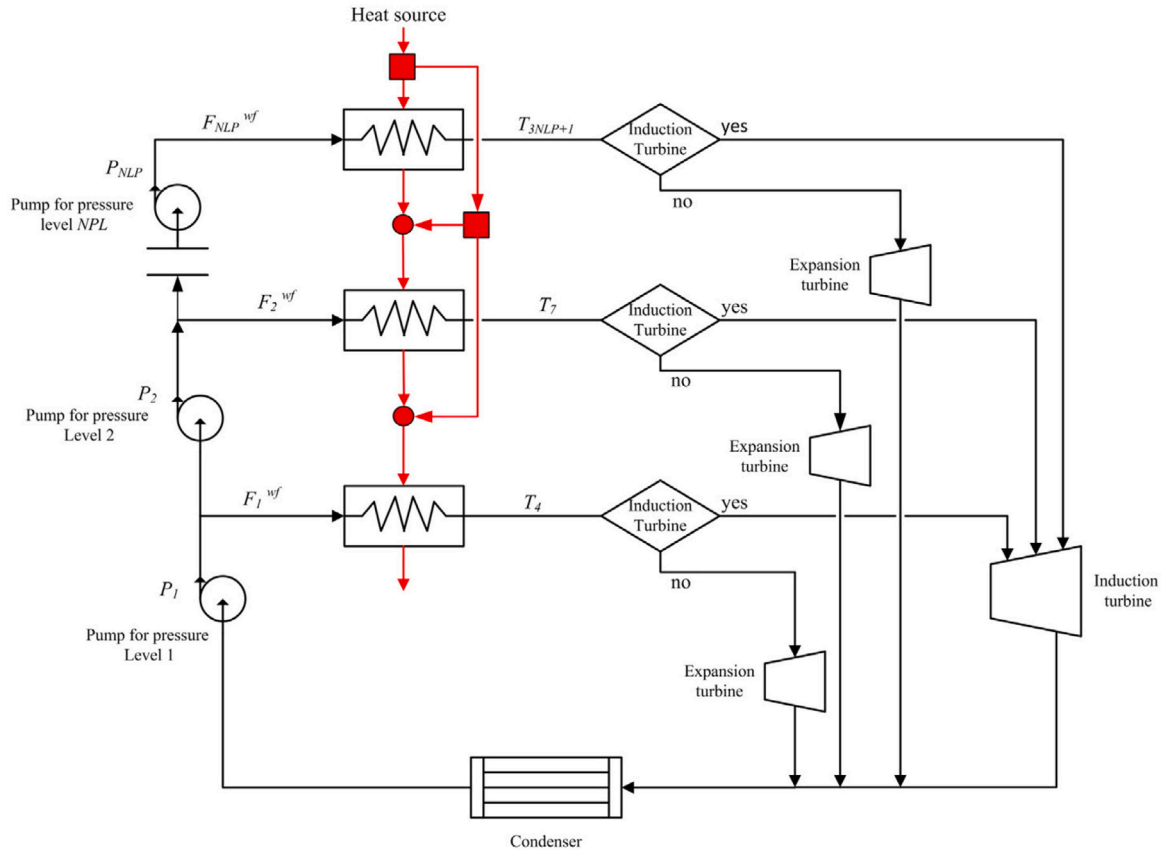
Fig. 11. Generic structure for representation of multi-pressure ORC network.
Source: Reprinted with permission from Stijepovic et al. [194].
© 2014 Elsevier.
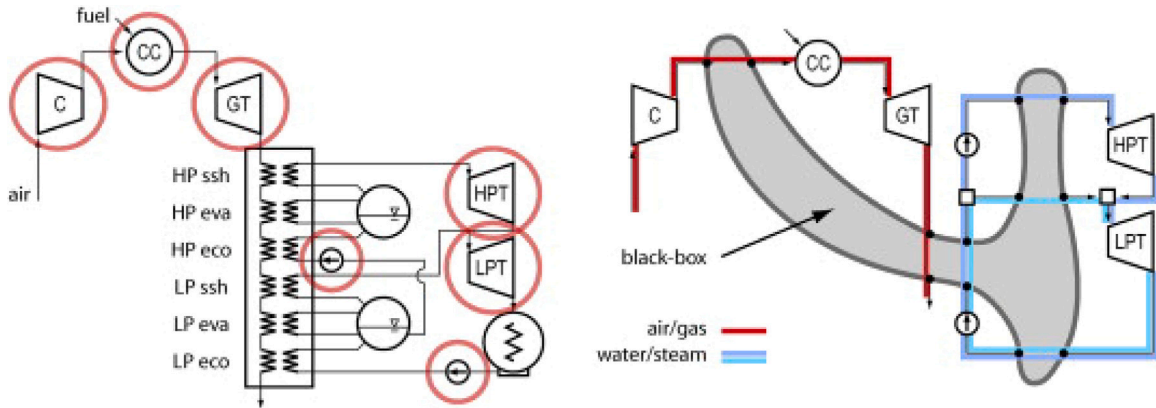
Fig. 12. Representation of a multi-pressure cycle (left) through the HEATSEP approach of Toffolo [196] (right).
Source: Reprinted with permission from Toffolo [196].
© 2014 Elsevier.

as GA, indicating how a move between states of the algorithmic operations represents a change in the structure of the designed ORC. Internally, for every generated structure, he proposed the use of an SQP to identify the optimum operating conditions of the structure. The implementation of the algorithm in a case study resulted in multi-pressure cycles that comprised various dependent loops, where the flow of the working fluid might be split and mixed, whereas heat might be drawn at different cycle points. The work was further extended to the SYNTHSEP framework [197] where rules were proposed for the framework of Toffolo [196] to allow for the implementation of reasonable thermal cuts in the generated structures.

Wang et al. [198] further proposed a rule-based approach for the generation of structural options during ORC system optimisation. The approach was based on the hierarchical imposition of rules, implemented through a mutation operation in an evolutionary optimisation algorithm. The latter was used to handle the discrete structural design variables, whereas, for each generated ORC structure, an NLP was used internally to optimise the continuous parameters. A notable feature of this work is that the authors discussed algorithmic convergence issues in the form of repeated execution of the evolutionary algorithm and the determination of optimality gaps. The work was extended by Wang et al. [199] to account for MOO.

Lee et al. [210] proposed a superstructure of a cryogenic ORC, which included several different alternatives such as multi-stream cryogenic heat exchangers, vapour flashes, multi-stage turbines, and vapour re-condensation processes. All these were pre-specified in the superstructure, and the GA algorithm could freely select different options.

Huster et al. [200] presented a superstructure approach for the design of ORCs that included various options, such as multiple pressure levels, additional superheating options, direct expansion from the higher to the lower pressure levels, omitting intermediate pressures and turbine bleeding. The heat sources could also be used in sequential or parallel modes (split into different streams). A key feature of this work was the use of ANNs for the prediction of the thermodynamic properties of the working fluid. Furthermore, the authors reduced the attainable design space by introducing logical propositions to rationalise the selection of different options and employed appropriate relaxations and constraints to facilitate the optimisation solver, while a parallel version of the optimisation algorithm was also used. Through the proposed approach, they managed to reduce the computational effort by 49 % using relaxations, in a superstructure that included 28 structural, integer combinations.

In all the previous works systematic approaches were presented for the design of advanced ORC configurations, which were implemented for one fluid. In the approaches reported below superstructures were employed where both the fluid and the final ORC configuration are selected from a set of available options.

Kermani et al. [201] proposed a superstructure that enables the selection of multiple different pressure levels, the addition of all the basic components of an ORC system at each level and the type of fluid that is used, out of a number of options. The problem again was solved at two levels, where a GA was used externally and mixed-integer linear programming (MILP) internally. Contrary to the previous works, it appears that the GA handled mainly the continuous variables, whereas the discrete variables were handled by the MILP. SOO and MOO formulations were further tested with different objective functions.

Bao et al. [202] proposed a superstructure for a three-stage condensation ORC that used the LNG cold energy. The working fluid was split into three streams after the expansion and was condensed at three temperature levels. After that, the fluid streams could be compressed in parallel pumps (parallel arrangement) prior to being mixed and entering the evaporator. Another alternative was to compress two streams in parallel and then mix them with the third stream and compress the final stream (partial parallel arrangement). The final alternative was to compress the first stream, then mix it with the second stream, compress the output and then mix this with the third stream and compress it (serial arrangement). Similarly, the superstructure could include parallel, partial parallel, and serial expansion. In the first case, the evaporator outlet was split and expanded using three turbines. In the partial parallel arrangement, the fluid was first expanded in one turbine and was then split into three streams that flowed in the partial parallel arrangement of the condensers. In the serial arrangement, after expanding all the fluid in one turbine, it was divided into two streams, one of them flowing in the first condenser, whereas the other was expanded in another turbine and was further divided into two streams prior to entering the two final condensers. The superstructure included nine structural options, which were represented by three ternary, discrete variables for the different configurations of the expansion and the compression processes. Each working fluid, out of 12 options, was also a binary variable. This superstructure was also optimised using GA.

Lin et al. [214] combined the HEATSEP representation of Toffolo [196] to select pure fluids and mixtures out of a set of pre-specified options. They used a similar solution approach to most of the previous studies, where an external evolutionary algorithm handled the discrete and binary structural and fluid option variables, whereas the ORC simulation was performed through an internal deterministic algorithm. The proposed work was implemented in a two-stage condensation ORC for LNG cold energy exploitation.

3.3.3. Integration of heat sources

The heat that is provided to the ORC may come from various systems that have different flows, operate at different temperatures or pressures and that simultaneously serve different purposes in an industrial or other site. The exchange of energy among such systems and the ORC needs to result from a design approach that is able to systematically capture and exploit all the interactions. In this section, we consider studies in which the heat source is integrated through systematic approaches with the ORC in order to improve the overall system performance. Often such approaches enable the design of a heat-recovery network which can be integrated with simpler or more-complex ORC configurations. Hipólito-Valencia et al. [203] proposed a superstructure-based approach for the design of the utility network that is used in a regenerative ORC (Fig. 13). The work was extended by Hipólito-Valencia et al. [227] in cases of inter-plant heat integration of utility networks, to serve either individual or shared regenerative ORCs. The work was further extended by Lira-Barragán [205] in the design of tri-generation systems. In this case, the utility superstructure was used to design a network that simultaneously served an ORC, a steam RC, and an absorption-refrigeration system.

Similarly to the previous study, Chen et al. [204] employed a superstructure to design a utility network. The first stage included the design of the utility network structure, and the second stage involved the design of the ORC for this structure.

Soffiato et al. [215] developed an algorithm that used the HEATSEP representation of Toffolo [196] and comprised three stages. The heat composite curves of the boiler-heat source were first calculated for a given set of design variables for the ORC, the latter was simulated, and the algorithm calculated the cold composite curves at the condenser. The mass flow rate of the working fluid was increased until the minimum temperature difference was reached at the boiler-heat source and condenser-cold sink sides. The net work output of the ORC was then generated, and the algorithm continued until a value for the working-fluid flow rate was found that violated the heat-transfer feasibility constraints at the hot and cold sides. The algorithm was implemented separately for each ORC configuration and fluid.

Yu et al. [206] further proposed an approach for the simultaneous design of the utility network and of the ORC operating conditions and equipment sizes. A major contribution was the use of the mathematical formulation of the pinch-based model of Duran and Grossmann [228], where the use of fixed temperature intervals is avoided in the design of the utility network.

Elsido et al. [207] proposed an optimisation approach for the design of complex ORC configurations and the corresponding utility network. The work was based on the generic superstructure of Elsido et al. [229]. The superstructure could capture multi-pressure cycles with turbine bleeding, saturated, superheated, reheated, or regenerative options, combined heat and power cycles, condensing and non-condensing turbines, import and export of liquid or vapour streams, subcooling of the evaporator inlet, deaerators or desuperheaters, *etc*. The work was focused on the efficient solution of the challenging MINLP formulation through a decomposition approach that included outer-approximation linearisation, McCormick relaxations, and adaptive piecewise linearisation of the cost functions. The problem was essentially decomposed into an MILP master and an NLP subproblem.

Marechal and Kalitventzeff [208] developed an approach based on exergy composite curves for exploiting the external heat and cooling utilities while designing an optimum ORC. The exergy curves allowed the targeting of the mechanical production potential from a set of heat-source streams. In the first stage, an MILP problem was solved to identify the temperature levels of the external utilities that minimised the exergy losses. Based on these temperature levels, the second stage included the design of ORC configurations together with the identification of the desired working fluid from a list of pre-determined options, with the aim again to minimise the exergy losses. In the third stage, an MILP problem was further solved to minimise the cost of the ORC
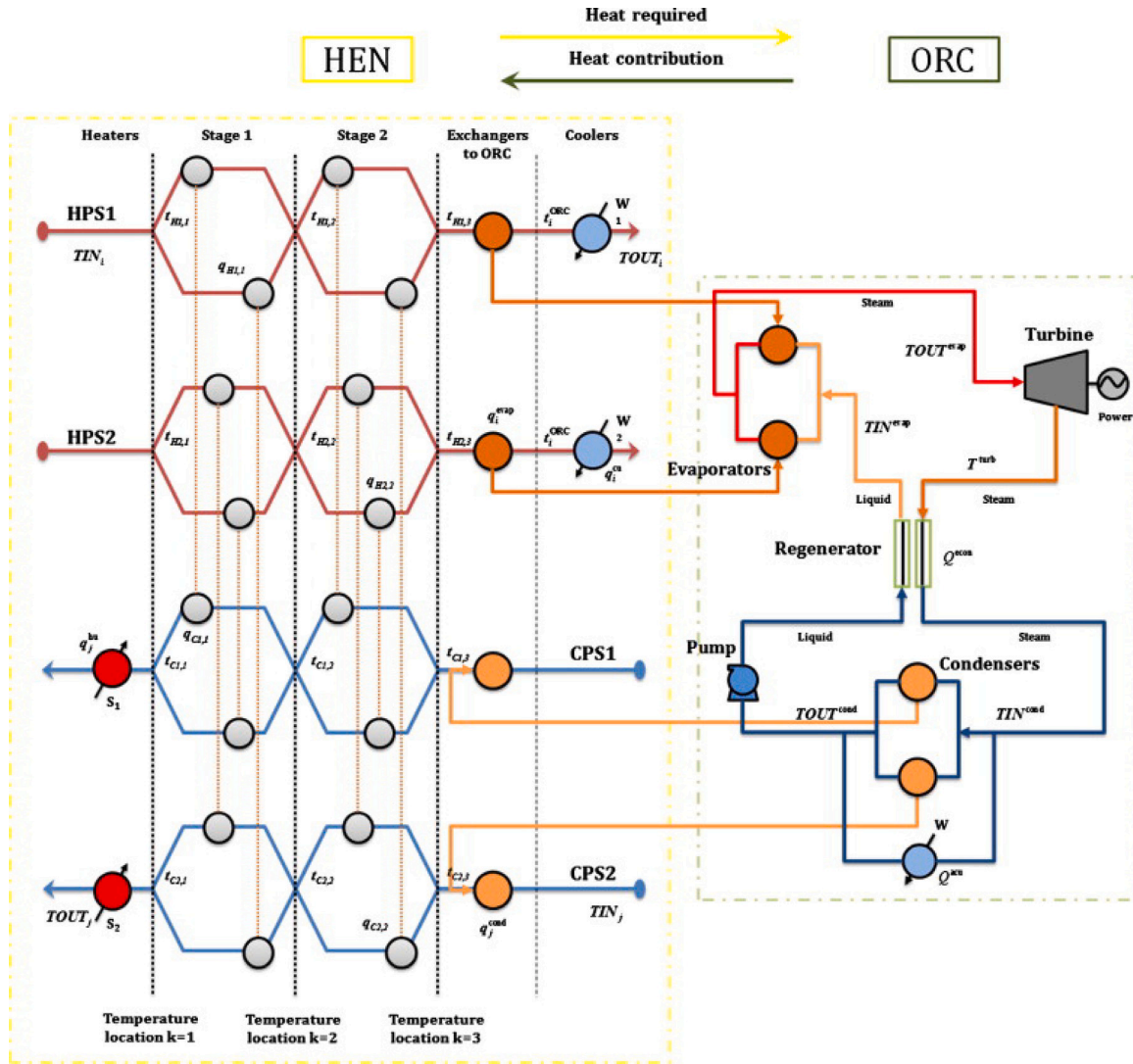
Fig. 13. Superstructure for optimum design of utility network in a simple ORC with recuperator.
Source: Reprinted with permission from Hipólito-Valencia et al. [203].
© 2013 Elsevier.

system from the list of options available from Stage 2. The approach essentially enabled the gradual addition of constraints in the exergy composite curves of a process.

Stijepovic et al. [195] proposed the integration of multiple heat sources of different temperatures into a superstructure, which can enable the simultaneous design of multiple cycles that share the heat-extraction section and the cooling utility, the design of the hot-utility network, and the selection (number and type) of the working fluid. The approach was based on the mathematical representation of the utility requirements through pinch analysis tools and the use of optimisation. A key finding was that when a dual (or higher) ORC cascade is the optimum solution, each one of them may operate with a different working fluid.

Scaccabarozzi et al. [211,212] presented an optimisation-based approach, where the concentration of different binary mixtures of pre-specified composition was optimised simultaneously with the cycle and the heat source. The ORC system was used to recover heat from an internal combustion engine. The PGS-COM evolutionary algorithm was used to maximise the cycle power output and efficiency. PGS-COM is a derivative-free algorithm for non-smooth constrained black-box models. For each set of design variables that was generated by the algorithm, the ORC model determined the stream temperatures. The

working-fluid mass flow rate was then optimised to maximise the heat recovery from the heat source. The heat cascade methodology was used for this purpose in the form of a linear programme [230], where the ORC system flows and the mass flow rates of the external utilities were used as optimisation variables. The execution of the PGS-COM was repeated five times to assess the quality of the optimum solution.

3.3.4. Key observations

The reviewed studies indicate that there are multiple ORC configurations that need to be considered prior to selecting the one that exhibits the optimum system performance. Approaches that enable the automated generation of such structures during optimisation are very important because the optimum results are highly dependent on both the employed working fluid and the availability of heat and cooling utilities. The approaches that integrate the design of the utility network and of the ORC structure indicate that it is also important to recover the heat and cooling resources within optimum networks. The consideration of working-fluid selection as part of the integration of ORC systems with multiple heat-source streams or heat-exchanger networks has been very limited to date, and only small sets of pre-defined fluids have been considered in ORC integration studies. The studies in which limited fluid-selection options are considered as part

of ORC design and system integration serve as a demonstration of the importance of integrated approaches to simultaneous cycle design, integration, and fluid selection. Similarly, while promising results have been reported in early studies, the simultaneous selection and design of working-fluid mixtures in heat-recovery-network design have received little attention to date.

Such approaches and their extensions to consider working-fluid design for both single fluids and mixtures constitute a promising direction for future research. However, as the optimisation problem is extended from the simultaneous selection of fluids and design of ORC structures to one that also requires the design of the corresponding heat-exchanger networks, the complexities incurred by the optimisation algorithms further increase. Huster et al. [200] and Elsido et al. [207] discussed the challenges in the development of efficient deterministic algorithms for global optimisation of such systems. Approaches that include meta-heuristics to handle the discrete variables and deterministic algorithms to handle the continuous variables have been quite popular, as shown in the Appendix (Table A.2). In such cases, it is important to perform different executions and fine-tune the algorithmic parameters in order to be able to assess the quality of the solutions.

Other than considering advanced and efficient optimisation algorithms, it is also important to exploit insights that are provided by the phase behaviour of the fluids to avoid examining options (e.g., working fluid candidates or ORC structural options) that may have detrimental effects on the ORC costs. For example, the shape of the temperature-entropy curves changes for different working fluids, resulting in their classification as wet, dry or isentropic. Györke et al. [104] noted that based on these fluid types different ORC structures or equipment may be necessary to avoid the appearance of liquid or of superheated vapour in the expander outlet. The former increases the equipment maintenance costs, whereas the latter increases the cooling utility costs. They further showed that this classification is not sufficient to predict the phase of the fluid after expansion and proposed up to 32 potential categories to ensure that all potential fluid phase outcomes can be attained. In combination with this classification approach, Györke et al. [231] developed a rule of thumb, based on a correlation related to molar isochoric specific heat capacity of saturated vapour states, to identify dry or isentropic fluids out of a database of 74 options. Imre and Groniewsky [232] applied the new classification to identify such fluids out of 30 options and mainly for cryogenic applications, within different upper and lower expansion temperature limits. The proposed approach was also extended to selection of working fluids for trilateral flash cycles [232]. Groniewsky et al. [233] extended the proposed approach to account for different expander efficiencies and source–sink temperatures that may be relevant for cryogenic, geothermal and industrial waste-heat recovery applications. The authors also developed a software that may select a working fluid from a database of 69 options for different temperature ranges. Such an approach may be integrated in ORC optimisation, introducing additional constraints and criteria to reduce the optimisation effort and to result in highly performing fluids and ORC systems.

Overall, there is a trend to formulate increasingly larger design problems to include a growing number of options in terms of cycle design, cycle integration with heat sources, and working-fluid selection, as well as more-detailed equipment models in single, comprehensive optimisation models that become increasingly challenging to solve. Research into problem-decomposition schemes, similar to the CAMPD problem decomposition using MOO CAMD [217,234,235], may be a promising direction for future research to enable the effective solution of the envisaged larger problems.

An important issue here is the reliability and reproducibility of the attained results. As the complexity of the ORC configurations increases or as new fluids are proposed through computational approaches, experimental validation is not easy because experimental data generally exist for simpler configurations (Lecompte et al. [80] and well-known working fluids, such as commercially available refrigerants [236,237].

Park et al. [236] indicate that experimental ORC layouts include mainly basic cycle configurations where different expanders or working fluids are tested. More complex experimental layouts are less frequent and include the use of ORCs in trigeneration systems [238] or the testing of multiple expanders in parallel [239]. The experimental testing of more advanced systems is clearly a key direction for future work. However, the motivation for building and testing experimental rigs of more advanced systems should come from optimisation studies that prove their economic and environmental benefits, as the capital costs may often make them unappealing.

In view of the lack of experimental data, as a minimum requirement, validations should be presented with experimental data of reference fluids for simpler models that are used as the basis for the development of more complex configurations. Additionally, all the details and data used in the model equations should always be presented so that the models may be reproduced. For design results that indicate improved performance through more complex configurations or fluids for which experimental data are not available, insights should always be provided regarding the key driving forces that enable performance improvements. An additional feature that could enhance the reliability of the attained results is the consideration of uncertainty in various models, parameters and correlations that are used. As discussed in Section 3.4.3 and 3.5, uncertainty significantly affects the attained results and the ranking of the fluids. By using systematic methods to address it during working fluid selection and ORC design, the results will become more robust and likelier to closely match experimental outcomes.

3.4. Fluid selection and rigorous equipment models

ORC performance improvements may be attained by designs that focus on expander or heat-exchanger internals such as blade and pipe geometries, to name but a few. The effects of the working fluids on such designs are very pronounced, but the highly detailed models that are needed result in challenging design problems. There are several studies in which such challenges have been addressed. Key features of the reviewed studies are summarised in Table 3 and presented in more detail in Tables A.3 (for expanders) and A.4 (for heat exchangers) in the Appendix, where additional information is presented regarding the modelling approaches and assumptions.

3.4.1. Expanders

The expansion stage is absolutely critical in the achieved performance of the ORC system. A variety of expansion devices can be employed in ORC systems, such as turbines (with radial and axial configurations being the most-common options), positive-displacement equipment (with scroll, screw, piston, and rotary vane expanders as possible and common alternatives), and ejectors [282]. The conversion of the potential energy (associated with the total pressure) of the working fluid upstream of the expander into either rotational or linear displacement work, depending on the expander type (positive-displacement or turbomachine) is closely related to the properties of the working fluid. Therefore, the design of the expander should be carefully considered with respect to the features and characteristics of the working fluid. A series of recent studies incorporating investigations of the interactions of working fluids with the expander design, the operating conditions prevailing in the expander, and the achieved expander efficiency in combination with the overall ORC system thermodynamic and economic performance are critically reviewed with the summary of their approaches and conclusions shown in the Appendix (Table A.3).

Yue et al. [283] presented a model where the internal geometric turbine and heat-exchanger features were considered. An axial flow turbine was modelled considering rotor, blade, and nozzle characteristics. Plate evaporator and condenser heat exchangers were also modelled considering plate dimensions, distances, numbers, and materials of construction, to name but a few. An important observation was that a zeotropic isobutane–isopentane mixture exhibited optimum thermal

Table 3

Overview of key features presented in Section 3.4 (details available in Tables A.3 and A.4, in the Appendix).

Work context	Categories		Reference (s)
Scope of work with respect to component	Pure fluid selection		[129,180,225,240–262]
	Mixture selection		[162,163,169,171,263–269]
	Consideration of pure and mixed fluids in selection		[155,161,270–272]
	Molecular design	Pure fluids	[98,273–276]
		Mixtures	[277,278]
Expander type	Radial		[240–246,248,249,270,271, 273,279,280]
	Axial		[247,263]
	Both		[245]
Cycle investigation scope (expander model cases)	Off-design cycle operation studies		[240,242,246,249,263,270, 271,279]
	Nominal cycle operation studies		[241,243–245,247,248,273,280]
Boiler type	Tube-based (mostly shell-and-tube, with some fin-and tube cases)		[98,155,156,161,162,169,171, 251–253,255,260,262,265–267,272,274,275,277,278,281]
	Plate-based		[250,254,256–258,276]
	Other		[163,255,259,261,269]
Condenser type	Tube-based		[98,155,161,162,169–171,198,250,251,255,258,264–268,272,274,275,277,278,281]
	Plate-based		[252–254,256,257,276]
	Other		[163,180,259–261]
Boiler and condenser model types	Steady-state		[98,180,250–258,264,272,274, 275,277,278,281]
	Dynamic		[259–262,265–269]

performance at compositions that did not exhibit the maximum temperature glide. Thus, proper accounting for equipment–working-fluid interactions is crucial, and purely thermodynamic design guidelines lead to suboptimal performance.

Song et al. [279] pointed out that failure to accurately estimate the turbine efficiency in ORC simulation calculations may lead to erroneous results regarding the assessment of the performance of various working fluids. In their work, a one-dimensional turbine-efficiency model was integrated within the thermodynamic ORC model for the evaluation of six working fluids. A breakdown into friction and leakage-related losses for a wide range of operating conditions for each working fluid enabled a reliable rank ordering of the investigated working fluids, in which R123 exhibited the highest overall efficiency.

Fiaschi et al. [242] focused on the radial-turbine design for two blade configurations and the accurate estimation of the losses for each specific design. The effect of key design parameters such as blade height, flow and load coefficients, and isentropic degree of expansion on the geometric features of the expander were calculated for six single-component fluids. An explicit mapping of working-fluid and radial-turbine expander design and operating conditions was then derived. In addition, a thorough analysis of the contribution of each loss factor in the overall losses was performed for each working fluid under consideration. Off-design studies for the two blade geometries were carried out, examining the influence of corrected rotational speed on the generated power. Fluids with higher average density and lower volumetric expansion, such as R134a and R1234yf, showed superior performance in terms of expander efficiency under nominal operating conditions.

Rahbar et al. [243,244] aimed at the optimisation of a small radial expander for ORC applications. Non-ideal gas behaviour was coupled with a mean-line model for the expander. A GA was employed [243] for the maximisation of the expander efficiency by calculation of a set of operating (*e.g.*, rotational speed, load and flow coefficient, degree of superheating and so forth) and geometric (*e.g.*, rotor exit flow angle, nozzle inlet to exit radii, rotor exit to inlet radii and so forth) characteristics. An optimised expander tailored for the selected working

fluid could increase its efficiency by a maximum of 14.7 %, with R152a resulting in the highest expander efficiency among the investigated working fluids. R123a and R236ea achieved the smallest expander size.

White and Sayma [240] investigated 18 single components as working fluids in a 10 kWe system using a thermodynamic model for the ORC and a simplified radial expander model. The optimisation approach used an aggregate objective function with multiple terms aiming at obtaining the optimal sizing of the ORC system equipment. Overall, fluids R1234ze and R142b demonstrated the best performance, as reflected in the objective function value, while exhibiting a condensation pressure below 3 bar.

Bekiloğlu et al. [241] screened 28 hydrocarbons based on their performance on two objective functions: the total heat-exchanger area and the maximum performance factor. Both objective functions considered implicitly the economic cost for equipment purchase and installation costs. A larger maximum performance factor indicated higher power generation from a smaller turbine. An iterative radial-inflow turbine design procedure was employed that determined the geometric features of the turbine in order to achieve operation within a desired regime and maintain the power losses due to friction and irregular flow patterns contributing to pressure losses within an acceptable level. Therefore, the direct impact of the working-fluid properties and behaviour was taken into account.

Meroni et al. [247] investigated the employment of multi-stage axial expanders for the evaluation of 11 working fluids. A sequence of optimisation steps that considered multiple expander stages was incorporated into the design procedure. For a conventional expander design, the ideal turbine was characterised by a two-stage configuration with supersonic converging nozzles and post-expansion. For a more extreme expander design, the ideal obtained choice was a single-staged supersonic converging–diverging nozzle with an achieved Mach number up to 2.

Lampe et al. [273] presented a holistic approach for the optimal selection of working fluids in ORC systems by considering a CAMD approach using group contribution and the PC-SAFT EoS to provide

the thermodynamic properties. A 1-D radial-expander model was incorporated into the design and the performance simulation of the ORC system for each working fluid that was generated by CAMD. The optimisation framework offered an integrated approach that can evaluate in a systematic way the interactions among the working-fluid properties, the thermodynamic features of the overall ORC, and the aerodynamic conditions of the expander for a very large set of fluids.

Bahadormanesh et al. [280] investigated the impact of mechanical vibrations in the radial expander on the optimal ORC design considering four pure organic refrigerants. The MOO approach that was employed considered the thermal efficiency of the cycle and the performance of the radial expander with respect to its size. The developed tension and vibrations in the radial expanders were explicitly considered in the optimisation problem as constraints, and their impact on the optimal solution was thoroughly explored. The trade-offs between thermal efficiency and expander size enabled the calculation of superior expander-design solutions.

Han et al. [249] and Li et al. [246] investigated the selection of working fluids under both constant and variable turbine efficiencies. Turbine efficiency may change due to variations in the operating conditions induced by hot-source temperature drifting. To this end, a turbine model accounting for losses due to friction, leakage, and other peripheral turbine features is absolutely necessary. Energy losses based on the relative velocity ratio and, subsequently, the geometric configuration of the turbine was estimated. Han et al. [249] considered exergy and thermal efficiency in addition to the cost per kW, whereas Li et al. [246] assessed exergy efficiency and total system cost, both within a MOO framework. Optimal working-fluid selection was influenced by the employed turbine-efficiency model. However, more-realistic conditions were considered with the variable turbine-efficiency approach. Han et al. [249] showed that cyclic and aromatic hydrocarbons were superior to chained hydrocarbons in performance, whereas Li et al. [246] identified highly performing fluorohydrocarbons. Peng et al. [263] compared the off-design performance of an ORC with a transcritical CO_2 power cycle in single-stage axial turbines. Mean-line model and velocity triangles were used for the geometric design of the axial turbines and the estimation of the off-design expander efficiency. The CO_2 power cycle exhibited a higher efficiency and improved ability to cope with the off-design operation.

In one of the limited number of studies that involve a detailed multi-dimensional expander model, Gad-el-Hak et al. [270] employed a numerical model that solved the Reynolds-averaged Navier–Stokes equations coupled with the k-ω turbulence model and a non-ideal EoS for the prediction of the thermodynamic properties. A relationship between isentropic efficiency and blade speed ratio was derived from the numerical implementation of the experimentally validated radial expander model. Zeotropic mixtures of R600a/R245fa at some concentrations showed an improvement in the efficiency in the range of 1.15 % to 1.6 %. Off-design operation increased the incidence losses in the expander due to irregular incidence angles in the rotor. However, the performance can be corrected to design levels by proper adjustment of the nozzle guide geometry. Wang et al. [271], through a similar approach, compared the performance of R245fa and an R245fa/R134a mixture in a radial expander by a set of rigorous CFD simulations and parametric sensitivity. Higher power output by more than 9 % and isentropic efficiency by about 2.5 % were achieved with a lower mass flow rate for the zeotropic mixture.

On a similar track, Jubori et al. [245] implemented rigorous simulation for the performance assessment of five organic fluids in low temperature (< 100 ℃) ORC systems. The investigation was performed for an axial and a radial inflow expander. It was shown that the key operating and design parameters that have a strong impact on the expander performance are the rotational speed, the expansion ratio in the cycle, the associated mass flow rate, and the expander size. A thermodynamic model and a mean-line model allowed the provision of the geometric characteristics of the turbine, whereas a

CFD model enabled an accurate expander-performance prediction for a wide range of the operational regime. Isopentane exhibited the highest efficiency, and in general, the axial turbine was smaller in size than the radial-inflow turbine. Jubori et al. [248] extended the work to include MOO in the design of the expander. CFD simulations were used in conjunction with a design space-filling technique to develop a response surface that acted as the surrogate model for the expander system. Nozzle and rotor-blade geometry, as defined by blade angle and blade-thickness distributions, were optimised for isopentane and R245fa based on efficiency and aerodynamic performance criteria. An impressive enhancement of more than 10 % in the overall efficiency of the expander was observed for both fluids. The optimal expander design was subsequently incorporated into the overall ORC system design.

As the model detail for the expander increases, the complexity of the optimisation problem becomes prohibitive from the computational point of view. The latter is more pronounced when working-fluid selection decisions are to be determined. An approach to tackle such a burden is the employment of simplified mathematical models that, however, encompass the fundamental relations and interactions between the key operating conditions and the performance indicators of the ORC system for accuracy in predictions. Neural networks and other data-driven modelling techniques that act as surrogate models have been widely utilised in the optimisation of ORC systems [180,248,284, 285]. For example, Palagi et al. [284] considered the development of a neural-network model that, apart from the thermodynamic ORC model, included a detailed model for an in-flow radial expander. Different architectures were tested, including a shallow network with 20, 50 and 100 neurons in the hidden layer and a deep network with two hidden layers, 30 neurons in the first layer and 10 in the second. The deep network exhibited the lowest error in all the used training sets. The neural-network model greatly facilitated the computational effort for the optimisation. The approach was implemented for one working fluid. Kim et al. [286] also developed a neural-network model for an in-flow radial expander. The model was fitted using experimental data. A deep network was used with two hidden layers. Different numbers of nodes per layer were tested, ranging between 10 and 30. The highest accuracy was attained when the first layer included 30 nodes and the second 10. A single fluid was used here too. The use of such surrogate models for the assessment of working fluids would require the development of as many training data sets as the number of fluids under consideration. Of critical importance is the accuracy of the developed data-based model, which depended on the quality of the training data set.

3.4.2. Heat exchangers

The heat-exchanger sizes are strongly dependent on working-fluid properties, *e.g.*, critical pressure, molecular weight, thermal conductivity, density, and the heat capacity [147]. The cost of heat exchangers in an ORC is a significant part of the cycle capital cost, and this is reflected in the proposed use of the ratio of ORC heat exchanger (HEX) area to ORC net power to produce an economic performance metric [287]. Bernal-Lara and Flores-Tlacuahuac [171] show that this cost may be up to 60%–70% of the total capital cost (with the rest being mainly from the turbine) for low thermal efficiencies of 1%–2%, respectively. It decreases to 45% for a thermal efficiency of 10%, with the contribution of the turbine capital cost exceeding 50%. The modelling of HEXs as part of ORC design has therefore received considerable attention. Both shell-and-tube, as well as plate HEXs, have been modelled in ORC studies. Key features of the HEX models used in different publications are shown in the Appendix (Table A.4).

Heberle and Brüggemann [155] investigated a layout with a preheater and evaporator, where the aim was to calculate the surface area. All the geometric parameters of the HEXs were pre-specified. Wang et al. [156] investigated a layout with three zones in the evaporator and two zones in the condenser, with the aim of determining their surface area. Details were not disclosed, but the employed heat-transfer coefficient correlation indicates that a shell-and-tube type HEX was

assumed. Each HEX was discretised in 30 finite elements to calculate heat transfer under the assumption of constant properties at each element. Andreasen et al. [161] provided more details about the heat exchangers, where the shell-and-tube geometry (including angles of tubes in their relative positioning) was used to calculate their surface area and pressure drops. Discretisation in 30 control volumes was performed in this case, too.

Oyewunmi and Markides [162] developed a model of shell-and-tube HEXs with two zones in the boiler and the condenser. Heat-transfer correlations were considered, with 100 segments of the variable size used for each HEX. The calculations included pre-specified geometric parameters and correlations for turbulent flow boiling of the mixtures. Noriega Sanchez et al. [163] used the logarithmic-mean temperature approach to determine the conductance and mentioned that the HEX were discretised to perform the heat balances.

Among the researchers who included the determination of both the mixture composition and concentration in their studies, few performed HEX calculations. Satanphol et al. [169] used HEX models from ASPEN Plus, assuming constant heat-transfer coefficients. Lee and Mitsos [170] modelled rigorously only the condenser, due to the needs of their application on LNG cold-energy recovery. They used 100 segments in the problem with the GA solver and 19 segments in the final subproblem of the NLP formulation (*cf.*, Section 3.1). Bernal-Lara and Flores-Tlacuahuac [171] calculated the surface area of the HEX, using correlations in the shell and tube sides for the heat transfer and pressure drops, for pre-specified geometric characteristics.

Studies are further reviewed that include the selection of pure fluids, with a focus on cases where geometrical characteristics of the HEX and their types are accounted for. Lecompte et al. [250] evaluated different pure fluids in an approach where the optimum part-load and year-round operation of the ORC were determined in a step-wise procedure. Pierobon et al. [251] presented a work where fluids from a pre-specified set were used as options in an optimisation algorithm that optimised the ORC and the geometric features of the HEX simultaneously. An MOO GA algorithm was used where 20 fluids were design options, together with the condenser outlet pressure and pinch point, the recuperator pinch point, the minimum temperature difference of the economiser and the vaporiser, the turbine inlet pressure, the superheating temperature difference and the target velocities in the tube and shell sides of the HEX. These velocities were determined by using the outer tube diameter, pitch, and baffle spacing as design variables in a separate, simplex direct-search algorithm that provided an optimum result for every vector of the ORC operating variables that was handled by the GA.

Tian et al. [264] investigated the performance of a few mixtures in a dual-loop ORC, where the geometric features of the employed shell-and-tube HEX were pre-determined. The number of tubes was manipulated in the parametric investigations in order to satisfy the pressure-drop constraint. Di Battista et al. [252] used a shell-and-tube HEX for the boiler, a plate-and-frame HEX for the recuperator, and a plate-and-tube HEX for the condenser. The latter was the same as a conventional car radiator. The plate-and-frame HEX enabled low minimum temperature approaches in smaller dimensions.

In Li et al. [281], the key feature was the method for the evaluation of the pressure drop. The calculated HEX pressure drop was used to iteratively update the cycle calculations until a threshold was met in the pressure-drop predictions between consecutive iterations. Different shell cross-sectional area sizes were also investigated. Huster et al. [180] developed an ANN for fluid–ORC system optimisation. The ANN was derived from a full-scale model where the moving boundary model (MBM) was used for the HEX, whose length was a design variable.

While the above studies included geometric features of the HEX as design variables, in several studies fixed HEX geometries were used. Le et al. [272] considered a shell-and-tube HEX, including equations to predict fouling. The discretisation of the HEXs in the case of two-phase

flows indicated that 50 segments were sufficient, as larger numbers up to 350 segments improved the predictions by less than 1 %. Yang et al. [253] investigated a dual-loop ORC with few pure fluids. A fin-and-tube type HEX was selected to recover heat from high-temperature flue gases, whereas plate HEXs were proposed for the intercooler, condenser, preheater, and second evaporator.

Wang et al. [254] used plate HEXs for all the heat-transfer processes. Rosset et al. [255] used HEX models in six ORC configurations to exploit engine waste heat, with all using an air-cooled condenser and a regenerator. The configurations included single-source heat using the engine coolant, single-source heat using exhaust gases, dual-source heat with series evaporators, dual-source heat, dual-regeneration with series evaporators, dual-source heat with parallel evaporators and dual-source heat, dual-pressure with parallel evaporators.

Jankowski and co-workers [256,257] proposed the use of plate HEXs, considering discretisation of 1000 finite elements in the two-phase regions. Bianchi et al. [258] used the moving-boundary model (MBM) for the HEX. In this case, the HEX had only three zones, whose limits were determined spatially by the phase-change features of the fluid.

The above studies refer to steady-state simulations; few of them contain explicit mention of the use of an MBM. This model is mainly used for dynamic modelling, but the division of the fluid flow in control volumes that equal the number of states (*e.g.*, subcooled, two-phase, and superheated-vapour) corresponds to a moving-boundary approach in steady-state [180]. The difference with the dynamic implementation of this model is that the size of the control volumes varies in time during transient operation, following the saturated-liquid and the saturated-vapour boundaries [288]. Another model that is used for dynamic HEX modelling is the finite-volume model (FVM). This consists in discretising the HEX volume into a number of equal and constant control volumes [288].

Grelet et al. [259] employed the FVM, where the HEX representation was based on discretisation into a number of longitudinal lumped volumes of equal length. In each volume, there were three zones; one representing the fluid state in the internal pipe, one representing the state of the metal of the pipe wall, and a final one representing the fluid state in the external pipe. Therefore, discretisation was implemented both horizontally and vertically.

Shu et al. [260], Wang et al. [261] and Chen et al. [268] employed the MBM in fluid-assessment studies. Cai et al. [269] compared the MBM and the FVM based on results from an experimental rig for a mixture at different concentrations. The authors noted that five ordinary differential equations need to be solved at each volume in the FVM, indicating that the need for multiple segments would increase the size and complexity of the simulations compared to the MBM, which only requires three segments. Both models matched the transient experimental results in the evaporator sufficiently, but the MBM simulation could not continue in cases where the superheated state disappeared during the experiment.

Zarogiannis and co-workers [265–267] further employed the FVM for the boiler and condenser. The surface areas of the HEX were design variables, together with other cycle parameters, in a challenging mixture-selection and optimum-ORC control problem. Pili et al. [262] employed the MBM for the boiler and considered several geometric parameters as design variables for the dynamic ORC performance assessment of pure fluids (see Table A.4, in the Appendix).

3.4.3. Key observations

Expander modelling is of paramount importance for the prediction of the overall ORC efficiency and performance. Working-fluid thermodynamic properties influence the conditions in the expander for a given set of geometric configurations. The proper adjustment of such configurations for optimal operation can be achieved through a combination of empirical strategies and systematic optimisation procedures. Since expander performance can significantly deteriorate at

off-design operating points, it is necessary that an optimisation procedure takes into consideration both the range of possible operating conditions and the frequency that such conditions will occur during the life span of the system. In this way, a robust expander performance can be achieved without the extra costs of overdesign. Truly, 3-D computational models offer good accuracy in expander-performance predictions, but the computational burden that is associated with such models is large, and their use in optimisation studies is prohibitive. However, 3-D expander models can provide a simulation test-bed for the generation of numerous datasets for various working fluids and geometric configurations that will enable the development of surrogate models for reliable performance predictions. The key challenges are the determination of the degree of model resolution for 3-D simulations to obtain accurate performance predictions, preferably validated in experimental test rigs, and the generation of sufficiently large data sets for the development of high-fidelity surrogate models.

In the case of HEX modelling, the MBM has been mentioned in both dynamic and steady-state simulations. The FVM has been used in dynamic simulations but has not been mentioned explicitly in steady-state simulations, although the discretisation rationale was similar to that of the dynamic implementation of the FVM. Xu et al. [289] noted that the computational effort of the MBM is lower because the model equations are solved only in three segments (*e.g.*, preheating, evaporation, and superheating in the boiler), whereas multiple segments are used in the FVM model. The downside of the MBM is that numerical challenges appear when one or more fluids in a mixture disappear from one of the phases or when different phases (*e.g.*, vapour or liquid) or states (*e.g.*, superheated fluid) disappear. Such problems were also reported by Cai et al. [269], who further compared predictions from the MBM and the FVM with experimental data and observed insignificant differences in both cases, despite the fact that the MBM is a lumped model. The number of segments selected in the FVM affects the attained accuracy. Xu et al. [289] reported errors that decrease from 10.5 % to 0.9 %, as the number of segments increases from five to 30.

In ORCs, system simulations rely on phase-equilibrium calculations that involve significant numerical challenges due to the appearance and disappearance of phases and states, especially as the number of mixture components and segments increases. In principle, the identification of a stable phase requires the global minimisation of the state function of interest, *e.g.*, of the Gibbs free energy. Such functions are usually nonconvex, and the identification of local minima results in states of metastable equilibrium, whereas the use of global optimisation incurs significant computational effort. To this end, advanced algorithms have been developed to address such issues, such as the Helmholtz free Energy Lagrangian Dual (HELD) algorithm [290] or the algorithm of Mitsos and Barton [291] that is also based on Lagrange duality. These algorithms are worth considering as a means of reducing the computational effort and of evaluating phase stability, formation of azeotropes, the appearance of minimum or maximum flash points, *etc.*, in ORC fluid selection and system design.

The two types of HEX that dominate the current literature are the shell-and-tube HEX and the plate HEX. The latter are more compact and enable better heat transfer at the expense of higher pressure drops [252]. This results in the need for higher pressure on the working-fluid side, higher backpressure on the heat-source side, and thus additional losses and costs if heat is to be extracted from flue gases; they are also susceptible to problems when used at higher temperatures or flows with particulates (*e.g.*, internal-combustion engines). Di Battista et al. [252] noted that shell-and-tube HEXs enable a reasonable trade-off between heat-transfer efficiency and pressure drop, while their costs are lower and their design is simpler. Different HEX types have also been proposed, such as the shell-and-louvered fin mini-tubes [292], the shell-and-tube HEX with plate baffles [293], the corrugated tube HEX with twisted tape inserts [294] or the tube-in-tube HEX with metal foam structures [295]. All these HEX types are worth investigating in the context of different fluids and ORC configurations.

The results attained by HEX models are affected by the use of different heat transfer correlations. Zhang et al. [296] investigated the effects of 8 two-phase heat transfer correlations, including 4 flow boiling and 4 flow condensation ones, in the operating, economic and environmental ORC performance. At design conditions they found that for different flow condensation correlations the relative difference between the maximum predicted condenser plate length and the minimum one is up to 103%, whereas different flow boiling correlations do not affect significantly the size of the evaporator. Under off-design conditions, they found that the net power output exhibits a relative difference of 1.1% for 4 different flow boiling correlations. Examining all combinations of the flow boiling and combination condensation correlations they reported that the relative difference of the electricity production cost is up to 11.2%, whereas the environmental performance, measured in total tons of CO_2 equivalents, changes by less than 1%. Deviations of similar ranges, due to the use of different heat transfer coefficients in the evaporator, were also reported by Calise et al. [297]. They additionally observed that for higher heat transfer areas the deviations are lower. These findings indicate clearly that the choice of the heat transfer coefficient incurs significant uncertainty and that systematic methods are necessary to address it, as discussed in the next section. If this uncertainty is not considered, then rankings of working fluids may change significantly depending on the choice of the heat transfer correlation or of other parameters with uncertainty, affecting especially those fluids that exhibit close performance and behaviour.

3.5. Uncertainty quantification approaches

In some studies on fluid selection sensitivity analysis has been employed to determine how certain cycle performance indicators change when different fluids are considered or when some cycle operating parameters change [19,298]. This is important as the performance of the fluids and the cycle may be affected by uncertainty in experimentally attained property values, in the underlying property- and process-prediction models, or by operating variability. The quantification of this uncertainty requires the use of approaches that can account simultaneously for the uncertain realisations of multiple parameters and systematically assess their effects on different performance indicators.

One such approach was presented by Papadopoulos et al. [141] to assess the effects of property uncertainties in the thermal and exergetic ORC efficiency, considering a set of mixtures that was identified as Pareto-optimum in computer-aided molecular-mixture design. The method included non-linear sensitivity analysis based on first-derivative information, where multiple parameter variations were propagated through the cycle model to determine their simultaneous effects on multiple performance indicators. Essentially, the proposed method quantified the sensitivity of the cycle performance indicators under changes in the multi-parametric space and determined the property parameters where the smallest variations incurred the highest performance changes. The results indicated that the performance of certain mixtures was sensitive to changes in property values such as the critical temperature and pressure, and the boiling point. Mixtures were also identified for which both the thermal and exergetic ORC predictions were robust, as they were not affected significantly by changes in the component property parameters. The approach was recently extended [299] by incorporating second-derivative information in the analysis and testing the robustness in the predictions of different EoS and activity-coefficient models under variability in property parameters. Sensitivity analysis based on second derivatives is vital in optimisation, as models that give rise to process state and performance profiles that are very non-linear may be avoided. The approach was implemented in a vapour absorption refrigeration cycle and can be easily tested in ORCs.

Frutiger and co-workers [300,301] developed an advanced, Monte Carlo-based approach for uncertainty quantification and selection of

ORC working fluids. 1965 pure working fluids were initially investigated with respect to their performance in an ORC model. In the first stage, two ORC operating parameters were sampled from a uniform distribution using the Latin-hypercube method. Each fluid was simulated for each pair of sampled parameters, and the ones that satisfied specific ORC operating constraints were selected. The process variables giving the highest net power output were then selected for each selected working fluid. In the second stage, 400 samples were drawn from a normal distribution using a Latin hypercube for each one of the eight fluid parameters. Each sample was then simulated through the ORC at the optimal operating parameter values identified in the previous stage. The fluids were then rank-ordered based on their net power output, with their 95 % confidence interval. The work showed that the ranking of fluids differed significantly when property uncertainty was considered.

The above uncertainty propagation approach was extended to investigate the sensitivity of the Soave–Redlich–Kwong (SRK) [302] and PC-SAFT [303] EoS, when they are used in ORC simulations [304]. Uncertainties were quantified for the critical temperature and pressure, and for the acentric factor in SRK, for the segment diameter, the chain length, and the energy parameters in PC-SAFT and the Aly-Lee, ideal-gas heat-capacity coefficients [305]. The uncertain distributions of these parameters were then propagated through the ORC model. It was then observed that the departure functions of these EoS dominated the total uncertainties in the ORC performance predictions and that SRK incurred lower uncertainty in the simulation output.

Frutiger et al. [306] further evaluated the Monte Carlo sampling and the Morris screening techniques to estimate the effects of different fluid parameters in ORC power output. Uncertainties in critical temperature and pressure, acentric factor, molecular weight, and the Aly-Lee, ideal-gas heat-capacity coefficients were propagated through the ORC model using the Peng–Robinson [307] EoS. It was observed that the Morris screening technique was more reliable, as it did not require the assumption of a linearisable model, as in the case of Monte Carlo. However, Morris screening did not account for correlation and interdependencies of the fluid parameters, which need to be filtered out. It was found that the critical temperature and pressure and the acentric factor incurred higher changes in the ORC net power output than the other investigated parameters. Hence it is important to have accurate values for these parameters.

Santos-Rodriguez et al. [308] addressed the mixture selection and ORC design problem under uncertainty through a stochastic optimisation framework. Using a set of four pre-specified pure fluids, the goal was to determine the optimum number and concentration of the mixtures, together with the optimum ORC operating characteristics. The first stage addressed the perfect information problem, where the effects of the heat-source temperature on the mixture composition and concentration and on the cycle efficiency were determined. This provided parameter sensitivity information and a target of ideal performance. The stochastic optimisation problem was solved in the second stage, where the optimum mixture was found that maximised the mean cycle efficiency over a desired heat-source temperature range. The approach employed risk measures in the form of the variance and the conditional value-at-risk in the formulation of the stochastic optimisation problem to facilitate the optimisation search across the uncertain realisations. The results indicated that different mixtures could be identified depending on the considered uncertain parameters.

Observations that are similar to the above last statement were made in several of the reviewed works. Uncertainty may occur in the employed thermodynamic or process models (*e.g.*, in parameters such as fluid properties, transfer coefficients, *etc.*). The consideration of uncertainty during fluid selection is important, but the need to evaluate multiple uncertain realisations increases the computational effort. It is therefore important to be able to identify the parameters that incur the highest changes in the ORC performance indicators and avoid the ones that exhibit low sensitivity to changes. The latter would increase

the computational effort without any significant effect on the attained results. When uncertainty is represented through continuous distributions, the choice of the distribution sampling method is important. Uniform sampling is needed to ensure efficient representation of the continuous distributions and to avoid oversampling some distribution areas at the expense of others. There are various sampling methods, such as Latin hypercube (LatHS), Hammersley sequence (HSS), and Sobol sampling (SS) [309]. A recent study [309] on the use of such methods in optimisation under uncertainty of various linear and non-linear objective functions indicated that HSS performs best for up to 40 uncertain variables, SS for up to 100 variables, LatHS-SS for over 100 variables and LatHS-HSS for up to 250 variables.

The impact of using different heat transfer correlations has been clearly highlighted in the previous section, however the underlying uncertainties have not been accounted for in ORC optimisation systematically. The different approaches outlined above may enable the identification of both the heat transfer correlations and even specific terms included in each one of them, that incur the highest impacts in multiple ORC performance indicator simultaneously. This could greatly help identify which correlations or which correlation terms need to be improved through further experiments, as well as the areas of the parameter space in which such experiments need to take place. Furthermore, through some of the reported methods, the existing correlations may be used simultaneously during ORC optimisation to identify optimum system conditions and working fluids in view of the uncertainty in such correlations.

3.6. Fluid selection and ORC off-design assessment

The key features of approaches pertaining to the use of advanced techniques for off-design ORC performance assessment considering different fluids are summarised in Table A.5, in Appendix. Deviation from the design point in an ORC system can result from the effects of disturbances affecting the system (*e.g.*, drifting in the hot- and cold-source stream temperatures and flow rates, fouling in the evaporator and condenser, and so forth), and output power level changes. The direct result is a quick deterioration of the overall efficiency of the system. A control system aims to maintain the efficiency at the highest possible level for the operating set of conditions. Working-fluid properties are influenced by the changes in the operating conditions. Depending on the sensitivity of the fluid properties to such changes, the speed of response of the control system is affected despite the employed control algorithm and its tuning [310]. Lu et al. [311] exploited this fact and proposed a concentration adjustment to the working fluid, a mixture of R245fa and R113, whenever the ORC system was in off-design operating regime. In this way, the temperature glide could be manipulated by altering the proportion of the most volatile to the least volatile components in the mixture so that the overall efficiency is maintained within the acceptable range.

Mavrou et al. [312,313] selected four novel and one conventional fluid mixture that exhibited high steady-state performance from the prior work of Mavrou et al. [314,315], to investigate their operability performance under the influence of disturbances. A systematic approach was used, where numerous disturbances were propagated simultaneously through a non-linear, equilibrium solar ORC model to investigate their impacts on multiple performance indicators. The overall design goal was to minimise a sensitivity index, expressed in the form of a control performance index that minimised the distance of the controlled variables (e.g. work output) from the desired operating set-point and the use of resources to bring the system back to its set-point. The authors did not consider dynamic models but highlighted in a systematic way, by considering a series of steady-state simulations, the importance of considering variability as part of working-fluid selection.

Chatzopoulou et al. [316] employed an approach that combined an optimisation algorithm with part-load operation. Initially, the authors addressed the optimum sizing of the components of an ORC under

steady-state operation. Subsequently, they optimised the operating conditions of the cycle, for the identified optimum cycle size, for a series of heat-source conditions. An interesting feature was how the simulation of the expanders was handled. The operating points generated by the optimiser at each iteration were introduced in expander maps to calculate updated isentropic efficiencies and mass flow rates. The iterations continued until the expander outputs matched those of the energy and mass balances.

Pang et al. [317] investigated the long-term operation of a 3 kW ORC under different control strategies for the pump head and, subsequently, the mass flow rate of the working fluid. They further developed a simulation model that could act as a platform for the determination of the optimal operational policies under off-design conditions. R245fa, R123, and their mixtures were systematically evaluated with a mixture achieving the highest system efficiency of 5.14 %.

Pili et al. [262] designed an ORC system for waste-heat recovery with an application for heavy-duty trucks that considered working-fluid interactions for a wide range of operating conditions. A dynamic model for the ORC with an incorporated control system consisted of one proportional-integral (PI) controller for the mass flow rate in the pump and one proportional controller for the exhaust by-pass valve in the evaporator. The time-averaged power generation of the ORC system was the criterion that was related to the off-design operation and closely linked to the controller performance. Toluene, followed by ethanol, exhibited the highest power generated, but the cost of the required installation of a vacuum system should be taken into account.

Zarogiannis [267] and Zarogiannis et al. [265,266] investigated the impact of different working fluids on the control system performance in an ORC system. A model predictive control (MPC) approach was developed to maintain the power output at the desired level. Dynamic models were utilised for the heat exchangers and pseudo-steady-state models for the pump and the expander in the ORC system. Novel and conventional hydrocarbon- and halogenated hydrocarbon-based mixtures were considered within an integrated framework featuring an ORC system model and a model predictive controller. Variation in the hot source streams was considered in the system where the employed MPC aimed to maintain the evaporator temperature at the desired level and achieve the maximum work in the expander. The simultaneous problem of working-mixture selection and ORC design under open and closed loop conditions was solved using the SA algorithm. It was proposed to deal with the design decisions through comprehensive criteria, which ensure the full inclusion of the underlying interactions simultaneously instead of the sequential design of individual parts of the cycle. The results provided significant insights into the behaviour of the ORC system under closed-loop conditions in view of different working media. For example, it was observed that the effort of the controller to compensate for the imposed disturbances is higher when the employed working fluid is sensitive to disturbances. A working fluid that is more resilient (less sensitive to disturbances) would be able to absorb disturbances of wider ranges without requiring significant effort from the underlying controller.

The integration of ORC design with the dynamic performance under closed-loop conditions for various working fluids and a wide range of operational conditions and disturbance scenarios is still at the initial stage of development. Even though expander and heat-exchanger models can capture the impact of off-design operation, the control system can alleviate such impact with the proper adjustment of the ORC system operation mode. Clearly, the effort of the control system to manipulate system operation depends on the ability of the equipment to accommodate the required corrective actions and the potential of the working fluid to absorb the effects of undesired deviations and favour high efficiency. The in-depth analysis of design decisions, as represented by equipment capacity, cycle configuration, and working-fluid selection, in accordance with the achievable dynamic performance has not yet been fully explored. For instance, the impact of the degree of over-design in equipment size on the ability of the system to quickly and

effectively compensate for disturbances needs to be carefully estimated in terms of cost for the design and economic benefit from minimising the time of operation away from the economic optimum. Optimisation-based controllers clearly provide insights into cycle operation in a direct link to the economics of the ORC system and could offer the solution to the outlined challenges.

4. Working-fluid property prediction

As discussed in the *Introduction*, the working fluid is an integral element of an ORC system, with a controlling role in determining its technical and thermodynamic performance. A key factor in ORC design is therefore the ability to provide accurate and reliable predictions of the thermophysical properties of the working fluid in conditions relevant to ORC operation, such as the changes in specific enthalpy and entropy undergone by the working fluid through each process in the overall cycle, as well its viscosity and thermal conductivity at each stage.

4.1. Empirical, highly accurate physical property models and their limitations

Highly accurate, empirical EoS have been developed for well-measured pure substances [318,319] and a small set of mixtures [320]. These models usually provide the most accurate representation of a species' physical properties if such a model exists for the substance of interest. Models of this class rely on the availability of sufficient experimental data and are not predictive in nature. Among the array of well-measured substances, it is possible to screen for ORC working fluids, whereas a wider design space of substances cannot be analysed. Further, highly accurate EoS can be used to unambiguously (concerning the static properties) determine the thermodynamic behaviour of a considered pure substance. In that sense, such models serve as a reference to assess other predictive models.

4.2. Models based on empirical group-contribution (GC) approaches

The philosophy of GC approaches is a simple one: properties of a substance are obtainable as a sum of contributions from appropriately designated chemical (functional) groups that together constitute the molecules of which the substance is comprised. GC methods are more successful for some physical properties and less so for others, which is caused by missing information of how functional groups are connected to one another. Both intra-molecular energies and inter-molecular energies (or the appropriate partition sums) suffer from the lack of detail on connectivity and proximity. For example, the effect of intra-molecular hydrogen bonding on the considered physical property cannot be properly predicted with a GC method. Making a distinction between a possibly incomplete description of intra-molecular energies and of inter-molecular energies rationalises why GC methods are rather successful for ideal-gas properties that only suffer from shortcomings in the representation of intra-molecular contributions but not by lack of effective inter-molecular detail.

An excellent summary of empirical GC methods is provided in the book of Poling et al. [321]; we note that an updated edition [322] of this classic text has recently been published. Another more-recent perspective on GC methods, in general, has been provided by Gani [323]. Lydersen [324] developed a successful GC method to estimate critical properties in the 1950s; his approach was later extended in the 1980s by Joback and Reid [64,325] to estimate a variety of pure-component thermodynamic properties, including (of particular importance in the context of ORC modelling) the critical pressure and temperature, the normal boiling temperature, the enthalpy of vaporisation (at the normal boiling point), and the temperature-dependent ideal-gas heat capacity, $c_p^0(T)$. In spite of their age, the Joback and Reid correlations remain especially popular; for example, they are incorporated in process-modelling software such as ASPEN PLUS [326] and

gPROMS [327]. They were adopted, together with the Riedel correlation [328] for saturation (or vapour) pressure, in the ORC CAMD work of Palma-Flores et al. [329]; these authors proposed a simultaneous product and process design method for waste-heat recovery using novel organic fluids, using "Rankine-like" cycles. They were also adopted by Lukawski et al. [330] in their development of molecular-property methods for assessing ORC efficiency. The early correlative approaches of this type (often referred to as first-order GC methods) were refined by Marrero-Morejón, Gani and co-workers [143,331,332] to incorporate isomerism and proximity effects through the introduction of secondary groups. For example, Lukawski et al. [330] found the second-order GC critical-temperature correlation of Marrero-Morejón and Pardillo-Fontdevila [332] to be more reliable than the first-order Joback and Reid correlation for cases where experimental values of normal boiling temperature were not available; more recently, Fanxiao et al. [333] found that the Marrero–Pardillo method provided for more-accurate exergy efficiency predictions of ORC systems (also reporting that PC-SAFT [144,303] (discussed below) performed better than either). Among the second-order approaches, the method of Constantinou and Gani [331] has become popular; this allows for the calculation of normal boiling point and melting point, critical pressure and temperature, and standard enthalpy of vaporisation at 298 K (among other pure-component thermodynamic properties). The approach has been used, for example, in the studies of Papadopoulos and co-workers [98,100,141,314,315,334–337]. In 2017, an extensive review of GC methods in the context of pure working fluids for thermodynamic cycles was undertaken by Su et al. [338]. These authors considered in turn thermodynamic (boiling temperature, critical properties, freezing temperature, enthalpy of vaporisation, isobaric heat capacity, density, and vapour pressure) and transport (viscosity and thermal conductivity) properties of interest, providing a near-comprehensive listing of GC methods available for each at the time of publication although, perhaps reflecting their relative infancy at the time, GC SAFT approaches were largely overlooked. These authors also discussed environmental, physicochemical and economic properties.

A weakness of empirical GC approaches is that their quality is constrained by the amount and quality of experimental data available for parameter refinement at the time of their development; any sort of extrapolation of their use, either in the context of their application to fluids not represented among the original data sets, or for predicting properties at thermodynamic conditions not considered during group development, is ill-advised; this could lead to inconsistencies in the treatment of different candidate working-fluid molecules, whereby care is required to ensure the selection of the most-appropriate correlations. Poling et al. provide useful comparisons for this purpose in relation to GC methods available at the turn of the millennium. In this context, we note that the contributions for the Joback and Reid $c_p^0(T)$ correlation were developed for temperatures from ambient to 1000 K, which should suffice for most ORC applications, but this range should be kept in mind should the low temperature of the cycle be below ambient. Recently, a statistical-mechanics-based alternative [339] has been proposed that retains better performance outside this temperature range, as well as providing a significant improvement in the case of halogenated compounds, for which the Joback and Reid approach suffers reduced accuracy [321,339].

GC approaches have also been developed for mixtures, initially focusing on activity coefficients in liquid mixtures. Indeed, perhaps the most important GC method historically is the well-known universal functional activity coefficient (UNIFAC) approach [65,340,341], that, together with its modifications, has been firmly established for many years.

4.3. Activity-coefficient models and cubic equations of state

Activity-coefficient models — in particular, local-composition activity-coefficient models, exemplified by the Wilson [342], non-random two-liquid (NRTL) [343], the universal quasichemical (UNIQUAC) [344,

345] models, and the GC variants, the analytical solution of groups (ASOG) model [346] and UNIFAC [65,340,341] – represent a route to thermodynamic properties of liquid mixtures that can be successfully applied in the case of working fluids. A useful discussion of the approach and its strengths and weaknesses (particularly in comparison to the use of EoS) has been provided in Chapters 5 and 6 of the book of Kontogeorgis and Folas [347]. The NRTL model has been employed for working-fluid modelling in the context of ORCs or related cycle devices [348–352] while UNIFAC has been used by Thierry et al. [278] in their work on simultaneous optimal design of multi-stage ORCs and working-fluid mixtures. However, in general, the approach has not been widely adopted in connection to ORCs and related systems.

In the context of CAMD, UNIFAC represents the most relevant of this class of model due to its GC nature allied to the substantial database of available parameters. Indeed, the feasibility of adopting GC approaches such as this rests on the availability of numerous adjustable parameters, which are obtained by adjustment ("fitting") using experimental data. Although, by now, the database of parameters available for UNIFAC is extensive, parameters for a particular group may nevertheless be unavailable, in which case the approach cannot be used — this is a problem that has its analogue in most GC approaches, including GC EoS (see below). We note, however, that recently, the challenge of missing UNIFAC parameters has been approached through the application of matrix-completion methods to predict the missing parameters [353].

The quantum-mechanical conductor-like screening (COSMO) methods, further developed by Klamt for describing real solvents (COSMO-RS) [354–356] offer a predictive alternative to activity coefficient models for the calculation of liquid thermodynamic properties. Despite their foundation in quantum mechanics, these methods possess adjustable parameters for size, short-ranged hydrogen-bonding energies, and element-specific van der Waals energies. COSMO-RS has been adopted in working-fluid screening for ORCs [148,216,357] and CAMD for chemical-engineering problems [358]. The more-transparent COSMO segment activity-coefficient model (COSMO-SAC) [359] has been adopted in ORC modelling [360] but, so far as we are aware, not yet in a CAMD context. Recently, an open-source implementation [361] of three versions [359,362,363] of COSMO-SAC has been made available by Bell and co-workers, together with an excellent exposition of the approach [364], which will make it a convenient option for use in future research.

In a recent ground-breaking enterprise, Winter and co-workers [365,366] have introduced further predictive power to activity-coefficient methods for binary mixtures through the so-called SMILES-to-Property Transformer (SPT)–NRTL [366] approach, a transformer-based machine-learning model to predict concentration-dependent thermodynamically consistent binary activity coefficients and their corresponding NRTL parameters, based solely on simplified molecular-input line-entry system (SMILES) codes. (SMILES [367–369] refers to a systematic procedure for translating the molecular structure of a compound into a string of symbols that is easily interpretable in a computer code.) These authors introduced a pre-training step on synthetic property data sampled from COSMO-RS and a second, fine-tuning step, training on experimental data. They have provided NRTL parameters for 100 000 000 mixtures with more than 10 000 unique molecules, and have demonstrated superior performance from SPT–NRTL compared with COSMO-RS and UNIFAC in most examples considered. There is clear potential for this approach in the design of binary-mixture working fluids for ORCs.

A drawback with the activity-coefficient or COSMO-based approaches is that one is obliged to adopt, in tandem, a different approach to obtain vapour-phase properties; care must therefore be exercised to ensure thermodynamic consistency. Typically, a cubic EoS is employed. For example, Thierry et al. adopted the SRK EoS [302] (for pure components) and the predictive-SRK (PSRK) [370] (for mixtures) together with UNIFAC; in the investigations of Preißinger and co-workers [148,216,357] the COSMO-RS theory was combined with a generalised Patel–Teja equation [371], while Xu et al. chose the Peng–Robinson

EoS [307] in their study with COSMO-SAC. We note that this type of combined approach is becoming more accessible to researchers outside the field of fluid-thermodynamic modelling with the emergence in recent times of open-source software, such as FeOs [372], that of Bell and co-workers [361,364,373], Phasepy [374], and Clapeyron.jl [375,376], wherein the Wilson, NRTL, UNIFAC and COSMO-SAC approaches, as well as a wide variety of EoS (both cubic and SAFT) have all been implemented and can be straightforwardly combined.

GC activity-coefficient methods such as UNIFAC, as well as the COSMO approaches, are well suited to a CAMD framework, however this may not be true of the equation (or equations) of state with which they are paired. For the approach to be completely versatile these EoS should also be amenable to application within a GC strategy.

Within the framework of EoS modelling of fluids, GC approaches evolved initially in relation to mixture calculations using cubic EoS through so-called EoS/G^E mixing rules. The link to GC approaches was through the incorporation, within the mixing rules, of activity coefficients that could, for example, be obtained from a GC approach, such as UNIFAC. The first of the EoS/G^E mixing rules was developed by Huron and Vidal [377]. Improved EoS/G^E mixing rules were later introduced by various researchers, including Michelsen and co-workers [378–380], and Wong and Sandler [381]; the PSRK EoS [370] is an example that falls into this category. Later, adopting a slightly different philosophy, a GC approach was introduced that enables the prediction of the binary interaction (or "k_{ij}") parameter used in mixture combining rules to characterise the unlike (cross) attractive EoS parameter [382,383]. Each of these two strategies confers predictive power on cubic EoS that had hitherto been largely correlative, thereby allowing for their use in the design of working-fluid mixtures.

More recently, GC approaches have been applied to pure-component modelling with cubic EoS in the context of ORC modelling. The use of standard cubic EoS such as SRK [302] or Peng–Robinson [307] requires prior knowledge of the critical temperature, T_c, and pressure, p_c, (to evaluate the EoS parameters a and b), and the acentric factor, ω (for the evaluation of the α function). GC methods are available for each of these and, by extension, can be used collectively for cubic EoS. For example, Chen et al. [384] recently applied the Peng–Robinson and the volume-translated Peng–Robinson (VTPR) [385] EoS in a CAMD study pertaining to ORC working fluids. Following Peng et al. [386] these authors used the GC methods of Su et al. [387] for T_c, p_c, ω and c_p^0, together with the GC method of Nannoola et al. [388] for the critical volume, V_c, which is required in addition for the VTPR EoS. The approach was tested on four commonly used working fluids, R245fa, R600a, R601a and R1234ze(E); in terms of the predicted thermodynamic properties it was observed that, although the deviations (from REFPROP [389] data) were higher than those obtained when using the Peng–Robinson and VTPR EoS parameterised in the conventional way, they were nevertheless within acceptable limits.

4.4. Statistical associating fluid theory (SAFT)

In essence, when adopting a traditional cubic EoS, one is assuming that the fluid molecule can be adequately represented as a sphere (in particular, of a hard spherical core surrounded by a region of attraction); there is recognition neither of asymmetry in molecular shape nor of polarity in the underlying molecular model. A consequence of the former is that cubic EoS are not well suited for modelling large, highly non-spherical molecules; this may not be a concern since such molecules are unlikely to be encountered in the context of working fluids for ORCs. The neglect of polarity, however, is of more significance; in particular, no account is taken of the possible impact of intermolecular association (often important in the case of polar molecules, which are commonly encountered in working-fluid design). Thus, when adopting cubic EoS within CAMD, the relative success of the strategy is dependent on the nature of molecules designed; in this sense, cubic EoS are not naturally well suited for CAMD. By contrast, a

conventional SAFT EoS is more versatile; the adoption of a molecular model comprising instead a chain of spherical segments allows better recognition of molecular shape. The segments, which interact with each other via a pair potential (such as Lennard-Jones, or Mie), can also be furnished with "sticky sites" (sometimes described as "intermolecular velcro"), thereby accounting for association interactions, such as hydrogen bonding. Moreover, the EoS parameters each have a clear physical meaning in relation to this molecular model; this is a key feature in CAMD, facilitating searches in molecular parameter space.

The Helmholtz free energy of the fluid is expressed as a sum of contributions, each arising from different features of the underlying molecular model, making the SAFT approach highly adaptable, as is reflected in the number of versions that have become available since the first SAFT equation [66,67] was introduced by Gubbins and co-workers, including soft-SAFT [390], SAFT-VR [391,392], PC-SAFT [144,303] and SAFT-VR Mie [145]. (We note that implementations of all the major SAFT versions are available open-source, together with coded algorithms for their use [372,375,376]). The inclusion of extra contributions in the free-energy expression has allowed the development of SAFT EoS for fluids of polar molecules [393–405], and of electrolyte solutions [406–418]. The extra versatility of SAFT, compared to cubic EoSs, comes at the price of greater computational expense. The majority of the increased computational cost comes from the evaluation of the association contribution, which includes numerical calculations (of the bonding volume and degree of association). In addition to the extra computational cost, a greater burden is placed on the numerical solvers when solving, for example, for fluid-phase equilibrium, so that robust solvers are required.

The first contribution to the free energy in any SAFT equation is the ideal free energy, A^{IDEAL}. However, strictly speaking, the evaluation of this contribution is *not* made using the SAFT theory, which provides only the residual (or non-ideal) part of the free energy; this subtlety is often overlooked or misunderstood. In practice, the ideal contribution is usually "backed out" from the ideal-gas heat capacity, whereby the user is required to choose the source of c_p^0 appropriate to the problem at hand — just as one would when using, for example, a cubic EoS; typically the Joback and Reid [64] correlation is adopted. (In some commercial software in which SAFT is implemented, the ideal contribution is hardwired; this may have contributed to the confusion over its role in the theory.) The relative importance of the ideal contribution to the whole free energy can be high, even in the liquid phase. This can be assessed by comparing the ideal-gas and total heat capacities; for example, at ambient conditions the ratio c_p^0/c_p for water is $\sim 45\%$. The significance of the ideal contribution has been discussed in some depth by Walker and Haslam [339], and is illustrated in Fig. 14, using n-butane as an example fluid. The calculated (p, T) fluid phase diagram of n-butane is presented as a colour map depicting the ratio c_p^0/c_p; calculations were performed using (in this case) SAFT-γ Mie [79] (the GC analogue of SAFT-VR Mie [145]), incorporating the c_p^0 model of Walker and Haslam [339]. One can see that the ideal contribution is dominant throughout much of the phase diagram, exceeding the residual contribution even throughout much of the liquid region. This emphasises the need for, at least, an awareness of the characteristics and range of applicability of the adopted correlation for c_p^0.

In the context of the current article, an important consequence of the adaptability of the SAFT approach is that SAFT equations are more suitable for CAMD modelling than, for example, their classical cubic counterparts. Bardow and co-workers [20,51,55,276,277,419–428] have exploited this in their pioneering CAMD work on ORC systems using PC-SAFT [144,303] (probably the most popular among the widely-used versions of SAFT), adapting the approach taken in related earlier work [57] on integrated solvent and process design. These authors showed that, by treating the PC-SAFT molecular parameters as continuous, they can be optimised together with other process parameters, searching for the optimal hypothetical working fluid (and corresponding ORC cycle). These parameters are mapped onto a database
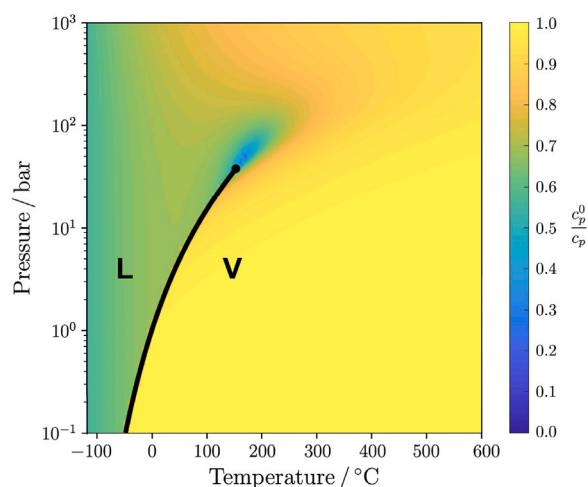
Fig. 14. Pressure–temperature colour map of the ratios between the ideal isobaric heat capacity and the total heat capacity of *n*-butane, as calculated using SAFT-*γ* Mie, incorporating the c_p^0 model of Walker and Haslam [339]. The black curve corresponds to the calculated saturation (vapour-pressure) curve, terminating at the critical point, represented by the black filled circle. "L" and "V" denote the liquid and vapour phases (respectively).
Source: Adapted from Ref. [339].

of parameters representing real fluids using an approximation of the process-based objective function to identify the best candidate working fluid. In subsequent work, the MINLP is solved using a GC approach both for the EoS and for transport coefficients [274,277,424,427,428]. Among other versions of SAFT, SAFT-VR Mie [145] has also found considerable use in the context of modelling ORC systems [18,89,193, 316,429–439]. Through the use of the highly adaptable Mie potential to represent the interaction between monomer segments, allied to greater sophistication in the statistical–mechanical foundation of the theory, this particular version of SAFT [145] was developed to provide improved descriptions of second-derivative properties, such as heat capacity and Joule–Thomson coefficient – properties that are highly relevant in the context of working fluids for ORCs and related devices – while retaining the all-round excellent description of traditionally targeted properties, such as fluid phase equilibrium and densities.

4.5. Group-contribution SAFT approaches

Conventional SAFT EoS such as SAFT-VR Mie and PC-SAFT – notwithstanding their innovative use in CAMD – are not, of themselves, GC equations. However, GC adaptions of these and other SAFT variants have been published; for a recent review see Shaahmadi et al. [440]. In some of these publications (Refs. [68,69,72,441–443] for PC-SAFT; Ref. [71] for original SAFT [67] and SAFT-VR [391]), GC approaches are introduced to characterise the (identical) segments of the *homonuclear* chain comprising the model molecule, after the fashion of a GC-based mixing rule for the molecular parameters [444]; the fluid properties are then evaluated using the existing SAFT theory. By contrast to these homonuclear approaches, in the GC-SAFT-VR [78], hs-PC-SAFT [444] and SAFT-*γ* [76,77,79] approaches, the GC concept is embedded within the SAFT formalism itself. A more-detailed molecular model is incorporated, wherein different types of monomeric segments are used to represent the individual chemical functional groups making up a molecule; the model molecule is, therefore, *heteronuclear*. A systematic comparison of a homonuclear GC PC-SAFT approach and a heteronuclear GC model showed that the heteronuclear leads to better correlation results [445]. Moreover, the retention of the functional-group information in the molecular model allows for the prediction of thermodynamic properties of mixtures based on pure-component

data alone [77–79,446], which can be an advantage. Markides and co-workers have pioneered the use of this class of GC-SAFT EoS in the context of ORCs or related systems, [146,275,447–451] adopting SAFT-*γ* Mie. As the GC analogue of SAFT-VR Mie, SAFT-*γ* Mie is particularly well suited for use in this setting. Recently, Rehner et al. [452] have been the first to use a heterosegmented GC PC-SAFT implementation [444] as the property-prediction model in a CAMPD application, highlighting the design of an ORC system as a case study. In another recent study, Rehner et al. [453] proposed a GC method for binary-interaction parameters for the homo- and heteronuclear GC methods for PC-SAFT. This advancement holds promise for enhancing the accuracy of mixture modelling in ORC CAMPD applications relying on PC-SAFT.

4.6. Equations of state informed by machine learning

Although a relatively new field, machine-learning (ML) techniques are already impacting thermodynamic-property prediction and have been applied to equations of state to improve their predictive power. For example, Chaparro and Müller [454] have developed an ML EoS by training a neural network on molecular-dynamics simulation data. In recent years, notable advancements have been made in leveraging ML techniques to predict EoS parameters. For example, Biswas et al. [455] presented a graph neural network that outputs the critical point and the acentric factor of a fluid, thereby providing a method to parameterise many types of cubic EoS. In pioneering endeavours, deep neural networks have been integrated to predict pure-component parameters of PC-SAFT, utilising either group counts [456] or extended-connectivity fingerprints [457] as inputs. In a comprehensive study, Felton et al. [458] evaluated various model architectures, with random forests emerging as the most accurate in predicting vapour pressures and liquid densities. However, these models encounter two primary limitations: firstly, the models are trained solely on pure-component parameters, failing to capture the sensitivity of the PC-SAFT model itself; secondly, the training of the models relies on existing databases of pure-component parameters, limiting applicability to molecules with adequate experimental data for parameter regression. To address these challenges, Winter et al. [459] recently embedded the PC-SAFT EoS directly into the training process of a transformer model. By doing so, the authors could train their SPT model directly on experimental vapour-pressure and liquid-density data, thereby capturing the PC-SAFT sensitivity on model parameters. The resulting SPT$_{\text{PC–SAFT}}$ model demonstrates remarkable performance, enabling the prediction of pure-component parameters from SMILES codes with an average percentage deviation of 13.5% for vapour pressures and 3% for liquid densities. Given the necessity of SMILES codes for model input, integrating the SPT$_{\text{PC–SAFT}}$ model into CAMPD for ORC systems would require a derivative-free optimisation algorithm (for details, see Section 5.2).

4.7. Prediction of transport coefficients

Transport coefficients, such as viscosity, thermal conductivity, or diffusion coefficients, play a significant role in determining ORC equipment dimensions, and thus the cost of the ORC system. Any meaningful objective function thus relies on sufficiently accurate estimates of transport coefficients [274]. GC models were developed for shear viscosity [64] and for thermal conductivity [460], although limited to liquid phases or to vapour phases [461]. Transport coefficients, like the viscosity $\eta(T, p)$ are functions of state variables temperature and pressure, or temperature and density. Models for transport coefficients are thus often based on input from thermal EoS, such as friction theory [462] or free-volume theory [463]. For constructing predictive models, the most successful approach is *excess entropy scaling* proposed by Rosenfeld [464,465]. The approach is suitable for viscosity, thermal conductivity, and self-diffusion coefficients and is very simple to implement. In view of this it is perhaps surprising that it was neglected for a number of years before being taken up by Novak [466–470] and by
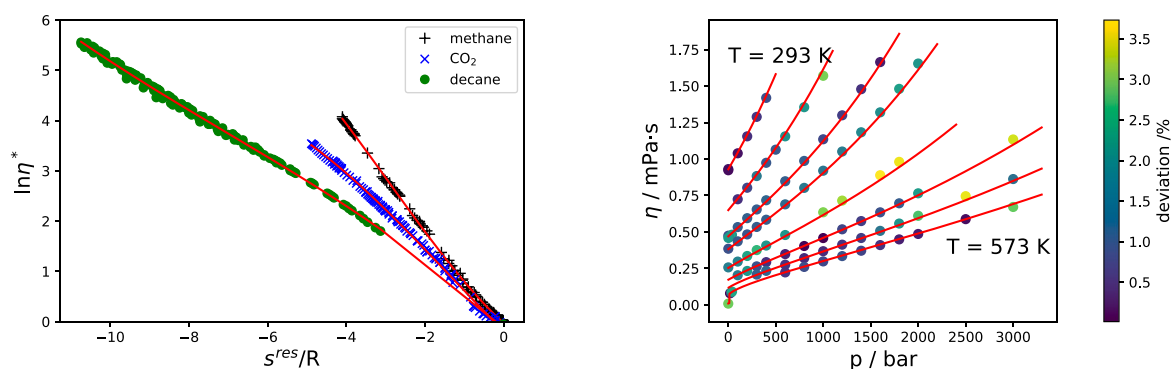
Fig. 15. Left: Logarithm of dimensionless shear viscosity η^* for methane, CO_2, and *n*-decane as a function of s^{res}/R. The curves represent cubic polynomials that correlate the experimental data [485] (symbols). The temperature and pressure ranges of the data are 91–450 K and 0.1–700 bar for methane, 219–500 K and 5.6–2600 bar for CO_2, and 289–709 K and 0.07–3000 bar for decane. Right: Viscosity of *n*-decane as a function of pressure for several isotherms. Experimental values [485] (symbols) and results of entropy scaling (curves) using the cubic polynomial from the diagram to the left. The symbol colour represents the model error for each data point.

Gross and co-workers [471–476]; subsequently the approach has been championed by Bell and co-workers [477–484].

Excess entropy scaling is based on the observation that transport coefficients, made dimensionless with a suitable reference value, are, to an excellent approximation, univariate functions only of residual (or excess) entropy s^{res}, with $s^{res}(T, \rho, x) = s(T, \rho, x) - s^{ig}(T, \rho, x)$, where s^{ig} is the entropy of an ideal gas. In Fig. 15, the principle of excess entropy scaling is illustrated for three substances (methane, CO_2, and *n*-decane). The left diagram gives experimental viscosity data η made dimensionless using a Chapman–Enskog equation, $\eta^* = \eta/\eta_{CE}$, covering a wide range of temperature and pressure. Simple Ansatz functions, such as low-order polynomials, can be used to correlate the logarithm of the scaled transport properties with residual entropy. The red curve of the left diagram (corresponding to *n*-decane) leads to the predictions (red curves) on the right diagram by back converting $\eta = \eta^* \cdot \eta_{CE}$.

Models for the shear viscosity [467,469] and self-diffusion coefficients [466] were proposed by Novak using the PC-SAFT EoS for the residual entropy s^{res}. Lötgering-Lin and Gross [471] developed a predictive GC method based on entropy scaling and PC-SAFT. For 100 pure species, the mean absolute relative deviation is about 5% for the entire fluid phase (*i.e.*, for vapour and liquid states); for three chemical families, the deviations are higher, reaching about 10%. Water is represented with deviations of 3.1%. In a subsequent study on mixtures, Lötgering-Lin et al. [472] determined a mixing rule from results of molecular simulations and applied the mixture model in a completely predictive manner to viscosities of real mixtures. For 566 mixtures (34,500 experimental data points), they obtained relative mean deviations of, on average, 6% for mixtures without hydrogen-bonding species. Deviations exceeded 10% for mixtures with hydrogen-bonding, indicating that such mixtures require an adjusted binary-interaction parameter ("k_{ij}") for improved results.

Thermal conductivity was studied by Hopp and Gross by parameterising pure substances individually [473] but also by a predictive GC method [475]. Both studies showed good agreement with experimental data for thermal conductivity, even for substances with strong hydrogen-bonds such as water and alcohols. Hopp et al. [474] proposed a model for the self-diffusion coefficients of pure substances. In practical applications, of course, one is interested in binary diffusion coefficients, say Maxwell–Stefan diffusion coefficients. Several approaches exist for estimating binary diffusion coefficients from self-diffusion coefficients [321,476,486].

In summary, entropy scaling has shown to be powerful in devising predictive models for transport coefficients. The ability to predict transport coefficients allows for a rough sizing and cost estimation of key process equipment, which in turn is a requirement for economic objective functions for process and working-fluid optimisation [274, 277,428].

4.8. Other properties

Other important working-fluid properties include environmental properties (ODP, GWP, flammability, and toxicity) physicochemical properties (molecular weight, stability against thermal decomposition, and chemical compatibility (with engine materials and, for example, with lubricating oil)); although not strictly fluid properties, both availability and cost may also be considered relevant in this context. The simplest approach is to exclude such properties from the CAMD itself, taking account of them instead in a post-processing step. For example, in a CAMD study for the selection of working fluids for refrigeration cycles, Essa and Mohamed [487] considered only fundamental thermodynamic criteria in the CAMD itself, considering the other properties in a subsequent step after generating a list of candidate molecules. However, GC methods are nevertheless available for all of these quantities, as discussed by Su et al. [338] in relation to pure (single-component) working fluids.

The flammability of mixtures has been discussed in Section 3.2.3, where it is noted that the prediction of this property requires vapour–liquid equilibrium calculations. For the flammability of pure components there are several GC methods that are either based on the prediction of the flash point [488] or on the calculation of upper and lower flammability limits [489–492]. The latter properties may be calculated by accounting for the oxidation reaction of generic formulas of organic compounds and for molecular characteristics such as the length of the carbon skeleton, the type of bonds in the molecule and others.

For ODP and GWP of pure components, there are GC methods available [338,488], although these are not comprehensive for all compounds. For example, GC methods are available for ODP of one- and two-carbon HFCs and HCFCs [493], and for one- and two-carbon CFCs [494]; the more-recent method of Al et al. [495] is applicable to CFCs, HCFCs, and haloalkanes. GC methods for predicting GWPs [495–497] are applicable to a somewhat wider range of species, although still focused on refrigerants and related fluids. In this context, we mention also GC methods for radiative efficiency [498,499], upon which the GWP is based.

In Section 3.2.3, we have mentioned the existence of holistic sustainability assessment frameworks that have been used in both CAMD [100] and CAMPD [188]. The first framework takes a cradle-to-gate approach, whereby the sustainability features of the fluids are calculated for both fluid production and fluid use. The calculations for the fluid use are based on pure-component properties, without accounting for the fluid quantities that are necessary and that may eventually vary the impacts of the fluids. In this context, the sustainability performance of the fluids is summarised into environmental, health, and safety scores which are calculated by various properties. The environmental score includes water- and air-mediated effects, accumulation into organisms and degradation in the environment of the chemicals. The

health impacts are associated with chronic toxicity, whereas the safety impacts are calculated from the mobility, fire potential, and acute toxicity of the chemicals. The sustainability performance during fluid production is used to assess the impacts of the production stage of the fluids and considers its cumulative energy demand, GWP, and eco-indicator 99 (EI99), which includes 11 properties that are associated with the environmental impact. The environmental impacts of chemical production were predicted from an ANN in this work [500], but they can also be predicted through a GC model [501], or machine-learning-based models [502]. A key feature of this work is a systematic approach to deal with data gaps in property models. In the absence of data, a data mining approach is used which deploys on-line similarity assessment against molecules whose properties are available or can be predicted through the employed models.

A cradle-to-grave approach for sustainability assessment in CAMPD has been demonstrated by Fleitmann et al. [188], in the so-called COSMO-susCAMPD framework. The authors demonstrate the approach for the integrated design of benign solvents and hybrid extraction–distillation processes. To capture the environmental impacts of solvent production, the authors integrate a predictive life-cycle-assessment (LCA) framework based on Kleinekorte et al. [502,503] into the COSMO-CAMPD framework, previously published by Scheffczyk et al. [504]. The predictive LCA framework is based on an ANN using molecular descriptors such as structure information or thermodynamic properties calculated from COSMO-RS. The environmental impacts of the solvent use are calculated using life-cycle inventory data directly obtained from the employed process model. The end-of-life of the solvent is modelled using an aggregated process model from the literature for wastewater treatment. The work highlights the importance of cradle-to-grave life cycle assessment in CAMPD for the design of environmentally benign fluids, as simplified cradle-to-gate or economic assessments alone can lead to suboptimal fluid selections. While the authors apply the COSMO-susCAMPD framework for a chemical-engineering application, the approach can be easily transferred to the design of working fluids for organic Rankine cycles.

In recent years, significant efforts have been observed for the prediction of various such properties through machine learning (ML) approaches. In typical GC methods, the property prediction model and the number of model parameters are fixed, whereas the latter are regressed through an appropriate algorithm. In GC-ML models, the number of parameters and the model structure are not fixed a priori [505]. There are various important properties that may be predicted through such methods, including toxicity, bioconcentration factor, auto-ignition temperature, photochemical oxidation potential, and others [506]. Purely ML-based models have also been developed for the prediction of the product carbon footprint of chemicals such as FineChem 2 [507], which has evolved from the ANN (FineChem) developed by Wernet et al. [500], or APPROPRIATE [502], which is based on Gaussian process regression combined with an encoder–decoder neural network.

5. Computer-aided molecular and process design for organic Rankine cycles

CAMPD for organic Rankine cycles aims to identify an optimal working fluid (or mixture) jointly with the corresponding ORC system that optimise an objective for a given ORC application. An optimal combination of working fluid and ORC system can be identified by directly linking ORC optimisation to a CAMD formulation. CAMD formulations allow for the *in silico* design of novel working fluids [134]. For this purpose, molecular building blocks are combined to molecular structures while still fulfilling chemical constraints. Thereby, a large molecular design space can be considered to select optimal working fluids. The link between a CAMD formulation and the ORC system model is most commonly established using GC approaches. In GC approaches, each functional group has a contribution to a certain

physical property or parameters used as input of a thermodynamic-property model (*cf.*, Section 4). By linking the ORC system optimisation to CAMD, working fluids can be chosen as a degree of freedom of the ORC system optimisation and designed simultaneously to the ORC conditions considering an objective function of the ORC system. Such an integrated design thus leads to an optimal combination of working fluid and ORC system for the considered design space (see Fig. 16).

5.1. General CAMPD problem formulation

The origins of CAMPD can be traced back to chemical-engineering problems, *e.g.*, aiming to identify optimal solvents for separation processes [508]. CAMPD problems are usually nonlinear due to the process and thermodynamic property models. Moreover, CAMPD problems generally include discrete degrees of freedom, *e.g.*, binary variables, to represent the molecular structure and the cycle configuration. Thus, mathematically, CAMPD problems can be formulated as mixed-integer nonlinear programmes [508]. A general MINLP problem formulation for CAMPD of pure molecules is given in Problem (1):

$$\min_{x,y} \ (f_1(x,y), f_2(x,y), \dots, f_k(x,y))^{\mathrm{T}}$$

$$\text{s.t.} \quad h(x,y) = 0$$

$$g(x,y) \le 0 \tag{1}$$

$$k(y) \le 0$$

$$x_{\mathrm{lb}} \le x \le x_{\mathrm{ub}} \quad \in \mathbb{R}^{\mathrm{n}} \times \mathbb{Z}^{\mathrm{m}}$$

$$y_{\mathrm{lb}} \le y \le y_{\mathrm{ub}} \quad \in \mathbb{Z}^{\mathrm{l}}.$$

The CAMPD model minimises a set of objective functions f_i of an ORC system. These objective functions are commonly either thermodynamic objectives, *e.g.*, the ORC thermal efficiency or net power output, or thermo-economic objectives, *e.g.*, specific investment cost or net present value. The objective functions depend on the cycle and equipment variables x and the molecular structure of the working fluid y. The cycle and equipment variables x can be continuous variables (*e.g.*, pressure levels or the degree of superheating after evaporation) or discrete variables (*e.g.*, the number of turbine stages or binaries describing the ORC configuration). The objective functions are minimised subject to equality constraints h and inequality constraints g and k. The equality constraints h represent the cycle and equipment models (*e.g.*, energy balances of the processes or sizing/costing correlations of the equipment) and the property model of the working fluid. The inequality constraints g represent design or operational limitations that ensure the feasibility of the application (*e.g.*, pressure limits or minimal approach temperatures) and limitations on molecular properties ensuring compliance with regulations or technical restrictions (*e.g.*, flammability or toxicity of the working fluid). The inequality constraints k represent the CAMD formulation and provide the structural feasibility of the working fluid during the molecular design, *e.g.*. For example, the octet rule prevents open bonds in molecular structures, while specific equations ensure the correct number of functional groups for ring structures or double bonds (for details, see Refs. [509,510]). The CAMPD problem in Problem (1) generally includes continuous and discrete degrees of freedom of the cycle processes and equipment x and the discrete degrees of freedom of the molecular structure of the working fluid y.

Solving the MINLP optimisation problem (Problem (1)) results in the optimal working fluid jointly with the optimal ORC system. Ranking the most-promising working fluids is usually beneficial to account for model uncertainties. Moreover, such a ranking enables assessing properties not captured within the integrated design due to missing predictive models (*e.g.*, chemical or thermal stability). The most-promising working fluids can be ranked by solving the MINLP repeatedly, considering additional constraints. The so-called integer-cut constraints prevent finding molecular structures identified in previous optimisations [511,512].
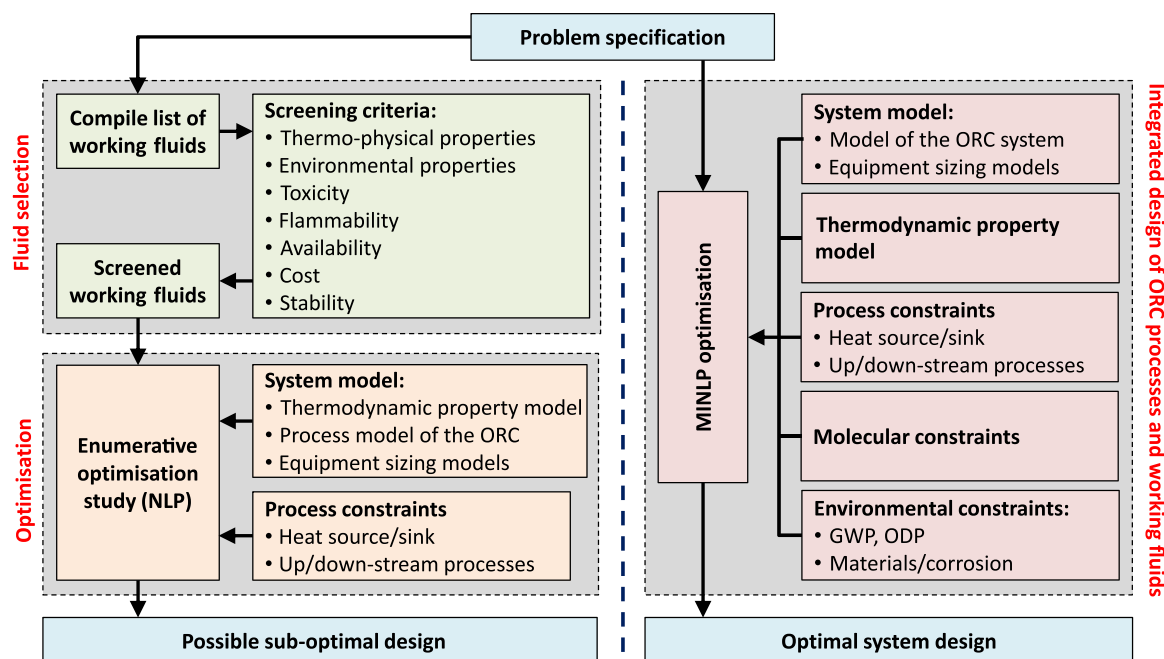
Table 4

Overview of CAMD and CAMPD methods proposed for the integrated design of working fluids for organic Rankine cycles.

Legend:

[a] Thermodynamic property model:
GC = group-contribution approach
EoS = equation of state

[b] Problem:
SOO = single-objective optimisation
MOO = multi-objective optimisation

[c] Solution Algorithm:
SA = simulated annealing
OA = outer-approximation
B&B = branch-and-bound
B&C = branch-and-cut
RO = robust optimisation
CMR = continuous molecular representation
GA = genetic algorithm

Category	Attribute	Papadopoulos et al. [98]	Palma-Flores et al. [137]	Andrés-Martínez and Flores-Tlacuahuac [514]	Lampe et al. [51, 419]	Roskosch and Atakan [516, 517]	Palma-Flores et al. [329]	Su et al. [488]	Cignitti et al. [518]	Frutiger et al. [519]	Schilling et al. [423, 424]	Wang et al. [523]	White et al. [146, 447]	Bowskill et al. [450]	Rehner et al. [452]	Lampe et al. [273]	Schilling et al. [274]	van Kleef et al. [275]	Schilling et al. [428]	Tillmanns et al. [526]	Schilling et al. [426, 427]	Tillmanns et al. [276]	Papadopoulos et al. [141]	Schilling et al. [277]	Rehner et al. [536]
Group		Molecular design (CAMD)	CAMD	CAMD	Integrated molecular and process design (CAMPD)	CAMPD	CAMPD	CAMPD	CAMPD	CAMPD	CAMPD	CAMPD	CAMPD	CAMPD	CAMPD	CAMPD	CAMPD	CAMPD	CAMPD	CAMPD	Integrated molecular and process design for transient operation	transient	Integrated mixture and process design (CAM^{b}PD)	CAM^{b}PD	CAM^{b}PD
	Objective function	Performance indicators based on physical properties	Performance indicators based on physical properties	Performance indicators based on physical properties	Thermodynamic	Thermodynamic	Thermodynamic	Thermodynamic	Thermodynamic	Thermodynamic	Thermodynamic	Thermodynamic	Thermodynamic	Thermodynamic	Thermodynamic	Thermodynamic	Thermo-economic + thermodynamic	Thermo-economic + thermodynamic	Thermo-economic + thermodynamic	Thermo-economic + thermodynamic	Thermodynamic	Thermodynamic	Thermodynamic	Thermo-economic + thermodynamic	Thermo-dynamic
ORC model	Thermodynamic model	After CAMD for selected fluids	After CAMD for selected fluids	After CAMD for selected fluids	integrated within design	integrated within design	integrated within design	integrated within design	integrated within design	integrated within design	integrated within design	integrated within design	integrated within design	integrated within design	integrated within design	integrated within design	integrated within design	integrated within design	integrated within design	integrated within design	integrated within design	integrated within design	integrated within design	integrated within design	integrated within design
	Process operation	steady-state	steady-state	steady-state	steady-state	steady-state	steady-state	steady-state	steady-state	steady-state	steady-state	steady-state	steady-state	steady-state	steady-state	steady-state	steady-state	steady-state	steady-state	steady-state	quasi-steady-state	dynamic	steady-state	steady-state	steady-state
	Equipment sizing	X														X	X	X	X	X		X		X	
	Costing	X															X	X	X	X				X	
	More than 2 configurations		X				X				X		Super-structure						Super-structure						
Thermodynamic property model	Equilibrium properties[a]	GC	GC	GC	GC-PC-SAFT	cubic EoS	GC	GC	GC + cubic EoS	GC + cubic EoS	GC-PC-SAFT	GC-PC-SAFT	SAFT-γ Mie	SAFT-γ Mie	Hetero-PC-SAFT	GC-PC-SAFT	GC-PC-SAFT	SAFT-γ Mie	GC-PC-SAFT	GC-PC-SAFT	GC-PC-SAFT	GC-PC-SAFT	GC + cubic EoS	GC-PC-SAFT	Hetero-PC-SAFT
	Transport properties[a]	GC	GC	GC													entropy scaling	GC	entropy scaling	entropy scaling				entropy scaling	
	Uncertainty analysis		X							X														X	
Solution	Problem[b]	MOO	SOO	SOO	SOO	SOO	SOO	SOO	SOO/MOO	SOO	SOO	SOO	SOO	SOO	SOO/MOO	SOO	SOO/MOO	SOO/MOO	SOO	SOO	SOO	SOO	MOO	SOO	SOO
	Strategy	Decomposition	Decomposition	Decomposition	Integrated/direct	Integrated/direct	Integrated/direct	Integrated/direct	Integrated/direct	Integrated/direct	Integrated/direct	Integrated/direct	Integrated/direct	Integrated/direct	Integrated/direct	Integrated/direct	Integrated/direct	Integrated/direct	Integrated/direct	Integrated/direct	Integrated/direct	Integrated/direct	Decomposition	Integrated/direct	Integrated/direct
	Algorithm class	Meta-heuristic	Deterministic	Deterministic	Deterministic	Deterministic	Deterministic	Generate-and-test	Deterministic	Deterministic	Deterministic	Generate-and-test	Deterministic	Deterministic	Deterministic	Deterministic	Deterministic	Meta-heuristic	Deterministic	Deterministic	Deterministic	Deterministic	Meta-heuristic	Deterministic	Deterministic
	Algorithm[c]	SA	OA / B&B	RO + OA	CMR + MIQP	r-algorithm	B&B		B&C	B&C	CMR + OA		CMR + OA	OA	B&B	CMR + OA	CMR + OA	GA	CMR + OA	CMR + OA	CMR + MIQP	CMR + MIQP	SA	CMR + OA	CMR + OA

proposed method identifies both conventional and novel working fluids outperforming working fluids proposed in the literature. Thus, the work highlights the advantages of CAMD for ORC working-fluid design. The multi-objective CAMD formulation is used to avoid the assumption that any particular pure-component property captures the ORC process performance drivers better than another. The considered properties are reasonable in terms of reflecting typical working-fluid requirements in the ORC, but they are not exhaustive, and the possibility of considering additional properties may not be excluded.

Palma-Flores et al. [137] analysed suitable physical-property targets to design working fluids for ORCs. Based on guidelines and rules for working-fluid selection, the authors defined four objective functions for the CAMD problem as combinations of molecular properties of the working fluid, *i.e.*, the enthalpy of vaporisation and the liquid heat capacity of the working fluid, and the Gibbs energy of formation of the ideal gas. The four objective functions are considered in individual single-objective molecular-design problems. Subsequently, the identified working fluids are assessed in detailed process optimisations for three cycle configurations. From the optimisations, the authors concluded that the most-promising working fluids can be identified for the considered ORC applications by minimising the liquid heat capacity of the working fluids because the heat duty in the evaporator is decreased.

Due to uncertainties in property prediction, Andrés-Martínez and Flores-Tlacuahuac [514] extended the work by an uncertainty analysis and a robust formulation of the linear constraints. Thereby, GC model uncertainties are considered during working-fluid design. The framework identifies working fluids that are robust against uncertainties in property prediction and different from those identified without considering GC model uncertainties.

The use of simplified cycle indicators based on physical-property targets enables the fast, straightforward, and robust design of molecular structures without the need for detailed modelling. The thermodynamic-property models that could be used to predict the desired physical properties may range from empirical models to robust EoS, such as SAFT (*cf.* Section 4). The molecular-design approaches described above result in promising working fluids compared to the traditional working-fluid selection, as shown by their subsequent performance assessment through ORC system simulations or in comparison with third-party investigations [148]. However, optimal target properties are typically case-specific, and defining proper physical-property targets thus requires experience with the investigated system and its specifications, which is often missing or unreliable. For example, the critical temperature of the working fluid should align with the maximum cycle temperature, which is influenced by the heat source temperature, to ensure the cycle operates in subcritical or supercritical conditions [98]. Typically, the rules and guidelines from the traditional working-fluid selection (*cf.*, Section 3.1) are used to define the physical property targets. However, knowing *a priori* which molecular property represents the ORC performance of a specific application most accurately in a single- or multi-objective optimisation is impossible. For chemical-engineering applications, Kossack et al. [515] have shown in early work that a single-objective CAMD approach may result in a different optimal solution than a CAMPD approach using a process-based objective. MOO formulations allow the capture of multiple physical-property targets and their trade-offs simultaneously, reducing the probability of excluding promising working fluids. However, even for MOO, it is challenging to know *a priori* how many and which physical properties precisely would capture the working-fluid behaviour in the ORC sufficiently. Considering different sets of objective functions or Pareto-approximation algorithms may affect the generated Pareto fronts, leading to the inclusion or omission of working fluids. Moreover, different pressures and temperatures are observed in the cycle depending on the working fluid. Such varying cycle conditions may not be captured by considering solely pure-component physical properties. These challenges can be tackled in an integrated CAMPD formulation considering an objective function that captures all trade-offs. Using an

ORC system model in a CAMPD formulation considers all necessary cycle processes and conditions, as well as heat transfer, and other phenomena in the ORC equipment while evaluating the working fluids using thermodynamic and/or sizing and economic indicators. In this context, CAMPD approaches may result in different optimal working fluids than CAMD approaches based solely on physical properties.

5.1.2. Integrated molecular and process design

The previously presented shortcomings of approaches based on molecular-property indicators can be overcome by considering ORC system-related objective functions for working-fluid design [48,337]. Thus, a substantial effort has been made in the last decade to solve the integrated molecular and process design problem as formulated in Problem (1). ORC system-related objective functions assess the performance of a working fluid within an ORC system and thus need reliable knowledge of the thermodynamic behaviour of the working fluid. The thermodynamic behaviour of a molecule can be estimated using predictive thermodynamic-property models (*cf.*, Section 4). Thermodynamic-property models link information on the molecular structure to the thermodynamic properties of a molecule. The thermodynamic properties can be used for ORC modelling, yielding ORC system-related objective functions. The employed thermodynamic-property model defines which model can be used and, thus, the objective function(s) and constraints of Problem (1). For example, a thermodynamic-equilibrium model enables the development of an ORC model based on phase equilibrium, mass, and energy balances, while additional models for transport properties are required for the sizing (and, if considering economic indicators, also the costing) of the equipment.

Integrated thermodynamic design with steady-state operation

A basic thermodynamic ORC model based on equilibrium thermodynamics requires equilibrium properties of the working fluid (*e.g.*, densities, enthalpies, or entropies) and, thus, a thermodynamic-property model (*cf.*, Section 4). In CAMPD for ORCs, most commonly, an EoS is used as the thermodynamic-property model combined with GC approaches to calculate the parameters representing a working fluid in the EoS from its molecular structure. A thermodynamic ORC model enables the consideration of thermodynamic objective functions (*e.g.*, the ORC net power output or thermal efficiency) and constraints (*e.g.*, limits on the pressure levels). Due to its simplicity, the first systematic design methods developed to solve the CAMPD problem for ORCs were focused on a thermodynamic ORC model.

In 2014 and 2015, Lampe et al. [51,419] proposed the so-called continuous-molecular targeting — computer-aided molecular design (CoMT-CAMD) approach for ORCs, which decomposes the integrated design problem in two subproblems (*cf.*, Fig. 17). The idea of the CoMT-CAMD approach originates from the work of Bardow et al. [57] on solvent selection for separation processes. Initially, the discrete fluid parameters are relaxed, representing the working fluid in the used thermodynamic-property model; here, the PC-SAFT EoS was adopted. The continuous molecular representation enables the identification of favourable working-fluid properties, so-called targets, by optimising the molecular parameters within an ORC optimisation. In a second step, real working fluids are identified with performance closest to the target either based on screening a database [51] or designing working fluids using CAMD [419,425] and homosegmented GC approach of PC-SAFT [445]. Importantly, the objective function in this second step approximates the objective used in the targeting step and does not simply aim to identify real working fluids with parameters closest to the target, as sometimes misinterpreted in the literature. The distance in parameter space depends on scaling and does not capture the different impacts of different properties on the objective. A detailed description of the solution strategy of the CoMT-CAMD method is given in Section 5.2.

Another decomposition method based on a continuous molecular representation has been proposed by Roskosch and Atakan [516] for
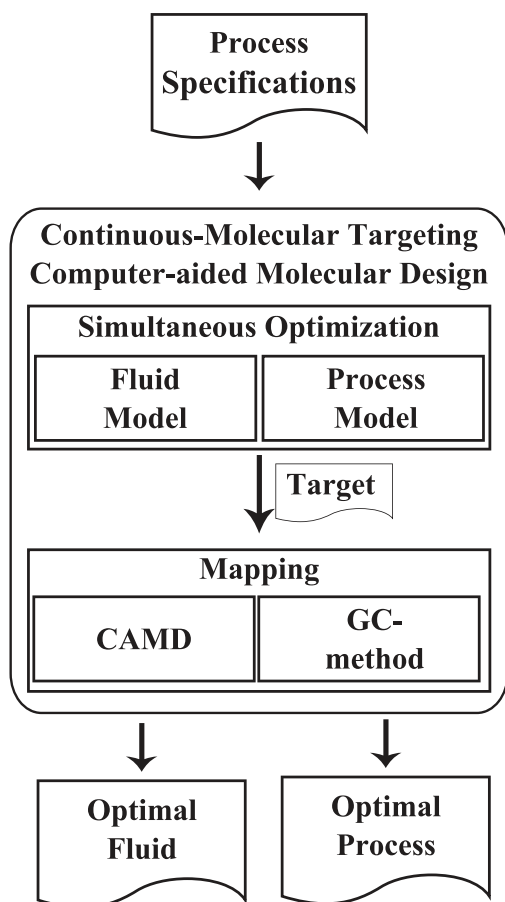
Fig. 17. CoMT-CAMD methodology proposed by Lampe et al. [419]: The continuous-molecular targeting defines the target for the CAMD optimisation.
Source: Reprinted with permission from Lampe et al. [419].
© 2015 Elsevier.

refrigerant design for compression heat pumps and applied to ORC working-fluid design [517], using the Peng–Robinson EoS [307]. The working fluids are characterised by their critical temperature and pressure, the acentric factor, and parameters of a correlation of the ideal-gas heat capacity. These discrete fluid parameters are initially treated as continuous within ORC optimisation. Subsequently, real working fluids are identified by screening a database using an approximation of the objective function around the hypothetical, optimal working fluid as an assessment criterion.

Decomposing the integrated design problem into smaller subproblems allows for a computationally efficient solution while still highlighting the benefits of system-related assessment criteria. However, the decomposition can introduce inaccuracies, which do not guarantee global optimal solutions [134].

The shortcomings of decomposition methods can be tackled by directly solving the integrated design problem in a single step. Such a direct solution to the integrated design problem has been supported in the past years by improved MINLP solvers and numerical techniques. Palma-Flores et al. [329] have presented the earliest work to our knowledge, which solves the MINLP problem of the integrated design of the ORC systems and working fluids in a single step. The study builds upon their earlier work on molecular design [137] but now directly links a thermodynamic model of the ORC to the GC approaches used to predict thermodynamic properties and the CAMD formulation. A numerical solver from the literature is used to solve the MINLP considering three cycle configurations (see Section 5.2). The authors highlight that integrated CAMPD identifies better working fluids than a molecular design based on simplified indicators using physical-property targets.

Su et al. [488] similarly use simple GC approaches for property prediction in their working-fluid design method. However, the authors solve the integrated design problem using a generate-and-test strategy, which can only be solved efficiently for a small molecular design space (*cf.*, Section 5.2.1).

Simple GC approaches are fast and straightforward for thermodynamic-property prediction but lack a consistent thermodynamic basis and, thus, accuracy. The accuracy of property prediction can be improved by using a thermodynamic-property model like an EoS (*cf.*, Section 4). Cignitti et al. [518] proposed a CAMPD method for the integrated design of ORCs and working fluids using the SRK EoS [302] and GC approaches for the parameters representing a molecule in the EoS. The MINLP is solved using an MINLP solver from the literature. The authors compare the results to traditional working-fluid selection and a decomposed molecular design and demonstrate the advantages of the integrated design in both the performance of the identified working fluids and the computational efficiency of the approach.

Due to the uncertainty in property prediction, Frutiger et al. [519] extended the work of Cignitti et al. [518] by a Monte Carlo-based uncertainty analysis and analysed the impact of property uncertainties on the identified ranking of the best working fluids. The proposed method determines a ranking of promising working fluids jointly with a probability distribution, indicating how likely a working fluid is to be the best solution depending on the chosen uncertainties. The probability distribution supports a reliable selection of working fluids and reduces the risk of suboptimal solutions due to property uncertainties. The results highlight the need for accurate property prediction models within an integrated design framework.

In general, cubic EoS are simple and reliable. However, they are known for limited model accuracy for mixtures with non-ideal fluid behaviour, *e.g.*, polar mixtures [347]. Thus, for mixture modelling, cubic EoS are often combined with G^E models requiring an assessment of thermodynamic consistency (*cf.*, Section 4).

The impact of property uncertainties on the ranking can be reduced by using an EoS based on SAFT, which has strong predictive power for liquid, vapour, and supercritical phases even for mixtures with non-ideal behaviour (*cf.*, Section 4.4). In one of the earliest direct integrated design methods, Schilling et al. [424] used the PC-SAFT EoS [144] and the corresponding homosegmented GC approach [445] as the thermodynamic-property model. The method is based on Lampe et al. [419] but directly integrates the CAMD formulation into the initial targeting stage, enabling the solution of the MINLP in an integrated optimisation. A commercial MINLP solver based on outer approximation (*cf.*, Fig. 18 (a)) is used to solve the integrated design problem. The MINLP solver initially relaxes the discrete molecular degrees of freedom as in the continuous-molecular targeting framework [419] (see Section 5.2).

The method is thus called 1-stage CoMT-CAMD. The authors showed that an integrated solution of the MINLP improves the robustness and quality of the results compared to the decomposition-based CoMT-CAMD method of Lampe et al. [419]. The work thus highlights the advantages of a fully integrated solution. The authors integrated the 1-stage CoMT-CAMD method into the commercial software gPROMS ProcessBuilder [327]. Recently, the two-stage CoMT-CAMD approach has also been integrated into the in-house simulator of BASF SE [520]. Both integrations enable using model libraries and, thus, a straightforward and efficient definition of the ORC system and the overall integrated design problem [423]. Besides the integrated design of working fluids and ORCs, 1-stage CoMT-CAMD has also been successfully applied to the integrated design of refrigerants and compression heat pumps by Neumaier et al. [521] and refrigerants and adsorption chillers by Mayer et al. [522]. The homo-segmented GC method of PC-SAFT was also used by Wang et al. [523]. The authors solved the CAMPD problem using a generate-and-test strategy (*cf.*, Section 5.2.1) and were thus limited to small molecular design space for efficient computation.
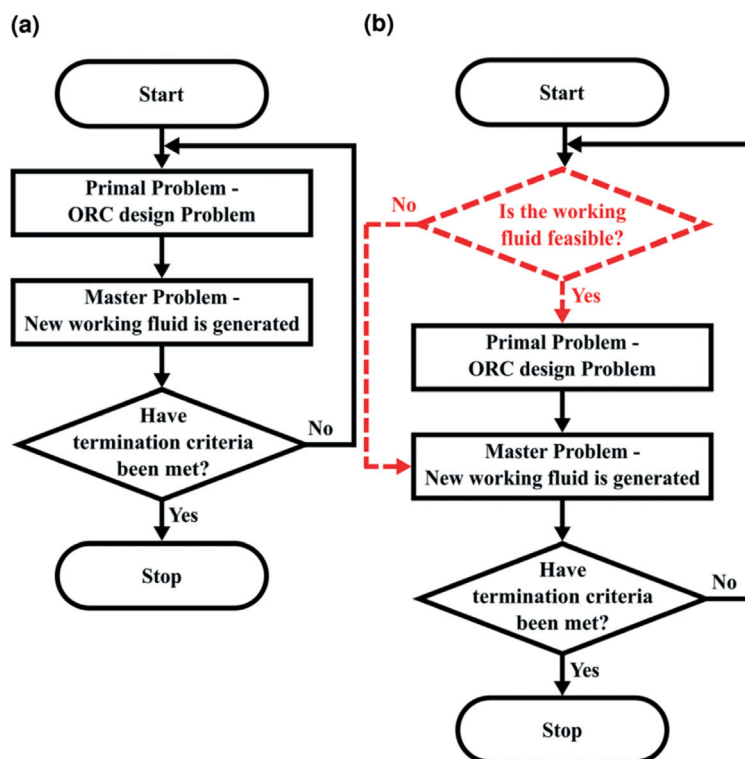
Fig. 18. (a) A standard outer-approximation algorithm and (b) the modified outer approximation algorithm proposed by Bowskill et al. [450] reinforced with feasibility tests. Red dotted sections correspond to algorithm modifications due to the introduction of feasibility tests.
Source: Reprinted with permission from Bowskill et al. [450].
© 2020 Royal Society of Chemistry.

In addition to PC-SAFT, a powerful SAFT-based fluid model is the predictive SAFT-γ Mie group-contribution EoS [79,145], used by White et al. [447] for integrated ORC design. The authors reduced the computational complexity within the proposed framework by decomposing the molecular design space and solving individual MINLP optimisations for *n*-alkanes, methyl alkanes, 1-alkenes, and 2-alkenes. The developed integrated design method has been applied for industrially relevant ORC waste-heat-recovery applications. Beyond integrated thermodynamic design, the authors discussed the identified working fluids in detail regarding their relevant characteristics within an ORC system, considering a simple model of a radial turbine [447] and sizing models for the heat exchangers and their thermo-economic performance using cost correlation for the equipment [146]. The work underlines the good performance of SAFT-based thermodynamic-property models for integrated molecular and power-cycle design frameworks.

However, increasing model complexity increases the computational time and the possibility that algorithms fail for diverse design spaces. One of the main challenges for a robust algorithm is working fluids tested during the optimisation (either real or hypothetical working fluids), which are infeasible for the considered ORC system due to a mismatch between the physical properties and the process constraints (*e.g.*, the saturation temperatures within the given pressure range is higher than the ORC heat-source temperature).

Therefore, Bowskill et al. [450] proposed an integrated design framework for ORCs based on the SAFT-γ Mie GC EoS, which extends an outer-approximation algorithm with a physical domain reduction by feasibility tests (*cf.*, Fig. 18(b)). The work is based on the CAMPD framework developed by Gopinath et al. [60] for the integrated design of solvents and separation processes. The feasibility tests of physical properties before the ORC optimisation reduce the execution of infeasible evaluations. Thus, the framework enables a faster and more robust integrated design and allows consideration of a more extensive and diverse molecular design space (*i.e.*, functional groups for branched alkanes, alkenes, ethers, esters, carboxylic acids, and 1-alcohols).

The CAMD formulations typically used in CAMPD methods for ORCs describe the molecular structures by the number of occurrences of a certain molecular group within the molecular structure. Such CAMD formulations are efficient and can be used with gradient-based optimisation if a proper thermodynamic-property model is used. However, the underlying molecular representation also has two disadvantages for CAMPD: (1) isomers cannot be distinguished; and (2) the CAMPD methods are limited to thermodynamic-property models that depend on the group counts solely (*e.g.*, classical GC methods). These disadvantages can be overcome by more-advanced CAMPD formulations. Recently, Rehner et al. [452] proposed a graph-based molecular representation, the so-called molecule superstructure, an approach inspired by the superstructures developed for flowsheet optimisation in chemical and energy engineering. The graph-based molecule superstructure includes the full connectivity information of the molecular groups and can thus distinguish between isomers. Moreover, the proposed molecule superstructure can be relaxed and thus be used within gradient-based optimisation algorithms. Due to the additional information on the group connectivity, higher-fidelity thermodynamic-property models can be used within CAMPD, as, for example, demonstrated by the authors for the hetero-segmented PC-SAFT EoS [445].

Equipment sizing, costing and integrated thermo-economic design

Thermodynamic process and cycle models based on equilibrium thermodynamics enable an efficient integrated design of working fluids based on thermodynamic objectives. However, thermodynamic models neglect equipment sizing (and costing) and thus have some shortcomings, which can lead to suboptimal solutions:

(1) Fluid-dependent parameters are usually fixed, *e.g.*, the isentropic turbine efficiency, neglecting significant impacts of fluid behaviour on overall operation and performance [524] (*cf.*; Section 3.4);

(2) The practical implementation of the optimum designs introduces additional design degrees of freedom and constraints of the equipment that could change significantly the anticipated thermodynamic and economic performance of the ORC system and fluid [273]; and

(3) Thermodynamic models do not ensure economically competitive ORC systems.

Thus, the integrated design of ORC systems and working fluids should include equipment sizing and costing to capture all relevant system-wide trade-offs. Sizing the equipment often requires additional thermophysical properties like transport properties (*e.g.*, viscosity or thermal conductivity) and thus the integration of proper property models (*cf.*, Section 4.7). Lampe et al. [273] captured the impact of the working fluid on the ORC turbine by integrating a model of a one-stage radial inflow turbine into the 1-stage CoMT-CAMD framework developed by Schilling et al. [424]. The model enables the calculation of fluid-dependent isentropic turbine efficiencies and crucial turbine design parameters, *e.g.*, blade heights, Mach numbers, and rotational speeds, limited within the integrated design. The authors showed that limiting turbine design parameters can strongly influence the ranking of the best working fluids, and that neglecting the turbine sizing can lead to infeasible turbine geometries for the identified optimal fluids and corresponding process settings. Thus, the study of Lampe et al. [273] highlights the need for capturing equipment behaviour within the working-fluid design.

Schilling et al. [274] extended the 1-stage CoMT-CAMD framework [424] by equipment models for sizing heat exchangers. The equipment models capture the heat transfer for single-phase, evaporation, and condensation. For this purpose, the authors integrated advanced models for calculating viscosity [471] and thermal conductivity [475] of molecules into the framework. These recently developed models for transport properties are based on the PC-SAFT EoS and entropy scaling (*cf.*, Section 4.7). Thus, equilibrium and transport properties are modelled consistently within the integrated design. The equipment sizing enables the calculation of the cost of the purchased equipment using costing correlations and, therefore, the investment cost of the ORC. Thereby, a thermo-economic objective function can be considered for the integrated design (*e.g.*, the specific investment cost or the net present value of the ORC). The authors demonstrated that the optimal working fluid identified using a thermo-economic objective can differ from that identified using a thermodynamic objective. Similarly, van Kleef et al. [275] integrated a thermo-economic assessment into the framework developed by White et al. [146,447]. For this purpose, the authors used GC approaches for transport properties (*cf.*, Section 4.7). Moreover, equipment models for sizing the heat exchangers and costing are directly linked to their integrated design framework. The trade-off between thermodynamic and thermo-economic performance was analysed using MOO. The authors investigated the impact of the ORC heat-source temperature on the working fluid ranking and identify novel working fluids for ORC applications. Both Schilling et al. [274] and van Kleef et al. [275] highlighted the need for integrated equipment sizing and a thermo-economic assessment for the integrated design of working fluids and ORC systems. However, integrating equipment sizing and cost estimation models into CAMPD problems can introduce considerable uncertainties, primarily due to cost estimations [525]. These uncertainties can worsen the accuracy of the objective function and constraints, potentially leading to less reliable optimisation results. A key aspect is whether these uncertainties result in systematic errors across all working fluids, keeping the ranking unchanged, or if they vary based on the specific working fluid and consequently can change the ranking. The impact of these uncertainties on the working fluid ranking must be carefully assessed to ensure that the thermo-economic design remains robust despite the inherent uncertainties in cost estimations.

The integrated design methods discussed so far allow for the integrated ORC and working-fluid design for a fixed ORC configuration.

This limit was overcome by Schilling et al. [428], who integrated a superstructure of the ORC system into the 1-stage CoMT-CAMD framework [274]. Thereby, the authors can design the ORC system simultaneously with the working fluid. The superstructure of the ORC system consists of optional internal heat regeneration, turbine bleeding, and reheating. The optimisation algorithm can choose these options by additional discrete degrees of freedom. The whole framework is integrated into the software gPROMS ProcessBuilder [327]. Thereby, the superstructure of the ORC configuration can be defined straightforwardly using equipment model libraries. The framework identifies the thermo-economically optimal working fluid jointly with the optimal ORC configuration, cycle settings, and equipment sizes. The authors showed that the optimal working fluid and cycle configuration depends on the chosen objective function. The work highlights the impact of the ORC configuration on the working-fluid selection. In recent work, Tillmanns et al. [526] applied the 1-stage CoMT-CAMD framework to the integrated thermo-economic design of an ORC-based pumped-thermal electricity storage (PTES) system. The authors designed the working fluid for an ORC and the refrigerant for a heat pump simultaneously, to obtain an optimal interaction between the ORC and heat pump within the PTES system. The work used the gPROMS ProcessBuilder [327] implementation of 1-stage CoMT-CAMD and corresponding equipment model libraries. The authors demonstrated the possibility of integrating CAMPD for ORCs in the design of larger background systems involving several thermodynamic cycles with a molecular degree of freedom.

Integrated design for off-design operation

The solution methods discussed so far focus on designing optimal working fluids for ORC systems with steady-state operation or a nominal operating point. However, heat sources can be transient, and thus, ORC systems have to be operated at varying off-design conditions. Because the heat source strongly impacts working-fluid selection [48], fluids selected for a fixed heat source can be suboptimal if the real heat-source behaviour is transient [312,527]. Thus, identifying optimal working fluids for off-design operation needs an integrated design that can capture the transient behaviour. In general, off-design operation can be captured using dynamic models. Considering dynamic models for integrated design leads to a computer-aided molecular process and control design (CAMPCD) problem [134]. Mathematically, CAMPCD problems can be formulated as mixed-integer optimal control problems (MIOCPs), which are challenging to solve.

Schilling et al. [427] captured the transient behaviour of the heat source by considering multiple operating points in the so-called 1-stage continuous-molecular targeting-computer-aided molecular and multi-operating process design (1-stage CoMT-CAM^{2}PD). Thereby, solving challenging optimal control problems is prevented. The authors described the transient heat-source behaviour by a time series of the steady-state heat-source settings (*i.e.*, heat-source temperature and mass flow rate). From this time series, operating points were selected for the integrated design based on time-series aggregation techniques [528]. The framework assumes quasi-steady-state operation and identifies the working fluids with optimal thermodynamic properties in the given range of off-design operations. The authors showed that working fluids identified considering multiple operating points outperform those identified with only a single nominal operating point.

While quasi-steady-state models are efficient and robust for working-fluid selection in early design stages, they do not capture the inertia and dynamic response of ORC systems. Thus, quasi-steady-state models cannot be used to find an optimal match of working fluid and ORC control strategy [529]. The heat source up to the ORC system is not always steady state, but is in fluctuation, especially the engine heat source, which exhibits a rapid fluctuation with a fluctuation period on the second-minute level [262,530]. The off-design performance of different working fluids is not the same, so it is necessary to study the design of working fluids in ORC in transient states. Therefore, Tillmanns et al. [276] directly integrated dynamic models for the

ORC equipment into the two-stage CoMT-CAMD method proposed by Lampe et al. [419]. The integration transforms the initial NLP relaxation problem (*i.e.*, the continuous-molecular targeting) into an optimal control problem (OCP). The entire problem is implemented into the software Modelica [531] and solved using the commercial OCP solver MUSCOD-II [532]. MUSCOD-II is a robust multiple-shooting OCP solver that efficiently handles complex dynamic systems by solving time intervals simultaneously. In order to have a better symbolisation, a sine was used to represent the transient state of the heat source, which is a commonly used method [533,534]. As a result of the OCP, a hypothetical, optimal working fluid is identified with the corresponding optimal ORC settings and control strategy. In the second stage, real working fluids are identified using CAMD according to the previous CoMT-CAMD method. The authors highlighted the advantages of integrating dynamic ORC modelling and integrated working fluid and ORC design for applications with a strong impact of the transient behaviour. Due to the challenges of dynamic system operation, the developed method relies on a decomposition strategy and is limited to a small molecular design space. Moreover, both methods developed for an integrated design with transient ORC behaviour only consider the thermodynamic performance of the cycle, neglecting the equipment cost. Nevertheless, the proposed methods underline the need for capturing transient behaviour for selecting working fluids for ORC systems within an integrated design framework.

5.1.3. Integrated mixture and process design problem

The systematic design methods discussed in Section 5.1.2 focus on the integrated design of ORCs and *pure* working fluids. However, working-fluid *mixtures* can have favourable properties for ORCs due to the temperature-glide during evaporation and condensation [21]. As for pure components, finding an optimal combination of a working-fluid mixture and ORC requires an objective function related to the wider ORC system within the design. The problem formulation in Problem (1) can be extended to design working-fluid mixtures. For this purpose, the following requirements have to be considered:

(1) A thermodynamic-property model is needed to predict mixture behaviour (see Section 4);
(2) The process and equipment-sizing/costing models have to be extended for mixtures. For example, appropriate models need to capture the temperature-glide of evaporation and condensation, and the equipment-sizing models need to capture the heat-transfer behaviour of mixtures;
(3) A computer-aided mixture and blend design (CAM^{b}D) formulation is required to design all mixture components. Due to the molecular and combinatorial complexity, the design space of CAM^{b}D formulation is much larger than for the design of pure working fluids;
(4) A powerful solution algorithm is needed to handle the increased number of discrete degrees of freedom and constraints and the nonlinearity of mixture behaviour.

Systematic solution methods have been developed, fulfilling the requirements to tackle the integrated design of working-fluid mixtures and ORC systems.

Papadopoulos et al. [141] linked a CAM^{b}D formulation to a thermodynamic ORC model. The thermodynamic-property model is a cubic EoS combined with GC approaches. In the presented integrated two-step approach, the authors first applied the chemical feasibility constraints only to the first component of the working-fluid mixture but relaxed the feasibility constraints for the second component. The optimal first component was then identified in the first step using MOO and fixed in the second step to identify the corresponding optimal second component. The authors performed a post-design, nonlinear sensitivity analysis of the employed thermodynamic property and cycle models on selected mixtures. The analysis considers the simultaneous effects of multiple different fluid properties on multiple ORC performance

indicators. The results indicate that some mixtures are more robust in property-value changes than others. Furthermore, it appears more important to have reliable predictions for the boiling points of the mixture components compared to their critical properties.

In recent work, Schilling et al. [277] extended the 1-stage CoMT-CAMD framework [274] for the integrated design of working-fluid mixtures and ORC systems, so-called 1-stage continuous-molecular targeting-computer-aided mixture and blend design (1-stage CoMT-CAM^{b}D). Following their approach for pure components, the authors use the PC-SAFT EoS as thermodynamic property model, which is suitable for accurate prediction of mixture behaviour, even for working-fluid mixtures with non-ideal behaviour (see Section 4 for details). Moreover, PC-SAFT has been proven suitable for designing working-fluid mixtures based on molecular relaxation [535]. PC-SAFT is used to calculate the equilibrium and transport properties of working-fluid mixtures in a thermodynamically consistent way. The authors integrated a CAM^{b}D formulation that allows the design of the molecular structure of two mixture components and the mixture composition as degrees of freedom of the optimisation. Moreover, the CAM^{b}D formulation incorporates inequality constraints to break the symmetry of the molecular design space and ensure that identical molecular structures are not selected for both components. Specifically, the authors found that the most effective approach is to apply inequality constraints on the pure component parameters of PC-SAFT, which successfully breaks symmetry in the molecular design space. The model of the ORC system captures the temperature-glide of the working fluid mixture during evaporation and condensation. Moreover, the ORC system model includes heat-exchanger sizing for working-fluid mixtures. Thereby, a thermodynamic and thermo-economic design of working-fluid mixtures is enabled. The authors applied their integrated mixture design framework for various ORC heat source and sink specifications demonstrating the strong impact of the ORC specifications on the optimal mixture. The results show a lower potential of improvement for working-fluid mixtures designed using a thermo-economic objective (*i.e.*, the specific investment cost) than for working-fluid mixtures designed using a thermodynamic objective (*i.e.*, the net power output). Rehner et al. [536] recently extended their CAMPD framework, originally based on molecule superstructures [452], to design working-fluid mixtures. This framework employs a graph-based molecular representation for both components, allowing the use of the accurate heterosegmented GC method of PC-SAFT [445], along with a recent GC method for binary interaction parameters [453], making it particularly well-suited for designing working-fluid mixtures. Overall, all discussed frameworks for ORC mixture design highlight the potential of a systematic, integrated design of working-fluid mixtures for ORCs.

5.2. Solution strategies

Due to the challenging nature of solving MINLP problems, computer-aided molecular design is not straightforward for the integrated design of molecules and processes. Thus, various systematic methods have been developed and applied for the integrated design of working fluids for organic Rankine cycles. Besides the employed ORC models and thermodynamic-property models, these systematic design methods differ in the employed solution strategy and algorithm.

The solution strategy and algorithm strongly depend on the employed thermodynamic-property and thermodynamic system model. For example, efficient gradient-based optimisation strategies require the calculation of analytical or numerical derivatives. Such derivatives, in turn, need a molecular description and thermodynamic-property model, allowing for a continuous molecular representation. A continuous molecular representation and, thus, a gradient-based optimisation is typically enabled by GC approaches and EoS. In contrast, quantum-mechanical calculations rely on a discrete molecular representation and require derivative-free optimisation strategies like metaheuristics [537]. Thus, a proper solution strategy and algorithm must

be chosen carefully to find suitable solutions for the integrated design of working fluids and ORC systems. In this section, we give a short overview of possible solution strategies. For a detailed overview of solution strategies, the reader is referred to the comprehensive review on CAMPD from Papadopoulos et al. [134].

5.2.1. Generate-and-test

The generate-and-test approach is the most intuitive and straightforward but computationally less efficient solution strategy for integrated design problems. Here, all molecular structures fulfilling the structural and property constraints of a CAMD formulation are generated initially and subsequently enumerated in process optimisation [56]. This strategy is comparable to screening a pre-defined database, but the employed molecule database is generated using CAMD. A generate-and-test strategy for designing working fluids for ORCs has been employed, *e.g.*, by Su et al. [488]. Since all structurally feasible molecular structures are assessed in enumerative ORC optimisations, a generate-and-test approach ensures finding the globally optimal working fluid of the considered design space. However, generate-and-test approaches are typically only applied if the molecular design space is small due to the high computational demand of the process optimisations during the enumerative search. The size of the molecular design space can be assessed by the initial generation of all feasible molecular structures, which is typically much more efficient than the subsequent process optimisation of each structure.

5.2.2. Decomposition methods

Decomposition methods aim to reduce the problem complexity of the integrated design by decomposing the problem into several smaller subproblems. The smaller subproblems can be solved more quickly and efficiently. Decomposition methods can be separated into: (1) molecular-design problems (see Section 5.1.1); and (2) molecular-targeting problems (see Section 5.1.2). Decomposition-based molecular-design problems initially reduce the molecular design space by considering low-resolution performance indicators and constraints based on physical properties to avoid needing a more detailed thermodynamic model of the ORC system that typically requires more demanding computations. If the reduced molecular design space is small, enumerative process optimisations can be performed, or the reduced MINLP can be solved. The size of the molecular design space can be assessed by generating all feasible molecular structures. Alternatively, molecular-clustering techniques can be employed to reduce the molecular design space further [98].

In contrast, decomposition-based molecular-targeting problems address the CAMPD problem by identifying favourable ORC system-related target properties. For this purpose, the discrete molecule parameters representing a working fluid in the thermodynamic-property model are typically relaxed, *i.e.*, treated as continuous variables, and optimised simultaneously with the ORC degrees of freedom considering an appropriate objective function [51,276,419,517]. For this purpose, a thermodynamic-property model is required allowing for a continuous molecular representation, *e.g.*, GC approaches that target pure-component properties or an EoS. The relaxation of discrete molecule parameters transforms the MINLP of the integrated design into an NLP, which can be solved efficiently using gradient-based NLP solvers. The relaxed MINLP results in a hypothetical molecular structure of the so-called target with optimal performance within the considered molecular design space. The target serves as the lower bound of the optimisation problem. A convex hull and proper bounds of the molecule parameters are typically required to ensure the target's similarity to real molecular structures. In the second step, real molecules are identified with similar performance as the target. To ensure similar performance, real molecules are assessed considering an approximation of the objective function and constraints, *e.g.*, by a first- or second-order Taylor approximation around the target. Thereby, trade-offs can be considered, which are not captured if solely molecule

parameters closest to the target are sought. Real molecular structures can be identified by a database screening [51,517] or CAMD [276,419]. CAMD, combined with a second-order Taylor approximation of the objective and constraints, can be solved as a mixed-integer quadratic problem (MIQP) using standard deterministic MIQP solvers.

5.2.3. Metaheuristic optimisation methods

Metaheuristics are optimisation strategies based on direct heuristic (biased random) searches to generate and test iteratively sampling points within the design space [538]. Unlike deterministic methods, metaheuristics typically do not require derivatives, making them suitable for thermodynamic-property models that use discrete molecular representations. Due to their systematically guided search approach, metaheuristics only need to explore a small fraction of the design space, which is computationally more efficient than exhaustive generate-and-test approaches that enumerate all options. However, finding globally optimal solutions is not guaranteed. Furthermore, defining proper stopping criteria can be challenging in ensuring a sufficiently good solution.

For instance, Papadopoulos et al. [98], used simulated annealing (SA) [539] to design working fluids for ORCs. The SA algorithm mimics the annealing process from metallurgy, where the solution "temperature" serves as the control parameter of the process. This "temperature" control parameter is gradually reduced, allowing the system to escape local optima but still approach a global optimum. Another example is the genetic algorithm (GA) NSGA-II [540] employed by van Kleef et al. [275], where potential solutions are treated as individuals in a population. These solutions evolve over iterations through selection, crossover, and mutation inspired by natural selection.

5.2.4. Deterministic optimisation methods

Deterministic optimisation follows a rigorous mathematical approach, leading to a replicable solution. Typically, deterministic optimisation methods decompose the MINLP into smaller subproblems of the MINLP [541]. For this purpose, strategies from mathematical programming are employed, *e.g.*, linear or quadratic approximations of the objective and constraints or relaxing or fixing variables or constraints. Grossmann and Kravanja [541] give an overview of deterministic solution strategies for solving MINLPs. These strategies commonly rely on calculating gradients, and sometimes also the Hessian, of the model variables. Thus, an ORC model and thermodynamic-property model are required, which allow for the calculation of analytical or numerical derivatives. Compared to metaheuristics, deterministic optimisation methods typically converge faster, offering a more efficient path to solving optimisation problems. For the integrated design of ORC systems and working fluids, deterministic solution methods have been successfully employed, such as those based on outer-approximation formulations [542] combined with equality relaxation [137,146,273, 274,277,423,424,428,447], branch-and-bound algorithms [137,329], or branch-and-cut algorithms [518]. These studies have demonstrated the effectiveness of deterministic solution methods in providing high-precision results, particularly when accurate gradients are available. However, a key insight is that while these approaches offer speed and precision, they are limited by their reliance on derivative information and may struggle with highly non-linear or discontinuous design spaces, potentially leading to only locally optimal solutions [277,424].

Deterministic optimisation algorithms, particularly global optimisation solvers, can rely on model equations given in their explicit form. Explicit model equations can be typically implemented for GC approaches and classical EoS, such as cubic EoS. However, more-advanced and accurate thermodynamic-property models like SAFT-based EoS are more demanding and typically evaluated in an external code to ensure stable computation. The external code typically provides a black-box model to the solver. If parts of the model are given in external code, an optimisation algorithm is required that can handle black-box modelling. However, black-box capable optimisation algorithms usually

only ensure a locally optimal solution. A multi-start procedure can be employed to account for locally optimal solutions, or a ranking of the most-promising candidates can be calculated using integer-cut constraints. Despite the potential challenge with black-box models, the ability of deterministic methods to systematically handle complex design problems with well-defined mathematical models makes them highly valuable for CAMPD problems.

5.2.5. Multi-objective design methods

Optimisation strategies usually enable the consideration of a single objective function. However, considering multiple objective functions is often desired for integrated molecular and process design problems (*e.g.*, the net power output of an ORC system, and its associated total capital investment). For this purpose, MOO strategies have been developed. The result of MOO is a Pareto front of optimal solutions. For CAMPD problems, the Pareto front can consist of several promising working fluids (*cf.*, Fig. 19). It is recommended to choose non-aggregated objective functions for MOO, *i.e.*, objective functions that do not compromise a trade-off, to maximise the information content of the result [543].

Most commonly, MOO strategies transform the problem into several SOO problems. The most intuitive and straightforward approach for MOO is a linear scalarisation of the objective function, *i.e.*, the weighting sum of all objective functions [544]. The Pareto front can be generated by repeating the integrated design problem with varying weighting factors. Other MOO strategies are, *e.g.*, the normalised normal constraint method [545], the epsilon-constraint method [546] or interactive multi-objective methods combining sandwiching and hyperboxing [547], which enable tailoring a Pareto front in the desired region and are suited for non-convex objectives. For example, the normalised normal constraint method has been applied in CAMPD for ORCs by Schilling et al. [274,424].

Due to its efficiency, another popular approach for multi-objective optimisation in CAMPD problems for ORCs is the stochastic non-dominated sorting genetic algorithm II (NSGA-II) [540]. The evolutionary NSGA-II algorithm employs a non-dominated sorting approach that classifies solutions into different Pareto fronts based on dominance. The algorithm has been applied to CAMPD for ORC, e.g., by van Kleef *et at.* [275].

5.3. Key observations on CAMPD for ORCs

The development of CAMPD solution methods for working-fluid selection for ORCs has gained considerable progress in the past decade. Significant steps could be achieved in all parts of CAMPD problems:

- **Thermodynamic-property models** have been integrated with increasingly higher predictive power, starting from simple GC approaches, progressing with cubic EoS, and finally using SAFT-based EoS or quantum-mechanical calculations — moreover, accurate models for the working fluid's transport properties and even non-conventional properties are incorporated, like safety or environmental properties;
- **ORC system and equipment models** have been integrated with increasing complexity, starting from pure-component molecular properties that provide indirect links with ORC performance, progressing with thermodynamic process models, and finally implementing sizing and costing of the equipment, cycle superstructures, and dynamic component models;
- The **molecular design space** has been increased, starting from the integrated design of pure working fluids towards the integrated design of working-fluid mixtures;
- Advanced **solution algorithms** are developed, starting from problem decomposition towards a direct solution of integrated design problem based on deterministic optimisation; and

- **Practicability and applicability** — while many developed solution algorithms are specific tools enforcing expert knowledge and experience, the first steps have been taken to achieve a more user-friendly application for inexperienced users by integrating CAMPD for ORCs into commercial software.

With these developments, the CAMPD solution methods achieve high integration and accuracy. Moreover, the developments enable the consideration of objective functions and constraints for working-fluid selection relevant for practical application (*e.g.*, economic objectives or sizing constraints for the equipment). Despite the increasing complexity of the models and the increasing computational cost, the required computational time is still reasonable. The integrated design can be solved in seconds to minutes considering a thermodynamic ORC model and GC approaches and/or a cubic EoS [137,518]. Even an integrated design using PC-SAFT with equipment sizing and costing and cycle configuration superstructure is still efficient and requires less than an hour to calculate a ranking of five promising working fluids and corresponding optimal cycle configurations [428]. However, it should be noted that time is usually not a limiting factor at the early design stages, for which an integrated design of working fluids and processes is most relevant. In general, an integrated design is computationally much more efficient than a decomposed generate-and-test procedure of the considered design space [274,277,424,518].

In CAMPD for ORCs, open science is essential for ensuring reproducibility and validation of the assumptions and identified working fluids. By sharing open-source models, datasets, and CAMPD frameworks, researchers can replicate studies, validate results, and build on each other's work. Open access to thermodynamic models and CAMPD frameworks ensures that advancements in CAMPD for ORCs are grounded in validated data.

6. Applications and case studies of ORC systems

The role and development trend of the application of CAMD techniques in ORC system design can be intuitively reflected by an examination of various case studies across multiple industries. In the more than a decade of theoretical research on the integration of CAMD methods into ORC system design, the developed approaches have been applied to the integrated design of processes and working fluids of ORC systems with low- and medium-temperature heat sources such as internal-combustion engine with combined heat and power (ICE-CHP) systems, industrial waste-heat recovery, geothermal, solar thermal and so on. It has been shown that CAMPD methods are practical, advanced, and have good application prospects; the specific application scenarios and corresponding CAMPD methods are reflected in Table 5 . In this section, we investigate selected CAMPD case studies in various application scenarios through enumeration and induction.

6.1. Internal-combustion engine with combined heat and power systems (ICE-CHP)

When the exhaust gas of an internal-combustion engine is used as the heat source of the ORC system, its temperature is usually higher than that of geothermal, biomass energy, and most industrial waste-heat sources. Simultaneously, the influence of the transient characteristics of the exhaust gas on the design of the ORC system should be specifically considered.

Cignitti et al. [518] applied a CAMPD approach to an ORC device for energy recovery from the exhaust gas of a 37 MW marine diesel engine from MAN Diesel & Turbo for the design of suitable working fluids. The ORC unit had a regenerator and was designed to take into account the 75% load point of the diesel engine, where the exhaust gas inlet temperature was 509 K. The GC prediction method was used to describe the physical properties of molecules and a simultaneous design method was proposed: an MINLP problem, to be solved using the LINGO Global solver on the GAMS platform. The integrated method
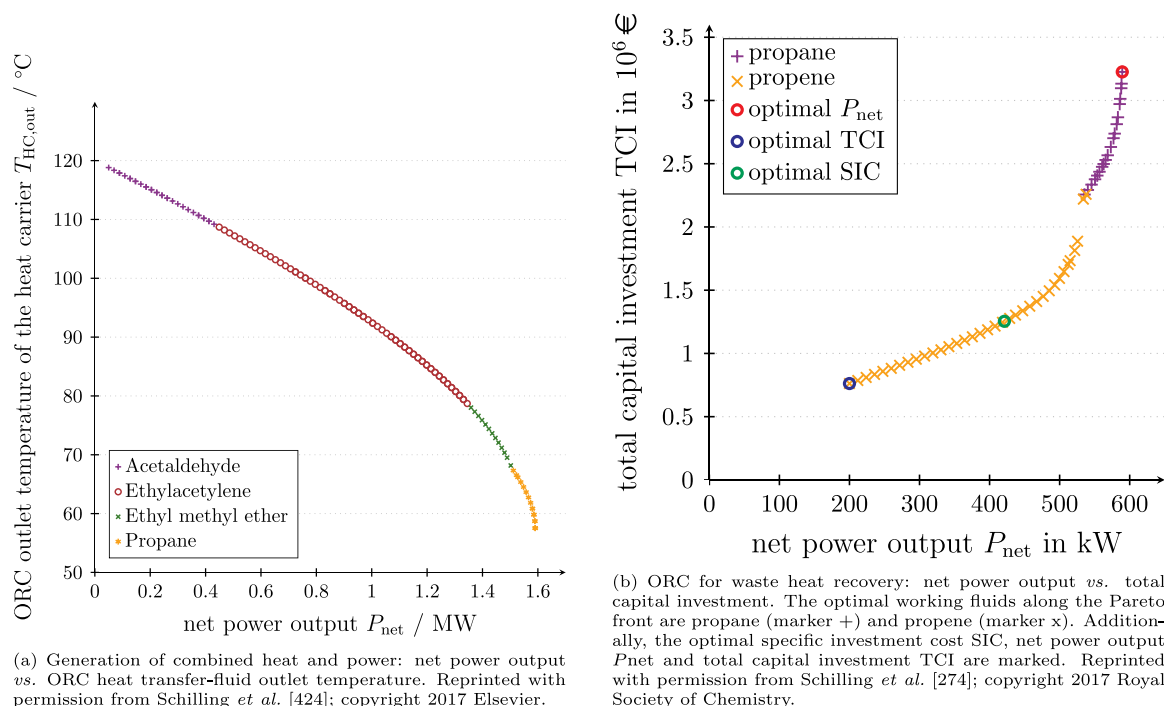
(a) Generation of combined heat and power: net power output *vs.* ORC heat transfer-fluid outlet temperature. Reprinted with permission from Schilling *et al.* [424]; copyright 2017 Elsevier.

(b) ORC for waste heat recovery: net power output *vs.* total capital investment. The optimal working fluids along the Pareto front are propane (marker +) and propene (marker x). Additionally, the optimal specific investment cost SIC, net power output P_{net} and total capital investment TCI are marked. Reprinted with permission from Schilling *et al.* [274]; copyright 2017 Royal Society of Chemistry.

Fig. 19. Examples for Pareto fronts resulting from multi-objective optimisation applied in CAMD for organic Rankine cycles.

Table 5
Case studies of CAMD technology in ORC system design.

Applications	Ref.	WF type[1]	ORC optimisation criteria[2]	ORC configuration	ORC state
ICE-combined heat and power system	[518,548]	pure	P_{net}	Regenerative	steady
	[148]	pure	P_{net}	Simple & mass flow splitting	steady
	[426,427]	pure	P_{net}	Simple	dynamic
	[276]	pure	P_{net}	Simple	dynamic
Industrial waste-heat recovery	[274,422]	pure	P_{net}, SIC, TIC	Simple	steady
	[421]	pure	NPV	Simple	steady
	[277]	mix	P_{net}, SIC	Simple	steady
	[428]	pure	NPV, SIC, P_{net}	Superstructure: simple, regenerative, turbine bleeding, and reheating	steady
	[450]	pure	P_{net}	Simple	steady
Geothermal and Biomass	[98,334, 335]	pure	P_{net}, TIC	Simple cycle	steady
	[141,336]	mix	η_{th}, η_{ex}	Simple	steady
	[51,425]	pure	P_{net}	Simple	steady
	[420,424]	pure	P_{net}	Simple	steady
	[549]	pure	P_{net}, η_{ex}	Simple & regenerative	steady
Solar thermal	[273,423, 424]	pure	P_{net}	regenerative	steady
Other power technologies	[55]	pure	η_{th}	Simple	steady
	[20,419]	pure	P_{net}	Simple	steady
	[550]	pure	P_{net}	Simple	steady
	[447,448]	pure	P_{net}	Simple	steady
	[146]	pure	SIC	Simple	steady
	[275]	pure	P_{net}, SIC, TIC	Simple	steady

[1] WF: working fluid.

[2] P_{net}: net power output; TIC: total investment costs; SIC: specific investment costs; NPV: net present value.

employed in this work is summarised in the workflow shown in Fig. 20. Considering the three cases of acyclic molecules, alicyclic molecules, and aromatic molecules, respectively, 2,2,3,3,4,4,5,5-octafluorohexane, 1,1,2,2,3,3,4-heptafluoro-4-(propan-2-yl)cyclobutane and 1,2-difluoro-6-methylcyclohexa-1,3-diene were judged the three best molecules, with the net power outputs of 1.21 MW, 1.20 MW, and 1.05 MW.

An analysis of all possible solutions using a decomposition method justified the results of the simultaneous design method while showing that the ORC performance was significantly correlated with the condenser and heat-exchanger UA values. Compared to conventional fluids used in similar ORC applications, such as MM, Toluene, i-Pentane, n-Pentane, Cyclopentane [551], the globally optimal fluid
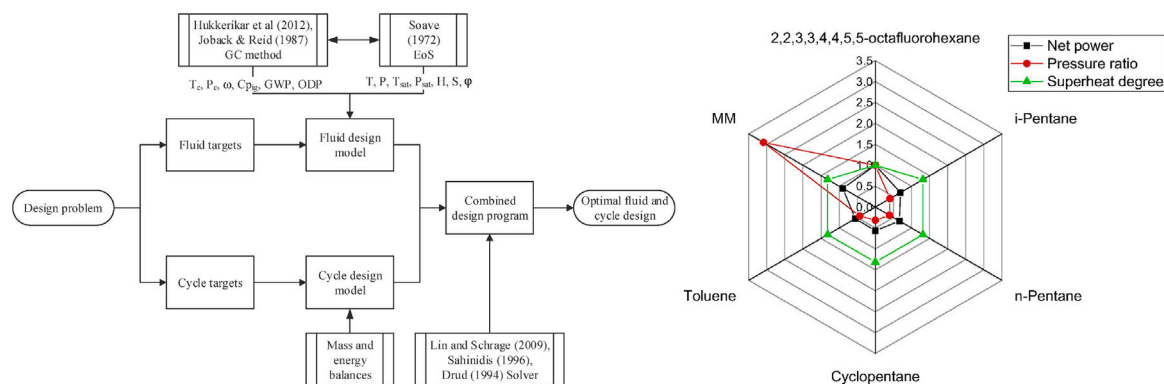
Fig. 20. Integrated design workflow (left) and optimal fluid comparison against conventional fluids used in similar ORC systems (right); workflow and results as presented in Ref. [518]. The three parameters of 2,2,3,3,4,4,5,5-octafluorohexane are plotted as unit 1, and the corresponding parameters of the conventional working fluid are expressed as ratios to 2,2,3,3,4,4,5,5-octafluorohexane.
Source: Reprinted with permission from Cignitti et al. [518].
© 2017 Elsevier.

(2,2,3,3,4,4,5,5-octafluorohexane) designed in the case study had the highest net power output and the lowest degree of superheat. In terms of pressure ratio, it was only second to hexamethyldisiloxane, as shown in Fig. 20. High net output power indicates good cycle performance, and low superheat means improved heat utilisation and reduced heat exchanger area requirements. High pressure ratios are a disadvantage, resulting in higher cost and lower performance of the turbine.

Frutiger et al. [548] conducted an uncertainty analysis of the properties of 15 candidate working fluids obtained using the CAMD method in the ORC of marine diesel exhaust-heat recovery by Cignitti et al. In the working-fluid design, the power output values of the CAMD solution of every working fluid were seen to be close, while the uncertainty analysis gave a significantly different ranking, providing an additional standard for the fluid class.

Schwobel et al. [148] designed working fluids for two thermodynamic ORCs for passenger cars and heavy-duty trucks. The first configuration is suitable for passenger cars without exhaust-gas recirculation. However, for the waste-heat recovery of heavy trucks, the exhaust energy from post-processing and the energy from exhaust-gas recirculation was considered according to the configuration of mass flow separation after the pump. To find the best fluids, a high-throughput screening (HTS) was performed, which covered almost all known chemical spaces with more than 72 million entries according to the structures provided in the PubChem database. A set of 3174 potential working fluids was considered for thermodynamic performance ranking after applying quantum-chemical calculation-based structural and thermodynamic filtering criteria to more than two million structures. Computational-chemistry methods were applied to predict all physicochemical properties of interest via COSMOtherm software (*e.g.*, vapour pressure, critical point) and thermodynamic-process simulations were performed (*e.g.*, net power output) via the fast simulation tool DetailSimORC. The state equation, combining the COSMO-RS theory with the generalised Patel–Teja [371] theory, extended the applicability of thermodynamic calculations to critical points. This quantum-chemistry-based COSMO-RS method is neither dependent on specific group contributions nor restricted to specific classes of compounds, enabling the analysis of millions of compounds in the complete known chemical space in a fully predictive manner of mass screening. A scheme of the calculation workflow is presented in Fig. 21. It is interesting to note that only 12 compounds in the top 100 resulting from this screening (ranked by thermodynamic properties) were previously classified as ORC working fluids.

Schilling et al. [427] used CAMD technology to design the working fluid for an ORC purposed to recover energy from the exhaust gas of heavy-duty vehicles. The authors proposed the 1-stage CoMT-CAM²PD algorithm, combining the 1-stage CoMT-CAMD with aggregation techniques, allowing the transient nature of the heat source to be integrated

in the design. Aggregation technology allows the representation of multiple operation points, caused by transient heat sources, using a few characteristic operating points. Subsequent evaluation of identified working fluids ensured safety and environmental friendliness. The algorithm was applied to the design of an ORC on a heavy-duty vehicle considering the newly developed VECTO Long Haul Cycle (LHC) as input; only six aggregated operating points were necessary to represent the transient exhaust gas. The optimal working fluid was identified as ethyl formate, which increased the net power output by 30% compared with the commonly used working fluid, ethanol.

The working conditions of the engine are more variable, especially for automotive engines. Therefore, it is necessary to conduct molecular-design research considering dynamic performance for ORCs of engine waste-heat recovery. Tillmanns et al. [276] proposed an integrated approach for optimising the ORC processes and working fluid that considers dynamics. The method is based on the CoMT-CAMD approach. The result is an OCP yielding the optimal working fluid and corresponding optimal system control given the dynamic inputs. Successful application of the approach was demonstrated; in this case, isobutane was identified as the best stable working fluid for dynamic applications. In contrast, the integrated design based on steady-state input (calculated as the average of temperature and mass flow of the dynamic heat source) failed, overestimating the average net power output of the top five identified working fluids by up to 30%.

6.2. Industrial waste-heat recovery

Waste heat recovery in plants is an important technology to improve efficiency and reduce emissions. There are various waste heat sources in plants, including boiler exhaust gas, reactor waste heat and cooler waste heat [552]. ORC is more advantageous in low-temperature heat recovery in plants, which has great potential [553,554]. The variety of heat sources and application scenarios require the support of the CAMD method to customise the best working fluid for an ORC.

Schilling et al. [274,422] considered a subcritical, non-regenerated ORC for waste-heat recovery, where the waste-heat source was waste water at 150 °C and the cooling source was cooled water at 15 °C. The authors utilised a consistent thermodynamic model for an integrated thermo-economic design approach for ORC processes, equipment, and working fluids. This method is based on the 1-stage CoMT-CAMD approach, in which the properties of the working fluid are modelled by the physically-based PC-SAFT EoS. A schematic illustration of the presented 1-stage CoMT–CAMD approach is shown in Fig. 22.

In this case study, only short-chain alkanes and olefins were identified. The ideal optimal working fluid was obtained under the relaxed NLP problem; the specific investment cost SIC = 3058 USD/kW, and the net power output P_{net} = 434 kW. The best practical working fluid
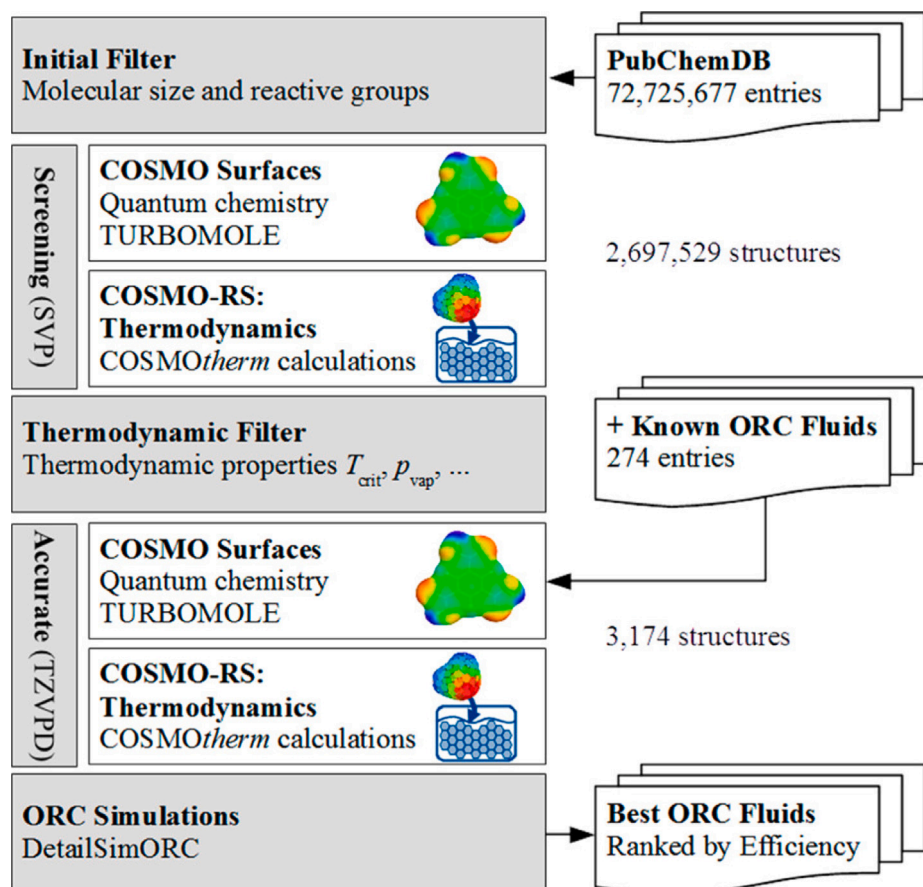
Fig. 21. Scheme of the PubChem database screening by COSMOtherm calculations and DetailSimORC.
Source: Reprinted with permission from Schwöbel et al. [148].
© 2016 American Chemical Society.

was identified as propylene, SIC = 3318 USD/kW, P_{net} = 422 kW. It was found that the final optimisation results were quite different from the thermodynamic optimisation results using the net power output as an objective function (here propane was ranked top; P_{net} = 589 kW, SIC = 6097 USD/kW). Multi-objective optimisation was used to more closely visualise the thermal-economic trade-off between net power output and total capital investment; the results displayed in Fig. 19(b) were obtained using multi-objective optimisation. Through this case study the authors also showed that the predicted specific purchased-equipment cost and the cost-sharing of purchased-equipment cost show good accordance with real ORC applications.

Using the above modelling method, ORC systems have been studied considering the net present value (NPV) as the design goal. For a case in which the waste-heat source was wastewater at 150 °C, and the cooling condition was cooling water at 15 °C Schilling et al. [421] obtained the ideal optimal working fluid under the relaxed NLP problem, with an NPV of €2.1 million. Next, the five best working fluids were determined, with the best actual working fluid being propylene with an NPV of €1.8 million and P_{net} = 489 kW. It was also found that the final optimisation results were quite different from the thermodynamic optimisation results wherein the net power output was the objective function (propane, NPV = €0.55 × 10^6, P_{net} = 589 kW).

Later, Schilling et al. [428] combined molecular design and super structure-based flowsheet design and optimised these simultaneously. This method was applied to the case of an ORC for waste-heat recovery. In the system design, regeneration, turbine bleeding, and reheating were considered as the expansion options of the basic cycle; NPV, SIC, and P_{net} were considered as the objective function. At the same time, the process settings and working fluid were optimised, leading to the

best combination of these. The accuracy and the great improvement of the calculation efficiency of the method were verified.

Based on the above-mentioned 1-stage CoMT-CAMD method, considering again an ORC system for which the waste-heat source was waste water at 150 °C and the cooling by water at 15 °C, Schilling et al. [277] extended the integrated design method of circulation and working fluid to mixed working-fluid design and proposed the 1-stage CoMT-CAM^{b}D method. The authors considered thermodynamic and thermo-economic objectives. The most-promising mixtures were effectively identified, maximising net power output or minimising SICs. Comparison with the best pure components showed the potential to use working-fluid mixtures. In particular, for the presented case study, the net power output could be increased by 7%. In contrast, for thermo-economic goals, the benefits of mixtures were generally lower compared to pure components. However, if the optimal pure component had a higher optimal superheat, the mixture could reduce certain investment costs. In addition, the effects of mixture composition, cooling medium, and heat source temperature were also analysed.

Bowskill et al. [450] studied an ORC system for typical industrial waste heat with a heat source temperature of 210 °C, with a cycle minimum and maximum temperature set to 20 °C and 200 °C, respectively. An algorithm using an outer-approximation (OA) and an augmented penalty scheme was proposed to calculate the chemical properties of the ORC working fluid using SAFT-γ Mie [79] and the GC method, and to enhance the performance of the algorithm, a feasibility test was embedded in the algorithm to eliminate the infeasible parts of the search space. The original OA framework and the version reinforced with feasibility tests proposed in this work are shown in Fig. 18. The algorithm yielded the top ten fluids, with *n*-butane ranking first. Using this model, Bowskill et al. [450] performed calculations for the ORC
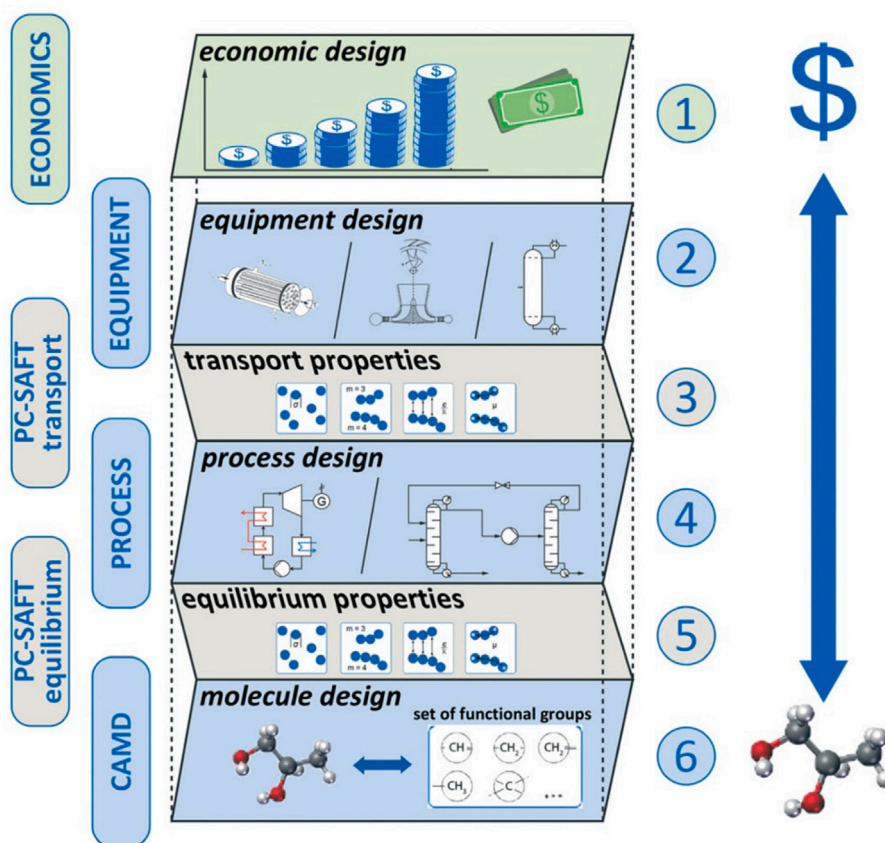
Fig. 22. Schematic illustration of the presented 1-stage CoMT-CAMD approach for the integrated thermo-economic design of the process, equipment, and molecule.
Source: Reprinted with permission from Schilling et al. [274].
© 2017 Royal Society of Chemistry.

application of a 120 ℃ geothermal heat source and a solar heat source with constant heat flow $\dot{Q} = 1$ MW, and obtained the optimal molecules propane and pent-1,4-diene, respectively, for each case study. Feasibility tests for the case studies revealed that low-molecular-weight alkanes (*e.g.*, propane), olefins (*e.g.*, pent-1,4-diene), and molecules containing ether groups (*e.g.*, methyl ethyl ether) are ideal ORC working fluids.

6.3. Geothermal and biomass

In the geothermal field, the design of working fluids for ORC has been realised for the first time through the CAMD approach. In 2010, Papadopoulos et al. [98,334] proposed the use of the CAMD approach to identify optimal working-fluid candidates for ORCs and conducted a case study on a representative low-enthalpy geothermal field with diverse temperature and flow characteristics. Multiple performance indicators were considered as design objectives in the study; particular attention was paid to safety and environmental characteristics such as flammability, toxicity, ODP and GWP. A performance ranking of molecules was obtained, including traditional and new working fluids. The most economically efficient molecule was found to be methyl-formate (R611), which was also favourably evaluated based on the other properties.

Extending the heat source range to 70–90 °C, Papadopoulos et al. [335] determined various performance characteristics of optimal working fluids under the variable-heat-source condition. For the first time, these authors addressed the design of binary working-fluid mixtures for CAMD-based ORC systems. This CAMD method exploits the beneficial properties of MOO technology by combining the proposed method with a nonlinear sensitivity-analysis method to quantify and evaluate the impact of inherent model uncertainty when selecting the highest-performing option among the best candidate mixtures obtained at the CAMD stage.

Papadopoulos et al. [141,336] illustrated the proposed approach by considering a case study of ORC power generation based on a 95 °C geothermal source at 9 kg/s flow rate, where the involved groups included $-CH_3$, $>CH_2$, $>CH-$, $>C<$, FCH_2O-, $-CF_3$, $>CF_2$, $>CF-$, with up to 16 groups allowed in each molecule. In this case, a series of mixtures were found, and their thermal efficiency and exergetic efficiency were higher than those of isopentane–isobutane mixtures proposed in the published literature. The sensitivity to the boiling point and critical properties of these mixtures was also analysed, indicating that for most mixtures accurate knowledge of the boiling point temperature is more important than of their critical properties. Details have been provided in Section 3.5.

Lampe et al. [51] proposed an overall ORC design framework that enables simultaneous optimisation of processes and working fluid based on system performance. The simultaneous optimisation was achieved by exploiting the molecular nature of the PC-SAFT EoS in the CoMT-CAMD approach. To predict thermal properties, a quantitative structure–property relationship (QSPR) for the heat capacity of ideal gases was proposed that relies on pure-component parameters of PC-SAFT. The two-step approach for the design of ORCs is shown in Fig. 17. This approach was applied in the optimisation of a geothermal ORC. Taking the net power output as the optimisation objective, the circulating parameters and circulating working fluid parameters were obtained. According to this, the ten most-promising working fluids were found from the database containing 200 substances, among which R227ea was judged the best practical candidate fluid, and it was observed that the top six working fluids from the real ranking list (used to assess the method) were all included in the ten working fluids found using this method.

Schilling et al. [420] applied the single-stage method of integrated design of ORC processes and working fluid to the case study of integrated design of a geothermal ORC. In this case, taking the net power

Table 6
Top five working fluids as identified in the study of Tillmans *et al* [425], with the net power output P_{net} as well as the process conditions; p_{cond} and p_{evap} are the pressure levels in the condenser and evaporator (respectively), $\dot{m}_{WF}$ is the mass flow rate of the working fluid and ΔT_{SH} is the degree of superheating determined in individual process optimisations. Adapted from Ref. [425].

Rank	Fluid	P_{net} / MW	$\dot{m}_{WF}$ / (kg s⁻¹)	p_{cond} / bar	p_{evap} / bar	ΔT_{SH} / K
–	target	1.95	71.5	7.0	25.5	0
1 (2)	Propene	1.48	47.1	11.0	32.0	0
2 (1)	Propane	1.50	47.8	9.2	27.4	0
3 (3)	Isobutane	1.44	41.4	2.8	9.3	0
4 (4)	1-Butene	1.43	40.0	2.9	9.6	0
5 (5)	Propyne	1.41	30.4	8.9	24.1	48.2

The order is according to the ranking of the CAMD step. The sorted rank according to the results of the individual process optimisations is shown in parentheses.

output as the objective function and considering 16 groups, the 1-stage method identified all the top ten working fluids in the database, and the computational effort was reduced by 94.1% compared to a single optimisation process for all molecular structures in the database.

Tillmanns et al. [425] integrated CoMT-CAMD into the object-oriented modelling language Modelica. Modelica's existing model library can be used to model the ORC system. The PC-SAFT state equation implemented using external functions provided the property prediction of the working fluid. The design method was applied to the integrated design of the ORC processes and working fluid of a geothermal power station, and the top five working fluids were successfully identified; these mainly consisted of short-chain alkanes and olefins, as shown in Table 6. The computational complexity of the optimisation process is high in this work, and if an uncertainty analysis can be carried out, it will make the results more informative.

Groniewsky et al. [549] used the Cycle-Tempo thermodynamic-modelling software to generate different ORC configurations, calling the FluidProp thermodynamic library and performing calculations with the PC-SAFT EoS, and implemented the CoMT-CAMD method using the optimisation process under MATLAB. Two different geothermal ORC configurations with heat-source temperatures between 80 and 180 °C were investigated using this method: a simple cycle, and a regenerative cycle. The initial working-fluid search space was established on the basis of PC-SAFT parameters of 60 real substances in the case. The results of CoMT-CAMD were checked against literature values obtained from conventional optimisation methods, and a more efficient loop configuration was determined for all 11 temperature terminations.

6.4. Solar thermal

The 1-stage CoMT-CAMD method for the integrated design of the ORC processes and working fluid proposed by Schilling et al. [423,424] was also applied to the ORC power generation of solar heat sources. The ORC structure included a reheater and a fixed solar thermal input of $Q = 463$ kW. Here, nine of the top ten working fluids in limited design space were identified by the 1-stage CoMT-CAMD method with integer cutting. Due to the local properties of the solver, the method missed the fifth-best molecular structure. Compared with the single process optimisation of all molecular structures in the database, the computational workload was reduced by 94.4%. The process model was extended by a detailed model of turbine design to demonstrate the possibility of modelling process components in a more detailed way. Compared to the constant turbine efficiency, the efficiency of the turbine in this study is calculated from the cycle process parameters and the properties of the fluid, providing a more accurate and realistic model. Of course, the calculations are more complex, but the 1-stage CoMT-CAMD methodology presented in this study allows for the simultaneous design of fluid properties and components.

On this basis, Lampe et al. [273] added the turbine meanline design procedure. A new design and optimisation method was proposed, which combines working-fluid selection, thermal cycle design, and preliminary turbine design. In the same case, the top ten organic working

fluids were obtained, mainly cyclopentane and cyclohexane derivatives, with alkyl side chains. The working fluid that allowed the maximum net power output was methylcyclohexane, with net power output P_{net} = 101.3 kW. This study demonstrated that in the case of small-scale ORC systems, turbine design constraints greatly affect the selection of the best working fluid and the corresponding thermodynamic cycle parameters.

6.5. Other technologies

Lampe et al. [55] used CoMT-CAMD to avoid complex MINLP problems, and the working-fluid characteristics were modelled using the PC-SAFT EoS. Using this method, an ORC driven by a waste-heat source at 360 °C was taken as an example to consider the linear siloxane family with the prospect of high-temperature application, and the thermal efficiency was taken as the optimisation goal. Based on the optimisation results, the best hypothetical working fluid was obtained. The most suitable real working fluid, octamethyltrisiloxane (MDM), was obtained through a mapping to a list of pure components. Finally, through the process optimisation of each of the working fluids considered, the result of the mapping step was verified. This was the first time that process optimisation was coupled with the selection of the working fluid, and the process goal was taken as the standard vertebra. Avoiding the use of targets other than process objectives in pre-selection may exclude the best fluid from further consideration.

Subsequently, Lampe et al. [20] developed a GC method to predict the pure-component parameters of PC-SAFT and realised the overall design of the new working fluid and the best system. The non-regenerative ORC with a waste-heat source at 320 °C was taken as a case study, and nine groups were considered to construct the working fluid. The optimal combination of working fluid and process parameters was obtained from the optimisation results, and the net power output of the resulting cycle is 19.6 MW. The CAMD step identified the actual working fluid with similar performance to the optimal fluid through database mapping and found the best actual working fluid to be chloroethane, with a net power output of 17.8 MW, which was only 9% less than that of the (hypothetical) optimal fluid. This is a good idea for optimisation. First find a fluid with ideal parameters, then optimise to get a practically feasible molecular structure based on the ideal parameters.

In the previously mentioned studies of Lampe and co-workers, due to the method of database mapping, the selection can only be made from known fluids; the actual design of a new fluid is impossible. Subsequently, Lampe et al. [419] integrated the CAMD method into the mapping steps of the CoMT-CAMD framework to achieve integrated process and fluid design. The CAMD method was based on a GC method for the PC-SAFT parameters (GC PC-SAFT) [445]. By investigating the case of non-regenerative ORC fluid design with a waste-heat source at 120 °C, the top ten working fluids were determined and verified by comparison to an existing database, demonstrating the general applicability of this method in the field of ORC working-fluid design.

White et al. [550] used the principle of CAMD to couple the thermodynamic model of a subcritical and non-regenerative cycle with the Peng–Robinson EoS [307] to optimise a subcritical and non-regenerative ORC to determine the relationship between the best working fluid and cycle operating conditions. They showed that when the temperature of the heat source is lower than 300 °C, the relationship between the working fluid and cycle operating conditions is determined. They observed and verified a linear relationship between the heat-source temperature, T_H and the optimal critical temperature for maximum power output ($T_c = 0.830 T_H + 41.27$ °C).

White et al. [447,448] proposed a CAMD-ORC optimisation method based on the SAFT-γ Mie GC EoS, implementing the model on the gPROMS platform. This method was used to study the optimal design of hydrocarbon working fluid in a simple ORC cycle for waste-heat recovery at three different heat-source temperatures (150 °C, 250 °C, or 350 °C). In this study, the CAMD-ORC MINLP optimisation model
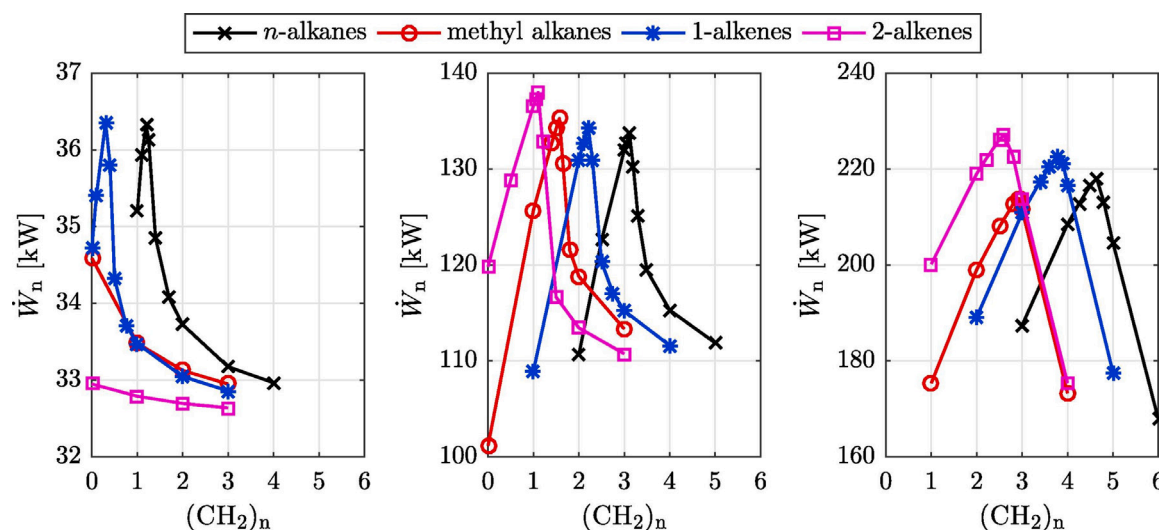
Fig. 23. The effect of the number of –CH$_2$– groups on the net power output from the ORC system for the four hydrocarbon families at three different heat-source temperatures; from left to right: 150 °C, 250 °C, 350 °C.
Source: Adapted from White et al. [447].

was used to investigate and optimise several different families of hydrocarbon working fluids, namely *n*-alkanes, methyl alkanes, 1-alkenes, and 2-alkenes. The results demonstrated that the theoretical optimal fluid for maximising power output should have the thermodynamic properties of maximising evaporation pressure and minimising superheat. This reduces the latent heat of evaporation and makes a better heat match between the working fluid and the heat source. As far as the actual working fluid is concerned, simple molecules such as propane and propylene were found to be especially suitable for low-temperature (150 °C) heat sources, and molecules with double bonds more suitable for medium-and high-grade heat sources with temperatures between 250 °C and 350 °C. Specifically, *n*-propane, 2-pentene, and 2-hexene were identified as the best working fluids at three heat-source temperatures, with optimal power output of 35.2 kW, 136.7 kW, and 219.0 kW, as shown in Fig. 23, and thermal efficiency of 9.7%, 16.9%, and 17.8%, respectively.

On this basis, the thermal economic analysis is incorporated into the CAMD-ORC framework, and the SIC of the system is taken as the optimisation objective.[146] In the same case, the working fluids of the ORC system with the lowest SIC were isoheptane, 2-pentene, and 2-heptene, with a SIC of £5620, £2760, and £2070 per kW, respectively. The importance of considering thermal economy within the framework of CAMD-ORC was demonstrated.

van Kleef et al. [275] further carried out multi-objective optimisation for the above case, taking into account the total investment cost and net power output, showing the relationship between net power output and SIC. These authors found that the molecular size of the optimal working fluid is related to the heat-source temperature. It was shown that multi-objective optimisation allows designers to choose work fluids that meet the requirements in a more flexible way.

In these case studies, it was found that different application scenarios lead to different optimal working fluids. From low-temperature wastewater to high-temperature heat sources in nuclear energy, no single fluid can be adapted to all working conditions, which is one of the driving forces behind the CAMD-ORC research. CAMD-ORC can customise the working fluids for various scenarios to guide the design of experiments as well as the development of related products. Considering the black-box nature of CAMD, it is necessary for researchers to provide as much analysis as possible on the cycle performance enhancement mechanism when designing working fluids to enhance the credibility and theoretical nature of the design. Providing uncertainty analysis can make the design results more informative. Based on the results and analysis of the CAMD-ORC, more focused experimental testing of application scenarios can be conducted to finalise the design of the ORC, including the structure and the working fluid.

7. Challenges, opportunities and outlook of ORC power systems

CAMPD methods for the integrated design of ORC systems and working fluids have rapidly evolved in the last decade. However, three main areas of further development of the methodology can be identified. These concern: (i) the prediction of the thermophysical properties of working fluids, (ii) the modelling of the system equipment characteristics both in on- and off-design conditions, as well as during transients, and (iii) the numerical algorithms and the extension of the methods to new applications.

7.1. Thermodynamic, transport, and other thermophysical properties

One of the main limitations of current CAMPD methods is that the working-fluid design space covers principally molecules containing carbon, hydrogen, and oxygen. A few studies additionally consider halogenated functional groups [98,141,518,519], given the advantageous thermodynamic properties of halogenated fluids for ORC applications. The main challenge with this class of fluids is that GC-based thermodynamic-property models tend to be less accurate due to their limitations in predicting the molecular dipole moment, especially in the case of multiple dipolar groups in the molecule. A potential solution to these limitations is represented by the vector GC method recently proposed by Hemprich et al. [555]. However, the modelling of halogenated substances may remain an academic problem given that these compounds are toxic or fall into the group of per- and poly-fluoroalkyl substances (PFAs) whose industrial use may be banned in the near future due to the health and environmental concerns they pose.

A fluid class which has not been considered in CAMPD for ORC systems so far is that of siloxanes, in spite of the fact that these compounds are frequently adopted in ORC gensets, especially for relatively high-temperature applications. It follows that the CAMPD solution methods still need the development of a comprehensive set of functional groups and a corresponding accurate property-prediction model for all molecular families relevant to ORC systems. This need is even more critical in the case of ORC systems operating with fluid mixtures, as current methods for the prediction of binary-interaction parameters lack sufficient accuracy or are applicable only to a restricted class of mixtures. On the contrary, the prediction of transport properties is performed in the more recent CAMPD implementations with high reliability, thanks to the development of the entropy scaling-based methods discussed in Section 4.

Besides thermodynamic properties, there are further properties that are critical for a proper assessment of the suitability of a candidate

working fluid for a given ORC application, *e.g.*, its flammability, toxicity, environmental impact, and thermal stability. These characteristics are, generally, assessed *a posteriori* for the best candidates identified by the CAMPD method, though there are research works where some of such properties were concurrently assessed via an automated procedure while ranking the optimal working fluids, see, *e.g.*, [98]. In principle, the ideal working fluid should be non-flammable, non-toxic, environmentally friendly, and thermally stable at temperature levels close to those of the heat sources. Given the expected evolution in environmental regulations, working fluids that exhibit high GWP will arguably not be feasible in the near future. Thus, the inclusion of an upper constraint for this characteristic in the CAMD problem formulation would be useful to prevent the optimiser from identifying molecules that are not viable. Regarding flammability and toxicity, one can, instead, argue that working fluids that are not fully satisfactory with respect to these properties can still be attractive [556].

For instance, a flammable working fluid enabling high conversion performance can still be the optimal choice. Appropriate measures to guarantee system safety are, after all, consolidated practice in industry, as also proven by the extensive use in ORC applications of fluids such as toluene, cyclopentane, and other hydrocarbons. The additional investment costs that the adoption of a flammable or toxic working fluid entails might be, indeed, compensated by the higher energy production of the plant or by the smaller size of the equipment. Such extra costs are, however, extremely difficult to estimate in a preliminary design phase and then accounted for in the CAMD model. The costs may also vary significantly based on the plant location. At the same time, there are applications such as waste-heat recovery from an industrial process, where the use of flammable or toxic working fluid may conflict with the environmental and safety regulation to which the industrial plant is subject. For these applications, the identification of the optimal working fluid cannot be performed without a qualitative estimation of the hazard profile of the molecules.

Predictive models for flammability, toxicity, and environmental properties of organic chemicals have been developed for decades, see, *e.g.*, Refs. [505,557] and show good reliability, at least for given fluid categories and a subset of these indicators. Such models can be incorporated into the CAMPD methodology to exclude molecules that do not meet certain targets, such as null ODP and low GWP values if their molecular representation matches that of the employed CAMD formulation. In other words, the additional thermo-physical properties of interest have to be modelled according to the molecular representation of the working fluid y in the optimisation problem (Problem (1)) of the CAMPD problem (see Section 5.1). The accuracy of the predictive model is key to ensuring that no molecule is discarded due to model uncertainties. Alternatively, more-advanced CAMD formulations can be developed, *e.g.*, molecule superstructures [452], that provide a higher degree of structural information than state-of-the-art CAMD formulations (*e.g.*, group counts of molecular groups). With a higher degree of structural information in the CAMD model, more-accurate predictive models for thermo-physical properties can be made available for CAMPD.

As far as thermal stability is concerned, no predictive models have been established so far. This is a strong limitation for current CAMD methods, as thermal stability data are available mainly for those molecules that are already of common use in the ORC technology. The potential of CAMD methods in identifying new molecules for high-temperature ORC systems is then considerably hindered. This is a knowledge gap that would deserve extensive research efforts in the future, and that is also of interest for other fields of application, such as heat-transfer fluids, high-temperature heat pumps, as well as gas-bearing technology. Predictive models for fluid thermal stability should not be limited to pure substances, as there is empirical evidence that mixtures may exhibit higher thermal stability than the single molecules in the blend at hand. An example is siloxane-based mixtures used as heat-transfer fluids in solar collectors, which can operate at temperatures exceeding $400\,°C$ [558], while the thermal stability of pure siloxanes is limited to appreciably lower temperature levels.

7.2. Preliminary design of system and equipment

State-of-the-art CAMPD frameworks for ORC systems enable, nowadays, the integrated optimisation of the thermodynamic cycle configuration and the main system equipment. This represents a key advancement in ORC system design with respect to conventional practice, where the various design phases are performed sequentially and iteratively repeated. The advantage of the integrated design approach is the possibility of accounting explicitly in the optimisation for the interdependency between the thermodynamic cycle parameters and the cost, performance, as well as design feasibility [273,275,281] of the various equipment. Due to the trade-off between such quantities, in a sequential design workflow, possible optimal solutions may be overlooked, as already recognised by White et al. [447,448]. At the same time, the consequence of a decision at one design stage can lead to challenging problems later on. For instance, the choice of the cycle maximum temperature and expansion ratio in the case of small power capacity applications may lead to an unfeasible turbine design, as the resulting rotational speed is too high or the height of the blade passages is too small for manufacturing. The implementation of a CAMPD methodology performing the integrated optimisation of the ORC system and the preliminary design of its main equipment arguably requires *ad-hoc* ORC equipment models. On the one hand, the equipment models have to be as detailed as possible since approximations can affect the working-fluid selection. On the other hand, the more detailed equipment models and larger ORC systems are considered in the CAMPD problem, the more design variables the optimisation algorithm has to deal with, and the higher the computational cost associated with the evaluation of the objective functions. Further developments in system and equipment modelling are envisaged in order to fully exploit the potential of the CAMPD methodology.

The key equipment for an ORC application essentially are the heat exchangers, which may belong not only to the working-fluid loop but also to auxiliary circuits of the plant, the expander, and, to a lower extent, given the limited size and consumed power, the pump. In the CAMPD studies targeting the simultaneous optimisation of the thermodynamic cycle and the related system equipment (see Table 4), the heat exchangers are typically modelled by assuming a counterflow configuration and discretising the heat-transfer area in several control volumes. The discretisation serves to capture the variation of the hot and cold stream thermodynamic properties and the consequent change in the heat-transfer coefficient and friction factor. These models are analogous to those used in industry for the preliminary design of heat-transfer equipment, and, as such, they exhibit adequate accuracy given the purpose of CAMPD studies. More-complex heat-exchanger topologies than those considered so far can be simulated with a similar modelling scheme by relying on the epsilon-NTU method or the cell method described in Ref. [559]. A limitation of the current modelling approach arguably consists in the fact that the flow configuration and the surface topology of the heat exchanger are to be chosen *a priori*. Consequently, the optimisation has to be repeated if the best heat-exchanger type is not known for the application of interest. As an example, think of extended surface heat exchangers where various fin topologies may be adopted. A solution to this limitation, which anyhow transcends the sole CAMPD methods, being inherent in heat-exchanger preliminary design practice, is currently unavailable.

Regarding the expander, this is often of the turbine type in ORC applications, apart from small power capacity systems. In standard design practice, the preliminary turbine design is performed based on the so-called mean-line flow model of the machine [560]. This model is formulated with a lumped-parameter approach, accounting for flow quantities only at the inlet and exit of each blade cascade, regardless of the detailed shape of the blades. In spite of the simple modelling approach, a mean-line code commonly features a relatively high computational cost for system simulations due to the various fluid-dynamic loss mechanisms that are to be considered and the nonlinearity

of the resulting system of equations. The work of Lampe et al. [273] is, at present, the sole CAMPD study that included a mean-line code in the system model to perform preliminary turbine sizing and performance estimation according to the characteristics of the working fluid. The code embeds some simplifications with respect to state-of-the-art mean-line models and allows only for radial-inflow turbine configurations. Though not demonstrated in their work, the authors assumed that the accuracy of their simplified mean-line code is adequate for working-fluid selection. A possible solution to prevent excessive simplifications that deserve future investigation may be offered by current advancements in reduced-order model techniques. A surrogate model of the turbine can be calibrated based on the results of a validated mean-line code for various working fluids, in analogy with the procedure described in Ref. [561] for the case of a centrifugal compressor. In principle, for efficiency prediction, the surrogate model can even be trained based on CFD results, thus enabling high accuracy with extremely low computational costs. To ease its integration into a CAMPD framework, the turbine reduced-order model must feature among the inputs the same parameters of the adopted EoS or thermodynamic properties representative of the working-fluid characteristics that can be calculated based on the molecular representation of the working fluid y in the optimisation problem (Problem (1)), such as the molecular complexity and the isentropic pressure–volume exponent [561]. A similar approach can also be adopted for the ORC pump. Moreover, the derivation of validated reduced-order models for the preliminary design of various turbine configurations, as well as of volumetric machines, may enable a thorough comparison of the different expander technologies for the application of interest. Notice that the CAMPD formulation would be the key enabler of such a comparison, as the traditional working-fluid selection process would arguably require an unfeasible simulation time or lead to non-definitive conclusions if the comparison is repeated only for a limited amount of compounds.

The improvement of the models for preliminary equipment design can also facilitate the implementation in CAMPD frameworks of more-accurate costing models for ORC equipment. In this regard, the models currently in use typically estimate the cost of ORC equipment based on the value of a single performance indicator. For example, the cost of an expander is often estimated based on its power output. However, its cost depends on the size and design complexity, which, in turn, are related to the characteristics of the working fluid and the thermodynamic cycle. Single performance indicators do not capture these dependencies and, thus, might lead to inaccurate cost estimations [562]. Furthermore, the cost of the working fluid should also be considered. Having additional charge in the system has a direct increase in the investment cost but also indirectly due to possibly more stringent safety or environmental constraints.

Another research area related to ORC system design that is still unexplored, except for the work of Schilling et al. [427], is multi-point design optimisation. In waste-heat-recovery applications, especially aboard vehicles or in solar plants, the operating conditions of the ORC system vary over time. Consequently, the definition of a single design point does not reflect the actual potential of the application and may lead to the selection of a suboptimal working fluid, as demonstrated by Schilling et al. [427]. In analogy with the design practice of aero-engines, a better strategy is, then, to optimise the ORC design for several operating conditions that are representative of the actual operating envelope of the system. A methodology to select a proper set of quasi-steady-state operating conditions based on the so-called aggregation techniques is described in Ref. [427]. The main limitation of this exploratory work is that no preliminary design of the equipment is performed, thus making the prediction of the ORC system performance in the various operating conditions arguably approximate. Proper evaluation of the objective functions in a multi-point design optimisation problem requires, instead, an ORC model allowing not only for equipment sizing but also for off-design simulation. The implementation of an off-design model in a CAMPD framework will

require an *ad-hoc* modelling strategy for the expander, as in system simulation, the off-design characteristics of an expander are commonly predicted through pre-calculated or even experimentally-based performance maps. Data-driven modelling techniques can provide a computationally efficient means for accurately predicting such performance maps based on working-fluid characteristics and the expander design inputs. On the contrary, for heat exchangers, similar models to those used for preliminary sizing can be adopted.

Finally, if the variation of the ORC system operating conditions is too fast to consider a set of quasi-steady-state operating points, the ORC off-design model is to be replaced by a dynamic model, as studied in [276]. In this case, the CAMPD formulation includes the set point of the manipulated variables of the control system. Consequently, an equivalent optimal control problem is solved in addition to the optimisation of the thermodynamic process and related equipment. The current challenge of the methodology is related to the computational cost associated with dynamic simulation. Notably, the simulation time must be reduced such that the design space considered in the optimisation or the level of detail of the models for preliminary sizing of the system equipment can remain similar to those of CAMPD frameworks for single steady-state design point optimisation. The ideal approach consists in replacing the dynamic model with an equivalent transfer function whose coefficients are expressed as a function of the characteristics of the working fluid and the system equipment. As an alternative, if the dynamic requirements of the application are stringent and then the controllability of the system is of concern, a design approach similar to that devised in Ref. [563] may be preferable for the CAMPD problem formulation. In this work, as the first step of the methodology, the design of the ORC system is optimised with respect to two objectives functions: one accounts for the thermodynamic performance of the system, *i.e.*, the net power output; the second objective function is instead representative of the dynamic characteristics of the plant. This quantity is the total volume of the more bulky equipment of the ORC module, namely, the primary heat exchanger and the recuperator. In the second step, the dynamic performance of the system is assessed by simulating, in an automated way, critical transients for each design on the Pareto front and by verifying whether the dynamic requirements of the application are met or not. A PI (Proportional-Integral) controller is tuned for each candidate solution by setting the proportional gain to a value that is proportional to the heat exchangers volume, thus accounting for the specific characteristics of the selected solution on the Pareto front while keeping the integral time at a suitable constant value. Based on the outcome of these simulations, a final optimal system design of the ORC plant can be selected, knowing that the equipment design characteristics, in particular the heat exchangers size, will not hinder the synthesis of the controller.

7.3. Optimisation algorithms and implementation opportunities

One of the key elements of a CAMPD method is the optimisation algorithm. Possible options considered in the past are derivative-free metaheuristic algorithms that include mechanisms to avoid locally optimum solutions. However, there is a large range of derivative-free algorithms other than metaheuristics [177] that are worth exploring, as they may facilitate the future incorporation of high-fidelity process and equipment models in CAMPD for ORC systems. Indeed, global gradient-based optimisation algorithms can be exploited for CAMPD problems if all equations of the models are given in an explicit form [518,519]. However, explicit formulations of the mathematical model are often possible only for simple thermodynamic ORC models and thermodynamic-property models, *e.g.*, GC approaches, or cubic EoS. More-complex system models are thus usually modelled by implicit functions, and local optimisation algorithms have to be used, with the consequence that locally optimal solutions may be found by

the optimiser. A solution to this limitation may be provided by the recent advancements in global optimisation algorithms for implicit functions [564,565] or using embedded machine-learning models [566]. The use of these algorithms for CAMPD deserves future investigations.

Regarding the applications, as shown in Section 6, CAMPD methods have already been applied to almost all kinds of processes and energy sources of economic relevance for ORC technologies. Only novel or niche applications have not been explored yet, such as ocean thermal energy conversion, waste-heat recovery aboard aircraft, or propulsion of satellites. The study of these applications does not require arguably additional developments in the CAMPD methods. In principle, only the system model must be adapted. A topic that requires, instead, further advancements is process integration. In current CAMPD studies on waste-heat recovery from industrial processes, the characteristics of the waste-heat source represent an input of the design problem. A more-efficient solution may be found by redesigning the thermal network or the process itself from which waste heat is recovered to optimise the ORC system integration and the overall energy consumption of the plant. Most of the studies, *e.g.*, Refs. [567,568], which explore this design problem, make use of pinch analysis to optimally integrate the ORC system with the multiple heat sources at different temperature levels of an industrial process. The most advanced methods dealing with ORC design and process integration, such as those proposed in Refs. [195,201,202], do not consider a predefined ORC configuration, but the same ORC system model, also called ORC superstructure. This model can be used to optimise the plant layout by means of additional discrete design parameters that can activate or deactivate some flow connections in the working-fluid loop(s). However, in these works, the working fluid of the ORC is selected from a small list of predefined organic compounds. At present, no CAMPD method has been implemented to tackle ORC design and process integration. Only the work of Schilling et al. [428] considered an ORC superstructure within a CAMPD framework, though the optimiser can choose only between three ORC configurations, while the ORC superstructures discussed in the literature offer multiple options. Further developments in this area are envisaged in the upcoming years since the choice of the ORC configuration impacts the ranking of optimal working fluids, as demonstrated by Schilling et al. [428]. Another interesting research area for CAMD methods is robust design. In the field of energy conversion technology, this involves designing a thermal machine or prime mover, or even one of their components, while accounting for uncertainty in the model as well as in the design specifications. The goal is to minimise the impact of the various uncertainty sources on the selection of the optimal solution. The outcome of a robust CAMD procedure would consist of a ranking of the optimal working fluids based on the chosen figure of merit along with its uncertainty, which should be fluid-dependent.

Despite the potential of the method, CAMPD is still marginally used in ORC design practice. The main reasons thereof are: (1) the risks felt by manufacturers in adopting novel working fluids, especially if limited experimental data about their thermochemical and thermophysical properties are available; and (2) the specific expertise needed to set up the optimisation problem and the system model in current CAMPD tools, as well as to analyse the results. To facilitate their deployment in ORC design practice, researchers should ensure that CAMPD methods can be easily replicated. This can be achieved by thoroughly documenting the methods' workflow or by making the CAMPD tools open source. Another solution is to implement the developed methods into software and tools of common use in the industry. In this way, the users can be guided in the CAMPD problem implementation through a graphical user interface and a sequential process, as in the case of software for process simulation. The first step in this direction is represented by the work of Schilling et al. [423,428], which shows that integrating CAMPD methods in commercial process flowsheeting software is possible. Just recently, an integrated molecule and process design approach has also been integrated into the in-house flowsheet simulator of BASF SE [520]. However, both implementations are so far not commercially available.

Tackling the challenges mentioned above will improve the relevance, reliability, and applicability of CAMPD for ORC systems. However, it should be noted that aiming for increased model complexity and more-accurate models in CAMPD may not always be worthwhile. As the main aim of CAMPD is the selection of optimal molecules, the key requirement for the adopted system and thermodynamic models is to be accurate enough to properly capture the trends between the various molecules with respect to the design objectives. Thus, the integration into CAMPD of more-accurate models and methods is meaningful only if they lead to the selection of different working fluids with respect to their less-accurate counterparts. The comparison of the solutions obtained with new CAMPD implementations against those of state-of-the-art methods is thus always crucial for CAMPD research.

CRediT authorship contribution statement

Christos N. Markides: Writing – review & editing, Writing – original draft, Visualization, Validation, Supervision, Resources, Project administration, Methodology, Funding acquisition, Formal analysis, Conceptualization. **André Bardow:** Writing – review & editing, Writing – original draft, Visualization, Supervision, Methodology, Formal analysis, Conceptualization. **Michel De Paepe:** Writing – review & editing, Writing – original draft, Visualization, Supervision, Methodology, Formal analysis, Conceptualization. **Carlo De Servi:** Writing – review & editing, Writing – original draft, Visualization, Methodology, Formal analysis, Conceptualization. **Joachim Groß:** Writing – review & editing, Writing – original draft, Visualization, Supervision, Methodology, Formal analysis, Conceptualization. **Andrew J. Haslam:** Writing – review & editing, Writing – original draft, Visualization, Methodology, Formal analysis, Conceptualization. **Steven Lecompte:** Writing – review & editing, Writing – original draft, Visualization, Supervision, Methodology, Formal analysis, Conceptualization. **Athanasios I. Papadopoulos:** Writing – review & editing, Writing – original draft, Visualization, Supervision, Methodology, Formal analysis, Conceptualization. **Oyeniyi A. Oyewunmi:** Writing – review & editing, Writing – original draft, Visualization, Methodology, Formal analysis, Conceptualization. **Panos Seferlis:** Writing – review & editing, Writing – original draft, Visualization, Supervision, Methodology, Formal analysis, Conceptualization. **Johannes Schilling:** Writing – review & editing, Writing – original draft, Visualization, Methodology, Formal analysis, Conceptualization. **Patrick Linke:** Writing – review & editing, Writing – original draft, Visualization, Supervision, Methodology, Formal analysis, Conceptualization. **Hua Tian:** Writing – review & editing, Writing – original draft, Visualization, Supervision, Methodology, Formal analysis, Conceptualization. **Gequn Shu:** Writing – review & editing, Writing – original draft, Visualization, Supervision, Methodology, Formal analysis, Conceptualization.

Declaration of competing interest

This manuscript has not been submitted to, nor is under review at, another journal or other publishing venue. They have no known competing financial interests or personal relationships that could have appeared to influence the work reported in this paper.

Acknowledgements

Appendix

See Tables A.1–A.5.

Table A.1

Overview of mixture selection approaches.

Ref.	Component features	Formulation and objective functions	Optimisation algorithm	Design variables
Pre-specified mixture compositions				
[150]	1 ternary mixture and pure components	SOO- Max net electric efficiency	Optimisation with ORCSim+ StanMix	Maximum temperature and minimum temperature in regenerator
[151]	10 binary, 3 ternary	SOO- Max net power output,	Generalised reduced gradient method [569] (NLP)	Mixture concentrations, cycle pressures, mass flows, and medium temperatures
[152]	4 binary and several pure component fluids	SOO- Max thermal efficiency	Simulated Annealing	Mixture concentration
[19]	8 binary	SOO- Max second law efficiency	Generalised Reduced Gradient (GRG) nonlinear multistart algorithm (NLP)	Evaporating pressure and mixture concentration
[153]	10 binary	SOO- Min ratio of the specific investment cost over the effectiveness of heat recovery	PSO	Mixture concentration, pinch temperatures in condenser, evaporator and regenerator, expander inlet pressure and air-cooled condenser area
[154]	6 binary	SOO- Max net power output	PSO (population up to 40, generations 60)	Mixture concentration, highest and lowest cycle operating temperatures
[155]	12 binary	SOO- Max second law efficiency	Cycle Tempo internal optimisation algorithm	Mixture concentration and re-injection geothermal fluid temperature are varied
[156]	7 binary	SOO- Max net power output without or with leakage, or minimise CO_2-eq emissions	PSO	Evaporating pressure, pinch-point temperature differences in evaporator and condenser, mass flow rates of working fluid and cooling source
[157]	6 binary	SOO- Max net power output	PSO	Mixture concentration, high and low cycle temperatures
[158,159]	1 binary mixture	MOO- Max exergy efficiency, Min levelised energy cost	NGSA II	Mixture concentration, evaporator and condenser temperature, pinch point temperature difference, degree of superheating
[160]	5 binary	MOO- Max exergy efficiency, expander-specific volume flow ratio	GA (Matlab), population size 60, generations 100	Mixture concentration, evaporation bubble point, condensation dew point, expander inlet temperature and
[161]	2 pure fluids and 1 fully specified mixture	MOO- Maximise net power output, Min total cycle cost	GA (Matlab), population size 30,000, generations 500	Turbine inlet pressure, degree of superheating, condensing temperature at bubble point, boiler and condenser pinch point temperature. For condenser and boiler: inlet tube diameter, number of tubes, baffle spacing
[162]	2 binary	MOO- Max net work output, Min equipment cost	Interior point algorithm (NLP), use of SAFT-VR	Evaporator and condenser temperature, degree of superheating, working fluid flowrate

Table A.1 (*continued*).

Ref.	Component features	Formulation and objective functions	Optimisation algorithm	Design variables
Pre-specified mixture compositions				
[163]	28 binary	MOO- Max net power output and second law efficiency, Min conductance (UA)	NSGA-II	Mixture concentration, evaporation pressure, condensation temperature, and minimum temperature difference approach in the evaporator.
[164]	12 combinations of pure fluids in ORC and VCC	MOO- Max second law efficiency, Min conductance (UA)	GA (Matlab)	VCC evaporator and condenser temperatures, condenser pinch point temperature and degree of superheating and of subcooling, ORC evaporator degree of superheating and pinch point, condenser temperature, degree of subcooling and pinch point, and mass flowrate
[165]	5 binary mixtures and 1 pure	MOO- Min conductance (UA), Max net electrical power and cooling power	NSGA-II, 729 individuals in initial population	Mixture concentration, condensation and evaporation pressures, degree of superheating, regenerator effectiveness, pinch temperature difference, mass fraction of fluids
Mixtures from combination of pure components				
[166]	11 pure components	SOO- Max cycle efficiency	Mode Frontier-evolutionary approach	Mixture composition and concentration
[167]	30 pure and mixed fluids	SOO- Max net power output	GA (Matlab), population size 100, generations 500 or 200	Binary mixture composition and concentration, expander inlet temperature and pressure and hot fluid outlet temperature.
[168]	19 pure components	SOO- Max absorbed heat, or net power output, or thermal efficiency, or second law efficiency, or Min the area of the temperature profiles between the working fluid and the heat source or sink	CONOPT (NLP)	Mixture composition and concentration, number of components in mixture, ORC operating conditions
[169]	24 pure components	SOO- Max net work output	SQP, tear stream approach, two internal loops used to converge the model simulation and cooling water flow	Mass flowrate of each pure component, considering 6 components at a time at each optimisation, evaporator pressure, condenser pressure and degree of superheating
[170]	23 pure components	SOO- Min area between hot and cold temperature curves in condenser	GA for MINLP (population 150, generations 50), BARON for NLP	Presence of pure component in mixture, concentration of components in ternary mixture, condenser pressure
[171]	10 pure components	MOO- Max thermal efficiency, Min total annualised cost	CONOPT (NLP) with ϵ-constraint method	Number of components in mixture, mixture composition, and concentration, ORC operating conditions and HEX surface areas

Table A.2

Approaches for systematic fluid selection and ORC process design and/or heat integration.

Ref.	Component features	Configuration features	Formulation and objective functions	Optimisation algorithm	Design variables
Pre-specified ORC configurations					
[189]	6 pure fluids	BORC, Single (SRORC) and dual (DRORC) stage regenerative ORC	SOO- Max exergy efficiency	GA (population 200, generations 2000)	Turbine inlet pressure and temperature (all cycles), split fractions of turbine outlet stream (SRORC, DRORC)
[190]	Ammonia-water (both ORCLFE and ORCSC), CO_2-acetone (ORCSC), pure fluids	Simple ORC, ORC with liquid-flooded expansion (ORCLFE), ORC with solution-circuit (ORCSC), transcritical conditions were considered for the ORC and the ORCLFE	SOO- Max second law efficiency	Optimisation (Engineering Equation Solver) performed separately for different source temperatures	ORC: evaporating pressure, ORCLFE: evaporating pressure, ratio of flooding liquid to working fluid, ORCSC: rich and weak solution concentration
[191]	9 pure fluids	Single pressure, recuperated and double pressure	SOO- Max net present value or investment cost	CasADi (automatic differentiation) and WORHP (SQP-interior point NLP solver)	Single pressure: Temperature before the turbine, saturation temperature at the pressure before the turbine, the pressure at the inlet of the pump, the mass flow of the working fluid, the recuperator effectiveness; Double pressure: All of single pressure and the temperature before the second turbine, the saturation temperature at the pressure before the second turbine and the mass flow rate through the second turbine. In both cases, for each HEX the shell diameter, the tube outside diameter, the tube pitch, the baffle cut and the distance between the baffles.
[209]	9 mixtures of up to 5 components with pre-specified concentrations	Simple ORC, parallel two-stage ORC, series two-stage ORC	SOO- 1st stage: 1st and 2nd law criteria; SOO- 2nd stage: STORC-all fluids parametric assessment, net power output and turbine size parameter; MOO- 3rd stage: STORC and R32/R125/R134a, net power output and turbine size parameter	1st and 2nd stage parametric simulations, 3rd stage GA (population 500, generations 600)	1st and 2nd evaporator pressure, pinch point temperature in evaporator 1, degree of superheating in evaporator 1
[192]	14 pure fluids	Subcritical, supercritical, trilateral	SOO-Max work output	Golden section search	Working fluid flowrate
[213]	5 mixed and 1 single fluid for HT, 3 mixed and 1 single fluid for LT	Dual loop	MOO- Thermal efficiency, payback period, annual CO_2 emission reduction	NSGA-II (population 120, generations 1000)	Evaporation temperature of HT loop, condensation pressures of the HT and LT loops, pinch point temperature of the HT evaporator, of the internal HEX and of the LT condenser, mass fraction of first component of the HT and LT loops.
[193]	2 single fluids for HT loop, 5 fluids for LT loop	Dual loop	MOO- Min capital cost, Max exergy efficiency	GA, ANN for the SOFC-GT-ORC model	Degree of superheating of HT loop, pinch point temperature differences in HT and LT loops, condenser temperatures of HT and LT loops HT loop pressure factor
Design of advanced ORC configurations					
[194]	1 pure fluid	Generic representation of multi-pressure ORC, pressure loops may be added, different turbine types may be used	SOO- Min exergy loss or Max work output	New pressure loop added automatically if it improves the performance, NLP within each pressure loop	Number of loops, flowrates of working fluid, saturation temperatures and temperature of the outlet of the heat extraction section for each loop, type of turbine (induction or expansion)

Table A.2 (*continued*).

Ref.	Component features	Configuration features	Formulation and objective functions	Optimisation algorithm	Design variables
Pre-specified ORC configurations					
[196,197]	1 pure fluid [196], 2 pure fluids [197]	Generic structural representation with thermal cuts between expansion and compression operations (HEATSEP and SYNTHSEP)	SOO-Max total electrical power	External level: GA to handle structural parameters; Internal level: SQP to handle continuous operating parameters	Number and interactions of pressure levels, expansion, compression and heat exchange stages
[198,199]	1 pure fluid	Generic representation of ORC, addition of multiple turbines with reheating and feedwater preheating	SOO- Max thermal efficiency [198]; MOO- Max thermal efficiency, Min cost of electricity [199]	External level: Evolutionary algorithm (population 25, generations 200, Internal level: NLP (CONOPT3)	Number of turbines, superheaters, feedwater preheaters stages, feedwater pumps
[210]	1 mixture of pre-specified composition and concentration	Superstructure for cryogenic ORC	SOO- Max Annual profit	GA (population 200, generations 50	Ten **binary variables** that activate or de-activate the multi-stream cryogenic heat exchanger, vapour flash, expansion and vapour re-condensation process; 9 **continuous variables**, including 5 for pressure change of pumps and 4 for split fractions of vapour re-condensation
[200]	1 pure fluid	Superstructure with ANN for fluid property predictions	SOO- Max work output or Min levelised electricity cost	MAiNGO (parallel version)	Low, medium and high pressure level, corresponding mass flows for these levels, superheating at high pressure level, enthalpies at turbine and preheater, existence of high pressure level, of parallel heating mode, of turbine bleeding, of compression at medium pressure level and of expansion directly to low pressure, of recuperator, of high and medium pressure superheater
[201]	Up to 14 pure organic fluids (simultaneous fluid selection)	Superstructure	SOO- Outer GA Max work output, Inner MILP Min operating cost; MOO- Outer GA Max work output, Min investment cost, Inner MILP Min total annualised cost	Outer level GA, Inner level MILP	Binary variables: pumps, turbines, condensation and evaporation levels, working fluid; Continuous variables: pressure and temperature levels
[202]	12 pure fluids (simultaneous fluid selection)	Superstructure with different condensation and expansion options	SOO- Max net power output	GA (population 800, generations 100)	Temperatures of the three condensation levels, condensation and expansion layout (parallel, partial parallel, serial), working fluid
[214]	12 pure fluids, 9 mixtures (simultaneous fluid selection)	HEATSEP approach	SOO- Max net power output	Outer and upper level: GA (population 20, generations 50, Lower level: SQP	Working fluid type (single fluids) or mixture composition (from pre-specified options) and concentration (for mixtures), binary option for sharing of compression, heating, expansion and cooling processes between two elementary cycles, initial states of compression and expansion process.

Table A.2 (*continued*).

Ref.	Component features	Configuration features	Formulation and objective functions	Optimisation algorithm	Design variables
Pre-specified ORC configurations					
Heat integration approaches					
[203]	3 pure fluids	Regenerative ORC, superstructure for utility network design	SOO-Min total annualised cost	MINLP (CPLEX, CONOPT, DICOPT)	Utility network structure, equipment sizes, flowrates *etc.* (up to 190 continuous and 39 binary variables)
[204]	3 pure fluids	Basic ORC, superstructure for utility network design	SOO- Stage 1: Min hot and cold utility, Stage 2: Max work output	BARON	Utility network structure, equipment sizes, operating optimisation of ORC, Stage 1: 295 continuous, 43 binary variables, Stage 2: 131 continuous 28 binary variables
[215]	6 pure fluids	HEATSEP approach for boiler-heat source integration in simple, regenerative and dual pressure ORC structures	SOO- Max net work output	Hybrid algorithm, development of hot composite curves, SQP for ORC simulation, development of cold composite curves	Evaporation pressure, superheating temperature (simple and regenerative), medium and high pressure, corresponding superheating temperatures, split fraction of working fluid, mass flowrate of fluid in all layouts)
[206]	4 pure fluids	Superstructure of heat and cold utility network	SOO- Min total annualise cos	NLP (CONOPT)	524 variables
[207]	1 pure fluid	Generic superstructure for ORC and utility network	SOO- Min Total annualised cost	BARON-CPLEX	Problems of up to 475 binary and 1599 continuous variables
[208]	2 pure fluids (simultaneous fluid selection)	Incorporation of basic cycle components based on exergy composite curve profiles	SOO-Level 1 and 2: Min exergy losses, Level 3: Min cost	MILP	Stage 1: Flowrate of external utilities (integer variables) to satisfy energy requirements of system and corresponding temperature levels; Stage 2: vaporisation and condensation temperatures, minimum liquid preheating and vaporisation heat load, working fluid and flowrates (defining a cycle structure); Stage 3: Select optimum cycle structure from the previous options
[195]	7 pure fluids (simultaneous fluid selection, different fluids may be used simultaneously in the overall ORC design)	ORC superstructure for design of multiple power generation cascades and the corresponding hot utility heat exchange network	SOO- Max power generation	BARON	Number and structure of ORC cascades, operating conditions (*e.g.*, flowrates, pressures, temperatures) number and types of working fluids, quantity and type of cooling utility
[211,212]	36 mixtures	Simple ORC, the minimum number of stages required by the turbine are also calculated	SOO-Max cycle exergy efficiency	PGS-COM evolutionary algorithm	Condenser and turbine inlet pressure, superheat temperature, mixture concentration, working fluid mass flowrate and flowrates of external utilities

Table A.3

Summary of ORC working fluid selection studies that incorporate a detailed model for the expander.

Ref.	Working fluids	Optimisation of operating conditions	Expander type	Expander design method	Off-design
[240]	17 pure components	1-D steady state model; aggregate objective function (equipment size, rotational speed, work generated)	Radial	1-D analysis; correlations, velocity triangles based on fixed isentropic velocity ratio and exit velocity ratio.	Yes
[241]	28 pure components	1-D steady state model; MOO on heat exchanger area and maximum performance factor	Radial	1-D analysis; deterministic and empirical models for operating regimes inside the expander; loss and turbine efficiency model.	No
[242]	6 pure components	1-D steady-state; parametric analysis for design and off-design operating conditions	Radial	1-D analysis; detailed modelling of expander and losses estimation. Parametric analysis of loading factor on expander design and velocity triangles for 6 WF.	Yes
[279]	7 pure components	1-D steady state thermodynamic	Radial	1-D analysis; velocity triangles; energy losses estimation; breakdown of losses per source	Yes
[243,244]	8 pure components	Expander optimisation	Radial	Mean-line model with estimation of losses.	No
[245]	5 pure components	1-D steady state thermodynamic	Radial and axial	3-D Reynolds-Averaged Navier–Stokes model, k-ω turbulence model	No
[280]	4 pure components	1-D steady-state thermodynamic; MOO	Radial	1-D model with tension and vibration constraints	No
[246]	5 pure components	1-D thermodynamic	Radial	Variable efficiency turbine model using velocity triangles and simplified models for energy losses	Yes
[263]	1 zeotropic mixture, CO_2	1-D thermodynamic model	Axial	Variable efficiency turbine model using velocity triangles and simplified models for energy losses	Yes
[270]	6 pure components, 1 zeotropic mixture	Only expander model — parametric analysis	Radial	3-D Reynolds-Averaged Navier–Stokes model, k-ω turbulence model, with Peng-Robinson equation of state for thermodynamic properties prediction	Yes
[247]	11 pure components	1-D thermodynamic model	Axial	1-D expander model; single and multi-stage expander	No
[245]	2 pure components	Only expander model	Radial	3-D Reynolds-Averaged Navier–Stokes model with Peng-Robinson	No
[248]	2 pure components	1-D thermodynamic with optimal expander design	Radial	3-D Reynolds-Averaged Navier–Stokes model	No
[249]	6 pure components	1-D thermodynamic model; multi-objective optimisation	Radial	1-D expander model with losses estimation and variable turbine efficiency	Yes
[271]	1 pure component and 1 zeotropic mixture	1-D thermodynamic model;	Radial	1-D expander design model; 3-D computational model for performance evaluation	Yes
[273]	CAMPD	1-D thermodynamic; integrated optimisation of working fluids and ORC (with expander model)	Radial	1-D expander design model; velocity triangles	No

Table A.4

Key features of heat exchanger modelling approaches.

Ref.	Fluid type	Boiler	Condenser	Modelling approach
Steady-state models- *cf.* Section 3.1				
[155]	Pure and binary mixtures	Shell-and-tube counter flow for pre-heater and evaporator	Air-cooled, cross-flow with finned tubes	Correlations of heat transfer coefficients
[156]	Binary mixtures	Shell-and-tube, preheating, evaporation and superheating zones	Shell-and-tube, cooling and condensing zones	Correlations of heat transfer coefficients, discretisation
[161]	Pure and binary mixture	TEMA E type shell-and-tube, one shell, one tube pass	TEMA E type shell-and-tube, one shell, one tube pass	Discretisation, correlations for heat transfer and pressure drops
[162]	Binary mixtures	Shell-and-tube, counter-current, double pipe, preheater and evaporator	Shell-and-tube, counter-current, double pipe, de-superheater and condenser	Discretisation, correlations of heat transfer coefficients
[163]	Binary mixtures	Counterflow	Counterflow	Discretisation
[169]	Mixtures from pure fluids	Floating head (tube only)	Floating head (shell-and-tube)	Constant heat transfer coefficients
[170]	Mixtures from pure fluids	–	Shell-and-tube, only condensation	Discretisation
[171]	Mixtures from pure fluids	Shell-and tube (one pass shell, two-pass tubes)	Shell-and tube (one pass shell, two-pass tubes)	Correlations for heat transfer and pressure drop
Steady-state models — other cases				
[250]	Pure	Plate (pre-heater, evaporator, superheater)	Finned tube with circular fins	Correlations of heat transfer; Design variables: number of plates and length in the evaporator, number of tube rows and frontal area in the condenser
[251]	Pure	Shell-and-tube	Shell-and-tube	Correlations for heat transfer and pressure drop; Design variables: geometrical features are design variables
[264]	Mixtures	Shell-and-tube (hexagonal arrangement tubes in tube side, baffle plates in shell side)	Shell-and-tube (hexagonal arrangement tubes in tube side, baffle plates in shell side)	Correlations for heat transfer and pressure drop; Design variable: Number of tubes (in parametric evaluation)
[252]	Pure	Shell-and-tube for preheating, evaporation and superheating	Plate-and-tube (two rows of single pass, flat tubes, plate fins used for finned surface)	Correlations for heat transfer, pressure drop through discretisation of duct length; Design variables: tube length and shell diameter in boiler, plate dimension and number of channels in the recuperator
[281]	Pure	Shell-and-tube (preheater, evaporator)	Shell-and-tube (desuperheater, condenser)	Heat transfer correlations, systematic calculation of pressure drop; Design variables: different HEX cross-sectional areas tested
[180]	Pure	Single rectangular channels with fixed channel width and height (pre-heater, evaporator, superheater)	Single rectangular channels with fixed channel width and height (pre-heater, evaporator, superheater)	Moving boundary model; Design variable: length of heat exchanger
[272]	Pure and a mixture	Shell-and tube	Shell-and tube	Discretisation, correlations for heat transfer and pressure drop
[253]	Pure	Fin-and-tube	Plate	Correlations for heat transfer

(*continued on next page*)

Table A.4 (*continued*).

Ref.	Fluid type	Boiler	Condenser	Modelling approach
Steady-state models- *cf.* Section 3.1				
[254]	Pure	Plate with counter current arrangement (boiler includes preheating, evaporation and superheating)	Plate with counter current arrangement (boiler includes preheating, evaporation and superheating)	Heat transfer correlations
[255]	Pure	General concentric-tube, counter-flow model with infinitely thin walls	General concentric-tube, counter-flow model with infinitely thin walls	6 different ORC configurations, 3 zones for each HEX, tube diameters determined from fluid flowrate, heat transfer coefficients
[256,257]	Pure	Plate with preheating, evaporation and superheating	Plate with condensation and superheated regions	Discretisation, heat transfer coefficients
[258]	Pure	Brazed plate (preheater-evaporator, superheater)	Shell-and-tube	Moving boundary model with variable heat transfer coefficients
Dynamic models				
[259]	Pure	Straight pipe in pipe counterflow	Straight pipe in pipe counterflow	Finite volume model
[260]	Pure	Finned tube represented as counter flow straight pipe, preheating, evaporation and superheating	Steady-state	Moving boundary model
[261]	Pure	Preheating, evaporation, superheating	Undisclosed	Moving boundary model
[266,267]	Mixtures	Shell-and-tube	Shell-and-tube	Finite volume model; Design variables: Evaporator and condenser surface areas
[268]	Mixtures	Shell-and-tube	Shell-and-tube	Moving boundary model
[269]	Mixture	Counter-current thimble HEX	Counter-current thimble HEX	Moving boundary and finite volume model
[262]	Pure	Fin-and-tube, cross-counter flow	—	Moving boundary; Design variables: fin height, tube outer diameter, fin pitch, tube length and tube spacing.
Molecular design approaches				
[98]	Pure	Shell-and-tube	Shell-and-tube	Aspen HTFS+, steady-state model; Design variables: Surface areas of evaporator and condenser
[278]	Mixtures	Tube and shell heat exchangers, with split-ring head construction (TEMA S)	Tube and shell heat exchangers, with split-ring head construction (TEMA S)	Constant overall heat transfer coefficients, no pressure drop along the exchangers, steady-state model; Design variables: Surface areas of evaporator and condenser
[274]	Pure	Shell-and-tube, counter flow, without baffles	Shell-and-tube, counter flow, without baffles	Discretisation, steady-state model; Design variables: Surface areas of evaporator and condenser
[275]	Pure	Counter-current, double-pipe tubular heat exchangers	Counter-current, double-pipe tubular heat exchangers	Discretisation, steady-state model; Design variables: Bulk liquid velocity of preheating section inlet, bulk liquid velocity of condensing section outlet
[276]	Pure	Single-pass plate heat exchangers, fixed heat transfer area	Single-pass plate heat exchangers, fixed heat transfer area	0-D model, constant heat transfer coefficients
[277]	Mixtures	Shell-and-tube, counter flow, without baffles	Shell-and-tube, counter flow, without baffles	Discretisation, steady-state model; Design variables: Surface areas of evaporator and condenser

Table A.5
Summary of approaches for off-design cycles assessment considering multiple fluids.

Ref.	Fluid type	Employed model	Approach	Varied parameters	Criterion
[312],[313]	9 conventional and 10 novel binary mixtures	Equilibrium, steady-state models for HEX, including solar collectors and thermal storage, efficiency models for expander and pump	Non-linear, multiparametric sensitivity analysis of consecutive steady-states, based on objective function represented as control structure	Mass flowrate of collectors, minimum temperature in storage tank, mass flowrate of heat carrier, total collector area, volume of storage tank	Net work output, thermal efficiency, volume ratio across turbine, evaporator temperature glide, irreversibility
[316]	5 pure fluids	Steady-state, moving boundary HEX model, screw and piston expander models (lumped mass)	Optimisation algorithm used to change operating parameters on a previously optimum sizing design solution	Working fluid and exhaust-gas temperature at evaporator exit, evaporator pressure, heat source mass flowrate, pressure ratio for every expansion stage	Net work output
[265–267]	4 novel and 1 conventional, binary mixture	Dynamic models for HEX, efficiency models for turbine and pump	Integrated fluid selection, ORC sizing optimisation and MPC	Heat exchanger areas (sizing), evaporator temperature (disturbance), working, heat source and cooling fluid flowrate (manipulated)	Net work output
[262]	8 pure components	Dynamic model, single loop controllers	Integrated fluid selection, ORC sizing and controller performance criterion	Equipment sizing, operating conditions	Net work output
[311]	1 mixture at variable concentrations	1-D steady state thermodynamic model	Concentration adjustment for working fluid in off-design operation	Equipment sizing, operating conditions	Net power output and ORC efficiency
[317]	2 pure components and their mixtures	1-D dynamic state model	Simulator model based on experimental test-rigs	Operating conditions	Efficiency

Data availability

Data will be made available on request.

References

[1] Lawrence Livermore National Laboratory, USDepartment of Energy. World energy flow in 2011. In: Energy flow charts: charting the complex relationships among energy, water, and carbon. 2014, URL https://flowcharts.llnl.gov.

[2] Handagama N, White M, Sapin P, Markides C. Renewable and waste-heat utilization technologies. Cambridge University Press; 2023, URL https://assets.cambridge.org/97811084/80772/frontmatter/9781108480772_frontmatter.pdf.

[3] Markides C, Wang K. Power generation technologies for low-temperature and distributed heat. Elsevier; 2023, URL https://www.sciencedirect.com/book/9780128180228/power-generation-technologies-for-low-temperature-and-distributed-heat.

[4] Oyewunmi OA. Heat recovery and conversion technologies with organic fluid cycles: optimal working fluid and system design (Ph.D. thesis), Imperial College London; 2018.

[5] Markides CN. Low-concentration solar-power systems based on organic Rankine cycles for distributed-scale applications: Overview and further developments. Front Energy Res 2015;3:47. http://dx.doi.org/10.3389/fenrg.2015.00047, URL http://journal.frontiersin.org/article/10.3389/fenrg.2015.00047.

[6] Oyewunmi OA, Kirmse CJW, Haslam AJ, Müller EA, Markides CN. Working-fluid selection and performance investigation of a two-phase single-reciprocating-piston heat-conversion engine. Appl Energy 2017;186:376–95. http://dx.doi.org/10.1016/j.apenergy.2016.05.008.

[7] Ibrahim MB, Kovach RM. A Kalina cycle application for power generation. Energy 1993;18(9):961–9. http://dx.doi.org/10.1016/s0360-5442(06)80001-0.

[8] Kalina AI, Tribus M. Advances in Kalina cycle technology 1980–1991: Part I: Development of a practical cycle. 1992.

[9] Zhang X, He M, Zhang Y. A review of research on the Kalina cycle. Renew Sustain Energy Rev 2012;16(7):5309–18. http://dx.doi.org/10.1016/J.RSER.2012.05.040, URL https://www.sciencedirect.com/science/article/pii/S1364032112003747.

[10] Kalina AI. Low temperature geothermal system. 2004, URL http://www.google.com/patents/US6820421, US Patent 6820421.

[11] Goswami DY. Solar thermal power technology: Present status and ideas for the future. Energy Sources 1998;20(2):137–45. http://dx.doi.org/10.1080/00908319808970052.

[12] Vijayaraghavan S, Goswami D. A combined power and cooling cycle modified to improve resource utilization efficiency using a distillation stage. Energy 2006;31(8–9):1177–96. http://dx.doi.org/10.1016/J.ENERGY.2005.04.014, URL https://www.sciencedirect.com/science/article/pii/S0360544205001167.

[13] Akbari AD, Mahmoudi SMS. Thermoeconomic analysis & optimization of the combined supercritical CO_2 (carbon dioxide) recompression Brayton/organic Rankine cycle. Energy 2014;78:501–12. http://dx.doi.org/10.1016/J.ENERGY.2014.10.037, URL https://www.sciencedirect.com/science/article/pii/S0360544214011864.

[14] Niu X-D, Yamaguchi H, Iwamoto Y, Zhang X-R. Optimal arrangement of the solar collectors of a supercritical CO_2-based solar Rankine cycle system. Appl Therm Eng 2013;50(1):505–10. http://dx.doi.org/10.1016/J.APPLTHERMALENG.2012.08.004, URL https://www.sciencedirect.com/science/article/pii/S135943111200525X.

[15] Chan CW, Ling-Chin J, Roskilly AP. A review of chemical heat pumps, thermodynamic cycles and thermal energy storage technologies for low grade heat utilisation. Appl Therm Eng 2013;50(1):1257–73. http://dx.doi.org/10.1016/j.applthermaleng.2012.06.041.

[16] Date A, Alam F, Khaghani A, Akbarzadeh A. Investigate the potential of using trilateral flash cycle for combined desalination and power generation integrated with salinity gradient solar ponds. Procedia Eng 2012;49:42–9. http://dx.doi.org/10.1016/j.proeng.2012.10.110.

[17] Fischer J. Comparison of trilateral cycles and organic Rankine cycles. Energy 2011;36:6208–19. http://dx.doi.org/10.1016/j.energy.2011.07.041.

[18] Oyewunmi OA, Taleb AI, Haslam AJ, Markides CN. On the use of SAFT-VR Mie for assessing large-glide fluorocarbon working-fluid mixtures in organic Rankine cycles. Appl Energy 2016;163:263–82. http://dx.doi.org/10.1016/j.apenergy.2015.10.040.

[19] Lecompte S, Ameel B, Ziviani D, van den Broek M, De Paepe M. Exergy analysis of zeotropic mixtures as working fluids in organic Rankine cycles. Energy Convers Manage 2014;85:727–39. http://dx.doi.org/10.1016/j.enconman.2014.02.028.

[20] Lampe M, Kirmse C, Sauer E, Stavrou M, Gross J, Bardow A. Computer-aided molecular design of ORC working fluids using PC-SAFT. In: Eden M, Siirola J, Towler G, editors. Proceedings of the 8th international conference on foundations of computer-aided process design. Computer aided chemical engineering, Vol. 34, Sara Burgerhartstraat 25, PO Box 211, 1000 AE Amsterdam, Netherlands: Elsevier Science BV; 2014, p. 357–62, 8th International Conference on the Foundations-of-Computer-Aided-Process-Design (FOCAPD), Cle Elum, WA, Jul 13-17, 2014.

[21] Angelino G, Colonna Di Paliano P. Multicomponent working fluids for organic Rankine cycles (ORCs). Energy 1998;23(6):449–63. http://dx.doi.org/10.1016/S0360-5442(98)00009-7.

[22] Freeman J, Hellgardt K, Markides CN. An assessment of solar-powered organic rankine cycle systems for combined heating and power in UK domestic applications. Appl Energy 2015;138:605–20. http://dx.doi.org/10.1016/j.apenergy.2014.10.035.

[23] Oyewunmi OA, Taleb AI, Haslam AJ, Markides CN. An assessment of working-fluid mixtures using SAFT-VR Mie for use in organic Rankine cycle systems for waste-heat recovery. Comput Therm Sci: Int J 2014;6(4):301–16. http://dx.doi.org/10.1615/.2014011116, URL http://dl.begellhouse.com/journals/648192910890cd0e,79df49661eac26ec,50af28c84073a421.html.

[24] Freeman J, Hellgardt K, Markides CN. An assessment of solar-thermal collector designs for small-scale combined heating and power applications in the United Kingdom. Heat Transf Eng 2015;36:1332–47. http://dx.doi.org/10.1080/01457632.2015.995037.

[25] Song J, Li X, Wang K, Markides CN. Parametric optimisation of a combined supercritical CO2 (S-CO_2) cycle and organic Rankine cycle (ORC) system for internal combustion engine (ICE) waste-heat recovery. Energy Convers Manage 2020;218:112999. http://dx.doi.org/10.1016/j.enconman.2020.112999.

[26] Song J, Wang Y, Wang K, Wang J, Markides CN. Combined supercritical CO_2 (SCO_2) cycle and organic Rankine cycle (ORC) system for hybrid solar and geothermal power generation: Thermoeconomic assessment of various configurations. Renew Energy 2021;174:1020–35. http://dx.doi.org/10.1016/j.renene.2021.04.124.

[27] Ceperley PH. A pistonless Stirling engine—The traveling wave heat engine. J Acoust Soc Am 1979;66(5):1508–13. http://dx.doi.org/10.1121/1.383505.

[28] Huang BJ, Chuang MD. System design of orifice pulse-tube refrigerator using linear flow network analysis. Cryogenics 1996;36(11):889–902. http://dx.doi.org/10.1016/s0011-2275(96)00064-1.

[29] Backhaus S, Swift GW. A thermoacoustic-Stirling heat engine: Detailed study. J Acoust Soc Am 2000;107(6):3148–66. http://dx.doi.org/10.1121/1.429343.

[30] Backhaus S, Swift GW. A thermoacoustic Stirling heat engine. Nature 1999;399:335–8. http://dx.doi.org/10.1038/20624.

[31] Markides CN, Smith TCB. A dynamic model for the efficiency optimization of an oscillatory low grade heat engine. Energy 2011;36(12):6967–80. http://dx.doi.org/10.1016/j.energy.2011.08.051.

[32] Solanki R, Galindo A, Markides CN. Dynamic modelling of a two-phase thermofluidic oscillator for efficient low grade heat utilization: Effect of fluid inertia. Appl Energy 2012;89(1):156–63. http://dx.doi.org/10.1016/j.apenergy.2011.01.007.

[33] Solanki R, Galindo A, Markides CN. The role of heat exchange on the behaviour of an oscillatory two-phase low-grade heat engine. Appl Therm Eng 2013;53(2):177–87. http://dx.doi.org/10.1016/j.applthermaleng.2012.04.019.

[34] Solanki R, Mathie R, Galindo A, Markides CN. Modelling of a two-phase thermofluidic oscillator for low-grade heat utilisation: Accounting for irreversible thermal losses. Appl Energy 2013;106:337–54. http://dx.doi.org/10.1016/j.apenergy.2012.12.069.

[35] Markides CN, Osuolale A, Solanki R, Stan G-BV. Nonlinear heat transfer processes in a two-phase thermofluidic oscillator. Appl Energy 2013;104:958–77. http://dx.doi.org/10.1016/j.apenergy.2012.11.056.

[36] Markides CN, Solanki R, Galindo A. Working fluid selection for a two-phase thermofluidic oscillator: Effect of thermodynamic properties. Appl Energy 2014;124:167–85. http://dx.doi.org/10.1016/j.apenergy.2014.02.042.

[37] Markides CN, Gupta A. Experimental investigation of a thermally powered central heating circulator: Pumping characteristics. Appl Energy 2013;110:132–46. http://dx.doi.org/10.1016/j.apenergy.2013.03.030.

[38] Kirmse CJW, Oyewunmi OA, Taleb AI, Haslam AJ, Markides CN. A two-phase single-reciprocating-piston heat conversion engine: Non-linear dynamic modelling. Appl Energy 2017;186:359–75. http://dx.doi.org/10.1016/j.apenergy.2016.05.140.

[39] Encontech BV. Up-THERM: Innovative high efficiency phase change fluid based heat engine. 2013, URL http://www.encontech.nl/papers/UpTHERM-Flyer.pdf.

[40] Glushenkov M, Sprenkeler M, Kronberg A, Kirillov V. Single-piston alternative to Stirling engines. Appl Energy 2012;97:743–8. http://dx.doi.org/10.1016/j.apenergy.2011.12.050.

[41] Taleb AI, Timmer MAG, El-Shazly MY, Samoilov A, Kirillov VA, Markides CN. A single-reciprocating-piston two-phase thermofluidic prime-mover. Energy 2016;104:250–65. http://dx.doi.org/10.1016/J.ENERGY.2016.02.113, URL https://www.sciencedirect.com/science/article/pii/S036054421630175X.

[42] Up-THERM Consortium. Up-THERM: Innovative high efficiency phase change fluid based heat engine. 2013, URL http://www.uptherm.net/#!consortium/c205a.

[43] Garg P, Kumar P, Srinivasan K, Dutta P. Evaluation of isopentane, R-245fa and their mixtures as working fluids for organic Rankine cycles. Appl Therm Eng 2013;51(1–2):292–300. http://dx.doi.org/10.1016/j.applthermaleng.2012.08.056.

[44] Wang JL, Zhao L, Wang XD. A comparative study of pure and zeotropic mixtures in low-temperature solar Rankine cycle. Appl Energy 2010;87(11):3366–73. http://dx.doi.org/10.1016/j.apenergy.2010.05.016.

[45] Lecompte S, Lemmens S, Huisseune H, den Broeck MV, Paepe MD. Multi-objective thermo-economic optimization strategy for ORCs applied to subcritical and transcritical cycles for waste heat recovery. Energies 2015;8:2714–41. http://dx.doi.org/10.3390/en8042714.

[46] Barse KA, Mann MD. Maximizing ORC performance with optimal match of working fluid with system design. Appl Therm Eng 2016;100:11. http://dx.doi.org/10.1016/j.applthermaleng.2016.01.167, URL http://www.sciencedirect.com/science/article/pii/S1359431116301405.

[47] Shu G, Gao Y, Tian H, Wei H, Liang X. Study of mixtures based on hydrocarbons used in ORC (organic Rankine cycle) for engine waste heat recovery. Energy 2014;74:428–38. http://dx.doi.org/10.1016/j.energy.2014.07.007.

[48] Bao J, Zhao L. A review of working fluid and expander selections for organic Rankine cycle. Renew Sust Energ Rev 2013;24:325–42. http://dx.doi.org/10.1016/j.rser.2013.03.040.

[49] Shu G, Li X, Tian H, Liang X, Wei H, Wang X. Alkanes as working fluids for high-temperature exhaust heat recovery of diesel engine using organic Rankine cycle. Appl Energy 2014;119:204–17. http://dx.doi.org/10.1016/j.apenergy.2013.12.056, URL http://www.sciencedirect.com/science/article/pii/S0306261913010659.

[50] Song J, Gu C-w. Analysis of ORC (organic Rankine cycle) systems with pure hydrocarbons and mixtures of hydrocarbon and retardant for engine waste heat recovery. Appl Therm Eng 2015;89:693–702. http://dx.doi.org/10.1016/j.applthermaleng.2015.06.055.

[51] Lampe M, Stavrou M, Buecker HM, Gross J, Bardow A. Simultaneous optimization of working fluid and process for organic Rankine cycles using PC-SAFT. Ind Eng Chem Res 2014;53(21):8821–30. http://dx.doi.org/10.1021/ie5006542.

[52] Imran M, Usman M, Park B-S, Yang Y. Comparative assessment of organic Rankine cycle integration for low temperature geothermal heat source applications. Energy 2016;102:473–90. http://dx.doi.org/10.1016/j.energy.2016.02.119, URL http://www.sciencedirect.com/science/article/pii/S0360544216301815.

[53] Freeman J, Hellgardt K, Markides CN. Working fluid selection and electrical performance optimisation of a domestic solar-ORC combined heat and power system for year-round operation in the UK. Appl Energy 2017;186:291–303. http://dx.doi.org/10.1016/j.apenergy.2016.04.041.

[54] Oyewunmi OA, Lecompte S, De Paepe M, Markides CN. Thermoeconomic analysis of recuperative sub- and transcritical organic Rankine cycle systems. Energy Procedia 2017;129:58–65. http://dx.doi.org/10.1016/j.egypro.2017.09.187.

[55] Lampe M, Gross J, Bardow A. Simultaneous process and working fluid optimisation for organic Rankine cycles (ORC) using PC-SAFT. In: Bogle I, Fairweather M, editors. 22 European symposium on computer aided process engineering. Vomputer aided chemical engineering, Vol. 30, Sara Burgerhartstraat 25, PO Box 211, 1000 AE Amsterdam, Netherlands: Elsevier Science BV; 2012, p. 572–6, 22nd European Symposium on Computer Aided Process Engineering (ESCAPE), Univ Coll London, London, England, Jun 17-20, 2012.

[56] Gani R, Brignole EA. Molecular design of solvents for liquid extraction based on UNIFAC. Fluid Phase Equilib 1983;13(C):331–40. http://dx.doi.org/10.1016/0378-3812(83)80104-6.

[57] Bardow A, Steur K, Gross J. Continuous-molecular targeting for integrated solvent and process design. Ind Eng Chem Res 2010;49:2834–40. http://dx.doi.org/10.1021/ie901281w.

[58] Stavrou M, Lampe M, Bardow A, Gross J. Continuous molecular targeting computer-aided molecular design (CoMT-CAMD) for simultaneous process and solvent design for CO_2 capture. Ind Eng Chem Res 2014;53(46):18029–41. http://dx.doi.org/10.1021/ie502924h.

[59] Burger J, Papaioannou V, Gopinath S, Jackson G, Galindo A, Adjiman C. A hierarchical method to integrated solvent and process design of physical CO_2 absorption using the SAFT-γ Mie approach. AIChE J 2015;61(10):3249–69. http://dx.doi.org/10.1002/aic.14838.

[60] Gopinath S, Jackson G, Galindo A, Adjiman CS. Outer approximation algorithm with physical domain reduction for computer-aided molecular and separation process design. AIChE J 2016;62:3484–504. http://dx.doi.org/10.1002/aic.15411.

[61] Gani R, Nielsen B, Fredenslund A. A group contribution approach to computer-aided molecular design. AIChE J 1991;37(9):1318–32. http://dx.doi.org/10.1002/aic.690370905.

[62] Odele O, Macchietto S. Computer aided molecular design: A novel method for optimal solvent selection. Fluid Phase Equilib 1993;82:47–54. http://dx.doi.org/10.1016/0378-3812(93)87127-m.

[63] Churi N, Achenie LEK. Novel mathematical programming model for computer aided molecular design. Ind Eng Chem Res 1996;35(96):3788–94. http://dx.doi.org/10.1021/ie9601920.

[64] Joback KG, Reid RC. Estimation of pure-component properties from group-contributions. Chem Eng Commun 1987;57:233–43. http://dx.doi.org/10.1080/00986448708960487.

[65] Fredenslund A, Jones RL, Prausnitz JM. Group-contribution estimation of activity coefficients in nonideal liquid mixtures. AIChE J 1975;21(6):1086–99. http://dx.doi.org/10.1002/aic.690210607.

[66] Chapman WG, Gubbins KE, Jackson G, Radosz M. SAFT: Equation of state solution model for associating fluids. Fluid Phase Equilib 1989;52:31–8. http://dx.doi.org/10.1016/0378-3812(89)80308-5.

[67] Chapman WG, Gubbins KE, Jackson G, Radosz M. New reference equation of state for associating liquids. Ind Eng Chem Res 1990;29(8):1709–21. http://dx.doi.org/10.1021/ie00104a021.

[68] Vijande J, Piñeiro MM, Legido JL, Bessières D. Group-contribution method for the molecular parameters of the PC-SAFT equation of state taking into account the proximity effect. Application to nonassociated compounds. Ind Eng Chem Res 2010;49(19):9394–406. http://dx.doi.org/10.1021/ie1002813.

[69] Vijande J, Piñeiro MM, Legido JL. Group-contribution method with proximity effect for PC-SAFT molecular parameters. 2. Application to association parameters: Primary alcohols and amines. Ind Eng Chem Res 2014;53(2):909–19. http://dx.doi.org/10.1021/ie4023786.

[70] Tamouza S, Passarello JP, Tobaly P, De Hemptinne JC. Group contribution method with SAFT EOS applied to vapor liquid equilibria of various hydro-carbon series. Fluid Phase Equilib 2004;222–223:67–76. http://dx.doi.org/10.1016/j.fluid.2004.06.038.

[71] Tamouza S, Passarello JP, Tobaly P, de Hemptinne JC. Application to binary mixtures of a group contribution SAFT EoS (GC-SAFT). Fluid Phase Equilib 2005;228–229:409–19. http://dx.doi.org/10.1016/j.fluid.2004.10.003.

[72] Nguyen-Huynh D, Passarello JP, Tobaly P, de Hemptinne JC. Modeling phase equilibria of asymmetric mixtures using a group-contribution SAFT (GC-SAFT) with a k_{ij} correlation method based on London's theory. 1. Application to CO_2 + n-alkane, Methane + n-alkane and ethane + n-alkane systems. Ind Eng Chem Res 2008;47(22):8847–58. http://dx.doi.org/10.1021/ie071644j.

[73] Tihic A, Kontogeorgis GM, von Solms N, Michelsen ML, Constantinou L. A predictive group-contribution simplified PC-SAFT equation of state: Application to polymer systems. Ind Eng Chem Res 2008;47:5092–101. http://dx.doi.org/10.1021/ie0710768.

[74] Nguyen Thi TX, Tamouza S, Tobaly P, Passarello J-P, de Hemptinne J-C. Application of group contribution SAFT equation of state (GC-SAFT) to model phase behaviour of light and heavy esters. Fluid Phase Equilib 2005;238(2):254–61. http://dx.doi.org/10.1016/J.FLUID.2005.10.009, URL https://www.sciencedirect.com/science/article/pii/S0378381205004085#!.

[75] Emami FS, Vahid A, Elliott JR, Feyzi F. Group contribution prediction of vapor pressure with SAFT, perturbed-chain statistical associating fluid theory, and Elliott-Suresh-Donohue equations of state. Ind Eng Chem Res 2008;47:8401–11. http://dx.doi.org/10.1021/ie800329r.

[76] Lymperiadis A, Adjiman CS, Galindo A, Jackson G. A group contribution method for associating chain molecules based on the statistical associating fluid theory (SAFT - γ). J Chem Phys 2007;127(23):234903. http://dx.doi.org/10.1063/1.2813894.

[77] Lymperiadis A, Adjiman CS, Jackson G, Galindo A. A generalisation of the SAFT - γ group contribution method for groups comprising multiple spherical segments. Fluid Phase Equilib 2008;274(1–2):85–104. http://dx.doi.org/10.1016/j.fluid.2008.08.005.

[78] Peng Y, Goff KD, dos Ramos MC, McCabe C. Developing a predictive group-contribution-based SAFT-VR equation of state. Fluid Phase Equilib 2009;277(2):131–44. http://dx.doi.org/10.1016/j.fluid.2008.11.008.

[79] Papaioannou V, Lafitte T, Avendaño C, Adjiman CS, Jackson G, Müller EA, et al. Group contribution methodology based on the statistical associating fluid theory for heteronuclear molecules formed from Mie segments. J Chem Phys 2014;140:054107. http://dx.doi.org/10.1063/1.4851455.

[80] Lecompte S, Huisseune H, van den Broek M, Vanslambrouck B, Paepe MD. Review of organic Rankine cycle (ORC) architectures for waste heat recovery. Renew Sustain Energy Rev 2015;47:448–61. http://dx.doi.org/10.1016/j.rser.2015.03.089.

[81] Tartière T. KCORC Science and Tech.. 2013, URL https://kcorc.org/technology/research-trends/.

[82] Colonna P, Casati E, Trapp C, Mathijssen T, Larjola J, Turunen-Saaresti T, et al. Organic Rankine cycle power systems: From the concept to current technology, applications, and an outlook to the future. J Eng Gas Turbines Power 2015;137(10). http://dx.doi.org/10.1115/1.4029884.

[83] Bertrand B, Lambrinos G, Frangoudakis A, Papadakis G. Low-grade heat conversion into power using organic Rankine cycles - A review of various applications. Renew Sustain Energy Rev 2011;15:3963–79. http://dx.doi.org/10.1016/j.rser.2011.07.024.

[84] Wieland C, Dawo F, Schifflechner C, Astolfi M. Market report on organic Rankine cycle power systems: recent developments and outlook. In: Proceedings of 6th international seminar on ORC Power Systems. 1, 2021, p. 1–10.

[85] Tartière T. KCORC Home. 2021, URL https://www.kcorc.org/en/.

[86] Firth A, Zhang B, Yang A. Quantification of global waste heat and its environmental effects. Appl Energy 2019;235:1314–34. http://dx.doi.org/10.1016/j.apenergy.2018.10.102.

[87] Forman C, Muritala I, Pardemann R, Meyer B. Estimating the global waste heat potential. Renew Sustain Energy Rev 2016;57:1568–79. http://dx.doi.org/10.1016/j.rser.2015.12.192.

[88] Maghrabi A, Song J, Sapin P, Markides C. Electricity demand reduction through waste heat recovery in olefins plants based on a technology-agnostic approach. Energy Convers Manag: X 2023;20:100419. http://dx.doi.org/10.1016/j.ecmx.2023.100419.

[89] Gangar N, Macchietto S, Markides CN. Recovery and utilization of low-grade waste heat in the oil-refining industry using heat engines and heat pumps: An international technoeconomic comparison. Energies 2020;13(10). http://dx.doi.org/10.3390/en13102560.

[90] Incorporated B. Waste heat recovery: Technology opportunities in the US industry. US Department of Energy; 2008, URL http://www1.eere.energy.gov/manufacturing/intensiveprocesses/pdfs/waste_heat_recovery.pdf.

[91] Element Energy Limited, Ecofys, Imperial College London. The potential for recovering and using surplus heat from industry: Final Report for DECC. 2014, URL https://www.gov.uk/government/uploads/system/uploads/attachment_data/file/294900/element_energy_et_al_potential_for_recovering_and_using_surplus_heat_from_industry.pdf.

[92] Markides CN. The role of pumped and waste heat technologies in a high-efficiency sustainable energy future for the UK. Appl Therm Eng 2013;53(2):197–209. http://dx.doi.org/10.1016/j.applthermaleng.2012.02.037.

[93] Tocci L, Pal T, Pesmazoglou I, Franchetti B. Small scale organic Rankine cycle (ORC): A techno-economic review. Energy 2017;10:413–39. http://dx.doi.org/10.3390/en10040413.

[94] Lemmens S. Cost engineering techniques and their applicability for cost estimation of organic Rankine cycle systems. Energies 2016;9:485–503. http://dx.doi.org/10.3390/en9070485.

[95] Calli O, Colpan C, Gunerhan H. Thermoeconomic analysis of a biomass and solar energy based organic Rankine cycle system under part load behavior. Sustain Energy Technol Assess 2021;46:101207. http://dx.doi.org/10.1016/j.seta.2021.101207.

[96] Macchi E. Theoretical basis of the Organic Rankine Cycle. Technol Appl 2017;3–24. http://dx.doi.org/10.1016/B978-0-08-100510-1.00001-6.

[97] Lecompte S. Performance evaluation of organic rankine cycle architectures: Application to waste heat valorisation. Ghent University: Faculty of Engineering and Architecture; 2016, p. 1–239. http://dx.doi.org/10.1016/j.rser.2015.03.089.

[98] Papadopoulos AI, Stijepovic M, Linke P. On the systematic design and selection of optimal working fluids for organic rankine cycles. Appl Therm Eng 2010;30:760–9. http://dx.doi.org/10.1016/j.applthermaleng.2009.12.006.

[99] Quoilin S, Declaye S, Legros A, Guillaume L. Working fluid selection and operating maps for organic rankine cycle expansion machines. In: Proceedings of international compressor engineering conference at purdue. 21, 2012, p. 1–10.

[100] Papadopoulos AI, Shavalieva G, Papadokonstantakis S, Seferlis P, Perdomo FA, Galindo A, et al. An approach for simultaneous computer-aided molecular design with holistic sustainability assessment: Application to phase-change CO_2 capture solvents. Comp Chem Eng 2020;135:106769. http://dx.doi.org/10.1016/j.compchemeng.2020.106769.

[101] Rayegan R, Tao Y. A procedure to select working fluids for solar organic Rankine cycles (ORCs). Renew Energy 2011;36:659–70. http://dx.doi.org/10.1016/j.renene.2010.07.010.

[102] Tabor H, Bronicki L. Establishing criteria for fluids for small vapor turbines. SAE Tech Pap., 1964.

[103] Badr O, Probert S, O'callaghan P. Selecting a working fluid for a rankine-cycle engine. Appl Energy 1985;21(1):1–42. http://dx.doi.org/10.1016/0306-2619(85)90072-8.

[104] Györke G, Deiters UK, Groniewsky A, Lassu I, Imre AR. Novel classification of pure working fluids for organic Rankine cycle. Energy 2018;145:288–300. http://dx.doi.org/10.1016/j.energy.2017.12.135.

[105] Maizza V, Maizza A. Working fluids in non-steady flows for waste energy recovery systems. Appl Therm Eng 1996;16:579–90. http://dx.doi.org/10.1016/1359-4311(95)00044-5.

[106] Hung T, Wang S, Kuo C, Pei B, Tsai K. A study of organic working fluids on system efficiency of an ORC using low-grade energy sources. Energy 2010;35:1403–11. http://dx.doi.org/10.1016/j.energy.2009.11.025.

[107] Larjola J. Electricity from industrial waste heat using high-speed organic Rankine cycle (ORC). Int J Prod Econ 1995;41:227–35. http://dx.doi.org/10.1016/0925-5273(94)00098-0.

[108] Yamamoto T, Furuhata T, Arai N, Mori K. Design and testing of the organic rankine cycle. Energy 2001;26:239–51. http://dx.doi.org/10.1016/S0360-5442(00)00063-3.

[109] Kroger D, Rohsenow W. Condensation heat transfer in the presence of a non-condensable gas. Int J Heat Mass Transfer 1968;11:15–26. http://dx.doi.org/10.1115/1.3688714.

[110] Saleh B, Koglbauer G, Wendland M, Fischer J. Working fluids for low-temperature organic Rankine cycles. Energy 2007;32:1210–21. http://dx.doi.org/10.1016/j.energy.2006.07.001.

[111] Wang E, Zhang H, Fan B, Ouyang M, Zhao Y, Mu Q. Study of working fluid selection of organic Rankine cycle (ORC) for engine waste heat recovery. Energy 2011;36:3406–18. http://dx.doi.org/10.1016/j.energy.2011.03.041.

[112] Dai Y, Wang J, Gao L. Parametric optimization and comparative study of organic Rankine cycle (ORC) for low grade waste heat recovery. Energy Convers Manage 2009;50:576–82. http://dx.doi.org/10.1016/j.enconman.2008.10.018.

[113] Hettiarachchi H, Mihajlo G, Worek W, Ikegami Y. Optimum design criteria for an organic Rankine cycle using low-temperature geothermal heat sources. Energy 2007;32:1698–706. http://dx.doi.org/10.1016/j.energy.2007.01.005.

[114] Masson-Delmotte V, Zhai P, Pirani A, Connors S, Péan C, Berger S, et al., editors. IPCC, 2021: Summary for policymakers. In: Climate change 2021: The physical science basis. contribution of working group I to the sixth assessment report of the intergovernmental panel on climate change. Vol. 6, Cambridge University Press; 2021, p. 1–3949.

[115] Bolaji B, Huan Z. Ozone depletion and global warming: Case for the use of natural refrigerant – a review. Renew Sustain Energy Rev 2013;18:49–54. http://dx.doi.org/10.1016/j.rser.2012.10.008.

[116] Zühlsdorf B, Jensen J, Cignitti S, Madsen C, Elmegaard B. Analysis of temperature glide matching of heat pumps with zeotropic working fluid mixtures for different temperature glides. Energy 2018;153:650–60. http://dx.doi.org/10.1016/j.energy.2018.04.048.

[117] Papadopoulos A, Kyriakides A, Seferlis P, Hassan I. Integrated design of working fluid mixtures and absorption refrigeration cycles. Front Chem Eng 2021;3. http://dx.doi.org/10.3389/fceng.2021.622998.

[118] Ng L, Chong F, Chemmangattuvalappil N. Challenges and opportunities in computer-aided molecular design. Comput Chem Eng 2015;81:115–29. http://dx.doi.org/10.1016/j.compchemeng.2015.03.009.

[119] Kuprasertwong N, Padungwatanaroj O, Robin A, Udomwong K, Tula A, Zhu L, et al. Computer-aided refrigerant design: New developments. In: Proceedings of the 31st european symposium on computer aided process engineering. Vol. 31, 2021, p. 19–24. http://dx.doi.org/10.1016/B978-0-323-88506-5.50004-8.

[120] Sadreddinia A, Ashjarib M, Fanic M, Mohammadia A. Thermodynamic analysis of a new cascade ORC and transcritical CO_2 cycle to recover energy from medium temperature heat source and liquefied natural gas. Energy Convers Manage 2018;167:9–20. http://dx.doi.org/10.1016/j.enconman.2018.04.093.

[121] Kosmadakis G, Manolakos D, Kyritsis S, Papadakis G. Economic assessment of a two-stage solar organic Rankine cycle for reverse osmosis desalination. Renew Energy 2009;34:1579–86. http://dx.doi.org/10.1016/j.renene.2008.11.007.

[122] Mago P, Chamra L, Srinivasan K, Somayaji C. An examination of regenerative organic Rankine cycles using dry fluids. Appl Therm Eng 2008;28:998–1007. http://dx.doi.org/10.1016/j.applthermaleng.2007.06.025.

[123] Dipippo R. Ideal thermal efficiency for geothermal binary plants. Geothermics 2007;36:276–85. http://dx.doi.org/10.1016/j.geothermics.2007.03.002.

[124] Lecompte S, van den Broek M, De Paepe M. Thermodynamic analysis of the partially evaporating trilateral cycle. In: Proceedings of the 2nd international seminar on ORC power systems. Vol. 2, 2013, p. 1–4.

[125] Schuster A, Karellas S, Aumann R. Efficiency optimization potential in super-critical organic rankine cycles. Energy 2010;35:1033–9. http://dx.doi.org/10.1016/j.energy.2009.06.019.

[126] Yu B, Yang J, Wang D, Shi J, Chen J. An updated review of recent advances on modified technologies in transcritical CO_2 refrigeration cycle. Energy 2019;189:116147. http://dx.doi.org/10.1016/j.energy.2019.116147.

[127] Radulovic J, Castaneda N. On the potential of zeotropic mixtures in super-critical ORC powered by geothermal energy source. Energy Convers Manage 2014;88:365–71. http://dx.doi.org/10.1016/j.enconman.2014.08.048.

[128] Yang K, Zhang H, Wang Z, Zhang J, Yang F, Yao E, et al. Study of zeotropic mixtures of ORC (organic Rankine cycle) under engine various operating conditions. Energy 2013;58:494–510. http://dx.doi.org/10.1016/j.energy.2013.04.074.

[129] Song J, Gu C, Ren X. Parametric design and off-design analysis of organic Rankine cycle (ORC) system. Energy Convers Manage 2016;112:157–65. http://dx.doi.org/10.1016/j.enconman.2015.12.085.

[130] Calise F, Capuozzo C, Carotenuto A, Vanoli L. Thermoeconomic analysis and off-design performance of an organic Rankine cycle powered by medium-temperature heat sources. Sol Energy 2014;103:595–609. http://dx.doi.org/10.1016/j.solener.2013.09.031.

[131] Ibarra M, Rovira A, Alarcón-Padilla D, Blanco J. Performance of a 5 kWe organic Rankine cycle at part-load operation. Appl Energy 2014;120:147–58. http://dx.doi.org/10.1016/j.apenergy.2014.01.057.

[132] Dickes R, Dumont O, Daccord R, Quoilin S, Lemort V. Modelling of organic rankine cycle power systems in off-design conditions: An experimentally-validated comparative study. Energy 2017;123:710–27. http://dx.doi.org/10.1016/j.energy.2017.01.130.

[133] Liu C, Gao T. Off-design performance analysis of basic ORC, ORC using zeotropic mixtures and composition-adjustable ORC under optimal control strategy. Energy 2019;171:95–108. http://dx.doi.org/10.1016/j.energy.2018.12.195.

[134] Papadopoulos AI, Tsivintzelis I, Linke P, Seferlis P. Computer-aided molecular design: Fundamentals, methods, and applications. In: Reedijk J, editor. Ref. modul. chem. mol. sci. chem. eng.. Elsevier; 2018, p. 1–76. http://dx.doi.org/10.1016/B978-0-12-409547-2.14342-2.

[135] Qyyum MA, Khan A, Ali S, Khurram MS, Mao N, Naquash A, et al. Assessment of working fluids, thermal resources and cooling utilities for organic Rankine cycles: State-of-the-art comparison, challenges, commercial status, and future prospects. Energy Convers Manage 2022;252:115055. http://dx.doi.org/10.1016/J.ENCONMAN.2021.115055.

[136] Bamorovat Abadi G, Kim KC. Investigation of organic Rankine cycles with zeotropic mixtures as a working fluid: Advantages and issues. Renew Sustain Energy Rev 2017;73:1000–13. http://dx.doi.org/10.1016/J.RSER.2017.02.020.

[137] Palma-Flores O, Flores-Tlacuahuac A, Canseco-Melchor G. Optimal molecular design of working fluids for sustainable low-temperature energy recovery. Comput Chem Eng 2015;72:334–49. http://dx.doi.org/10.1016/j.compchemeng.2014.04.009.

[138] Reid R, Prausnitz JM, Poling B. The properties of gases and liquids. fourth ed.. New York: MacGraw-Hill; 1987.

[139] Austin ND, Sahinidis VN, Trahan DW. Computer-aided molecular design: An introduction and review of tools, applications, and solution techniques. Chem Eng Res Des 2016;116:2–26. http://dx.doi.org/10.1016/j.cherd.2016.10.014.

[140] Samudra A, Sahinidis N. Optimization-based framework for computer-aided molecular design. AIChE J 2013;59(10):3686–701. http://dx.doi.org/10.1002/aic.14112.

[141] Papadopoulos AI, Stijepovic M, Linke P, Seferlis P, Voutetakis S. Toward optimum working fluid mixtures for organic Rankine cycles using molecular design and sensitivity analysis. Ind Eng Chem Res 2013;52(34):12116–33. http://dx.doi.org/10.1021/ie400968j.

[142] Adjiman CS, Sahinidis VN, Vlachos DG, Bakshi B, Maravelias CT, Georgakis C. Process systems engineering perspective on the design of materials and molecules. Ind Eng Chem Res 2021;60(14):5194–206. http://dx.doi.org/10.1021/ACS.IECR.0C05399.

[143] Marrero-Morejón J, Gani R. Group-contribution based estimation of pure component properties. Fluid Phase Equilib 2001;183–184:183. http://dx.doi.org/10.1016/s0378-3812(01)00431-9.

[144] Gross J, Sadowski G. Perturbed-chain SAFT: An equation of state based on a perturbation theory for chain molecules. Ind Eng Chem Res 2001;40(4):1244–60. http://dx.doi.org/10.1021/ie0003887.

[145] Lafitte T, Apostolakou A, Avendaño C, Galindo A, Adjiman CS, Müller EA, et al. Accurate perturbation theory for chains of Mie soft-core segments (SAFT-VR Mie) for the description of vapour-liquid equilibria and derivative properties. J Chem Phys 2013;139:154504. http://dx.doi.org/10.1021/acs.iecr.1c00480.s001.

[146] White MT, Oyewunmi OA, Chatzopoulou MA, Pantaleo AM, Haslam AJ, Markides CN. Computer-aided working-fluid design, thermodynamic optimisation and thermoeconomic assessment of ORC systems for waste-heat recovery. Energy 2018;161:1181–98. http://dx.doi.org/10.1016/j.energy.2018.07.098.

[147] Stijepovic M, Linke P, Papadopoulos A, Grujic A. On the role of working fluid properties in organic Rankine cycle performance. Appl Therm Eng 2012;36(1):406–13. http://dx.doi.org/10.1016/j.applthermaleng.2011.10.057.

[148] Schwöbel J, Preißinger M, Brüggemann D, Klamt A. High-throughput screening of working fluids for the organic rankine cycle (ORC) based on conductor-like screening model for realistic solvation (COSMO-RS) and thermodynamic process simulations. Ind Eng Chem Res 2017;56:788–98. http://dx.doi.org/10.1021/acs.iecr.6b03857.

[149] Wang J, Zhang J, Chen Z. Molecular entropy, thermal efficiency, and designing of working fluids for organic Rankine cycles. Int J Thermophys 2012;33(6):970–85. http://dx.doi.org/10.1007/s10765-012-1200-6.

[150] Angelino G, Di Paliano PC. Organic Rankine cycles (ORCs) for energy recovery from molten carbonate fuel cells. In: Proceedings of the intersociety energy conversion engineering conference. Vol. 2, 2000, p. 1400–9. http://dx.doi.org/10.1109/IECEC.2000.870957.

[151] Chys M, van den Broek M, Vanslambrouck B, De Paepe M. Potential of zeotropic mixtures as working fluids in organic Rankine cycles. Energy 2012;44(1):623–32. http://dx.doi.org/10.1016/J.ENERGY.2012.05.030.

[152] Victor RA, Kim JK, Smith R. Composition optimisation of working fluids for organic Rankine cycles and Kalina cycles. Energy 2013;55:114–26. http://dx.doi.org/10.1016/J.ENERGY.2013.03.069.

[153] Garg P, Orosz MS. Economic optimization of organic Rankine cycle with pure fluids and mixtures for waste heat and solar applications using particle swarm optimization method. Energy Convers Manage 2018;165:649–68. http://dx.doi.org/10.1016/J.ENCONMAN.2018.03.086.

[154] Kolahi MR, Nemati A, Yari M. Performance optimization and improvement of a flash-binary geothermal power plant using zeotropic mixtures with PSO algorithm. Geothermics 2018;74:45–56. http://dx.doi.org/10.1016/J.GEOTHERMICS.2018.02.004.

[155] Heberle F, Brüggemann D. Thermo-economic evaluation of organic rankine cycles for geothermal power generation using zeotropic mixtures. Energies 2015;8(3):2097–124. http://dx.doi.org/10.3390/EN8032097.

[156] Wang S, Liu C, Ren J, Liu L, Li Q, Huo E. Carbon footprint analysis of organic Rankine cycle system using zeotropic mixtures considering leak of fluid. J Clean Prod 2019;239:118095. http://dx.doi.org/10.1016/J.JCLEPRO.2019.118095.

[157] Han J, Wang X, Xu J, Yi N, Ashraf Talesh SS. Thermodynamic analysis and optimization of an innovative geothermal-based organic Rankine cycle using zeotropic mixtures for power and hydrogen production. Int J Hydrog Energy 2020;45(15):8282–99. http://dx.doi.org/10.1016/J.IJHYDENE.2020.01.093.

[158] Feng Y, Hung TC, Greg K, Zhang Y, Li B, Yang J. Thermoeconomic comparison between pure and mixture working fluids of organic Rankine cycles (ORCs) for low temperature waste heat recovery. Energy Convers Manage 2015;106:859–72. http://dx.doi.org/10.1016/J.ENCONMAN.2015.09.042.

[159] Feng Y, Hung TC, Zhang Y, Li B, Yang J, Shi Y. Performance comparison of low-grade ORCs (organic Rankine cycles) using R245fa, pentane and their mixtures based on the thermoeconomic multi-objective optimization and decision makings. Energy 2015;93:2018–29. http://dx.doi.org/10.1016/J.ENERGY.2015.10.065.

[160] Tiwari D, Sherwani AF, Arora A. Thermodynamic and multi-objective optimisation of solar-driven organic Rankine cycle using zeotropic mixtures. Int J Ambient Energy 2017;40(2):135–51. http://dx.doi.org/10.1080/01430750.2017.1378718.

[161] Andreasen JG, Kærn MR, Pierobon L, Larsen U, Haglind F. Multi-objective optimization of organic Rankine cycle power plants using pure and mixed working fluids. Energies 2016;9(5):322. http://dx.doi.org/10.3390/EN9050322.

[162] Oyewunmi OA, Markides CN. Thermo-economic and heat transfer optimization of working-fluid mixtures in a low-temperature organic Rankine cycle system. Energies 2016;9(6):448. http://dx.doi.org/10.3390/EN9060448.

[163] Noriega Sanchez CJ, Gosselin L, K. da Silva A. Designed binary mixtures for subcritical organic Rankine cycles based on multiobjective optimization. Energy Convers Manage 2018;156:585–96. http://dx.doi.org/10.1016/J.ENCONMAN.2017.11.050.

[164] Nasir MT, Ali MA, Khan TS, Al-Hajri E, Kadri MB, Kim KC. Performance assessment and multi objective optimization of an organic Rankine cycle driven cooling air conditioning system. Energy Build 2019;191:13–30. http://dx.doi.org/10.1016/J.ENBUILD.2019.03.012.

[165] Rodriguez Sotomonte CA, Correa Veloso TG, Coronado CJ, Rosa do Nascimento MA. Multi-objective optimization for a small biomass cooling and power cogeneration system using binary mixtures. Appl Therm Eng 2021;182:116045. http://dx.doi.org/10.1016/J.APPLTHERMALENG.2020.116045.

[166] Micheli D, Pinamonti P, Reini M, Taccani R. Performance analysis and working fluid optimization of a cogenerative organic Rankine cycle plant. J Energy Resour Technol Trans ASME 2013;135(2). http://dx.doi.org/10.1115/1.4023098/365899.

[167] Andreasen JG, Larsen U, Knudsen T, Pierobon L, Haglind F. Selection and optimization of pure and mixed working fluids for low grade heat utilization using organic Rankine cycles. Energy 2014;73:204–13. http://dx.doi.org/10.1016/J.ENERGY.2014.06.012.

[168] Molina-Thierry DP, Flores-Tlacuahuac A. Simultaneous optimal design of organic mixtures and Rankine cycles for low-temperature energy recovery. Ind Eng Chem Res 2015;54(13):3367–83. http://dx.doi.org/10.1021/IE503675V.

[169] Satanphol K, Pridasawas W, Suphanit B. A study on optimal composition of zeotropic working fluid in an organic Rankine cycle (ORC) for low grade heat recovery. Energy 2017;123:326–39. http://dx.doi.org/10.1016/J.ENERGY.2017.02.024.

[170] Lee U, Mitsos A. Optimal multicomponent working fluid of organic Rankine cycle for exergy transfer from liquefied natural gas regasification. Energy 2017;127:489–501. http://dx.doi.org/10.1016/J.ENERGY.2017.03.126.

[171] Bernal-Lara RO, Flores-Tlacuahuac A. Thermo-economic multiobjective optimization of a LOW temperature organic Rankine cycle for energy recovery. Ind Eng Chem Res 2017;56(40):11477–95. http://dx.doi.org/10.1021/ACS.IECR.7B01198.

[172] Tzeng G-H, Huang J-J. Multiple attribute decision making: methods and applications. Boca Raton, Florida, USA: CRC Press; 2011.

[173] Shannon C. A mathematical theory of communication. Bell Syst Tech J 1948;27(3):379–423. http://dx.doi.org/10.4135/9781412959384.n229.

[174] Srinivasan V, Shocker AD. Linear programming techniques for multidimensional analysis of preferences. Psychometrika 1973;38(3):337–69. http://dx.doi.org/10.1007/BF02291658.

[175] Micheli D, Reini M, Taccani R. Application of biomass fed ORC power systems in the furniture manufacturing industrial district of pordenone: Part II: Development of thermodynamic cycle simulation model. In: Proceedings of 3rd international symposium on energy and environment. ITA; 2004.

[176] Sahinidis VN. BARON: A general purpose global optimization software package. J Glob Optim 1996;8(2):201–5. http://dx.doi.org/10.1007/BF00138693.

[177] Boukouvala F, Misener R, Floudas CA. Global optimization advances in mixed-integer nonlinear programming, MINLP, and constrained derivative-free optimization, CDFO. European J Oper Res 2016;252(3):701–27. http://dx.doi.org/10.1016/j.ejor.2015.12.018.

[178] Papadopoulos A, Linke P. On the synthesis and optimization of liquid-liquid extraction processes using stochastic search methods. Comput Chem Eng 2004;28(11):2391–406. http://dx.doi.org/10.1016/j.compchemeng.2004.06.008.

[179] Küçükoğlu İ, Ene S, Aksoy A, Öztürk N. A memory structure adapted simulated annealing algorithm for a green vehicle routing problem. Environ Sci Pollut Res 2015;22(5):3279–97. http://dx.doi.org/10.1007/s11356-014-3253-5.

[180] Huster WR, Schweidtmann AM, Mitsos A. Working fluid selection for organic Rankine cycles via deterministic global optimization of design and operation. Optim Eng 2020;21(2):517–36. http://dx.doi.org/10.1007/s11081-019-09454-1.

[181] Leigh MJ. A computer flowsheeting programme incorporating algebraic analysis of the problem structure (Ph.D. thesis), Imperial College London; 1973.

[182] Letsios D, Baltean-Lugojan R, Ceccon F, Mistry M, Wiebe J, Misener R. Approximation algorithms for process systems engineering. Comput Chem Eng 2020;132:106599. http://dx.doi.org/10.1016/J.COMPCHEMENG.2019.106599.

[183] Bongartz D, Mitsos A. Deterministic global optimization of process flowsheets in a reduced space using McCormick relaxations. J Global Optim 2017;69(4):761–96. http://dx.doi.org/10.1007/S10898-017-0547-4.

[184] Vasilas N, Papadopoulos A, Papadopoulos L, Salamanis A, Kazepidis P, Soudris D, et al. Approximate computing, skeleton programming and run-time scheduling in an algorithm for process design and controllability in distributed and heterogeneous infrastructures. Comput Chem Eng 2022;164:107874. http://dx.doi.org/10.1016/j.compchemeng.2022.107874.

[185] Hu S, Yang Z, Li J, Duan Y. A review of multi-objective optimization in organic Rankine cycle (ORC) system design. Energies 2021;14(20):6492. http://dx.doi.org/10.3390/EN14206492.

[186] Lee YS, Graham EJ, Galindo A, Jackson G, Adjiman CS. A comparative study of multi-objective optimization methodologies for molecular and process design. Comput Chem Eng 2020;136:106802. http://dx.doi.org/10.1016/J.COMPCHEMENG.2020.106802.

[187] Liaw HJ, Lee TP, Tsai JS, Hsiao WH, Chen MH, Hsu TT. Binary liquid solutions exhibiting minimum flash-point behavior. J Loss Prev Process Ind 2003;16(3):173–86. http://dx.doi.org/10.1016/S0950-4230(03)00004-4.

[188] Fleitmann L, Kleinekorte J, Leonhard K, Bardow A. COSMO-susCAMPD: Sustainable solvents from combining computer-aided molecular and process design with predictive life cycle assessment. Chem Eng Sci 2021;245:116863. http://dx.doi.org/10.1016/J.CES.2021.116863.

[189] Xi H, Li MJ, Xu C, He YL. Parametric optimization of regenerative organic Rankine cycle (ORC) for low grade waste heat recovery using genetic algorithm. Energy 2013;58:473–82. http://dx.doi.org/10.1016/J.ENERGY.2013.06.039.

[190] Woodland BJ, Krishna A, Groll EA, Braun JE, Horton WT, Garimella VS. Thermodynamic comparison of organic Rankine cycles employing liquid-flooded expansion or a solution circuit. Appl Therm Eng 2013;61(2):859–65. http://dx.doi.org/10.1016/J.APPLTHERMALENG.2013.05.020.

[191] Walraven D, Laenen B, D'haeseleer W. Economic system optimization of air-cooled organic Rankine cycles powered by low-temperature geothermal heat sources. Energy 2015;80:104–13. http://dx.doi.org/10.1016/J.ENERGY.2014.11.048.

[192] Theamtat T, Koonsrisuk A. Fluid selection and optimal operating conditions of an ORC, and trilateral Rankine cycle power plant for a heat source temperature of 210° C – 250° C. Trans TSME, J Res Appl Mech Eng 2020;8(2):135–47. http://dx.doi.org/10.14456/jrame.2020.14.

[193] Emadi MA, Chitgar N, Oyewunmi OA, Markides CN. Working-fluid selection and thermoeconomic optimisation of a combined cycle cogeneration dual-loop organic Rankine cycle (ORC) system for solid oxide fuel cell (SOFC) waste-heat recovery. Appl Energy 2020;261:114384. http://dx.doi.org/10.1016/J.APENERGY.2019.114384.

[194] Stijepovic M, Papadopoulos A, Linke P, Grujic A, Seferlis P. An exergy composite curves approach for the design of optimum multi-pressure organic Rankine cycle processes. Energy 2014;69:285–98. http://dx.doi.org/10.1016/j.energy.2014.03.006.

[195] Stijepovic MZ, Papadopoulos AI, Linke P, Stijepovic V, Grujic AS, Kijevčanin M, et al. Organic Rankine cycle system performance targeting and design for multiple heat sources with simultaneous working fluid selection. J Clean Prod 2017;142:1950–70. http://dx.doi.org/10.1016/j.jclepro.2016.11.088.

[196] Toffolo A. A synthesis/design optimization algorithm for Rankine cycle based energy systems. Energy 2014;66:115–27. http://dx.doi.org/10.1016/J.ENERGY.2014.01.070.

[197] Lazzaretto A, Manente G, Toffolo A. SYNTHSEP: A general methodology for the synthesis of energy system configurations beyond superstructures. Energy 2018;147:924–49. http://dx.doi.org/10.1016/J.ENERGY.2018.01.075.

[198] Wang L, Voll P, Lampe M, Yang Y, Bardow A. Superstructure-free synthesis and optimization of thermal power plants. Energy 2015;91:700–11. http://dx.doi.org/10.1016/J.ENERGY.2015.08.068.

[199] Wang L, Lampe M, Voll P, Yang Y, Bardow A. Multi-objective superstructure-free synthesis and optimization of thermal power plants. Energy 2016;116:1104–16. http://dx.doi.org/10.1016/J.ENERGY.2016.10.007.

[200] Huster WR, Schweidtmann AM, Lüthje JT, Mitsos A. Deterministic global superstructure-based optimization of an organic Rankine cycle. Comput Chem Eng 2020;141:106996. http://dx.doi.org/10.1016/J.COMPCHEMENG.2020.106996.

[201] Kermani M, Wallerand AS, Kantor ID, Maréchal F. Generic superstructure synthesis of organic Rankine cycles for waste heat recovery in industrial processes. Appl Energy 2018;212:1203–25. http://dx.doi.org/10.1016/j.apenergy.2017.12.094.

[202] Bao J, Zhang R, Lin Y, Zhang N, Zhang X, He G. Simultaneous optimization of system structure and working fluid for the three-stage condensation Rankine cycle utilizing LNG cold energy. Appl Therm Eng 2018;140:120–30. http://dx.doi.org/10.1016/J.APPLTHERMALENG.2018.05.049.

[203] Hipólito-Valencia BJ, Rubio-Castro E, Ponce-Ortega JM, Serna-González M, Nápoles-Rivera F, El-Halwagi MM. Optimal integration of organic Rankine cycles with industrial processes. Energy Convers Manage 2013;73:285–302. http://dx.doi.org/10.1016/j.enconman.2013.04.036.

[204] Chen CL, Chang FY, Chao TH, Chen HC, Lee JY. Heat-exchanger network synthesis involving organic Rankine cycle for waste heat recovery. Ind Eng Chem Res 2014;53(44):16924–36. http://dx.doi.org/10.1021/IE500301S.

[205] Lira-Barragán LF, Ponce-Ortega JM, Serna-González M, El-Halwagi MM. Sustainable integration of trigeneration systems with heat exchanger networks. Ind Eng Chem Res 2014;53(7):2732–50. http://dx.doi.org/10.1021/IE4021232.

[206] Yu H, Eason J, Biegler LT, Feng X. Simultaneous heat integration and techno-economic optimization of organic Rankine cycle (ORC) for multiple waste heat stream recovery. Energy 2017;119:322–33. http://dx.doi.org/10.1016/J.ENERGY.2016.12.061.

[207] Elsido C, Martelli E, Grossmann IE. A bilevel decomposition method for the simultaneous heat integration and synthesis of steam/organic Rankine cycles. Comput Chem Eng 2019;128:228–45. http://dx.doi.org/10.1016/J.COMPCHEMENG.2019.05.041.

[208] Marechal F, Kalitventzeff B. A methodology for the optimal insertion of organic Rankine cycles in industrial processes. In: 2nd international symposium on process integration halifax Canada. 2004, p. 1–15.

[209] Sadeghi M, Nemati A, ghavimi A, Yari M. Thermodynamic analysis and multi-objective optimization of various ORC (organic Rankine cycle) configurations using zeotropic mixtures. Energy 2016;109:791–802. http://dx.doi.org/10.1016/J.ENERGY.2016.05.022.

[210] Lee U, Jeon J, Han C, Lim Y. Superstructure based techno-economic optimization of the organic Rankine cycle using LNG cryogenic energy. Energy 2017;137:83–94. http://dx.doi.org/10.1016/J.ENERGY.2017.07.019.

[211] Scaccabarozzi R, Tavano M, Invernizzi CM, Martelli E. Thermodynamic optimization of heat recovery ORCs for heavy duty internal combustion engine: pure fluids vs. zeotropic mixtures. Energy Procedia 2017;129:168–75. http://dx.doi.org/10.1016/J.EGYPRO.2017.09.099.

[212] Scaccabarozzi R, Tavano M, Invernizzi CM, Martelli E. Comparison of working fluids and cycle optimization for heat recovery ORCs from large internal combustion engines. Energy 2018;158:396–416. http://dx.doi.org/10.1016/J.ENERGY.2018.06.017.

[213] Wang Z, Xia X, Pan H, Zuo Q, Zhou N, Xie B. Fluid selection and advanced exergy analysis of dual-loop ORC using zeotropic mixture. Appl Therm Eng 2021;185:116423. http://dx.doi.org/10.1016/J.APPLTHERMALENG.2020.116423.

[214] Lin S, Zhao L, Deng S, Zhao D, Wang W, Chen M. Intelligent collaborative attainment of structure configuration and fluid selection for the organic Rankine cycle. Appl Energy 2020;264:114743. http://dx.doi.org/10.1016/J.APENERGY.2020.114743.

[215] Soffiato M, Frangopoulos CA, Manente G, Rech S, Lazzaretto A. Design optimization of ORC systems for waste heat recovery on board a LNG carrier. Energy Convers Manage 2015;92:523–34. http://dx.doi.org/10.1016/j.enconman.2014.12.085.

[216] Preißinger M, Schwöbel JA, Klamt A, Brüggemann D. Multi-criteria evaluation of several million working fluids for waste heat recovery by means of organic Rankine cycle in passenger cars and heavy-duty trucks. Appl Energy 2017;206:887–99. http://dx.doi.org/10.1016/J.APENERGY.2017.08.212.

[217] Papadopoulos A, Linke P. Multiobjective molecular design for integrated process-solvent systems synthesis. AIChE J 2006;52(3):1057–70. http://dx.doi.org/10.1002/aic.10715.

[218] Papadopoulos A, Gkouletsos D, Champilomatis V, Giannakakis A, Kousidis V, Hassan I, et al. Systematic assessment of working fluid mixtures for absorption refrigeration based on techno-economic, environmental, health and safety performance. Energy Convers Manage 2020;223:113262. http://dx.doi.org/10.1016/j.enconman.2020.113262.

[219] Papadopoulos AI, Kyriakides A-S, Seferlis P, Hassan I. Absorption refrigeration processes with organic working fluid mixtures- a review. Renew Sustain Energy Rev 2019;109:239–70. http://dx.doi.org/10.1016/j.rser.2019.04.016.

[220] Buskens C, Wassel D. The ESA NLP solver WORHP. Springer Optim Appl 2012;73:85–110. http://dx.doi.org/10.1007/978-1-4614-4469-5_4.

[221] Andersson J, Åkesson J, Diehl M. CasADi: A symbolic package for automatic differentiation and optimal control. Lect Notes Comput Sci Eng 2012;87 LNCSE:297–307. http://dx.doi.org/10.1007/978-3-642-30023-3_27.

[222] Walraven D, Laenen B, D'haeseleer W. Optimum configuration of shell-and-tube heat exchangers for the use in low-temperature organic Rankine cycles. Energy Convers Manage 2014;83:177–87. http://dx.doi.org/10.1016/J.ENCONMAN.2014.03.066.

[223] Linnhoff B, Dhole VR. Shaftwork targets for low-temperature process design. Chem Eng Sci 1992;47(8):2081–91. http://dx.doi.org/10.1016/0009-2509(92)80324-6.

[224] Linnhoff B, Flower JR. Synthesis of heat exchanger networks: I. Systematic generation of energy optimal networks. AIChE J 1978;24(4):633–42. http://dx.doi.org/10.1002/aic.690240411.

[225] Li J, Ge Z, Liu Q, Duan Y, Yang Z. Thermo-economic performance analyses and comparison of two turbine layouts for organic rankine cycles with dual-pressure evaporation. Energy Convers Manage 2018;164:603–14. http://dx.doi.org/10.1016/j.enconman.2018.03.029.

[226] Lazzaretto A, Toffolo A. A method to separate the problem of heat transfer interactions in the synthesis of thermal systems. Energy 2008;33(2):163–70. http://dx.doi.org/10.1016/J.ENERGY.2007.07.015.

[227] Hipólito-Valencia BJ, Rubio-Castro E, Ponce-Ortega JM, Serna-González M, Nápoles-Rivera F, El-Halwagi MM. Optimal design of inter-plant waste energy integration. Appl Therm Eng 2014;62(2):633–52. http://dx.doi.org/10.1016/J.APPLTHERMALENG.2013.10.015.

[228] Duran MA, Grossmann IE. Simultaneous optimization and heat integration of chemical processes. AIChE J 1986;32(1):123–38. http://dx.doi.org/10.1002/AIC.690320114.

[229] Elsido C, Mian A, Martelli E. A systematic methodology for the techno-economic optimization of organic Rankine cycles. Energy Procedia 2017;129:26–33. http://dx.doi.org/10.1016/J.EGYPRO.2017.09.171.

[230] Papoulias SA, Grossmann IE. A structural optimization approach in process synthesis—II: Heat recovery networks. Comput Chem Eng 1983;7(6):707–21. http://dx.doi.org/10.1016/0098-1354(83)85023-6.

[231] Györke G, Groniewsky A, Imre AR. A simple method of finding new dry and isentropic working fluids for organic rankine cycle. Energies 2019;12(3):480. http://dx.doi.org/10.3390/en12030480.

[232] Imre AR, Groniewsky A. Various ways of adiabatic expansion in organic rankine cycle (ORC) and in trilateral flash cycle (TFC). Z Phys Chem 2019;233(4):577–94. http://dx.doi.org/10.1515/zpch-2018-1292.

[233] Groniewsky A, Kústán R, Imre AR. Simultaneous working fluid and expander selection method for reaching low-threshold technology organic rankine cycle (ORC) design. Energy Sci Eng 2023;11(7):2330–50. http://dx.doi.org/10.1002/ese3.1457.

[234] Papadopoulos A, Linke P. Efficient integration of optimal solvent and process design using molecular clustering. Chem Eng Sci 2006;61(19):6316–36. http://dx.doi.org/10.1016/j.ces.2006.06.006.

[235] Papadopoulos A, Linke P. A unified framework for integrated process and molecular design. Chem Eng Res Des 2005;83(6 A):674–8. http://dx.doi.org/10.1205/cherd.04349.

[236] Park B-S, Usman M, Imran M, Pesyridis A. Review of organic rankine cycle experimental data trends. Energy Convers Manag 2018;173:679–91. http://dx.doi.org/10.1016/j.enconman.2018.07.097.

[237] Pardiñas ÁÁ, Pilarczyk M, Agromayor R, Nord LO. Design of an experimental orc expander setup using natural working fluids. In: Proceedings of the fifth international seminar on ORC power systems. 2019, p. 1–8.

[238] Jradi M, Riffat S. Experimental investigation of a biomass-fuelled micro-scale tri-generation system with an organic rankine cycle and liquid desiccant cooling unit. Energy 2014;71:80–93. http://dx.doi.org/10.1016/j.energy.2014.04.077.

[239] Yun E, Kim D, Yoon SY, Kim KC. Experimental investigation of an organic rankine cycle with multiple expanders used in parallel. Appl Energy 2015;145:246–54. http://dx.doi.org/10.1016/j.apenergy.2015.02.022.

[240] White M, Sayma AI. System and component modelling and optimisation for an efficient 10kWe low-temperature organic Rankine cycle utilising a radial inflow expander. In: Proceedings of the institution of mechanical engineers, part a: journal of power and energy. Vol. 229, 2015, http://dx.doi.org/10.1177/0957650915574211.

[241] Bekiloğlu HE, Bedir H, Anlaş G. Multi-objective optimization of ORC parameters and selection of working fluid using preliminary radial inflow turbine design. Energy Convers Manage 2019;183. http://dx.doi.org/10.1016/j.enconman.2018.12.039.

[242] Fiaschi D, Manfrida G, Maraschiello F. Design and performance prediction of radial ORC turboexpanders. Appl Energy 2015;138:517–32. http://dx.doi.org/10.1016/J.APENERGY.2014.10.052.

[243] Rahbar K, Mahmoud S, Al-Dadah RK, Moazami N. Modelling and optimization of organic Rankine cycle based on a small-scale radial inflow turbine. Energy Convers Manage 2015;91. http://dx.doi.org/10.1016/j.enconman.2014.12.003.

[244] Rahbar K, Mahmoud S, Al-Dadah RK, Moazami N. Parametric analysis and optimization of a small-scale radial turbine for organic Rankine cycle. Energy 2015;83:696–711. http://dx.doi.org/10.1016/j.energy.2015.02.079.

[245] Al Jubori A, Daabo A, Al-Dadah RK, Mahmoud S, Ennil AB. Development of micro-scale axial and radial turbines for low-temperature heat source driven organic Rankine cycle. Energy Convers Manage 2016;130:141–55. http://dx.doi.org/10.1016/j.enconman.2016.10.043.

[246] Li P, Mei Z, Han Z, Jia X, Zhu L, Wang S. Multi-objective optimization and improved analysis of an organic Rankine cycle coupled with the dynamic turbine efficiency model. Appl Therm Eng 2019;150:912–22. http://dx.doi.org/10.1016/j.applthermaleng.2019.01.058.

[247] Meroni A, Andreasen JG, Persico G, Haglind F. Optimization of organic Rankine cycle power systems considering multistage axial turbine design. Appl Energy 2018;209:339–54. http://dx.doi.org/10.1016/j.apenergy.2017.09.068.

[248] Al Jubori AM, Al-Dadah R, Mahmoud S. Performance enhancement of a small-scale organic Rankine cycle radial-inflow turbine through multi-objective optimization algorithm. Energy 2017;131:297–311. http://dx.doi.org/10.1016/j.energy.2017.05.022.

[249] Han Z, Mei Z, Li P. Multi-objective optimization and sensitivity analysis of an organic Rankine cycle coupled with a one-dimensional radial-inflow turbine efficiency prediction model. Energy Convers Manage 2018;166. http://dx.doi.org/10.1016/j.enconman.2018.04.022.

[250] Lecompte S, Huisseune H, van den Broek M, De Schampheleire S, De Paepe M. Part load based thermo-economic optimization of the organic Rankine cycle (ORC) applied to a combined heat and power (CHP) system. Appl Energy 2013;111:871–81. http://dx.doi.org/10.1016/J.APENERGY.2013.06.043.

[251] Pierobon L, Nguyen VT, Larsen U, Haglind F, Elmegaard B. Multi-objective optimization of organic Rankine cycles for waste heat recovery: Application in an offshore platform. Energy 2013;58:538–49. http://dx.doi.org/10.1016/J.ENERGY.2013.05.039.

[252] Di Battista D, Di Bartolomeo M, Villante C, Cipollone R. On the limiting factors of the waste heat recovery via ORC-based power units for on-the-road transportation sector. Energy Convers Manage 2018;155:68–77. http://dx.doi.org/10.1016/J.ENCONMAN.2017.10.091.

[253] Yang F, Cho H, Zhang H, Zhang J. Thermoeconomic multi-objective optimization of a dual loop organic Rankine cycle (ORC) for CNG engine waste heat recovery. Appl Energy 2017;205:1100–18. http://dx.doi.org/10.1016/J.APENERGY.2017.08.127.

[254] Wang M, Jing R, Zhang H, Meng C, Li N, Zhao Y. An innovative organic Rankine cycle (ORC) based ocean thermal energy conversion (OTEC) system with performance simulation and multi-objective optimization. Appl Therm Eng 2018;145:743–54. http://dx.doi.org/10.1016/J.APPLTHERMALENG.2018.09.075.

[255] Rosset K, Mounier V, Guenat E, Schiffmann J. Multi-objective optimization of turbo-ORC systems for waste heat recovery on passenger car engines. Energy 2018;159:751–65. http://dx.doi.org/10.1016/J.ENERGY.2018.06.193.

[256] Jankowski M, Borsukiewicz A, Szopik-Depczyńska K, Ioppolo G. Determination of an optimal pinch point temperature difference interval in ORC power plant using multi-objective approach. J Clean Prod 2019;217:798–807. http://dx.doi.org/10.1016/J.JCLEPRO.2019.01.250.

[257] Jankowski M, Borsukiewicz A. Multi-objective approach for determination of optimal operating parameters in low-temperature ORC power plant. Energy Convers Manage 2019;200:112075. http://dx.doi.org/10.1016/J.ENCONMAN.2019.112075.

[258] Bianchi M, Branchini L, De Pascale A, Melino F, Ottaviano S, Peretto A, et al. Performance and total warming impact assessment of pure fluids and mixtures replacing HFCs in micro-ORC energy systems. Appl Therm Eng 2022;203:117888. http://dx.doi.org/10.1016/J.APPLTHERMALENG.2021.117888.

[259] Grelet V, Reiche T, Guillaume L, Lemort V. Optimal waste heat recovery Rankine based for heavy duty applications. In: Fista world automotive congress. Maastricht; 2014.

[260] Shu G, Wang X, Tian H, Liu P, Jing D, Li X. Scan of working fluids based on dynamic response characters for organic Rankine cycle using for engine waste heat recovery. Energy 2017;133:609–20. http://dx.doi.org/10.1016/J.ENERGY.2017.05.003.

[261] Wang X, Shu G, Tian H, Liu P, Li X, Jing D. Dynamic response performance comparison of Rankine cycles with different working fluids for waste heat recovery of internal combustion engines. Energy Procedia 2017;105:1600–5. http://dx.doi.org/10.1016/J.EGYPRO.2017.03.512.

[262] Pili R, Jørgensen SB, Haglind F. Multi-objective optimization of organic Rankine cycle systems considering their dynamic performance. Energy 2022;246:123345. http://dx.doi.org/10.1016/J.ENERGY.2022.123345.

[263] Peng N, Wang E, Meng F. Off-design performance comparison of single-stage axial turbines using CO_2 and zeotropic mixture for low-temperature heat source. Energy Convers Manage 2020;213. http://dx.doi.org/10.1016/j.enconman.2020.112838.

[264] Tian H, Chang L, Gao Y, Shu G, Zhao M, Yan N. Thermo-economic analysis of zeotropic mixtures based on siloxanes for engine waste heat recovery using a dual-loop organic Rankine cycle (DORC). Energy Convers Manage 2017;136:11–26. http://dx.doi.org/10.1016/J.ENCONMAN.2016.12.066.

[265] Zarogiannis T, Papadopoulos A, Seferlis P, Linke P. The impact of novel and conventional working fluids on the control performance in organic Rankine cycles. Comput Aided Chem Eng 2017;40. http://dx.doi.org/10.1016/B978-0-444-63965-3.50409-8.

[266] Zarogiannis T, Papadopoulos A, Seferlis P. Control studies of organic Rankine cycles with different working fluid mixtures. Chem Eng Trans 2017;61. http://dx.doi.org/10.3303/CET1761233.

[267] Zarogiannis T. Systematic selection of working fluid mixtures for optimum solvent-based CO_2 capture processes and organic rankine cycles (Ph.D. thesis), Aristotle University of Thessaloniki; 2019.

[268] Chen X, Liu C, Li Q, Wang X, Wang S. Dynamic behavior of supercritical organic Rankine cycle using zeotropic mixture working fluids. Energy 2020;191:116576. http://dx.doi.org/10.1016/J.ENERGY.2019.116576.

[269] Cai J, Shu G, Tian H, Wang X, Wang R, Shi X. Validation and analysis of organic Rankine cycle dynamic model using zeotropic mixture. Energy 2020;197:117003. http://dx.doi.org/10.1016/J.ENERGY.2020.117003.

[270] Gad-el Hak I, Hussin A, Hamed AM, Mahmoud NA. 3D numerical modeling of zeotropic mixtures and pure working fluids in an ORC turbo-expander. Int J Turbomach Propul Power 2017;2(1):2. http://dx.doi.org/10.3390/ijtpp2010002.

[271] Wang Z, Zhang Z, Xia X, Zhao B, He N, Peng D. Preliminary design and numerical analysis of a radial inflow turbine in organic Rankine cycle using zeotropic mixtures. Appl Therm Eng 2019;162:114266. http://dx.doi.org/10.1016/J.APPLTHERMALENG.2019.114266.

[272] Le VL, Kheiri A, Feidt M, Pelloux-Prayer S. Thermodynamic and economic optimizations of a waste heat to power plant driven by a subcritical ORC (organic Rankine cycle) using pure or zeotropic working fluid. Energy 2014;78:622–38. http://dx.doi.org/10.1016/J.ENERGY.2014.10.051.

[273] Lampe M, De Servi C, Schilling J, Bardow A, Colonna P. Toward the integrated design of organic Rankine cycle power plants: A method for the simultaneous optimization of working fluid, thermodynamic cycle, and turbine. J Eng Gas Turbines Power-Trans Asme 2019;141(11):111009. http://dx.doi.org/10.1115/1.4044380.

[274] Schilling J, Tillmanns D, Lampe M, Hopp M, Gross J, Bardow A. From molecules to dollars: integrating molecular design into thermo-economic process design using consistent thermodynamic modeling. Mol Syst Des Eng 2017;2(3):301–20. http://dx.doi.org/10.1039/c7me00026j.

[275] van Kleef LMT, Oyewunmi OA, Markides CN. Multi-objective thermo-economic optimization of organic Rankine cycle (ORC) power systems in waste-heat recovery applications using computer-aided molecular design techniques. Appl Energy 2019;251:112513. http://dx.doi.org/10.1016/j.apenergy.2019.01.071.

[276] Tillmanns D, Petzschmann J, Schilling J, Gertig C, Bardow A. ORC on tour: Integrated design of dynamic ORC processes and working fluids for waste-heat recovery from heavy-duty vehicles. In: Kiss A, Zondervan E, Lakerveld R, Ozkan L, editors. 29th European symposium on computer aided process engineering, pt a. Computer aided chemical engineering, Vol. 46, Sara Burger-hartstraat 25, PO Box 211, 1000 AE Amsterdam, Netherlands: Elsevier Science BV; 2019, p. 163–8, 29th European Symposium on Computer-Aided Process Engineering (ESCAPE), Eindhoven, Netherlands, Jun 16–19, 2019.

[277] Schilling J, Entrup M, Hopp M, Gross J, Bardow A. Towards optimal mixtures of working fluids: Integrated design of processes and mixtures for organic Rankine cycles. Renew Sustain Energy Rev 2021;135:110179. http://dx.doi.org/10.1016/j.rser.2020.110179.

[278] Thierry DM, Flores-Tlacuahuac A, Grossmann IE. Simultaneous optimal design of multi-stage organic Rankine cycles and working fluid mixtures for low-temperature heat sources. Comput Chem Eng 2016;89:106–26. http://dx.doi.org/10.1016/J.COMPCHEMENG.2016.03.005.

[279] Song J, Gu Cw, Ren X. Influence of the radial-inflow turbine efficiency prediction on the design and analysis of the organic Rankine cycle (ORC) system. Energy Convers Manage 2016;123. http://dx.doi.org/10.1016/j.enconman.2016.06.037.

[280] Bahadormanesh N, Rahat S, Yarali M. Constrained multi-objective optimization of radial expanders in organic Rankine cycles by firefly algorithm. Energy Convers Manage 2017;148:1179–93. http://dx.doi.org/10.1016/j.enconman.2017.06.070.

[281] Li X, Song J, Yu G, Liang Y, Tian H, Shu G, et al. Organic Rankine cycle systems for engine waste-heat recovery: Heat exchanger design in space-constrained applications. Energy Convers Manage 2019;199:111968. http://dx.doi.org/10.1016/J.ENCONMAN.2019.111968.

[282] Zhao Y, Liu G, Li L, Yang Q, Tang B, Liu Y. Expansion devices for organic Rankine cycle (ORC) using in low temperature heat recovery: A review. Energy Convers Manage 2019;199:111944. http://dx.doi.org/10.1016/J.ENCONMAN.2019.111944.

[283] Yue C, Han D, Pu W, He W. Thermal matching performance of a geothermal ORC system using zeotropic working fluids. Renew Energy 2015;80:746–54. http://dx.doi.org/10.1016/j.renene.2015.02.063.

[284] Palagi L, Sciubba E, Tocci L. A neural network approach to the combined multi-objective optimization of the thermodynamic cycle and the radial inflow turbine for organic Rankine cycle applications. Appl Energy 2019;237. http://dx.doi.org/10.1016/j.apenergy.2019.01.035.

[285] Pantaleo AM, Simpson M, Rotolo G, Distaso E, Oyewunmi OA, Sapin P, et al. Thermoeconomic optimisation of small-scale organic Rankine cycle systems based on screw *vs.* piston expander maps in waste heat recovery applications. Energy Convers Manage 2019;200. http://dx.doi.org/10.1016/j.enconman.2019.112053.

[286] Kim J-S, Kim D-Y, Kim Y-T. Experiment on radial inflow turbines and performance prediction using deep neural network for the organic Rankine cycle. Appl Therm Eng 2019;149:633–43. http://dx.doi.org/10.1016/j.applthermaleng.2018.12.084.

[287] Madhawa Hettiarachchi HD, Golubovic M, Worek WM, Ikegami Y. Optimum design criteria for an organic Rankine cycle using low-temperature geothermal heat sources. Energy 2007;32(9):1698–706. http://dx.doi.org/10.1016/J.ENERGY.2007.01.005.

[288] Desideri A, Dechesne B, Wronski J, Van Den Broek M, Gusev S, Lemort V, et al. Comparison of moving boundary and finite-volume heat exchanger models in the Modelica language. Energies 2016;9(5):339. http://dx.doi.org/10.3390/EN9050339.

[289] Xu B, Rathod D, Kulkarni S, Yebi A, Filipi Z, Onori S, Hoffman M. Transient dynamic modeling and validation of an organic Rankine cycle waste heat recovery system for heavy duty diesel engine applications. Appl Energy 2017;205:260–79. http://dx.doi.org/10.1016/J.APENERGY.2017.07.038.

[290] Pereira FE, Jackson G, Galindo A, Adjiman CS. The HELD algorithm for multicomponent, multiphase equilibrium calculations with generic equations of state. Comput Chem Eng 2012;36(1):99–118. http://dx.doi.org/10.1016/j.compchemeng.2011.07.009.

[291] Mitsos A, Barton PI. A dual extremum principle in thermodynamics. AIChE J 2007;53(8):2131–47. http://dx.doi.org/10.1002/aic.11230.

[292] Mastrullo R, Mauro AW, Revellin R, Viscito L. Modeling and optimization of a shell and louvered fin mini-tubes heat exchanger in an ORC powered by an internal combustion engine. Energy Convers Manage 2015;101:697–712. http://dx.doi.org/10.1016/J.ENCONMAN.2015.06.012.

[293] Yang J, Liu W. Numerical investigation on a novel shell-and-tube heat exchanger with plate baffles and experimental validation. Energy Convers Manage 2015;101:689–96. http://dx.doi.org/10.1016/j.enconman.2015.05.066.

[294] Mokkapati V, Lin SC. Numerical study of an exhaust heat recovery system using corrugated tube heat exchanger with twisted tape inserts. Int Commun Heat Mass Transfer 2014;57:53–64. http://dx.doi.org/10.1016/J.ICHEATMASSTRANSFER.2014.07.002.

[295] Chen T, Shu G, Tian H, Ma X, Wang Y, Yang H. Compact potential of exhaust heat exchangers for engine waste heat recovery using metal foams. Int J Energy Res 2019;43(4):1428–43. http://dx.doi.org/10.1002/er.4340.

[296] Zhang J, Hu X, Wu D, Huang X, Wang X, Yang Y, et al. A comparative study on design and performance evaluation of organic rankine cycle (ORC) under different two-phase heat transfer correlations. Appl Energy 2023;350:121724. http://dx.doi.org/10.1016/j.apenergy.2023.121724.

[297] Calise F, Macaluso A, Pelella P, Vanoli L. A comparison of heat transfer correlations applied to an organic rankine cycle. Eng Sci Technol, Int J 2018;21(6):1164–80. http://dx.doi.org/10.1016/j.jestch.2018.09.009.

[298] Heberle F, Brüggemann D. Thermo-economic analysis of zeotropic mixtures and pure working fluids in organic Rankine cycles for waste heat recovery. Energies 2016;9(4):226. http://dx.doi.org/10.3390/EN9040226.

[299] Gkouletsos D, Papadopoulos AI, Seferlis P, Hassan I. Systematic modeling under uncertainty of single, double and triple effect absorption refrigeration processes. Energy 2019;183:262–78. http://dx.doi.org/10.1016/j.energy.2019.06.067.

[300] Frutiger J, Andreasen J, Liu W, Spliethoff H, Haglind F, Abildskov J, et al. Working fluid selection for organic Rankine cycles – Impact of uncertainty of fluid properties. Energy 2016;109:987–97. http://dx.doi.org/10.1016/J.ENERGY.2016.05.010.

[301] Frutiger J. Property uncertainty analysis and methods for optimal working fluids of thermodynamic cycles (Ph.D. thesis), Technical University of Denmark; 2017.

[302] Soave G. Equilibrium constants from a modified Redlich-Kwong equation of state. Chem Eng Sci 1972;27(6):1197–203. http://dx.doi.org/10.1007/978-3-319-26362-5_26.

[303] Gross J, Sadowski G. Application of perturbation theory to a hard-chain reference fluid: an equation of state for square-well chains. Fluid Phase Equilib 2000;168:183–99. http://dx.doi.org/10.1016/s0378-3812(00)00302-2.

[304] Frutiger J, Bell I, O'Connell JP, Kroenlein K, Abildskov J, Sin G. Uncertainty assessment of equations of state with application to an organic Rankine cycle. 115, (9–12):2017, p. 1225–44. http://dx.doi.org/10.1080/00268976.2016.1275856.

[305] Aly FA, Lee LL. Self-consistent equations for calculating the ideal gas heat capacity, enthalpy, and entropy. Fluid Phase Equilib 1981;6(3–4). http://dx.doi.org/10.1016/0378-3812(81)85002-9.

[306] Frutiger J, Abildskov J, Sin G. Global sensitivity analysis of computer-aided molecular design problem for the development of novel working fluids for power cycles. In: Computer aided chemical engineering. vol. 38, Elsevier; 2016, p. 283–8. http://dx.doi.org/10.1016/B978-0-444-63428-3.50052-7.

[307] Peng D-Y, Robinson DB. A new two-constant equation of state. Ind Eng Chem Fundam 1976;15(1):59–64. http://dx.doi.org/10.1021/i160057a011.

[308] Santos-Rodriguez MM, Flores-Tlacuahuac A, Zavala VM. A stochastic optimization approach for the design of organic fluid mixtures for low-temperature heat recovery, Appl Energy 198. http://dx.doi.org/10.1016/J.APENERGY.2017.04.047.

[309] Dige N, Diwekar U. Efficient sampling algorithm for large-scale optimization under uncertainty problems. Comput Chem Eng 2018;115:431–54. http://dx.doi.org/10.1016/j.compchemeng.2018.05.007.

[310] Zarogiannis T, Papadopoulos A, Seferlis P. Simultaneous process design and control in integrated energy conversion systems – Application to organic Rankine cycles. In: Klemes J, editor. Handbook of process integration. second ed.. Elsevier; 2022, p. 765–82.

[311] Lu P, Luo X, Wang J, Chen J, Liang Y, Yang Z, et al. Thermo-economic design, optimization, and evaluation of a novel zeotropic ORC with mixture composition adjustment during operation. Energy Convers Manage 2021;230. http://dx.doi.org/10.1016/j.enconman.2020.113771.

[312] Mavrou P, Papadopoulos AI, Seferlis P, Linke P, Voutetakis S. Selection of working fluid mixtures for flexible organic Rankine cycles under operating variability through a systematic nonlinear sensitivity analysis approach. Appl Therm Eng 2015;89:1054–67. http://dx.doi.org/10.1016/j.applthermaleng.2015.06.017.

[313] Mavrou P, Papadopoulos A, Seferlis P, Linke P, Voutetakis S. Systematic nonlinear sensitivity analysis of working fluid mixtures for flexible solar Rankine cycles. Chem Eng Trans 2015;45. http://dx.doi.org/10.3303/CET1545297.

[314] Mavrou P, Papadopoulos AI, Stijepovic MZ, Seferlis P, Linke P, Voutetakis S. Novel and conventional working fluid mixtures for solar Rankine cycles: Performance assessment and multi-criteria selection. Appl Therm Eng 2015;75(SI):384–96. http://dx.doi.org/10.1016/j.applthermaleng.2014.10.077.

[315] Mavrou P, Papadopoulos AI, Stijepovic M, Seferlis P, Linke P, Voutetakis S. Assessment of working fluid mixtures for solar organic Rankine cycles. In: Varbanov P, Klemes J, Liew P, Yong J, Stehlik P, editors. PRES 2014, 17th conference on process integration, modelling and optimisation for energy saving and pollution reduction, pts 1–3. Chemical engineering transactions, 39, 2014, p. 283–8, 17th Conference on Process Integration, Modelling and Optimisation for Energy Saving and Pollution Reduction (PRES 2014), Prague, Czech Republic, Aug 23–27, 2014.

[316] Chatzopoulou MA, Lecompte S, De Paepe M, Markides CN. Off-design optimisation of organic Rankine cycle (ORC) engines with different heat exchangers and volumetric expanders in waste heat recovery applications. Appl Energy 2019;253:113442. http://dx.doi.org/10.1016/j.apenergy.2019.113442.

[317] Pang KC, Hung TC, He YL, Feng YQ, Lin CH, Wong KW. Developing ORC engineering simulator (ORCES) to investigate the working fluid mass flow rate control strategy and simulate long-time operation. Energy Convers Manage 2020;203:112206. http://dx.doi.org/10.1016/J.ENCONMAN.2019.112206.

[318] Span R. Multiparameter equations of state: an accurate source of thermodynamic property data. Springer Science & Business Media; 2013.

[319] Vogel E, Kuechenmeister C, Bich E, Laesecke A. Reference correlation of the viscosity of propane. J Phys Chem Ref Data 1998;27(5):947–70. http://dx.doi.org/10.1063/1.556025.

[320] Kunz O, Wagner W. The GERG-2008 wide-range equation of state for natural gases and other mixtures: an expansion of GERG-2004. J Chem Eng Data 2012;57(11):3032–91. http://dx.doi.org/10.1021/je300655b.

[321] Poling BE, Prausnitz JM, O'Connell JP. The properties of gases and liquids. fifth ed.. McGraw Hill; 2001.

[322] Elliott JR, Diky V, Knotts IV TA, Wilding WV. The properties of gases and liquids. Sixth ed.. McGraw Hill; 2023.

[323] Gani R. Group contribution-based property estimation methods:advances and perspectives. Curr Opin Chem Eng 2019;23:184–96. http://dx.doi.org/10.1016/j.coche.2019.04.007.

[324] Lydersen AL. Estimation of critical properties of organic compounds. University of Wisconsin College Engineering, Eng. Exp. Stn. Rep. 3, Madison, WI 1955. http://dx.doi.org/10.1093/oso/9780195096897.003.0008.

[325] Joback KG. A unified approach to physical property estimation using multivariate statistical techniques. (Master's thesis), Cambridge, MA, USA: Massachusetts Institute of Technology, Dept of Chemical Engineering; 1984.

[326] ASPEN PLUS: user guide. Aspen Technology Inc.; 2000.

[327] Process Systems Enterprise. gPROMS. 1997–2020, http://www.psenterprise.com/products/gproms.

[328] Riedel L. Kritischer Koeffizient, Dichte des gesättigten Dampfes und Verdampfungswärme. Untersuchungen über eine Erweiterung des Theorems der übereinstimmenden Zustände. Teil III. Chem Ing Tech 1954;26:679–83. http://dx.doi.org/10.1002/cite.330261208.

[329] Palma-Flores O, Flores-Tlacuahuac A, Canseco-Melchor G. Simultaneous molecular and process design for waste heat recovery. Energy 2016;99:32–7. http://dx.doi.org/10.1016/j.energy.2016.01.024.

[330] Lukawski MZ, DiPippo R, Tester JW. Molecular property methods for assessing efficiency of organic Rankine cycles. Energy 2018;142:108–20. http://dx.doi.org/10.1016/j.energy.2017.09.140.

[331] Constantinou L, Gani R. New group contribution method for estimating the properties of pure compounds. AIChE J 1994;40(10):1697–710. http://dx.doi.org/10.1002/aic.690401011.

[332] Marrero-Morejón J, Pardillo-Fontdevila E. Estimation of pure compound properties using group-interaction contributions. AIChE J 1999;45(3):615–21. http://dx.doi.org/10.1002/aic.690450318.

[333] Fanxiao M, Enhua W, Bo Z. Possibility of optimal efficiency prediction of an organic Rankine cycle based on molecular property method for high-temperature exhaust gases. Energy 2021;222. http://dx.doi.org/10.1016/j.energy.2021.119974.

[334] Papadopoulos AI, Stijepovic M, Linke P, Seferlis P, Voutetakis S. Power generation from low enthalpy geothermal fields by design and selection of efficient working fluids for organic Rankine cycles. In: Klemes J, Lam H, Varbanov P, editors. PRES 2010: 13th international conference on process integration, modelling and optimisation for energy saving and pollution reduction. Chem. eng. trans., 21, 2010, p. 61–6, 13th Conference on Process Integration, Modelling and Optimisation for Energy Saving and Pollution Reduction, Prague, Czech Republic, Aug 28-Sep 01, 2010.

[335] Papadopoulos AI, Stijepovic M, Linke P, Seferlis P, Voutetakis S. Multi-level design and selection of optimum working fluids and ORC systems for power and heat cogeneration from low enthalpy renewable sources. In: Bogle I, Fairweather M, editors. 22nd European symposium on computer aided process engineering. Computer aided chemical engineering, 30, 2012, p. 66–70, 22nd European Symposium on Computer Aided Process Engineering (ESCAPE), Univ Coll London, London, England, Jun 17–20, 2012.

[336] Papadopoulos AI, Stijepovic M, Linke P, Seferlis P, Voutetakis S. Molecular design of working fluid mixtures for organic Rankine cycles. In: Kraslawski A, Turunen I, editors. 23rd European symposium on computer aided process engineering. Comp. aid. chem. eng., Vol. 32, 2013, p. 289–94, 23rd European Symposium on Computer Aided Process Engineering (ESCAPE), Lappeenranta Univ Technol, Lappeenranta, Finland, Jun 09–12, 2013.

[337] Linke P, Papadopoulos AI, Seferlis P. Systematic methods for working fluid selection and the design, integration and control of organic Rankine cycles-a review. Energies 2015;8(6):4755–801. http://dx.doi.org/10.3390/en8064755.

[338] Su W, Zhao L, Deng S. Group contribution methods in thermodynamic cycles: Physical properties estimation of pure working fluids. Renew Sustain Energy Rev 2017;79:984–1001. http://dx.doi.org/10.1016/j.rser.2017.05.164.

[339] Walker PJ, Haslam AJ. A new predictive group-contribution ideal-heat-capacity model and its influence on second-derivative properties calculated using a free-energy equation of state. J Chem Eng Data 2020;65(12):5809–29. http://dx.doi.org/10.1021/acs.jced.0c00723.s001.

[340] Fredenslund A, Gmehling J, Rasmussen P. Vapor-liquid equilibria using UNIFAC: A Group-Contribution method. Amsterdam: Elsevier; 1977.

[341] Weidlich U, Gmehling J. A modified UNIFAC model. 1. prediction of VLE, h^E and γ^∞. Ind Eng Chem Res 1987;26(7):1372–81. http://dx.doi.org/10.1007/978-3-319-26362-5_26.

[342] Wilson G. J Am Chem Soc 1964;86:127.

[343] Renon H, Prausnitz JM. Local compositions in thermodynamic excess functions for liquid mixtures. AIChE J 1968;14:135. http://dx.doi.org/10.1002/aic.690140124.

[344] Abrams DS, Prausnitz JM. Statistical thermodynamics of liquid mixtures: A new expression for the excess gibbs energy of partly or completely miscible systems, AIChE J. 21, 116–128. http://dx.doi.org/10.1002/aic.690210115.

[345] Maurer G, Prausnitz JM. On the derivation and extension of the uniquac equation, Fluid Phase Equilib. 2, 91–99. http://dx.doi.org/10.1016/0378-3812(78)85002-x.

[346] Derr EL, Deal CH. Analytical solutions of groups: correlation of activity coefficients through structural group parameters. Int Chem Eng Symp Ser No. 32 1969;3:44–51. http://dx.doi.org/10.1021/i160001a003.

[347] Kontogeorgis GM, Folas GK. Thermodynamic models for industrial applications. From classical and advanced mixing rules to association theories. Chichester, UK: John Wiley and Sons; 2010.

[348] Madani H, Valtz A, Coquelet C. Isothermal vapor-liquid equilibrium data for the decafluorobutane (R3110)+1,1,1,3,3-pentafluorobutane (R365mfc) system at temperatures from 333 K to 441 K. Fluid Phase Equilib 2013;354:109–13. http://dx.doi.org/10.1016/j.fluid.2013.06.031.

[349] Privat R, Qian JW, Alonso D, Jaubert JN. Quest for an efficient binary working mixture for an absorption-demixing heat transformer. Energy 2013;55:594–609. http://dx.doi.org/10.1016/j.energy.2013.03.081.

[350] Zhang M, Zheng DX, Yang WZ, Li XX. Measurement and Correlation of Isothermal Vapor-Liquid Equilibrium of 1,1,1,3,3-Pentafluoropropane plus N,N-Dimethylacetamide and 1,1,1,3,3,3-Hexafluoropropane plus N,N-Dimethylacetamide/Diethylene Glycol Dimethyl Ether Systems. J Chem Eng Data 2014;59:3912–9. http://dx.doi.org/10.1021/je500801w.

[351] Li XX, Zheng DX, Zhang M, Dong L. Vapor-liquid equilibrium measurement of 1,1,1,3,3-pentafluoropropane plus N,N-dimethylformamide/diethylene glycol dimethyl ether/N-methyl-2-pyrrolidone working fluids for absorption power cycle. Fluid Phase Equilib 2014;366:1–8. http://dx.doi.org/10.1016/j.fluid.2014.01.007.

[352] Panesar AS. An innovative organic Rankine cycle approach for high temperature applications. Energy 2016;115:1436–50. http://dx.doi.org/10.1016/j.energy.2016.05.135.

[353] Jirasek F, Hayer N, Abbas R, Schmid B, Hasse H. Prediction of parameters of group contribution models of mixtures by matrix completion. Phys Chem Chem Phys 2023;25(2):1054–62. http://dx.doi.org/10.31224/3063.

[354] Klamt A. Conductor-like Screening Model for Real Solvents: A new approach to the quantitative calculation of solvation phenomena. J Phys Chem 1995;99:2224. http://dx.doi.org/10.1007/978-3-319-26362-5_26.

[355] Klamt A, Jonas V, Bürger T, Lohrenz JCW. Refinement and parameterization of COSMO-RS. J Phys Chem A 1998;102:5074. http://dx.doi.org/10.1021/jp980017s.

[356] Klamt A, Eckert F. COSMO-RS: a novel and efficient method for the a priori prediction of thermophysical data of liquids. Fluid Phase Equilib 2000;172:43–72. http://dx.doi.org/10.1016/s0378-3812(00)00357-5.

[357] Preißinger M, Schwöbel J, Klamt A, Brüggemann D. High-throughput screening of ORC fluids for mobile applications. In: Junior C, Jänsch D, O. D, editors. Energy and thermal management, air conditioning, waste heat recovery: 1st ETA conference, December 1-2, 2016, berlin, Germany 1. Springer, Cham; 2016, p. 35–40. http://dx.doi.org/10.1007/978-3-319-47196-9_3, 1st ETA Conference.

[358] Scheffczyk J, Fleitmann L, Schwarz A, Lampe M, Bardow A, Leonhard K. COSMO-CAMD: A framework for optimization-based computer-aided molecular design using COSMO-RS. Chem Eng Sci 2017;159:84–92. http://dx.doi.org/10.1016/j.ces.2016.05.038.

[359] Lin S-T, Sandler SI. A priori phase equilibrium prediction from a segment contribution solvation model. Ind Eng Chem Res 2002;41:899–913. http://dx.doi.org/10.1021/ie001047w.

[360] Xu J, Scurto AM, Shiflett MB, Lustig SR, Hung FR. Power generation from waste heat: Ionic liquid-based absorption cycle versus organic Rankine cycle. AIChE J 2021;67:e17038. http://dx.doi.org/10.1002/aic.17038.

[361] https://github.com/usnistgov/COSMOSAC, 2020.

[362] Hsieh C-M, Sandler SI. Improvements of COSMO-SAC for vapor-liquid and liquid-liquid equilibrium predictions. Fluid Phase Equilib 2010;297:90–7. http://dx.doi.org/10.1016/j.fluid.2010.06.011.

[363] Hsieh C-M, Lin S-T, Vrabec J. Considering the dispersive interactions in the COSMO-SAC model for more accurate predictions of fluid phase behavior. Fluid Phase Equilib 2014;367:109–16. http://dx.doi.org/10.1016/j.fluid.2014.01.032.

[364] Bell IH, Mickoleit E, Hsieh C-M, Lin S-T, Vrabec J, Breitkopf C, et al. A Benchmark Open-Source Implementation of COSMO-SAC. J Chem Theory Comput 2020;16:2635–46. http://dx.doi.org/10.1021/acs.jctc.9b01016.

[365] Winter B, Winter C, Esper T, Schilling J, Bardow A. A smile is all you need: predicting limiting activity coefficients from SMILES with natural language processing. Digit Discov 2022;1:859. http://dx.doi.org/10.1039/d2dd00058j.

[366] Winter B, Winter C, Esper T, Schilling J, Bardow A. SPT-NRTL: A physics-guided machine learning model to predict thermodynamically consistent activity coefficients. Fluid Phase Equilib 2023;568:113731. http://dx.doi.org/10.1016/j.fluid.2023.113731.

[367] Weininger D. SMILES, a chemical language and information system. 1. Introduction to methodology and encoding rules. J Chem Inf Comput Sci 1988;28(1):31–6. http://dx.doi.org/10.1021/ci00057a005.

[368] Weininger D, Weininger A, Weininger J. SMILES. 2. Algorithm for generation of unique SMILES notation. J Chem Inf Model 1989;29(2):97–101. http://dx.doi.org/10.1021/ci00062a008.

[369] Weininger D. SMILES. 3. DEPICT. Graphical depiction of chemical structures. J Chem Inf Model 1990;30(3):237–43. http://dx.doi.org/10.1021/ci00067a005.

[370] Holderbaum T, Gmehling J. PSRK: A group contribution equation of state based on UNIFAC. Fluid Phase Equilib 1991;70(2–3):251–65. http://dx.doi.org/10.1016/0378-3812(91)85038-v.

[371] Patel NC, Teja AS. A new cubic equation of state for fluids and fluid mixtures. Chem Eng Sci 1982;37:463–73. http://dx.doi.org/10.1016/0009-2509(82)80099-7.

[372] Rehner P, Bauer G, Gross J. FeOs - an open-source framework for equations of state and classical density functional theory. Ind Eng Chem Res 2023;62(12):5347–57. http://dx.doi.org/10.1021/acs.iecr.2c04561.s001, URL https://github.com/feos-org/feos.

[373] Bell IH, Deiters UK, Leal AMM. Implementing an equation of state without derivatives: teqp. Ind Eng Chem Res 2022;61(17):6010–27. http://dx.doi.org/10.1021/acs.iecr.2c00237.

[374] Chaparro G, Mejía A. Phasepy: A Python based framework for fluid phase equilibria and interfacial properties computation. J Comput Chem 2020;41(29):2504–26. http://dx.doi.org/10.1002/jcc.26405, URL https://onlinelibrary.wiley.com/doi/10.1002/jcc.26405.

[375] Yew H-W, Walker PJ, Riedeman A. Clapeyron.jl. 2022, https://github.com/ClapeyronThermo/Clapeyron.jl/.

[376] Walker PJ, Yew H-W, Riedeman A. Clapeyron.jl: An extensible, open-source thermodynamics toolkit. Ind Eng Chem Res 2022;61(20):7130—7153. http://dx.doi.org/10.1021/acs.iecr.2c00326.

[377] Huron MJ, Vidal J. New mixing rules in simple equations of state for representing vapour-liquid equilibria of strongly non-ideal mixtures. Fluid Phase Equilib 1979;3:255. http://dx.doi.org/10.1016/0378-3812(79)80001-1.

[378] Michelsen ML. A modified Huron-Vidal mixing rule for cubic equations of state. Fluid Phase Equilib 1990;60:213. http://dx.doi.org/10.1007/978-3-319-26362-5_26.

[379] Dahl S, Michelsen ML. High-pressure vapor-liquid equilibrium with a UNIFAC-based equation of state. AIChE J 1990;36:1829. http://dx.doi.org/10.1002/aic.690361207.

[380] Dahl S, Fredenslund A, Rasmussen P. The MHV2 model: A UNIFAC-based equation of state model for prediction of gas solubility and vapor-liquid equilibria at low and high pressures. Ind Eng Chem Res 1991;30:1936. http://dx.doi.org/10.1021/ie00056a041.

[381] Wong DSH, Sandler SI. A theoretically correct mixing rule for cubic equations of state. AIChE J 1992;38:671. http://dx.doi.org/10.1002/aic.690380505.

[382] Jaubert J-N, Mutelet F. VLE predictions with the Peng-Robinson equation of state and temperature dependent k_{ij} calculated through a group contribution method. Fluid Phase Equilib 2004;224(2):285–304. http://dx.doi.org/10.1007/978-3-319-26362-5_26.

[383] Jaubert J-N, Privat R. Relationship between the binary interaction parameters (k_{ij}) of the Peng–Robinson and those of the Soave–Redlich–Kwong equations of state: Application to the definition of the PR$_2$SRK model. Fluid Phase Equilib 2010;295:26–37. http://dx.doi.org/10.1016/j.fluid.2010.03.037.

[384] Chen C, Su W, Yu A, Lin X, Zhou N. Combining cubic equations with group contribution methods to predict cycle performances and design working fluids for four different organic Rankine cycles. Energy Convers Manag X 2022;15:10025. http://dx.doi.org/10.1016/j.ecmx.2022.100245.

[385] Ahlers J, Gmehling J. Development of a universal group contribution equation of state. I. Prediction of liquid densities for pure compounds with a volume translated Peng-Robinson equation of state. Fluid Phase Equilib 2001;191(1–2):177–88. http://dx.doi.org/10.1021/ie0210356.

[386] Peng Y, Su W, Zhou N, Zhao L. How to evaluate the performance of subcritical organic rankine cycle from key properties of working fluids by group contribution methods? Energy Convers Manag 2020;221:113204. http://dx.doi.org/10.1016/j.enconman.2020.113204.

[387] Su W, Zhao L, Deng S. Developing a performance evaluation model of organic rankine cycle for working fluids based on the group contribution method. Energy Convers Manag 2017;132:307–15. http://dx.doi.org/10.1016/j.enconman.2016.11.040.

[388] Nannoolal Y, Rarey J, Ramjugernath D. Estimation of pure component properties. Part 2. Estimation of critical property data by group contribution. Fluid Phase Equilib 2007;252(1–2):1–27. http://dx.doi.org/10.1016/j.fluid.2006.11.014.

[389] Lemmon EW, Bell IH, Huber ML, McLinden MO. NIST standard reference database 23: Reference fluid thermodynamic and transport properties-REFPROP, version 10.0, national institute of standards and technology. 2018, http://dx.doi.org/10.18434/T4/1502528, URL https://www.nist.gov/srd/refprop.

[390] Blas FJ, Vega LF. Thermodynamic behaviour of homonuclear and heteronuclear Lennard-Jones chains with association sites from simulation and theory. Mol Phys 1997;92:135. http://dx.doi.org/10.1080/002689797170707.

[391] Gil-Villegas A, Galindo A, Whitehead PJ, Mills SJ, Jackson G, Burgess AN. Statistical associating fluid theory for chain molecules with attractive potentials of variable range. J Chem Phys 1997;106(10):4168–86. http://dx.doi.org/10.1063/1.473101.

[392] Galindo A, Davies LA, Gil-Villegas A, Jackson G. The thermodynamics of mixtures and the corresponding mixing rules in the SAFT-VR approach for potentials of variable range. Mol Phys 1998;93(2):241–52. http://dx.doi.org/10.1080/00268979809482207.

[393] Müller EA, Gubbins KE. An equation of state for water from a simplified intermolecular potential. Ind Eng Chem Res 1995;34:3662–73. http://dx.doi.org/10.1021/ie00037a055.

[394] Xu K, Li Y, Liu W. Application of perturbation theory to chain and polar fluids pure alkanes, alkanols and water. Fluid Phase Equilib 1998;142:55–66. http://dx.doi.org/10.1016/s0378-3812(97)00217-3.

[395] Jog PK, Chapman WG. Application of Wertheim's thermodynamic perturbation theory to dipolar hard sphere chains. Mol Phys 1999;97:307. http://dx.doi.org/10.1080/002689799163703.

[396] Jog PK, Sauer SG, Blaesing J, Chapman WG. Application of dipolar chain theory to the phase behavior of polar fluids and mixtures. Ind Eng Chem Res 2001;40:4641. http://dx.doi.org/10.1021/ie010264+.

[397] Tumakaka F, Sadowski G. Application of the perturbed-chain SAFT equation of state to polar systems. Fluid Phase Equilib 2004;217:233–9. http://dx.doi.org/10.1016/j.fluid.2002.12.002.

[398] Gross J, Vrabec J. An equation of state contribution for polar components: Dipolar molecules. AIChE J 2005;52(3):1194–204. http://dx.doi.org/10.1002/aic.10683.

[399] Gross J. An equation of state contribution for polar components: Quadrupolar molecules. AIChE J 2005;51(9):2556–68. http://dx.doi.org/10.1002/aic.10502.

[400] Karakatsani EK, Spyriouni T, Economou IG. Extended statistical associating fluid theory (SAFT) equations of state for dipolar fluids. AIChE J 2005;51:2328–42. http://dx.doi.org/10.1002/aic.10473.

[401] Karakatsani EK, Kontogeorgis GM, Economou IG. Evaluation of the truncated perturbed chain-polar statistical associating fluid theory for complex mixture fluid phase equilibria. Ind Eng Chem Res 2006;45(17):6063–74. http://dx.doi.org/10.1021/ie060313o.

[402] Karakatsani EK, Economou IG. Perturbed chain-statistical associating fluid theory extended to dipolar and quadrupolar molecular fluids. J Phys Chem B 2006;110:9252–61. http://dx.doi.org/10.1021/jp056957b.

[403] Zhao H, McCabe C. Phase behavior of dipolar fluids from a modified statistical associating fluid theory for potentials of variable range. J Chem Phys 2006;125:104504. http://dx.doi.org/10.1063/1.2337624.

[404] Leonhard K, Van Nhu N, Lucas K. Making equation of state models predictive-part 3: Improved treatment of multipolar interactions in a PC-SAFT based equation of state. J Phys Chem C 2007;111:15533–43. http://dx.doi.org/10.1021/jp0726081.

[405] Kleiner M, Sadowski G. Modeling of polar systems using PCP-SAFT: An approach to account for induced-association interactions. J Phys Chem C 2007;111:15544–53. http://dx.doi.org/10.1021/jp072640v.

[406] Liu W-B, Li Y-G, Lu J-F. A new equation of state for real aqueous ionic fluids based on electrolyte perturbation theory, mean spherical approximation and statistical associating fluid theory. Fluid Phase Equilib 1999;158–160:595–606. http://dx.doi.org/10.1016/s0378-3812(99)00082-5.

[407] Galindo A, Gil-Villegas A, Jackson G, Burgess AN. SAFT-VRE: Phase behavior of electrolyte solutions with the statistical associating fluid theory for potentials of variable range. J Phys Chem B. 1999;103:10272–81. http://dx.doi.org/10.1021/jp991959f.

[408] Patel BH, Paricaud P, Galindo A, Maitland GC. Prediction of the salting-out effect of strong electrolytes on water + alkane solutions. Ind Eng Chem Res 2003;42(16):3809–23. http://dx.doi.org/10.1021/ie020918u.

[409] Behzadi B, Patel B, Galindo A, Ghotbi C. Modeling electrolyte solutions with the SAFT-VR equation using Yukawa potentials and the mean-spherical approximation. Fluid Phase Equilib 2005;236(1–2):241–55. http://dx.doi.org/10.1016/j.fluid.2005.07.019.

[410] Cameretti LF, Sadowski G, Mollerup JM. Modeling of aqueous electrolyte solutions with perturbed-chain statistical associated fluid theory. Ind Eng Chem Res 2005;44:3355–62. http://dx.doi.org/10.1021/ie0488142.

[411] Zhao H, dos Ramos MC, McCabe C. Development of an equation of state for electrolyte solutions by combining the statistical associating fluid theory and the mean spherical approximation for the nonprimitive model. J Chem Phys 2007;126(24):244503. http://dx.doi.org/10.1063/1.2733673.

[412] Held C, Cameretti LF, Sadowski G. Modeling aqueous electrolyte solutions. Fluid Phase Equilib 2008;270(1–2):87–96. http://dx.doi.org/10.1016/j.fluid.2008.06.010.

[413] Held C, Sadowski G. Modeling aqueous electrolyte solutions. Part 2. Weak electrolytes. Fluid Phase Equilib 2009;279(2):141–8. http://dx.doi.org/10.1016/j.fluid.2009.02.015.

[414] Rozmus J, de Hemptinne J-C, Galindo A, Dufal S, Mougin P. Modeling of strong electrolytes with ePPC-SAFT up to high temperatures. Ind Eng Chem Res 2013;52(29):9979–94. http://dx.doi.org/10.1021/ie303527j.

[415] Schreckenberg JMA, Dufal S, Haslam AJ, Adjiman CS, Jackson G, Galindo A. Modelling of the thermodynamic and solvation properties of electrolyte solutions with the statistical associating fluid theory for potentials of variable range. Mol Phys 2014;112(17):2339–64. http://dx.doi.org/10.1080/00268976.2014.910316.

[416] Maribo-Mogensen B, Thomsen K, Kontogeorgis GM. An electrolyte CPA equation of state for mixed solvent electrolytes. AIChE J 2015;61:2933–50. http://dx.doi.org/10.1002/aic.14829.

[417] Eriksen DK, Lazarou G, Galindo A, Jackson G, Adjiman CS, Haslam AJ. Development of intermolecular potential models for electrolyte solutions using an electrolyte SAFT-VR Mie equation of state. Mol Phys 2016;114:2724–49. http://dx.doi.org/10.1080/00268976.2016.1236221.

[418] Selam MA, Economou IG, Castier M. A thermodynamic model for strong aqueous electrolytes based on the eSAFT-VR Mie equation of state. Fluid Phase Equilib 2018;47–63:464. http://dx.doi.org/10.1016/j.fluid.2018.02.018.

[419] Lampe M, Stavrou M, Schilling J, Sauer E, Gross J, Bardow A. Computer-aided molecular design in the continuous-molecular targeting framework using group-contribution PC-SAFT. Comput Chem Eng 2015;81:278–87. http://dx.doi.org/10.1016/j.compchemeng.2015.04.008.

[420] Schilling J, Lampe M, Gross J, Bardow A. One-stage approach for the integrated design of ORC processes and working fluid using PC-SAFT. In: Kravanja Z, Bogataj M, editors. 26th European symposium on computer aided process engineering (ESCAPE), PT b. Computer aided chemical engineering, 38B, Sara Burgerhartstraat 25, PO BOX 211, 1000 AE Amsterdam, Netherlands: Elsevier Science BV; 2016, p. 1335–40. http://dx.doi.org/10.1016/B978-0-444-63428-3.50227-7, 26th European Symposium on Computer Aided Process Engineering (ESCAPE), Portoroz, Slovenia, Jun 12-15, 2016.

[421] Schilling J, Tillmanns D, Lampe M, Hopp M, Gross J, Bardow A. Integrated thermo-economic design of ORC process, working fluid and equipment using PC-SAFT. In: Espuna A, Graells M, Puigjaner L, editors. 27th European symposium on computer aided process engineering (ESCAPE), PT b. Computer aided chemical engineering, 40, Sara Burgerhartstraat 25, PO Box 211, 1000 AE Amsterdam, Netherlands: Elsevier Science BV; 2017, p. 1795–800, 27th European Symposium on Computer-Aided Process Engineering (ESCAPE), Barcelona, Spain, Oct 01-05, 2017.

[422] Schilling J, Tillmanns D, Lampe M, Hopp M, Gross J, Bardow A. Integrating working fluid design into the thermo-economic design of ORC processes using PC-SAFT. In: Dossena V, Guardone A, Astolfi M, editors. 4th international seminar on ORC power systems. Energy procedia, 129, Sara Burgerhartstraat 25, PO Box 211, 1000 AE Amsterdam, Netherlands: Elsevier Science BV; 2017, p. 121–8, 4th International Seminar on Organic Rankine Cycle Power Systems (ORC), Politecnico Milano Bovisa Campus, Milano, Italy, Sep 13–15, 2017.

[423] Schilling J, Gross J, Bardow A. Integrated design of ORC process and working fluid using process flowsheeting software and PC-SAFT. In: Dossena V, Guardone A, Astolfi M, editors. 4th international seminar on ORC power systems. Energy procedia, 129, Sara Burgerhartstraat 25, PO Box 211, 1000 AE Amsterdam, Netherlands: Elsevier Science BV; 2017, p. 129–36, 4th International Seminar on Organic Rankine Cycle Power Systems (ORC), Politecnico Milano Bovisa Campus, Milano, Italy, Sep 13–15, 2017.

[424] Schilling J, Lampe M, Gross J, Bardow A. 1-stage CoMT-CAMD: An approach for integrated design of ORC process and working fluid using PC-SAFT. Chem Eng Sci 2017;159:217–30. http://dx.doi.org/10.1016/j.ces.2016.04.048.

[425] Tillmanns D, Gertig C, Schilling J, Gibelhaus A, Bau U, Lanzerath F, et al. Integrated design of ORC process and working fluid using PC-SAFT and Modelica. In: Dossena V, Guardone A, Astolfi M, editors. 4th international seminar on ORC power systems. Energy procedia, 129, Sara Burgerhartstraat 25, PO Box 211, 1000 AE Amsterdam, NetherlandS: Elsevier Science BV; 2017, p. 97–104. http://dx.doi.org/10.1016/j.egypro.2017.09.169, 4th International Seminar on ORC Power Systems (ORC), Politecnico Milano Bovisa Campus, Milano, ITALY, SEP 13-15, 2017.

[426] Schilling J, Eichler K, Pischinger S, Bardow A. Integrated design of ORC process and working fluid for transient waste-heat recovery from heavy-duty vehicles. In: Eden MR, Ierapetritou MG, Towler GP, editors. 13th international symposium on process systems engineering (PSE 2018). Computer aided chemical engineering, Vol. 44, Elsevier; 2018, p. 2443–8.

[427] Schilling J, Eichler K, Kölsch B, Pischinger S, Bardow A. Integrated design of working fluid and organic Rankine cycle utilizing transient exhaust gases of heavy-duty vehicles. Appl Energy 2019;255:e16903. http://dx.doi.org/10.1016/j.apenergy.2019.05.010.

[428] Schilling J, Horend C, Bardow A. Integrating superstructure-based design of molecules, processes and flowsheets. AIChE J 2020;66(5):e16903. http://dx.doi.org/10.1002/aic.16903.

[429] Zhang K, Chen X, Markides CN, Yang Y, Shen S. Evaluation of ejector performance for an organic Rankine cycle combined power and cooling system. Appl Energy 2016;184:404–12. http://dx.doi.org/10.1016/j.apenergy.2016.10.017.

[430] Pantaleo AM, Camporeale SM, Sorrentino A, Miliozzi A, Shah N, Markides CN. Solar/biomass hybrid cycles with thermal storage and bottoming ORC: System integration and economic analysis. In: Dossena V, Guardone A, Astolfi M, editors. 4th international seminar on ORC power systems. Energy procedia, 129, 2017, p. 724–31, 4th International Seminar on Organic Rankine Cycle Power Systems (ORC), Politecnico Milano Bovisa Campus, Milano, Italy, Sep 13–15, 2017.

[431] Pantaleo AM, Camporeale SM, Miliozzi A, Russo V, Mugnozza GS, Markides CN, et al. Thermo-economic assessment of an externally fired hybrid CSP/biomass gas turbine and organic Rankine combined cycle. In: Yan J, Sun F, Chou S, Desideri U, Li H, Campana P, Xiong R, editors. 8th international conference on applied energy (ICAE2016). Energy procedia, 105, 2017, p. 174–81, 8th International Conference on Applied Energy (ICAE), Beijing Inst Technol, Beijing, Peoples R China, Oct 08-11, 2016.

[432] Pantaleo AM, Camporeale SM, Miliozzi A, Russo V, Shah N, Markides CN. Novel hybrid CSP-biomass CHP for flexible generation: Thermo-economic analysis and profitability assessment. Appl Energy 2017;204:994–1006. http://dx.doi.org/10.1016/j.apenergy.2017.05.019, 8th International Conference on Applied Energy (ICAE), Beijing Inst Technol, Beijing, Peoples R China, Oct 08–11, 2016.

[433] Oyewunmi OA, Ferre-Serres S, Lecompte S, van den Broek M, de Paepe M, Markides CN. An assessment of subcritical and trans-critical organic Rankine cycles for waste-heat recovery. In: Yan J, Sun F, Chou S, Desideri U, Li H, Campana P, Xiong R, editors. 8th international conference on applied energy (ICAE2016). Energy procedia, 105, 2017, p. 1870–6, 8th International Conference on Applied Energy (ICAE), Beijing Inst Technol, Beijing, Peoples R China, Oct 08–11, 2016.

[434] Oyewunmi OA, Pantaleo AM, Markides CN. ORC cogeneration systems in waste-heat recovery applications. In: Yan J, Wu J, Li H, editors. Proceedings of the 9th international conference on applied energy. Energy procedia, 142, 2017, p. 1736–42, 9th International Conference on Applied Energy (ICAE), Cardiff, England, Aug 21-24, 2017.

[435] Oyewunmi OA, Lecompte S, De Paepe M, Markides CN. Thermoeconomic analysis of recuperative sub- and transcritical organic Rankine cycle systems. In: Dossena V, Guardone A, Astolfi M, editors. 4th international seminar on ORC power systems. Energy procedia, 129, 2017, p. 58–65, 4th International Seminar on ORC Power Systems (ORC), Politecnico Milano Bovisa Campus, Milano, Italy, Sep 13–15, 2017.

[436] Ramos A, Chatzopoulou MA, Freeman J, Markides CN. Optimisation of a high-efficiency solar-driven organic Rankine cycle for applications in the built environment. Appl Energy 2018;228:755–65. http://dx.doi.org/10.1016/j.apenergy.2018.06.059, 30th International Conference on Efficiency, Cost, Optimisation, Simulation and Environmental Impact of Energy Systems (ECOS), San Diego State Univ, San Diego, CA, Jul 02–06, 2017.

[437] Unamba CK, Sapin P, Li X, Song J, Wang K, Shu G, et al. Operational optimisation of a non-recuperative 1-kWe organic Rankine cycle engine prototype. Appl Sci-Basel 2019;9(15). http://dx.doi.org/10.3390/app9153024.

[438] Simpson MC, Chatzopoulou MA, Oyewunmi OA, Le Brun N, Sapin P, Markides CN. Technoeconomic analysis of internal combustion engine - organic Rankine cycle systems for combined heat and power in energy-intensive buildings. Appl Energy 2019;253. http://dx.doi.org/10.1016/j.apenergy.2019.113462.

[439] Pantaleo AM, Camporeale SM, Sorrentino A, Miliozzi A, Shah N, Markides CN. Hybrid solar-biomass combined Brayton/organic Rankine-cycle plants integrated with thermal storage: Techno-economic feasibility in selected Mediterranean areas. Renew Energy 2020;147(3):2913–31. http://dx.doi.org/10.1016/j.renene.2018.08.022, 4th International Seminar on Organic Rankine Cycle Power Systems (ORC), Politecnico Milano Bovisa Campus, Milano, Italy, Sep 13-15, 2017.

[440] Shaahmadi F, Smith SAM, Schwarz CE, Burger AJ, Cripwell JT. Group-contribution SAFT equations of state: A review. Fluid Phase Equilib 2023;565:113674. http://dx.doi.org/10.1016/j.fluid.2022.113674.

[441] Vijande J, Piñeiro MM, Bessières D, Saint-Guirons H, Legido JL. Description of PVT behaviour of hydrofluoroethers using the PC-SAFT eos. Phys Chem Chem Phys 2004;6(4):766–70. http://dx.doi.org/10.1007/978-3-319-26362-5_26.

[442] Thi TXN, Tamouza S, Tobaly P, Passarello JP, de Hemptinne JC. Application of group contribution SAFT equation of state (GC-SAFT) to model phase behaviour of light and heavy esters. Fluid Phase Equilib 2005;238:254. http://dx.doi.org/10.1016/j.fluid.2005.10.009.

[443] Nguyen-Huynh D, de Hemptinne JC, Lugo R, Passarello JP, Tobaly P. Modeling liquid–liquid and liquid–vapor equilibria of binary systems containing water with an alkane, an aromatic hydrocarbon, an alcohol or a gas (methane, ethane, CO_2, or H_2S), using group contribution polar perturbed-chain statistical associating fluid theory. Ind Eng Chem Res 2011;50(12):7467–83. http://dx.doi.org/10.1021/ie102045g.

[444] Paduszyński K, Domańska U. Heterosegmented perturbed-chain statistical associating fluid theory as a robust and accurate tool for modeling of various alkanes. 1. Pure fluids. Ind Eng Chem Res 2012;51:12967–83. http://dx.doi.org/10.1021/ie301998j.

[445] Sauer E, Stavrou M, Gross J. Comparison between a homo-and a heterosegmented group contribution approach based on the perturbed-chain polar statistical associating fluid theory equation of state. Ind Eng Chem Res 2014;53(38):14854–64. http://dx.doi.org/10.1021/ie502203w.

[446] dos Ramos MC, Haley JD, Westwood JR, McCabe C. Extending the GC-SAFT-VR approach to associating functional groups: Alcohols, aldehydes, amines and carboxylic acids. Fluid Phase Equilib 2011;306:97–111. http://dx.doi.org/10.1016/j.fluid.2011.03.026.

[447] White MT, Oyewunmi OA, Haslam AJ, Markides CN. Industrial waste-heat recovery through integrated computer-aided working-fluid and ORC system optimisation using SAFT-γ Mie. Energy Convers Manage 2017;150:851–69. http://dx.doi.org/10.1016/j.enconman.2017.03.048.

[448] White MT, Oyewunmi OA, Chatzopoulou MA, Pantaleo AM, Haslam AJ, Markides CN. Integrated computer-aided working-fluid design and thermoeconomic ORC system optimisation. In: Dossena V, Guardone A, Astolfi M, editors. 4th international seminar on ORC power systems. Energy procedia, Vol. 129, 2017, p. 152–9.

[449] Harraz AA, Freeman J, Wang K, Mac Dowell N, Markides CN. Diffusion-absorption refrigeration cycle simulations in gPROMS using SAFT-γ Mie. Energy Procedia 2019;158:2360–5. http://dx.doi.org/10.1016/j.egypro.2019.01.284.

[450] Bowskill D, Tropp UE, Gopinath S, Jackson G, Galindo A, Adjiman CS. Beyond a heuristic analysis: integration of process and working-fluid design for organic Rankine cycles. Mol Syst Des Eng 2020;5:493–510. http://dx.doi.org/10.1039/c9me00089e.

[451] Harraz AA, Haslam AJ, Najjaran A, Mac Dowell N, Markides CN. An integrated computer-aided molecular design framework for a diffusion-absorption refrigeration system. Energy Convers Manag 2024. http://dx.doi.org/10.1016/s1474-6670(17)67325-7, in preparation, to be submitted 2024.

[452] Rehner P, Schilling J, Bardow A. Molecule superstructures for computer-aided molecular and process design. Mol Syst Des Eng 2023;8:488–99. http://dx.doi.org/10.1039/D2ME00230B.

[453] Rehner P, Bardow A, Gross J. Modeling mixtures with PCP-SAFT: Insights from large-scale parametrization and group-contribution method for binary interaction parameters. Int J Thermophys 2023;44(12):179. http://dx.doi.org/10.1007/s10765-023-03290-3.

[454] Chaparro G, Müller EA. Development of thermodynamically consistent machine-learning equations of state: Application to the Mie fluid. J Chem Phys 2023;158(18):184505. http://dx.doi.org/10.1063/5.0146634.

[455] Biswas S, Chung Y, Ramirez J, Wu H, Green WH. J Chem Inf Model 2023;63(15):4574–88. http://dx.doi.org/10.1021/acs.jcim.3c00546.

[456] Matsukawa H, Kitahara M, Otake K. Estimation of pure component parameters of PC-SAFT EoS by an artificial neural network based on a group contribution method. Fluid Phase Equilib 2021;548:113179. http://dx.doi.org/10.1016/j.fluid.2021.113179.

[457] Habicht J, Brandenbusch C, Sadowski G. Predicting PC-SAFT pure-component parameters by machine learning using a molecular fingerprint as key input. Fluid Phase Equilib 2023;565:113657. http://dx.doi.org/10.1016/j.fluid.2022.113657.

[458] Felton KC, Raßpe-Lange L, Rittig JG, Leonhard K, Mitsos A, Meyer-Kirschner J, et al. ML-SAFT: a machine learning framework for PCP-SAFT parameter prediction. Chem Eng J 2024;151999. http://dx.doi.org/10.1016/j.cej.2024.151999.

[459] Winter B, Rehner P, Esper T, Schilling J, Bardow A. Understanding the language of molecules: Predicting pure component parameters for the PC-SAFT equation of state from SMILES. 2023, http://dx.doi.org/10.1021/ie034258k, arXiv preprint arXiv:2309.12404.

[460] Sastri S, Rao K. A new temperature–thermal conductivity relationship for predicting saturated liquid thermal conductivity. Chem Eng J 1999;74(3):161–9. http://dx.doi.org/10.1016/s1385-8947(99)00046-7.

[461] Chung TH, Lee LL, Starling KE. Applications of kinetic gas theories and multiparameter correlation for prediction of dilute gas viscosity and thermal conductivity. Ind Eng Chem Fundam 1984;23(1):8–13. http://dx.doi.org/10.1021/i100013a002.

[462] Quiñones-Cisneros SE, Zéberg-Mikkelsen CK, Stenby EH. The friction theory (f-theory) for viscosity modeling. Fluid Phase Equilib 2000;169(2):249–76. http://dx.doi.org/10.1016/s0378-3812(00)00310-1.

[463] Allal A, Boned C, Baylaucq A. Free-volume viscosity model for fluids in the dense and gaseous states. Phys Rev E 2001;64(1):011203. http://dx.doi.org/10.1103/physreve.64.011203.

[464] Rosenfeld Y. Relation between the transport coefficients and the internal entropy of simple systems. Phys Rev A 1977;15(6):2545. http://dx.doi.org/10.1103/physreva.15.2545.

[465] Rosenfeld Y. A quasi-universal scaling law for atomic transport in simple fluids. J Phys: Condens Matter 1999;11(28):5415. http://dx.doi.org/10.1051/jp4:2000517.

[466] Novak L. Self-diffusion coefficient and viscosity in fluids. Int J Chem React Eng 2011;9(1). http://dx.doi.org/10.1515/1542-6580.2640.

[467] Novak LT. Fluid viscosity-residual entropy correlation. Int J Chem React Eng 2011;9(1). http://dx.doi.org/10.2202/1542-6580.2839.

[468] Novak LT. Predicting natural gas viscosity with a mixture viscosity model for the entire fluid region. Ind Eng Chem Res 2013;52(45):16014–8. http://dx.doi.org/10.1021/ie402245e.

[469] Novak LT. Predictive corresponding-states viscosity model for the entire fluid region: n-alkanes. Ind Eng Chem Res 2013;52(20):6841–7. http://dx.doi.org/10.1021/ie400654p.

[470] Novak LT. Predicting fluid viscosity of nonassociating molecules. Ind Eng Chem Res 2015;54(21):5830–5. http://dx.doi.org/10.1021/acs.iecr.5b01526.

[471] Lötgering-Lin O, Gross J. Group contribution method for viscosities based on entropy scaling using the perturbed-chain polar statistical associating fluid theory. Ind Eng Chem Res 2015;54(32):7942–52. http://dx.doi.org/10.1021/acs.iecr.5b01698.

[472] Lötgering-Lin O, Fischer M, Hopp M, Gross J. Pure substance and mixture viscosities based on entropy scaling and an analytic equation of state. Ind Eng Chem Res 2018;57(11):4095–114. http://dx.doi.org/10.1021/acs.iecr.7b04871.

[473] Hopp M, Gross J. Thermal conductivity of real substances from excess entropy scaling using PCP-SAFT. Ind Eng Chem Res 2017;56(15):4527–38. http://dx.doi.org/10.1021/acs.iecr.6b04289.s001.

[474] Hopp M, Mele J, Gross J. Self-diffusion coefficients from entropy scaling using the PCP-SAFT equation of state. Ind Eng Chem Res 2018;57(38):12942–50. http://dx.doi.org/10.1021/acs.iecr.8b02406.

[475] Hopp M, Gross J. Thermal conductivity from entropy scaling: A group-contribution method. Ind Eng Chem Res 2019;58(44):20441–9. http://dx.doi.org/10.1021/acs.iecr.9b04289.

[476] Zmpitas J, Gross J. Modified Stokes–Einstein equation for molecular self-diffusion based on entropy scaling. Ind Eng Chem Res 2021;60(11):4453–9. http://dx.doi.org/10.1021/acs.iecr.0c06090.

[477] Bell IH, Messerly R, Thol M, Costigliola L, Dyre JC. Modified entropy scaling of the transport properties of the Lennard-Jones fluid. J Phys Chem B 2019;123:6345–63. http://dx.doi.org/10.1021/acs.jpcb.9b05808.

[478] Bell IH. Probing the link between residual entropy and viscosity of molecular fluids and model potentials. Proc Natl Acad Sci 2019;116(10):4070–9. http://dx.doi.org/10.1073/pnas.1815943116.

[479] Bell IH, Dyre JC, Ingebrigtsen TS. Excess-entropy scaling in supercooled binary mixtures. Nat Commun 2020;11:4300. http://dx.doi.org/10.1038/s41467-020-17948-1.

[480] Bell IH, Hellmann R, Harvey AH. Zero-density limit of the residual entropy scaling of transport properties. J Chem Eng Data 2020;65(3):1038–50. http://dx.doi.org/10.1021/acs.jced.9b00455.

[481] Bell IH. Entropy scaling of viscosity–I: A case study of propane. J Chem Eng Data 2020;65:3203–15. http://dx.doi.org/10.1021/acs.jced.0c00209.

[482] Bell IH. Entropy scaling of viscosity–II: Predictive scheme for normal alkanes. J Chem Eng Data 2020;65(11):5606–16. http://dx.doi.org/10.1021/acs.jced.0c00749.

[483] Yang X, Xiao X, May EF, Bell IH. Entropy scaling of viscosity–III: Application to refrigerants and their mixtures. J Chem Eng Data 2021;66(3):1385–98. http://dx.doi.org/10.1021/acs.jced.0c01009.

[484] Yang X, Xiao X, Thol M, Richter M, Bell IH. Linking viscosity to equations of state using residual entropy scaling theory. Int J Thermophys 2022;43:183. http://dx.doi.org/10.1007/s10765-022-03096-9.

[485] Dortmund Data Bank, 2015, www.ddbst.com.

[486] Liu X, Vlugt TJ, Bardow A. Predictive Darken equation for Maxwell-Stefan diffusivities in multicomponent mixtures. Ind Eng Chem Res 2011;50(17):10350–8. http://dx.doi.org/10.1021/ie201008a.

[487] Essa GA, Mohamed AA. Selection of optimal fluid for refrigeration cycles. World J Adv Eng Technol Sci 2020;01(02):021–36. http://dx.doi.org/10.30574/wjaets.2020.1.2.0031.

[488] Su W, Zhao L, Deng S. Simultaneous working fluids design and cycle optimization for organic Rankine cycle using group contribution model. Appl Energy 2017;202:618–27. http://dx.doi.org/10.1016/j.apenergy.2017.03.133.

[489] Kondo S, Urano Y, Tokuhashi K, Takahashi A, Tanaka K. Prediction of flammability of gases by using F-number analysis. J Hard Mater 2001;82(2):113–28. http://dx.doi.org/10.1016/S0304-3894(00)00358-7.

[490] Albahri TA. Flammability characteristics of pure hydrocarbons. Chem Eng Sci 2003;58(16):3629–41. http://dx.doi.org/10.1016/S0009-2509(03)00251-3.

[491] Catoire L, Naudet V. Estimation of temperature-dependent lower flammability limit of pure organic compounds in air at atmospheric pressure. 24, 2005, p. 130–7. http://dx.doi.org/10.1002/prs.10072.

[492] Gharagheizi F. A new group contribution-based model for estimation of lower flammability limit of pure compounds. J Hard Mater 2009;170(2–3):595–604. http://dx.doi.org/10.1016/j.jhazmat.2009.05.023.

[493] S. NJ, Skaggs SR. Estimating tropospheric lifetimes and ozone-depletion potentials of one- and two-carbon hydrofluorocarbons and hydrochlorofluorocarbons. Environ Sci Technol 1992;26(4):739–44. http://dx.doi.org/10.1021/es00028a011.

[494] Duvedi AP, Achenie LEK. Designing environmentally safe refrigerants using mathematical programming. Chem Eng Sci 1996;51(15):3727–39. http://dx.doi.org/10.1016/0009-2509(96)00224-2.

[495] Al R, Frutiger A, Zubov A, Sin G. Prediction of environmental properties using a hybrid group contribution approach. Comput Aided Chem Eng 2018;44:1723–8. http://dx.doi.org/10.1016/B978-0-444-64241-7.50282-2.

[496] An Q-S, Ma Y-T, Tian H. Discussion of refrigerant GWP calculation based on group contribution method. Kung Cheng Je Wu Li Hsueh Pao/J Eng Thermophys 2008;29(11):1826–30.

[497] Devotta S, Chelani A, Vonsild A. Prediction of global warming potentials of refrigerants and related compounds from their molecular structure – An artificial neural network with group contribution method. Int J Refrig 2021;131:756–65. http://dx.doi.org/10.1016/j.ijrefrig.2021.08.011.

[498] Zhang X, Kobayashi N, He M, Wang J. Radiative efficiency estimation of organic substance based on group contribution method. Energy Proc 2014;61:492–5. http://dx.doi.org/10.1016/j.egypro.2014.11.1156.

[499] Zhang X, Kobayashi N, He M, Wang J. An organic group contribution approach to radiative efficiency estimation of organic working fluid. Appl Energy 2016;162:1205–10. http://dx.doi.org/10.1016/j.apenergy.2015.08.032.

[500] Wernet G, Papadokonstantakis S, Hellweg S, Hungerbühler K. Bridging data gaps in environmental assessments: Modeling impacts of fine and basic chemical production. Green Chem 2009;11(11):1826–31. http://dx.doi.org/10.1039/B905558D.

[501] Baxevanidis P, Papadokonstantakis S, Kokossis A, Marcoulaki E. Group contribution-based LCA models to enable screening for environmentally benign novel chemicals in CAMD applications. AIChE J 2022;68(3):e17544. http://dx.doi.org/10.1002/aic.17544.

[502] Kleinekorte J, Kleppich J, Fleitmann L, Beckert V, Blodau L, Bardow A. Appropriate life cycle assessment: A process-specific, predictive impact assessment method for emerging chemical processes. ACS Sustain Chem Eng 2023;11(25):9303–19. http://dx.doi.org/10.1021/acssuschemeng.2c07682.

[503] Kleinekorte J, Kröger L, Leonhard K, Bardow A. A neural network-based framework to predict process-specific environmental impacts. In: Kiss A, Zondervan E, Lakerveld R, Özkan L, editors. 29th European symposium on computer aided process engineering. Computer aided chemical engineering, vol. 46, Elsevier; 2019, p. 1447–52. http://dx.doi.org/10.1016/B978-0-12-818634-3.50242-3.

[504] Scheffczyk J, Schäfer P, Fleitmann L, Thien J, Redepenning C, Leonhard K, et al. COSMO-campd: a framework for integrated design of molecules and processes based on COSMO-RS. Mol Syst Des Eng 2018;3(4):645–57. http://dx.doi.org/10.1039/C7ME00125H.

[505] Alshehri A, Tula A, You F, Gani R. Next generation pure component property estimation models: With and without machine learning techniques. AIChE J 2022;68(6):e17469. http://dx.doi.org/10.1002/aic.17469.

[506] Cao X, Gong M, Tula A, Chen X, Gani R, Venkatasubramanian V. An improved machine learning model for pure component property estimation. Engineering 2024;39:61–73. http://dx.doi.org/10.1016/j.eng.2023.08.024.

[507] Zhang D, Wang Z, Oberschelp C, Bradford E, Hellweg S. Enhanced deep-learning model for carbon footprints of chemicals. ACS Sustain Chem Eng 2024;12(7):2700–8. http://dx.doi.org/10.1021/acssuschemeng.3c07038.

[508] Gani R. Chemical product design: Challenges and opportunities. Comput Chem Eng 2004;28(12):2441–57. http://dx.doi.org/10.1016/j.compchemeng.2004.08.010.

[509] Struebing H. Identifying optimal solvents for reactions using quantum mechanics and computer-aided molecular design (Ph.D. thesis), London, UK: Department of Chemical Engineering, Imperial College London; 2011.

[510] Struebing H, Adjiman CS, Galindo A. Optimal solvent design for reactions using computer-aided molecular design. 2011, http://www.minlp.org/library/problem/mod/index.php?lib=MINLP&i=180&pi=-137, (accessed on November 09, 2015).

[511] Balas E, Jeroslow R. Canonical cuts on the unit hypercube. SIAM J Appl Math 1972;23(1):61–9. http://dx.doi.org/10.1137/0123007.

[512] Fazlollahi S, Mandel P, Becker G, Maréchal F. Methods for multi-objective investment and operating optimization of complex energy systems. Energy 2012;45(1):12–22. http://dx.doi.org/10.1016/j.energy.2012.02.046.

[513] Fink T, Bruggesser H, Reymond J. Virtual exploration of the small-molecule chemical universe below 160 Daltons. Angew Chem Int Ed 2005;44(10):1504–8. http://dx.doi.org/10.1002/anie.200462457.

[514] Andrés-Martínez O, Flores-Tlacuahuac A. Optimal molecular design of low-temperature organic fluids under uncertain conditions. Ind Eng Chem Res 2018;57(14):5058–69. http://dx.doi.org/10.1021/acs.iecr.8b00302.

[515] Kossack S, Kraemer K, Gani R, Marquardt W. A systematic synthesis framework for extractive distillation processes. Chem Eng Res Des 2008;86(7):781–92. http://dx.doi.org/10.1016/j.cherd.2008.01.008.

[516] Roskosch D, Atakan B. Reverse engineering of fluid selection for thermodynamic cycles with cubic equations of state, using a compression heat pump as example. Energy 2015;81:202–12. http://dx.doi.org/10.1016/j.energy.2014.12.025.

[517] Roskosch D, Atakan B. Reverse engineering of fluid selection for ORCs using cubic equations of state. In: Lemort V, Quoilin S, Paepe MD, van den Broek M, editors. proceedings of the 3rd international seminar on ORC power systems ASME-ORC 2015. Vol. 3, 2015, p. 570–9.

[518] Cignitti S, Andreasen JG, Haglind F, Woodley JM, Abildskov J. Integrated working fluid-thermodynamic cycle design of organic Rankine cycle power systems for waste heat recovery. Appl Energy 2017;203:442–53. http://dx.doi.org/10.1016/j.apenergy.2017.06.031.

[519] Frutiger J, Cignitti S, Abildskov J, Woodley JM, Sin G. Computer-aided molecular product-process design under property uncertainties–A Monte Carlo based optimization strategy. Comput Chem Eng 2019;122:247–57. http://dx.doi.org/10.1016/j.compchemeng.2018.08.021.

[520] Stavrou M, Hoeller J, Seidel T, Mairhofer J, Asprion N. Simultaneous optimization of process design and solvent in a flowsheet simulator. Chem Ing Tech 2023;95(3):391–404. http://dx.doi.org/10.1002/cite.202200100.

[521] Neumaier L, Roskosch D, Schilling J, Bauer G, Gross J, Bardow A. Refrigerant selection for heat pumps: The compressor makes the difference. Energy Technol 2023;11(4):2201403. http://dx.doi.org/10.1002/ente.202201403.

[522] Mayer F, Spiekermann L, Neumaier L, Rehner P, Seiler J, Schilling J, et al. Computer-aided molecular refrigerant design for adsorption chillers based on classical density functional theory and PC-SAFT. Comput Chem Eng 2024;108629. http://dx.doi.org/10.1016/j.compchemeng.2024.108629.

[523] Wang E, Mao J, Zhang B, Wang Y. On the CAMD method based on PC-SAFT for working fluid design of a high-temperature organic Rankine cycle. Energy 2022;125935. http://dx.doi.org/10.1016/j.energy.2022.125935.

[524] White MT, Sayma AI. Simultaneous cycle optimization and fluid selection for ORC systems accounting for the effect of the operating conditions on turbine efficiency. Front Energy Res 2019;7:50. http://dx.doi.org/10.3389/fenrg.2019.00050.

[525] Lemmens S. A perspective on costs and cost estimation techniques for Organic Rankine Cycle systems. In: Lemort V, Quoilin S, Paepe MD, van den Broek M, editors. proceedings of the 3rd international seminar on ORC power systems ASME-ORC 2015. Vol. 3, 2015, p. 181–90.

[526] Tillmanns D, Pell D, Schilling J, Bardow A. The thermo-economic potential of ORC-based pumped-thermal electricity storage: Insights from the integrated design of processes and working fluids. Energy Technol 2022;10:2200182. http://dx.doi.org/10.1002/ente.202200182.

[527] Xu B, Rathod D, Yebi A, Filipi Z, Onori S, Hoffman M. A comprehensive review of organic Rankine cycle waste heat recovery systems in heavy-duty diesel engine applications. Renew Sust Energy Rev 2019;107:145–70. http://dx.doi.org/10.1016/j.rser.2019.03.012.

[528] Teichgraeber H, Brandt AR. Time-series aggregation for the optimization of energy systems: Goals, challenges, approaches, and opportunities. Renew Sust Energy Rev 2022;157:111984. http://dx.doi.org/10.1016/j.rser.2021.111984.

[529] Quoilin S, van Broek MD, Declaye S, Dewallef P, Lemort V. Techno-economic survey of organic Rankine cycle (ORC) systems. Renew Sust Energ Rev 2013;22:168–86. http://dx.doi.org/10.1016/j.rser.2013.01.028.

[530] Jiménez-Arreola M, Pili R, Dal Magro F, Wieland C, Rajoo S, Romagnoli A. Thermal power fluctuations in waste heat to power systems: An overview on the challenges and current solutions. Appl Therm Eng 2018;134:576–84. http://dx.doi.org/10.1016/j.applthermaleng.2018.02.033, URL https://www.sciencedirect.com/science/article/pii/S1359431117370710.

[531] Fritzson P. Modelica—A language for equation-based physical modeling and high performance simulation. In: International workshop on applied parallel computing. Springer; 1998, p. 149–60.

[532] Leineweber DB, Schäfer A, Bock HG, Schlöder JP. An efficient multiple shooting based reduced SQP strategy for large-scale dynamic process optimization: Part II: Software aspects and applications. Comput Chem Eng 2003;27(2):167–74. http://dx.doi.org/10.1016/S0098-1354(02)00195-3.

[533] Li Z, Yu X, Wang L, Jiang R, Yu X, Huang R, et al. Comparative investigations on dynamic characteristics of basic ORC and cascaded LTES-ORC under transient heat sources. Appl Therm Eng 2022;207:118197. http://dx.doi.org/10.1016/j.applthermaleng.2022.118197, URL https://www.sciencedirect.com/science/article/pii/S1359431122001594.

[534] Hernandez A, Desideri A, Ionescu C, De Keyser R, Lemort V, Quoilin S. Real-time optimization of organic rankine cycle systems by extremum-seeking control. Energies 2016;9(5). http://dx.doi.org/10.3390/en9050334, URL https://www.mdpi.com/1996-1073/9/5/334.

[535] Lampe MHF. Integrated design of process and working fluids for organic rankine cycles (Ph.D. thesis), Aachen, Germany: Wissenschaftsverlag Mainz GmbH, RWTH Aachen University; 2016.

[536] Rehner P, Schilling J, Bardow A. Computer-aided mixture design using molecule superstructures. In: Proceedings of the 10th international conference on foundations of computer aided process design (FOCAPD 2024). Vol. 3, PSE Press; 2024, p. 876–82. http://dx.doi.org/10.69997/sct.187490.

[537] Gertig C, Leonhard K, Bardow A. Computer-aided molecular and processes design based on quantum chemistry: current status and future prospects. Curr Opin Chem Eng 2020;27:89–97. http://dx.doi.org/10.1016/j.coche.2019.11.007.

[538] Blum C, Roli A. Metaheuristics in combinatorial optimization: Overview and conceptual comparison. ACM Comput Surv (CSUR) 2003;35(3):268–308. http://dx.doi.org/10.1007/s10479-005-3971-7.

[539] Kirkpatrick S, Gelatt Jr. CD, Vecchi MP. Optimization by simulated annealing. Science 1983;220(4598):671–80. http://dx.doi.org/10.1126/science.220.4598.671.

[540] Deb K, Pratap A, Agarwal S, Meyarivan T. A fast and elitist multiobjective genetic algorithm: NSGA-II. IEEE Trans Evol Comput 2002;6(2):182–97. http://dx.doi.org/10.1109/4235.996017.

[541] Grossmann IE, Kravanja Z. Mixed-integer nonlinear programming techniques for process systems engineering. Comput Chem Eng 1995;19:189–204. http://dx.doi.org/10.1016/0098-1354(95)00072-a.

[542] Duran MA, Grossmann IE. An outer-approximation algorithm for a class of mixed-integer nonlinear programs. Math Program 1986;36(3):307–39. http://dx.doi.org/10.1007/bf02592081.

[543] Hennen M, Postels S, Voll P, Lampe M, Bardow A. Multi-objective synthesis of energy systems: Efficient identification of design trade-offs. Comput Chem Eng 2017;97:283–93. http://dx.doi.org/10.1016/j.compchemeng.2016.10.010.

[544] Pardalos PM, Žilinskas A, Žilinskas J. Scalarization. In: Non-convex multi-objective optimization. Springer; 2017, p. 13–8.

[545] Messac A, Ismail-Yahaya A, Mattson CA. The normalized normal constraint method for generating the Pareto frontier. Struct Multidiscip Optim 2003;25:86–98. http://dx.doi.org/10.1007/s00158-002-0276-1.

[546] Haimes YY, Lasdon LS, Wismer DA. On a bicriterion formulation of the problems of integrated system identification and system optimization. IEEE Trans Syst Man Cybern Syst 1971;1(3):296–7. http://dx.doi.org/10.1109/tsmc.1971.4308298.

[547] Bortz M, Burger J, Asprion N, Blagov S, Böttcher R, Nowak U, et al. Multi-criteria optimization in chemical process design and decision support by navigation on Pareto sets. Comput Chem Eng 2014;60:354–63. http://dx.doi.org/10.1016/j.compchemeng.2013.09.015.

[548] Frutiger J, Cignitti S, Abildskov J, Woodley JM, Sin G. Computational chemical product design problems under property uncertainties. In: 27th European symposium on computer-aided process engineering. ESCAPE, Computer aided chemical engineering, Vol. 40A, AMSTERDAM: Elsevier Science Bv; 2017, p. 973–8. http://dx.doi.org/10.1016/b978-0-444-63965-3.50164-1.

[549] Groniewsky A, Wagner C. Investigation of the effect of the regenerative heat exchanger on the performance of organic Rankine cycles using perturbed chain-statistical associating fluid theory equation of state. Ind Eng Chem Res 2020;59(44):19643–56. http://dx.doi.org/10.1021/acs.iecr.0c03782.

[550] White MT, Sayma AI. A generalised assessment of working fluids and radial turbines for non-recuperated subcritical organic Rankine cycles. Energies 2018;11(4):26. http://dx.doi.org/10.3390/en11040800.

[551] Andreasen JG, Meroni A, Haglind F. A comparison of organic and steam rankine cycle power systems for waste heat recovery on large ships. Energies 2017;10(4). http://dx.doi.org/10.3390/en10040547, URL https://www.mdpi.com/1996-1073/10/4/547.

[552] Miró L, Gasia J, Cabeza LF. Thermal energy storage (TES) for industrial waste heat (IWH) recovery: A review. Appl Energy 2016;179:284–301. http://dx.doi.org/10.1016/j.apenergy.2016.06.147, URL https://www.sciencedirect.com/science/article/pii/S0306261916309357.

[553] Oluleye G, Jobson M, Smith R, Perry SJ. Evaluating the potential of process sites for waste heat recovery. Appl Energy 2016;161:627–46. http://dx.doi.org/10.1016/j.apenergy.2015.07.011, URL https://www.sciencedirect.com/science/article/pii/S0306261915008405.

[554] Hsieh J-C, Fu B-R, Wang T-W, Cheng Y, Lee Y-R, Chang J-C. Design and preliminary results of a 20-kW transcritical organic rankine cycle with a screw expander for low-grade waste heat recovery. Appl Therm Eng 2017;110:1120–7. http://dx.doi.org/10.1016/j.applthermaleng.2016.09.047, URL https://www.sciencedirect.com/science/article/pii/S135943111631643X.

[555] Hemprich C, Rehner P, Esper T, Gross J, Roskosch D, Bardow A. Modeling dipolar molecules with PCP-SAFT: A vector group-contribution method. ACS omega 2024. http://dx.doi.org/10.1021/acsomega.4c04867.

[556] Ten JY, Hassim MH, Chemmangattuvalappil N, Ng DKS. A novel chemical product design framework with the integration of safety and health aspects. J Loss Prev Process Ind 2016;40:67–80. http://dx.doi.org/10.1016/j.jlp.2015.11.027.

[557] Hukkerikar AS, Kalakul S, Sarup B, Young DM, Sin G, Gani R. Estimation of environment-related properties of chemicals for design of sustainable processes: Development of group-contribution+ (GC+) property models and uncertainty analysis. J Chem Inf Model 2012;52(11):2823–39. http://dx.doi.org/10.1021/ci300350r.

[558] Jung C, Dersch J, Nietsch A, Senholdt M. Technological perspectives of silicone heat transfer fluids for concentrated solar power. Energy Procedia 2015;69:663–71. http://dx.doi.org/10.1016/j.egypro.2015.03.076.

[559] Roetzel W, Spang B. C1 thermal design of heat exchangers. VDI Heat Atlas 2010;33. http://dx.doi.org/10.1007/978-3-540-77877-6_4.

[560] Persico G, Pini M. 8 - fluid dynamic design of organic rankine cycle turbines. In: Macchi E, Astolfi M, editors. Organic rankine cycle (ORC) power systems. Woodhead Publishing; 2017, p. 253–97.

[561] Giuffre' A, Ascione F, Servi CD, Pini M. Data driven modeling of high-speed centrifugal compressors for aircraft environmental control system. In: Proceedings of global power and propulsion society conference, chania, Greece. 2022.

[562] Astolfi M, Romano MC, Bombarda P, Macchi E. Binary ORC (organic Rankine cycles) power plants for the exploitation of medium–low temperature geothermal sources – Part B: Techno-economic optimization. Energy 2014;66:435–46. http://dx.doi.org/10.1016/j.energy.2013.11.057.

[563] Pierobon L, Casati E, Casella F, Haglind F, Colonna P. Design methodology for flexible energy conversion systems accounting for dynamic performance. Energy 2014;68:667–79. http://dx.doi.org/10.1016/j.energy.2014.03.010, URL https://www.sciencedirect.com/science/article/pii/S0360544214002631.

[564] Bongartz D, Najman J, Sass S, Mitsos A. MAiNGO: McCormick based algorithm for mixed integer nonlinear global optimization. Tech. rep., Process Systems Engineering (AVT.SVT), RWTH Aachen University; 2018, p. 1–7, URL http://permalink.avt.rwth-aachen.de/?id=729717.

[565] Bongartz D, Mitsos A. Deterministic global flowsheet optimization: Between equation-oriented and sequential-modular methods. AIChE J 2019;65(3):1022–34. http://dx.doi.org/10.1002/aic.16507.

[566] Schweidtmann AM, Mitsos A. Deterministic global optimization with artificial neural networks embedded. J Optim Theory Appl 2019;180(3):925–48. http://dx.doi.org/10.1007/s10957-018-1396-0.

[567] Romeo LM, Lara Y, González A. Reducing energy penalties in carbon capture with organic Rankine cycles. Appl Therm Eng 2011;31(14):2928–35. http://dx.doi.org/10.1016/j.applthermaleng.2011.05.022, URL https://www.sciencedirect.com/science/article/pii/S1359431111002742.

[568] DiGenova KJ, Botros BB, Brisson J. Method for customizing an organic Rankine cycle to a complex heat source for efficient energy conversion, demonstrated on a Fischer Tropsch plant. Appl Energy 2013;102:746–54. http://dx.doi.org/10.1016/j.apenergy.2012.08.029, URL https://www.sciencedirect.com/science/article/pii/S0306261912006034, Special Issue on Advances in sustainable biofuel production and use - XIX International Symposium on Alcohol Fuels - ISAF.

[569] Lasdon LS, Waren AD, Jain A, Ratner M. Design and testing of a generalized reduced gradient code for nonlinear programming. ACM Trans Math Softw 1978;4(1):34–50. http://dx.doi.org/10.1145/355769.355773.

Christos N. Markides, B.A., M.Eng., M.A., Ph.D.
Contact details:
- Email: c.markides@imperial.ac.uk
- Web: www.imperial.ac.uk/people/c.markides & www.imperial.ac.uk/cep
Expertise:
Professor Markides' interests lie in fundamental aspects of thermodynamics, fluid flow, heat/mass transfer processes, and their applications to a range of components, devices, technologies and systems for energy recovery, conversion and storage, in particular for solarenergy and waste-heat conversion. His research covers theoretical, experimental and modelling approaches and the full range of scales from molecules to systems.

Professor Markides has been active in ORC research, both experimentally and computationally, for about 15 years, and in the development and application of statistical associating fluid theory (SAFT), including variable range and group contribution approaches, to ORC systems since 2012. Recent highlights include leading as primary investigator a £1.6M, 5-year research programme funded by the UK Engineering & Physical Sciences Research Council (EPSRC) on CAMD of ORC systems since 2016, and a more recent grant on the application of similar methods to heat pumps.

He has been sole author of review articles on ORC technology in waste-heat recovery as well as distributed solar applications, has given >30 plenary or keynote talks on related topics, and assisted as scientific or organising committee member in >20 conferences and other events on ORC technology and SAFT-based CAMD methods. He also won the Best Paper Award at the 4th International Seminar on Organic Rankine Cycle Power Systems (ORC 2017).

Dr.-Ing. André Bardow
Contact details:
- Email:
abardow@ethz.ch
- Web: https://epse.ethz.ch/the-group/people/bardow-andre & https://epse.ethz.ch
Expertise:
Professor Bardow's research focuses on the design of sustainable energy and chemical process systems by integrating energy systems engineering, adsorption-based systems, physical property measurements, and CAMD approaches combined with life cycle assessment.

Specifically in relation to the topic of this review paper, Professor Bardow has been working on integrating workingfluid selection and design into process design. Jointly with the group of Professor Groß, a framework for the integrated design has been developed based on the PC-SAFT equation of state. The framework allows the integrated design of fluid, process, equipment, and flowsheet configuration based on techno-economic objectives. The work has been recognised by several awards such as, e.g., the Recent Innovative Contribution Award 2019 of the Working Party for Computer-Aided Process Engineering of European Federation of Chemical Engineering (EFCE), PSE Model-Based Innovation (MBI) Prize 2018 by Process Systems Enterprise, and Professor Angelino Award at the 4th International Seminar on Organic Rankine Cycle Power Systems (ORC 2017).

Dr. Ir. Michel De Paepe
Contact details:
- Email: michel.depaepe@ugent.be
- Web: https://biblio.ugent.be/person/801001009059
Expertise:
Professor De Paepe's research focuses on developing energy efficient systems and contributing to the formulation of technical solutions for the reduction of CO2 emissions in compliance with the 20-20-20 directive of the European Union and the 2030 framework for climate and energy policies. He graduated with a Master of Science in ElectroMechanical Engineering from Ghent University in 1995. In 1999, he obtained a Ph.D. in Electro-Mechanical Engineering at Ghent University, with a thesis on 'Steam Injected Gas Turbines with Water Recovery'. For his master's thesis and his Ph.D. dissertation he received the WEL Energy prize. In 2005, he spent 3 months as a Visiting Professor at the University of Pretoria (South Africa), researching flow regime detection.

Professor De Paepe is currently Head of the Applied Thermodynamics and Heat Transfer (ATHT) research group at the Faculty of Engineering and Architecture of Ghent University. The research in this group focuses on: thermodynamics of new energy systems, performance of HVAC systems and energy in buildings and complex heat transfer phenomena in industrial applications, design of compact heat exchangers, combustion engines, refrigerant two-phase flow and electronics cooling. Since 2014, he has been a member of the Eurotherm Committee which aims to promote and foster European cooperation in thermal sciences and heat transfer by fostering collaboration between scientists and engineers working in specialised areas; he received the Prix Burnay from ATIC in 2015. Professor De Paepe is (co)author of 100 papers published in international peer reviewed journals and more than 280 conference papers.

Dr. Carlo De Servi, Dr.-Ing.
Contact details:
- Email: c.m.deservi@tudelft.nl
- Web: https://www.tudelft.nl/staff/c.m.deservi/?cHash=be4d915baab9a74c22f64c0239203af7
Expertise:
Dr. Carlo De Servi is a senior researcher at the Technical University of Delft, and VITO, a Belgian research and technology organisation in the areas of cleantech and sustainable development. He graduated in Mechanical Engineering at Politecnico di Milano in 2008. In 2009, he started working as a research engineer at the Energy Department of the same institution, where he earned his Ph.D. in 2014. Afterwards, he further specialised in the Propulsion & Power group of TU Delft, becoming an expert in energy system analysis and design. His professional experience revolves around energy conversion technologies, in particular on organic Rankine cycles turbogenerators, as well as modelling and simulation techniques for the same systems. In the last years, he also started investigating new CFD-based design methods for compact heat exchangers, and novel propulsion system concepts for future zero-emission aircraft.

Specifically, concerning this review paper, Dr. De Servi has been working on methods for preliminary design of ORC systems and optimal working-fluid selection.

Dr.-Ing. Joachim
Contact details:
- Email: gross@itt.uni-stuttgart.de
- Web: www.itt.uni-stuttgart.de
Expertise:
Professor Gross's research focus is on molecular thermodynamics. Together with his team he proposes methods and models for predicting physical properties of mixtures, with emphasis on fluid mixtures. His research covers static bulk fluid phases and phase equilibria using analytic models, such as the perturbed-chain statistical associating fluid theory (PC-SAFT), developed together with Professor Sadowski. Predictive models for dynamic properties, such as shear viscosity, thermal conductivity and diffusion coefficients, were recently developed based on the entropy scaling principle. A significant emphasis is also placed on interfacial properties, where predictive models from classical density functional theory (DFT) were developed in his group, and applied to various applications, such as fluid–liquid interfaces, adsorption phenomena, contact angles, but also the coupling of DFT with continuum models from fluid mechanics.

With regard to this review paper, he worked on integrated design of fluids and processes, in long-term cooperation with Professor Bardow and his group (CoMT-CAMD). Predictive thermodynamic models, including transport properties, are a prerequisite for conducting meaningful optimisations of fluids and processes. He thereby considered both applications in separation technology and in power cycles, mainly the organic Rankine cycle (ORC).

Dr. Andrew J. Haslam
Contact details:
- Email: a.haslam@imperial.ac.uk
- Web: www.imperial.ac.uk/people/a.haslam
Expertise:
Dr. Haslam's principal research interests reflect his background in statistical mechanics and thermodynamics, and can be summed up as investigating how fundamental understanding of physics at the molecular level can be applied to tackle real-life engineering problems. He is a member of the Molecular Systems Engineering (MSE) research group and the Clean Energy Processes (CEP) Laboratory in the Department of Chemical Engineering. The MSE group has an interest in the intelligent molecular design of materials for engineering applications. The research combines a fundamental physical understanding, mathematical models and numerical methods into new techniques and tools for the design of better products and processes. The emphasis is on integration of models across different scales so that

molecular-level models can be used at the larger scale of products and processes.

His role in the CEP Laboratory follows the same philosophy, applied in the context of the working fluids utilised in a wide range of heat engines and refrigerators, and primarily, ORC systems. He has a track record in research and publications relating to statistical associating fluid theory (SAFT) methods as applied to the computer-aided molecular design of working fluids and ORC systems.

Dr. Steven Lecompte
Contact details:
- Email: steven.lecompte@ugent.be
- Web: https://telefoonboek.ugent.be/en/people/802001235875
Expertise:
Dr. Steven Lecompte is an Assistant Professor at the Department of Electrical Energy, Metals, Mechanical Construction and Systems, Ghent University, Belgium. His research focuses on thermal machines, including thermo-economic optimisation, multiphase processes, expanders and compressors. His work is mainly oriented towards experimental research with almost a decade of experience in organic Rankine cycle (ORC) technology. Recent research projects include the H2020 EU projects CHESTER and RES4LIVE. Between 2016 and 2018 he was a visiting researcher at Imperial College London for in total 5 months doing research on multiphase flows. Steven Lecompte is chair of the Knowledge Center on Organic Rankine Cycle Technology (KCORC) editorial board. He is the author or co-author of more than 70 scholarly articles and conference papers on ORC systems, including review papers on ORC technology and its applications. Publication record.

Dr. Athanasios I. Papadopoulos
Contact details:
- Email: spapadopoulos@certh.gr
- Web: https://psdi.cperi.certh.gr/~spapadopoulos
Expertise:
Dr. Papadopoulos' research interests are in the areas of process and renewable energy systems synthesis, integration and optimisation as well as integrated product and process design for applications in chemical, hybrid renewable power generation systems and heat-to-power or heat-to-cooling transformation and co-generation systems. In the area of organic Rankine cycles (ORC) he has been the first to propose (jointly with P. Linke and P. Seferlis) innovative methods for both molecular and mixture design using optimisation-based computer-aided molecular design (CAMD) approaches. The novel working fluids proposed in his work have been verified repeatedly by third-party research results. Recently, he filed a patent application with the US Patent Office for novel working fluid mixtures in heat-to-cooling systems.

Dr. Papadopoulos was the first recipient of the prestigious Professor Angelino award in the field of ORCs (jointly with P. Linke and P. Seferlis), and was also awarded the prestigious John. S. Latsis public benefit foundation research grant for work in ORCs. He has also received the Collin McGreavy award from the Institute of Chemical Engineers (UK), a highly competitive advanced fellowship from the Institute of State Scholarships Foundation (GR), as well as best paper (Energies) and front cover awards (Green Chemistry) for work in ORCs and CAMD.

Oyeniyi A. Oyewunmi
Contact details:
- Email: o.oyewunmi@imperial.ac.uk
- Web: www.imperial.ac.uk/people/oyeniyi.oyewunmi12
Expertise:
Dr. Oyewunmi's research interests reflect the application of the principles of thermodynamics, heat transfer, economics and process systems engineering to the design and operations of renewable and non-conventional energy and power systems. He focuses on the following topics: optimal system design of non-conventional and renewable power

and cooling technologies; economic and life cycle analysis of current and emerging energy technologies; computer-aided molecular and process design of organic Rankine cycle systems and other waste-heat recovery technologies; dynamic behaviour and operational control of energy systems; and transport processes of multiphase flow in energy systems. He has been active in organic Rankine cycle (ORC) research for over 5 years, including the application of the statistical associating fluid theory (SAFT) to working fluid and ORC system design. He has authored over 50 original research articles on ORC systems for waste-heat recovery and/or combined heat and power (CHP) applications in peer-reviewed journal publications and conference proceedings. He currently serves as a certified subject reviewer for over 10 journals including Applied Energy, Applied Thermal Engineering, Energies, Energy, Energy Conversion and Management, and a guest editor on a special issue of Sustainability.

Panos Seferlis
Contact details:
- Email: seferlis@auth.gr
- Web: https://users.auth.gr/seferlis
Expertise:
Professor Seferlis' interests lie in process systems engineering with particular emphasis in the modelling, design, optimisation and control of complex process, and energy conversion systems. Gas–liquid and liquid–liquid physical separation and reactive separation, reaction process systems, renewable energy systems with storage, smart grids cover a large range of applications with contributions in the systematic selection of solvent and working media, modelling for accurate but compact representation of physical and chemical phenomena, optimal design and interactions with control system and achieved dynamic performance.

Specifically, in relation to this review paper, he has been active in organic Rankine cycle (ORC) research through the involvement in working-fluid mixture selection, the optimal design and the investigation of the working-fluid interactions with the control system performance. He has been involved in several projects at the European and national level utilising CAMD for energy conversion and separation systems such as CO2 capture exceeding €1.2M in the last 4 years. During the last 5 years, he has co-authored several articles including review articles in CAMD technology in separation and energy conversion systems, including ORC systems.

Dr.-Ing. Johannes Schilling
Contact details:
- Email: jschilling@ethz.ch
- Web: https://epse.ethz.ch/the-group/people/schilling-johannes & https://epse.ethz.ch
Expertise:
Dr. Schilling has a research interest in the integrated design of processes and molecules in energy and chemical engineering, exploring links between predictive thermodynamics, process modelling, and optimisation in an integrated design framework with a high level of integration.

Specifically in relation to this review paper, Dr. Schilling has been working on the computer-aided design of ORC systems using SAFT-based thermodynamic models for equilibrium and transport properties for over six years. In his research, he gained broad experience in integrating the ORC equipment sizing, e.g., for heat exchangers or turbines, superstructure-based design, and pure working fluid as well as mixture design into ORC process optimisation. The work has been recognised by several scientific awards and appreciated in research communities for ORC technology, thermodynamics, and computer-aided process engineering.

Over the last six years, he has published several journal papers on the integrated design of ORC systems and participates in 14 conferences on ORC technology and computer-aided process design.

Patrick Linke
Contact details:
- Email: patrick.linke@tamu.edu
- Web: https://engineering.tamu.edu/chemical/profiles/linke-patrick
Expertise:

Professor Linke is a process systems engineer and his on-going activities focus on the design of efficient processes, integrated systems and associated infrastructures. He currently leads research into innovating process designs with a focus on methods to support in silico screening and process synthesis, the efficient use of energy and materials in industrial clusters and the synthesis of novel materials for heat-to-power conversion devices, systems and applications.

Professor Linke has been active in organic Rankine cycle (ORC) research, both experimentally and computationally, for >15 years, and in the development and application of computer-aided product and process design or CAM(P)D approaches for >20 years. He and his co-workers were the first to propose CAM(P)D approaches for ORC working fluid selection and ORC design and have since made numerous further contributions relating to ORC mixture design, ORC optimisation for renewable energy applications and ORC cycle integration considering multiple heat sources.

Hua Tian
Contact details:
- Email: thtju@tju.edu.cn
- Web: http://skle.tju.edu.cn/kydw/show.jsp?informationid=201810181346330431
Expertise:

Hua Tian is a Professor at the State Key Laboratory of Engines, with over 12 years' research experience in engine waste-heat recovery using ORC or sCO2 power systems.

He developed the CO2-based working-fluid matching theory of efficient waste-heat recovery and system miniaturisation. Automotive engine needs system miniaturisation, which requires efficient recovery of waste heat by working-fluid matching design in the simple cycle mode, but there is no effective working-fluid scheme at present. Starting from the exploration of new working fluids, he discovered the correlation law between physical property of working

fluid and cycle efficiency, dynamic response and system miniaturisation, and put forward a new idea of defining the physical property of ideal working fluid and actual working fluid. The matching rule of physical property and characteristic of CO2-hydrocarbon mixture was explored, and a new working fluid and its optimisation design method were put forward to realise the efficient recovery of waste heat under the miniaturisation system.

He has published more than 110 journal papers that have been cited more than 2320 times, 1 English book chapter and 2 Chinese book chapters. As PI, he has received ¥14M in research funding, including NFSC and a major research programme supported by the governments of China and USA. Over the past five years, he received the Second Prize of State Natural Science Award (2020), National Science Fund for Excellent Young Scholars (2020), "Huoyingdong scholar" by Ministry of Education, China (2019) and the First Prize in Tianjin's Natural Science Award (2017).

Gequn Shu
Contact details:
- Email: sgq@tju.edu.cn
- Web: https://tsee.ustc.edu.cn/2018/1015/c3267a341742/page & http://skle.tju.edu.cn/kydw/show.jsp?informationid=201111291519345805
Expertise:

Professor Gequn has been engaged in the research of internal combustion engine design and waste heat energy conversion and utilisation for a long time. As the chief scientist, he has undertaken national 973 Project of China: "basic research on cascade utilisation of waste heat energy of efficient, energy-saving and low-carbon internal combustion engine". He has presided over more than 30 national, provincial and ministerial level scientific research projects, including key projects of intergovernmental international scientific and technological innovation cooperation: "Sino US joint research on key technologies for improving energy efficiency of medium and heavy haul trucks". More than 120 SCI papers have been published and more than 20 invention patents have been authorised.